

Polyelectrolytes for Therapeutic Cell Encapsulation

By

Mohammad Abu Jafar Mazumder, M.Sc.

A Thesis

Submitted to the School of Graduate Studies

in Partial Fulfillment of the Requirements

For the Degree

Doctor of Philosophy in Chemistry

McMaster University

© By Mohammad Abu Jafar Mazumder, June 2009

Polyelectrolytes for Therapeutic Cell Encapsulation

DOCTOR OF PHILOSOPHY (2009)
(Chemistry)

McMaster University
Hamilton, Ontario

TITLE: Polyelectrolytes for Therapeutic Cell Encapsulation

AUTHOR: Mohammad Abu Jafar Mazumder (McMaster University)

SUPERVISOR: Professor Harald D. H. Stöver

NUMBER OF PAGES: xxviii, 231

Abstract

Cell encapsulation aims at the delivery of a therapeutic protein to a patient from transplanted cells. Conventional approaches involve immune-isolating cell lines that have been genetically modified to express a therapeutic protein, in alginate-based microcapsules. The long-term success of this approach hinges on the structural stability of the microcapsules, as well as their ability to maintain an environment suitable for the long-term survival of encapsulated cells. The most commonly studied type of microcapsule is the alginate-poly-L-lysine-alginate (APA) microcapsule. However, the main concern with APA microcapsules is the loss of structural integrity during long-term implantation due to the exchange of calcium ions with other physiological ions, as well as the loss of the polyelectrolyte overcoats.

In order to increase the structural stability of the microcapsules, we developed and characterized a number of synthetic polyelectrolytes that undergo phase separation upon complexation, and which are capable of forming covalent cross-links. These reactive polyelectrolytes are designed to take the place of poly-L-lysine and the outer alginate layer. We also explored combining cross-linkable synthetic polyanions with sodium alginate to strengthen the Ca Alginate core, by forming a core cross-linked network extending throughout the microcapsules. The polyelectrolyte complexes, encapsulation processes and microcapsule properties were studied in detail using extensive characterization techniques, including collaborative work on cell viability and host-immune response.

Overall, this thesis describes a novel approach and promising materials for cell encapsulations that offer enhanced microcapsule resistance to chemical and mechanical stresses, while preserving the desired biocompatibility. These materials may ultimately be useful for clinical immunosuppressive therapies.

Acknowledgements

I would like to thank Professor Harald D. H. Stöver for supervising my thesis work and for the opportunity to work in his laboratory. More than just a supervisor, he has been a great mentor offering motivation, advice and guidance throughout my time in graduate studies. His patience, ability to identify and positively respond to several of my academic as well as social needs is highly appreciated and will be remembered. Many thanks go to those on my advisory committee, Professor Gillian Goward and Professor Shiping Zhu, for their help, taking the time out of their busy schedules to sit on my committee and their critical comments and constructive suggestions to keep my research in terms of content and direction.

I would also like to express my gratitude to our collaborator Professor Murray A. Potter for his fundamental advice on this project. Dr. Feng Shen, Research Associate in Professor Potter's group provided invaluable input and guidance in the cell related work made in this thesis.

Special thanks are due to Dr. Nicholas A. D. Burke. This thesis would not have been possible without the kind, patient, and hard work of him, whose presence and expertise in the group are invaluable and greatly appreciated. I would like to recognize the following members in Stöver group: Dr. Lisa M. Croll, Dr. Xiangchung Yin, Dr. M. M. Ali, Dr. Wen Hui Li, Yan Xia, Janice Hickey, Jian Li, Casey Mills and Rachelle, who were all invaluable for their kind friendship and insightful discussions.

Many thanks go to the following: Dr Don Hughes and Dr Steve Kornick (NMR facility); Mr. Chris Butcher (BIMR electron microscopy facility); Mrs. Marnie Timleck (Health Science Electron Microscopy Facility); Dr Alex Adronov's group for using UV-

Vis spectrometer. Carol Dada and entire Chemistry Department Staff, who have been wonderful and caring over the past years.

I could not have endured for so long without my family and friends. My late father, whom I miss dearly, inspired me to follow my dreams. I immensely grateful to my mother, Afia Khatun for love, emotional support, care and concern, despite my lengthy and attention demanding academic and other pursuits over the years. I thank my brother Shah Jahan Mazumder and sister Salina Akhter for support and encouragement when I needed it. Lastly, I wish to acknowledge and thank my wife Nazneen Akhter (Sumi). She had endured the brunt of my frustrations and was always understanding and encouraging.

To all of those above, I am most grateful.

Table of Contents

	Page
Abstract	iv
Acknowledgements	v
List of Figures	xv
List of Tables	xxvi
List of Schemes	xxvii
List of Abbreviations	xxviii
Preface – Thesis Outline	1
Chapter 1 Introduction to cell encapsulation	9
1.1 Aim of the thesis	9
1.2 Cell Encapsulation	9
1.3 Brief history of Cell Encapsulation	12
1.4 Encapsulation Technique	14
1.4.1 Macroencapsulation	14
1.4.2 Microencapsulation	15
1.5 Present methods in Microcapsule preparation	16
1.5.1 Dropping Method	16
1.5.2 Simple Coacervation Method	17
1.5.3 Complex Coacervation Method	19
1.5.4 Spraying Method	19

1.5.5 Interfacial Reaction	20
1.5.6 Layer by Layer Method	22
1.5.7 Moulding Method	23
1.6 Polyelectrolyte Complex	24
1.7 Materials in Cell Encapsulation	29
1.8 Research Objectives	37
1.9 References	38
Chapter 2: Polyelectrolyte Complexation between Poly(methacrylic acid, sodium salt) and Poly(diallyldimethylammonium chloride) or Poly[2-(methacryloyloxyethyl) trimethyl ammonium chloride]	48
Abstract	49
2.1 Introduction	50
2.2 Experimental	53
2.2.1 Materials	53
2.2.2 Low MW P(MOETAC)	54
2.2.3 PMOETAC-770	55
2.2.4 PMOETAC-300	56
2.2.5 P(MAA-co-LMA)	56
2.2.6 P(MAA-co-MEGMA)	56
2.2.7 P(MAA-co-MOEAA)	56
2.2.8 Characterization	57
2.2.9 Coacervation Efficiency	58

2.2.10 Encapsulation	58
2.2.11 Encapsulation and Cross linking	59
2.3 Results and Discussion	59
2.3.1 Nature of the Complexes of PMAANa with PDADMAC-20, PDADMAC-450 and PMOETAC-300	60
2.3.2 Factors affecting Complexation Efficiency	62
2.3.3 Charge Ratio	63
2.3.4 Ionic Strength	65
2.3.5 Polymer Loading	71
2.3.6 Effect of Co-Monomers	75
2.3.7 Encapsulation of Oils with Complex Coacervates	79
2.3.8 Encapsulation and Cross linking of the Capsule Walls	80
2.4 Conclusion	82
2.5 References	84
Chapter 3: Self Cross linking Polyelectrolytes Complexes for Therapeutic Cell Encapsulation	88
Abstract	89
3.1 Introduction	90
3.2 Experimental	94
3.2.1 Materials	94
3.2.2 P(MOETAC) (C100) and (p(MOETAC-co-AEMA)[70:30], (C70)	95
3.2.3 P(MAANa)(A100) and p(MAANa-co-MOEAA)[70:30](A70)	96

3.2.4 FITC-Labelled Polymers, C70f and A70f	96
3.2.5 Characterization	97
3.2.6 MW Determination	97
3.2.7 Spin Coating	98
3.2.8 Preparation and Coating of Ca –Alg beads	99
3.2.9 Mechanical Stability	100
3.2.10 Permeability Studies	100
3.2.11 Cell Culture	101
3.2.12 Encapsulation of Cells	102
3.2.13 Cell Viability	102
3.2.14 Implantation	102
3.3 Results and Discussion	103
3.3.1 Ca-Alg Model Films Coated with C70/A70	104
3.3.2 Polyelectrolyte Coating of Ca-Alg Microcapsules	107
3.3.3 Microcapsule Stability	112
3.3.4 Permeability of AC70A70 Capsules	116
3.3.5 Cell viability in Microcapsules with Cross linked Shells	117
3.4 Conclusion	120
3.5 References	122
Chapter 4: Mechanically Enhanced Microencapsulated Cellular Gene Therapy	126
Abstract	127

4.1 Introduction	128
4.2 Materials and Methods	130
4.2.1 Chemicals	130
4.2.2 Polymer Synthesis	131
4.2.3 Encapsulation	131
4.2.4 Luciferase Activity Assay In Vitro	132
4.2.5 Pore Size Measurement	133
4.2.6 Bovine Serum Albumin (BSA) Uptake	134
4.2.7 Confocal Microscopy	134
4.2.8 Stress Test	134
4.2.9 Cell Viability	135
4.2.10 In Vivo Assessment of Capsules	135
4.3 Results	138
4.3.1 Capsule Structure and Strength Testing	138
4.3.2 Biocompatibility Tests	141
4.3.3 Protein Expression and Release from Encapsulated Cells	149
4.4. Discussion	150
4.4.1 Stability	150
4.4.2 Permeability	151
4.4.3 Biocompatibility	152
4.5 References	155

Chapter 5: Primary Amine Based Polyelectrolytes for Cell Encapsulation	159
Abstract	160
5.1 Introduction	161
5.2 Experimental	164
5.2.1 Materials	164
5.2.2 Synthesis of Poly(N-(3-aminopropyl)methacrylamide hydrochloride), PAPM and Poly(2-aminoethyl methacrylate), C0	165
5.2.3 Molecular Weight Determination	166
5.2.4 Determination of pKa	166
5.2.5 Preparation and Coating of Ca-Alg beads	166
5.2.6 Characterization	167
5.2.7 Chemical and Mechanical Stress Test	167
5.2.8 Mechanical Stability	168
5.2.9 Encapsulation of Cells	168
5.2.10 Cell Viability	168
5.2.11 Bovine Serum Albumin (BSA)Uptake by Capsules	169
5.3 Results and Discussion	169
5.3.1 Coating of Ca-Alg beads	171
5.3.2 Capsule Stability	175
5.3.3 Cell Viability	178
5.3.4 Protein Binding	180
5.4 Conclusion	182
5.5 References	183

Chapter 6: Core Cross linked Microcapsules for Cell Encapsulation	186
Abstract	187
6.1 Introduction	188
6.2 Experimental	192
6.2.1 Materials	192
6.2.2 Synthesis of Fluorescent Version of PMAANa, A100f	193
6.2.3 Poly(methacrylic acid, sodium salt-co-2-[methacryloyloxy]ethyl acetoacetate) p(MAA-co-MOEAA), 70:30 (A70) of different molecular weights	193
6.2.4 Rhodamine- Labeled poly-L-lysine (PLLr)	194
6.2.5 Characterization	194
6.2.6 Preparation of Ca(A/A70) Composite beads	195
6.2.7 Coating of Ca(A/A70) Composite Beads with Poly-L-lysine and Sodium alginate to form (A/A70)PA Capsules	196
6.2.8 Capsule Characterization	196
6.2.9 Chemical and Mechanical Stress Test	197
6.2.10 Cell Culture	197
6.2.11 Cell Viability	197
6.2.12 Permeability Measurements	198
6.3 Results and Discussion	199
6.3.1 (A(1.5%)A70(0.5%))PA Composite Capsules, (A/A70)PA	201
6.3.2 Core-Cross linked (A/A70)PA Capsules	207

6.3.3 In Vitro Cell Viability	212
6.3.4 MW cut-off of APA and Shell Cross linked Microcapsules	215
6.4 Conclusion	218
6.5 References	219
Chapter 7: Summary and Future Work for Cell Encapsulation	224
7.1 Summary	224
7.2 Future Work	228
7.2.1 Study new Series of Polyelectrolytes	228
7.2.2 Optimization of Composite Capsules	229
7.3 References	231

List of Figures

No.	Caption	Page
1.1	A schematic representation of the basic principle of artificial cells.	11
1.2	Schematic representation of cell encapsulation process: a) Macroencapsulation, b) Microencapsulation.	15
1.3	Schematic representation of entrapment of cells in gel beads using the dropping method.	17
1.4	Schematic representation of encapsulation of cells using the coacervation technique.	18
1.5	Schematic representation of encapsulation of cells using the spraying method.	20
1.6	Schematic representation of microcapsule preparation by interfacial reaction.	21
1.7	Schematic representation of the preparation process of layer-by-layer microcapsules.	22
1.8	Schematic representation of entrapment of cells using moulds. a) The warm polymer-cell suspension solution is cast into moulds, b) after the gel setting time, c) entrapped cells are carefully taken out of the moulds, and then stored in a buffer solution.	23
1.9	Schematic representation of formation of polyelectrolyte complexes.	25
1.10	Calcium cross-linking of Alginate bead formation in Calcium Chloride bath.	30

- 2.1 Optical microscope images of polyelectrolyte complexes: a) liquid complex coacervate PMAANa/PDADMAC-20 (no added NaCl). b) – d) PMAANa / PMOETAC-300, in presence of b) 200 mM, c) 300 mM and d) 400 mM added NaCl. All complexes were formed by combining the polyelectrolytes in ratios that result in 1 wt% total polymer loading with 1:1 charge ratios. 61
- 2.2 Complex yield as a function of the charge ratio, for complexes formed between PMAANa and a) PDADMAC-20 or b) PMOETAC-300. Total polymer loading is 1 wt%, with no added NaCl. 63
- 2.3 Complexation efficiency as a function of the charge ratio for complexes formed between PMAANa and a) PDADMAC-20 or b) PMOETAC-300. Total polymer loading was 1 wt%, with no added NaCl. Also shown are the two curves for efficiency, expected if there were quantitative formation of a 1:1 complex and complete loss of associated Na^+ and Cl^- ions – c) PDADMAC-20 and d) PMOETAC-300. 64
- 2.4 Complex yield as a function of ionic strength for PMAANa complexation with a) PDADMAC-20 or b) PDADMAC-150, c) PDADMAC-450 d) PMOETAC-13 or e) PMOETAC-300. 1:1 Charge ratio, 1 wt% polymer loading. 67
- 2.5 Complexation efficiency as a function of ionic strength for complexation of PMAANa with a) PDADMAC-20 or b) PDADMAC-150, c) PDADMAC-450, d) PMOETAC-13 or e) PMOETAC-300. 1:1 Charge ratio, 1 wt% polymer loading. 67

- 2.6 Polymer fraction in the complex phase as a function of ionic strength for complexation of PMAANa with a) PDADMAC-20 or b) PDADMAC-150, c) PDADMAC-450, d) PMOETAC-13 or e) PMOETAC-300. 1:1 Charge ratio, 1 wt% polymer loading. 69
- 2.7 The effect of ionic strength on PMAANa/PMOETAC-300 complexation efficiency at various charge ratios for 1 wt% polymer loading. Added NaCl: a) 0 mM, b) 100 mM, c) 200 mM and d) 300 mM. Also shown is the curve (e) for “maximum” efficiency if there were quantitative formation of 1:1 complex and loss of associated small ions (NaCl). 70
- 2.8 Complex yield as a function of total polymer loading for complexation of PMAANa with a) PDADMAC-20, b) PDADMAC-450, c) PMOETAC-13, d) PMOETAC-300 and e) PMOETAC-770. Charge ratio = 1:1, no added NaCl. 72
- 2.9 The polymer fraction in the complex (closed symbols) and the supernatant (open symbols) as a function of the total polymer loading for complexation of PMAANa with a) PDADMAC-20, b) PDADMAC-450, c) PMOETAC-13, d) PMOETAC-300 and e) PMOETAC-770. Charge ratio = 1:1. 73
- 2.10 The effect of temperature on the PMAANa/PDADMAC-400 complexes formed at a) 11.5 wt% and b) 12 wt% total polymer loading. 75
- 2.11 The effect of total polymer loading (wt%) on the A) complex yield and B) complexation efficiency for the complex formed between PDADMAC-20 and a) PMAANa, b) P(MAANa-LMA)[95:5] and c) P(MAANa-

	PEGMA)[70:30]. Charge ratio = 1:1.	77
2.12	The effect of ionic strength on A) complex yield and B) complexation efficiency for the complex formed between PDADMAC-20 and a) PMAANa, b) P(MAANa-LMA)[95:5] and c) P(MAANa-PEGMA) [70:30]. Charge ratio = 1:1.	78
2.13	Optical microscopic image of methyl benzoate encapsulated with a complex made from PMAANa/PMOETAC-300 at a 1:1 charge ratio. Polymer loading: 1%, ionic strength: 325 mM.	80
2.14	Optical microscopic image of paraffin oil encapsulated with a complex made from P(MAANa-co-MOEAA)/PMOETAC-300 at a 1.05:1 charge ratio and an ionic strength of 375 mM: a) after cross-linking with PEI, and b) after addition of excess 4% NaCl (684 mM).	81
3.1	Film weights during formation of Ca-Alg- (C70-A70) 10 multilayer film on a glass cover slide.	106
3.2	Phase contrast microscope images of Ca-Alg beads exposed to a 0.05% solution of PLL for a) 10 minutes, b) 30 minutes, or to a 0.05% solution of C70 for c) 10 minutes, d) 30 minutes, followed by saline washing.	108
3.3	Confocal laser scanning microscopy image showing an equatorial section of representative Ca-Alg capsules exposed to a 0.5% solution of C70f for a) 10 minutes, and b) 120 minutes.	110
3.4	CLSM optical sections in the equatorial region of Ca-Alg beads exposed to 0.5% solution of polycation and polyanion for a) C70f and A70f; 30 sec each, b) C70f and A70f; 10 min each, c) C70f and A70; 10 min each d)	

	C70 and A70f; 10 min each, e) intensity line profile of microcapsules c and d showing the distribution of C70f and A70f.	111
3.5	Optical microscope image of APA (0.05/0.03) (top row), AC70A70 (0.5/0.5) (middle row) and AC70A100 (0.5/0.5) (bottom row) microcapsules in saline (left column), after exposure to 170 mM sodium citrate (centre column) and then 2M NaCl (right column).	113
3.6	Percentage of intact cell containing APA (0.05/0.03) and AC70A70 (0.5/0.5) capsules after osmotic pressure test.	115
3.7	GPC traces of a) the original PEG mixture and the solution in the sink compartment of the stirred diffusion cell(s) separated by b) AC70A70 (0.5/0.5), and c) APA (0.05/0.03) membranes after 24h at room temperature.	117
3.8	Phase contrast microscope image of C ₂ C ₁₂ cells encapsulated in AC70A70 after in vitro incubation for 1 week.	119
3.9	In vitro cell viability for C ₂ C ₁₂ cells encapsulated in APA and AC70A70 microcapsules.	119
4.1	Construction of 4-layer capsule.	131
4.2	Light microscopy phase contrast images (A, C, E, G) of capsules before stress test, and optical pictures (B, D, F, H) of petri dishes containing the same capsules shaken in 0.003% EDTA solution for 15 min and then stained with trypan blue. (A, B) Empty APA capsules, stored in saline for 3 days. (C, D) Empty 4-layer capsules, stored in saline for 3 days. (E, F) Empty 4-layer capsules, retrieved from mice after 1- week implantation.	

- (G, H) Empty 4-layer capsules, retrieved from mice after 4 weeks implantation. 137
- 4.3 GPC traces of: (a) the original PEG solution; and the solutions in the receptor compartments at $t = 24$ h for (b) Ca-alginate membrane; (c) Ca-alginate-PLL-alginate membrane; and (d) Ca-alginate-C70-A70-PLL-alginate membrane. 137
- 4.4 Confocal images of APA (A) and 4-layer (B) capsules containing C2C12 cells that were incubated with fluorescently labeled BSA at 37°C for 24 h. 139
- 4.5 A series of optical slices taken with a Confocal microscope from the top to the bottom of a 4-layer-capsule labeled with C70 before (A) and after (B) four weeks implantation in mice. The fluorescence intensity (corrected for capsule diameter) of capsules retrieved from mice after implantation for one and four weeks (C). 140
- 4.6 Effect of the C70 and A70 coating on survival of encapsulated cells. C₂C₁₂ Myoblasts were encapsulated in 4-layer-capsules or APA capsules. The viable cell number per capsule was assayed after incubation for up to 14 days. (** $p < 0.01$; no statistical difference between the two kinds of capsules at day 14. 142
- 4.7 Phase contrast images of capsules retrieved from mice after one-week implantation. (A) 4-layer capsules (Ca-alginate beads sequentially coated with 0.5% C70, 0.5% A70, 0.05% PLL, 0.03% alginate). (B) “0.50% C70” capsules (Ca-alginate beads sequentially coated with 0.50% C70, 0.03% alginate). (C) “0.10% C70” capsules (Ca-alginate beads

sequentially coated with 0.10% C70, 0.03% alginate). (D) “0.50% A70” capsules (Ca-alginate beads sequentially coated with 0.05% PLL, 0.50% A70, 0.05% PLL, 0.03% alginate). (E) “0.10% A70” capsules (Ca-alginate beads sequentially coated with 0.05% PLL, 0.10% A70, 0.05% PLL, 0.03% alginate). (F) “0.05% A70” capsules (Ca-alginate beads sequentially coated with 0.05% PLL, 0.05% A70, 0.05% PLL, 0.03% alginate). Data for “0.05% C70” capsules (Ca-alginate beads sequentially coated with 0.05% C70, 0.03% alginate) is absent because C70 concentrations lower than 0.1% cause the beads to clump together.

143

4.8 Summary of the surface analysis of capsules retrieved from mice that were implanted after 3-days in culture media (A) or implanted directly after manufacture (B). Capsules (~200) were randomly selected and the percentage of visible surface area coated by opaque materials was visually determined by light microscopy and the mean values are shown. 4-layer-capsules: Ca-alginate beads sequentially coated with 0.5% C70, 0.5% A70, 0.05% PLL, 0.03% alginate. “0.50% C70” capsules: Ca-alginate beads sequentially coated with 0.50% C70, 0.03% alginate. “0.10% C70” capsules: Ca-alginate beads sequentially coated with 0.10% C70, 0.03% alginate. “0.50% A70” capsules: Ca-alginate beads sequentially coated with 0.05% PLL, 0.50% A70, 0.05% PLL, 0.03% alginate. “0.10% A70” capsules: Ca-alginate beads sequentially coated with 0.05% PLL, 0.10% A70, 0.05% PLL, 0.03% alginate. “0.05% A70” capsules: Ca-alginate beads sequentially coated with 0.05% PLL, 0.05% A70, 0.05% PLL,

	0.03% alginate.	145
4.9	Confocal image through middle of capsules incubated in 0.05% FITC labeled BSA solution at 37 °C for 24 h. Line profiles are shown to the right for each kind of capsule. (A) 4-layer-capsules (Ca-alginate bead sequentially coated with 0.50% C70, 0.50% A70, 0.05% PLL, 0.03% alginate). (B) Reduced C70/A70 4-layer-capsules (Ca-alginate bead sequentially coated with 0.10% C70, 0.10% A70, 0.05% PLL, 0.03% alginate). (C) APA capsules.	146
4.10	Top – Confocal images through the middle of a) APA, b) <i>APA100PA</i> , c) <i>APA70PA</i> , d) <i>AC70A100PA</i> and e) 4-layer (<i>AC70A70PA</i>) microcapsules exposed to 0.05 w/v% BSA-FITC at 20 °C for 24 h. Bottom f) Line profiles of microcapsules shown at top.	148
4.11	Four layer-capsules (cultured in serum-free medium for 72 hours in advance of implantation) were retrieved after one week of mouse implantation.	149
5.1	Optical microscope image of aggregated Ca-Alg-PAPM capsules formed by exposure of Ca-Alg beads to 0.5wt% PAPM solution in saline for 10 min. Points of contact (white arrows) between capsules and detached patches (black arrows) are visible.	172
5.2	Effect of [NaCl] and [CaCl ₂] on capsule aggregation during coating with 0.5% PAPM.	172
5.3	Optical microscope image of Ca-Alg beads exposed for 10 minutes to 0.5% PAPM in 1.1% CaCl ₂ /0.45% NaCl, followed by washing and trypan	

	blue staining.	173
5.4	Ca-Alg beads, coated with 0.5 wt% C70 for 10 min, followed by washing and trypan blue staining.	174
5.5	Optical microscope images of a) APA (0.05/0.03), b) A-PAPM-A (0.5/0.03), c) A-PAPM-A70 (0.5/0.5), d) A-C0-A (0.5/0.03), and e) A-C0-A70 (0.5/0.5) capsules. After treatment with 170 mM sodium citrate and then 2 M NaCl, followed by trypan blue staining a, b, d have dissolved, while c and e shells survive and are shown in insets.	176
5.6	Phase contrast microscope image of C ₂ C ₁₂ cells encapsulated in a) APA (0.05/0.03), b) A-PAPM-A (0.5/0.03), c) A-PAPM-A70 (0.5/0.5), and d) A-C0-A70 (0.5/0.5) after in vitro incubation for 1 week.	179
5.7	In vitro cell viability for C ₂ C ₁₂ cells encapsulated in a: APA (0.05/0.03), b: A-PLL-A(0.5/0.03), c: A-PLL-A70(0.5/0.5), d: A-PAPM-A (0.5/0.03), e: A-PAPM-A70(0.5/0.5), and f: A-C0-A70(0.5/0.5) capsules.	180
5.8	Top: Confocal microscopy optical sections in the equatorial region of A-C70-A, A-C0-A, A-PLL-A, and A-PAPM-A capsules, all prepared from Novamatrix alginate, and incubated in 0.05% BSA _f at 20 °C for 24h. Bottom: line intensity profiles of capsules shown at top.	181
6.1	Percentage of A70 _f remaining in the composite microcapsules at different stages of the capsule preparation.	203
6.2	CLSM equatorial optical section of Ca(A/A70 _f) composite capsule: a) uncoated and b) coated with PLL (15-30 kDa) (0.05%, 6 min) and then alginate (0.03%, 4 min).	204

- 6.3 Top: CLSM equatorial optical sections of (A/A70) PA capsules made with PLL_r of a) 15-30 kDa; b) 4-15 kDa; and c) 1-4 kDa. Bottom: 25 pixel wide line profiles taken from the images. 205
- 6.4 Fluorescence microscopy images (grayscale) of (A/A70f) P (4-15 kDa, 0.05%) A(0.03%) capsules; a) as formed, and b) after being exposed to citrate (170 mM) and NaCl (2 M), and manually cut with a micro-knife. 206
- 6.5 Fluorescence microscopy images of a) (A/A70f) P (4-15k, 0.5%)A (0.03%) and d) (A/A100f) P (4-15k, 0.5%)A(0.03%); b, e) the beads were manually cut, and then exposed to excess 70 mM sodium citrate; c, f) after further treatment with 2 M NaCl. 208
- 6.6 Fluorescence microscopy images of core-cross linked (A/A70) PLL_r (4-15k, 0.5%)A (0.03%) composite capsules to show the location of PLL_r (4-15 kDa). a) As formed; b) after addition of excess 70 mM sodium citrate and crushing; c) following addition of excess 2 M NaCl. The scale bar is 500 μm. d) CLSM middle optical section, and intensity line profile, of a capsule such as in a). 210
- 6.7 Fluorescence microscopy images of (A/A70f) PA capsule prepared by exposure to both high and medium MW PLL. Ca(A/A70f) composite beads were coated with 0.05% PLL (15-30k) (1 min), and then with 0.5%PLL (4-15k) (6 min), followed by 0.03% Alg (4 min). a. As formed, b. After challenge with citrate and manual cutting. c. After exposure to excess 2 M NaCl. 212
- 6.8 Phase contrast microscope image of C₂C₁₂ mouse cells 7 days after being

- encapsulated in a) APA and b) (A/A70) PA microcapsules. Coating conditions: PLL (15-30 kDa, 0.05%)/6 min; Na-Alg (0.03%)/4 min. 212
- 6.9 In vitro cell viability of C₂C₁₂ cells encapsulated in APA and (A/A70) PA capsules over time. a) APA and shell-cross linked (A/A70) P (15-30k, 0.05%)A capsules and b) APA and core-cross linked (A/A70) P (4-15k, 0.5%)A capsules. Coating conditions: APA - PLL (15-30k, 0.05 % w/v, 6 min), Alg (0.03% w/v, 4 min); shell-cross linked (A/A70) PA: PLL (15-30k, 0.05 % w/v, 6 min) Alg (0.03% w/v, 4 min); core-cross linked (A/A70) PA: PLL (4-15k, 0.5 % w/v, 6 min) Alg (0.03% w/v, 4 min. 213
- 6.10 Top: CLSM middle sections of cell containing (A/A70) P(4-15k, 0.5%)A(0.03%) capsules exposed for 24h at room temperature to 0.05% dextran-FITC with nominal MWs of a) 10k, b) 70k, c) 150k, d) 250k, and e) 500k. Coating conditions - PLL (0.5 % w/v, 6 min); Alg (0.03% w/v, 4 min). Bottom: Line profile from images as above. 216
- 6.11 CLSM equatorial optical sections of a) APA and b) (A/A70) P(15-30k, 0.05%)A microcapsules exposed to BSA-FITC. 217

List of Tables

No.	Caption	Page
1.1	Cell encapsulation approaches based on alginate matrices	32
3.1	Polyelectrolyte properties	103
3.2	Weight and thickness of hydrogel films prepared on glass cover slides	105
3.3	Performance of empty APA and AC70A70 microcapsules in the OPT and calcium chelation test	114
5.1	Properties of polycations	170
5.2	Performance of empty and cell-containing capsules in the OPT and Ca chelation test	177
6.1	Polymer properties	200

List of Schemes

No.	Caption	Page
2.1	Polyelectrolytes used in this study	53
2.2	Reaction between acetoacetate and amine groups to form cross-linked polyelectrolyte complex	81
3.1	Natural and synthetic polyelectrolytes used to prepare coated capsules	93
3.2	Formation of cross linked shells on Ca-Alg capsules by sequential coating with self-cross linking polyelectrolytes having complementary reactive groups, amino (C70) and acetoacetate (A70)	94
3.3	Formation of C70A70 bilayer or multilayers films by sequential coating of Ca-Alg hydrogel films on glass slides	106
5.1	Polyelectrolytes used in this study	164
6.1	Schematic representation of the capsule morphologies formed when embedding reactive polyanion within the CaAlg capsule, followed by reaction with high MW PLL, low MW PLL, and sequentially with high and low MW PLL	191
6.2	Natural and synthetic polyelectrolytes used in this study	201

List of Abbreviations

AEMA	2-aminoethyl methacrylate
AIBN	2,2' Azobisisobutyronitrile
APM	N-(3-Aminopropyl)methacrylamide hydrochloride
CHES	2-(Cyclohexylamino)ethanesulfonic acid
CLSM	Confocal Laser Scanning Microscopy
FITC	Fluorescein isothiocyanate
GPC	Gel Permeation Chromatography
LMA	Lauryl methacrylate
MeiBrB	Methyl isobromobutyrate
MOEAA	2-(methacryloyloxy)ethyl acetoacetate
NMR	Nuclear Magnetic Resonance
OM	Optical Microscopy
PDADMAC	Poly(diallyldimethylammonium chloride)
PEGMA	Poly(ethylene glycol) monomethyl ether methacrylate
PEI	Polyethyleneimine
PLL	Poly(L-lysine)
PMAANa	Poly(methacrylic acid, sodium salt)
PMOETAC	Poly([2-(methacryloyloxy)ethyl] trimethylammonium chloride)
RITC	Rhodamine B isothiocyanate
SFM	Serum free media
THF	Tetrahydrofuran

Preface - Thesis outline

As this research has generated several published and one soon-to-be published manuscript, the results of this thesis are prepared in the so-called “sandwich” style. The first chapter starts with a general introduction to cell encapsulation for the immunisation of transplanted cells, including a literature review on techniques and methods used. Each subsequent chapter comprises a publication or a manuscript. The final chapter summarizes the results and outlines future work.

Chapter 1: Introduction to Cell Encapsulation

The aim of chapter 1 is to review the background of cell encapsulation. This chapter will discuss the cell encapsulation processes, different techniques and material involved in cell encapsulation, and with focus on polyelectrolyte complexation used in designing stable and biocompatible microcapsules.

Chapter 2: Polyelectrolyte Complexation between Poly(methacrylic acid, sodium salt) and Poly(diallyldimethylammonium chloride) or Poly[2-(methacryloyloxyethyl) trimethyl ammonium chloride]

Research Objective:

The aim of chapter 2 is to study the polyelectrolyte complexation between poly(methacrylic acid, sodium salt) and poly(diallyldimethylammonium chloride) or poly[2-(methacryloyloxyethyl) trimethyl ammonium chloride]. It will aid in

understanding the properties of polyelectrolytes that can be used in a wide variety of applications in the form of layer-by-layer assemblies, soluble complexes, solid precipitates, and liquid coacervate.

Synopsis:

The physical nature of the complexes and the efficiency of polyelectrolyte complexes between poly(methacrylic acid, sodium salt) and poly(diallyldimethylammonium chloride) or poly[2-(methacryloyloxyethyl) trimethyl ammonium chloride] to form gels, liquid phases, or soluble complexes depend on variables such as charge ratio, ionic strength, polymer concentration, and polymer molecular weight. Highest complexation efficiency was obtained when 1:1 charge ratios were used. Liquid coacervates were favoured by higher ionic strength, whether from added NaCl or from higher polymer loading, and by using polyelectrolytes of lower MW. The encapsulation of oils with a two-polyelectrolyte system forming a complex coacervate was demonstrated, as was the feasibility of cross-linking the resulting coacervate capsule walls via complementary polymer-bound reactive groups with polymer-bound amine groups in polyethyleneimine.

Associated Publication:

Burke, N. A. D.; Mazumder, M. A. J.; Hanna, M.; Stöver, H. D. H. "Polyelectrolyte complexation between poly(methacrylic acid, sodium salt) and poly(diallyldimethylammonium chloride) or poly[2-(methacryloyloxyethyl) trimethyl ammonium chloride]" *Journal of Polymer Science: Part A: Polymer Chemistry*, **2007**, *45*, 4129-4143.

Chapter 3: Self-cross-linking polyelectrolyte complexes for therapeutic cell encapsulation

Research Objective:

The aim of chapter 3 is to study the feasibility of using self-cross-linking synthetic polyelectrolytes capable of forming covalent cross-links around calcium alginate beads, and to replace the conventional poly-L-lysine (PLL) and outer alginate, respectively, of Alginate-PLL-Alginate (APA) microcapsules, leading to the preparation of stronger microcapsules for therapeutic cell encapsulation, yet with similar biocompatibility and permeability.

Synopsis:

We developed a number of self-cross-linking polyelectrolytes, which were used to strengthen the surface of calcium alginate beads for cell encapsulation. The synthetic copolymers of methacryloyl oxyethyl trimethyl ammonium hydrochloride with amino ethyl methacrylate [70:30] as a polycation (C70) and copolymers of methacrylic acid sodium salts with methacryloyl oxyethyl acetoacetate [70:30] as polyanions (A70) were prepared by free radical polymerization to strengthen calcium alginate capsules through the formation of a covalently cross-linked skin around the calcium alginate core. The covalent cross-linking is achieved by using complementary reactive groups (amino and acetoacetate) that are attached to two different polyelectrolytes that undergoes reaction once the polyelectrolytes are brought together by electrostatic interactions. The reactive groups are polymer-bound and hence their bioavailability to the encapsulated cells or the host will be reduced and they should not pose a toxicity concern during encapsulation.

CaAlg-C70-A70 capsules are shown to be more resistant to chemical and mechanical stresses, compared to APA capsules. The molecular weight cut off (MWCO) of CaAlg-C70-A70 capsules was shown to be similar to that of control APA capsules. The encapsulated cells were shown to be viable within calcium alginate capsules coated with C70 and A70 even though some of the capsules showed fibroid overcoats when implanted in mice, due to an immune response.

Associated Publication:

Mazumder, M. A. J.; Shen, F.; Burke, N. A. D.; Potter, M. A.; Stöver, H. D. H. “Self-cross-linking polyelectrolytes complexes for therapeutic cell encapsulation.” *Biomacromolecules*, **2008**, *9(9)*, 2292-2300.

Chapter 4: Mechanically enhanced microencapsulated cellular gene therapy

Research Objective:

The aim of chapter 4 is to develop mechanically enhanced multilayer capsules through the formation of a covalently cross-linked skin around the calcium alginate core to overcome the host immune response to the microcapsules or microencapsulated cells after implantation without losing permeability.

Synopsis:

To optimize all the required properties for a successful clinical application, we developed covalently cross-linked microcapsules in which calcium alginate beads were sequentially coated with C70, A70, PLL and Alginate. The multilayer capsules immune

stimulating effect (fibroid overgrowth) was studied by varying the concentration and compositions of polyelectrolytes, and changing the media used. Interaction between the FITC labeled protein (BSAf) (analogous to media protein) and the multilayer capsules was studied by CLSM, and it was observed that C70 significantly bound protein to the microcapsules surface, while A70 had a lesser effect. Reducing the concentration of C70 and A70 lessened this effect. Using serum-free media to culture the microcapsules post fabrication instead of regular medium eliminates this host reaction. Ca Alg-C70-A70-PLL-Alg multilayer capsules are more resistant to chemical and mechanical stress tests, compared with APA microcapsules. The pore size and *in vitro* and *in vivo* biocompatibilities of the multilayer capsules were shown to be similar to those of control APA microcapsules, and are suitable for cell encapsulation.

Associated Publication:

Shen, F.; Mazumder, M. A. J.; Burke, N. A. D.; Stöver, H. D. H.; Potter, M. A. “Mechanically enhanced microencapsulated cellular gene therapy” *Journal of Biomedical Material Research, Part B. Applied Biomaterials*, **2009**, *90B(1)*, 350-361

Chapter 5: Primary amine based polyelectrolytes for cell encapsulation**Research Objective:**

The aim of chapter 5 is to screen a number of self cross-linkable methacrylate or methacrylamide-based polyelectrolytes containing primary amine, which can facilitate covalent cross-linking, but not react with cellular media, and can potentially replace PLL for the preparation of stable alginate based microcapsules for long-term applications.

Synopsis:

A number of self-cross-linking polyelectrolytes have been developed, which were used to replace the PLL and to strengthen the surface of calcium alginate beads for cell encapsulation. The synthetic copolymers of [2-(methacryloyloxy) ethyl] trimethylammonium chloride (MOETAC) with 0 to 100% 2- aminoethylmethacrylate hydrochloride (AEM.HCl), and the homopolymer of N- (3- aminopropyl) methacrylamide hydrochloride (APM) were prepared by free radical polymerization. Polyelectrolyte complexes of all these amine-based polyelectrolytes including PLL with a polyanion alginate, poly (methacrylic acid, sodium salt) (A100), and A70 have been studied. The resistance of these complexes to ionic strength, and the cross-linked nature of the microcapsules shell, was demonstrated using tests involving exposure to citrate, sodium chloride, sodium hydroxide and dilute EDTA. The viability of encapsulated cells and biocompatibility of the Ca-Alg microcapsules coated with the complexes were explored with the goal of forming a self-cross-linked polyelectrolyte skin without sacrificing biocompatibility.

Associated Publication:

Mazumder, M. A. J.; Burke, N. A. D.; Shen, F.; Potter, M. A.; Stöver, H. D. H. "Primary amine based polyelectrolytes for cell encapsulation" To be submitted.

Chapter 6: Core cross-linked microcapsules for cell encapsulation

Research Objective:

The aim of chapter 6 is to study the feasibility of using cross-linkable synthetic polyanions (A70) to strengthen the Ca Alginate bead cores, by forming a core cross-linked interpenetrating network of covalently cross linked polymer within the conventional APA microcapsules.

Synopsis:

Synthetic reactive polyelectrolytes based on methacrylic acid (A70) are used to form covalently cross-linked network within calcium- gelled Alginate-Poly-L-lysine-Alginate (APA) microcapsules. The distribution of A70 and PLL in the modified capsules were studied by confocal laser scanning microscope (CLSM) using FITC labeled A70 (A70f) and Rhodamine labeled PLL (PLLr), and found that by varying the molecular weight of PLL and A70 it should be possible to localize the cross-linking reaction at the capsule surface or in the interior for the formation of an interpenetrating network within the calcium alginate matrix. The resulting cross-linked capsules are resistant to chemical stress tests (citrate, sodium chloride, sodium hydroxide and dilute EDTA). The molecular weight cut off (MWCO) of core cross-linked microcapsules were examined by CLSM using BSA_f and different molecular weight of FITC labelled saccharides (FITC-Dextran), and found that the MWCO of modified capsules was shown to be similar to that of control APA capsules. The viability of encapsulated cells and biocompatibility of the core cross-linked microcapsules was similar to the control APA microcapsules.

Associated Publication:

Mazumder, M. A. J.; Burke, N. A. D.; Shen, F.; Potter, M. A.; Stöver, H. D. H. “Core cross-linked microcapsules for cell encapsulation” *Biomacromolecules*, **2009**, *10(6)*, 1365-1373.

Chapter 7: Summary and future work for cell encapsulation

The aim of chapter 7 is to summarize the results and outline future work based on the completed research.

Chapter 1: Introduction to Cell Encapsulation

1.1 Aim of the Thesis

To develop synthetic polymers to be used as reinforcing materials in cell encapsulation for the treatment of several human diseases such as lysosomal storage diseases (LSD), diabetes, Parkinson's disease and cancer using immuno-isolated, genetically modified cells. In particular, this thesis focuses on polyelectrolytes that undergo phase separation upon complexation and which can be self-cross linked to form protective shells.

1.2 Cell Encapsulation

T.M.S. Chang in Montreal introduced the concept of using encapsulation for the immunoprotection of transplanted cells in the early 1960s.¹ The concept is well described by this quote: "Microencapsulated cells might be protected from destruction and from participation in immunological processes, while the enclosing membrane would be permeable to small molecules of specific cellular product which could then enter the general extra cellular compartment of the recipient. For instance, encapsulated endocrine cells might survive and maintain an effective supply of hormone."²

The implantation of non-autologous cells is complicated by the recipient's immune system, often leading to rejection of the transplant unless immune-suppressing drug regimes are used. The most direct way to avoid this problem is to transplant cells and tissues that are histocompatible with the host. However, this is not always possible due to the poor availability of donor tissues. Even partially histocompatible tissues still

require immunosuppression that could compromise the health of the host as well as the transplant. However, non-autologous tissue implantation is greatly facilitated if the cells were physically isolated from the immune response. For this purpose, immuno-isolation devices have been developed with the potential to physically enclose cells within a biocompatible membrane. The biocompatible and selectively permeable features of an immuno-isolation barrier protect foreign cells from immune rejection after transplantation, while permitting the continuous passage of secreted therapeutic products. This immuno-isolation could result in a reduction or even avoidance of long-term administration of immunosuppressants, provided that fully biocompatible materials that do not interfere with cell function can be used. The encapsulation of cells instead of therapeutic products allows the delivery of the product for a longer period of time as cells release the products continuously. It has a great potential to reduce the need for human donors for tissue and organ transplantations since it allows the transplantation of cells derived from standard human cell lines, human stem-cell derived cells, and animal cells. Immunoprotection may allow transplantation of cells without the need for immunosuppression, and transplantation of cells from non-human species (xenograft).³ In addition, genetically modified cells can be immobilized to express any desired protein *in vivo* without the modification of the host's genome. Immobilization of cells shows an important advantage compared with encapsulation of proteins because it allows a sustained and controlled delivery of produced therapeutic products at a constant rate. The concept of cell encapsulation is shown in Figure 1.1.

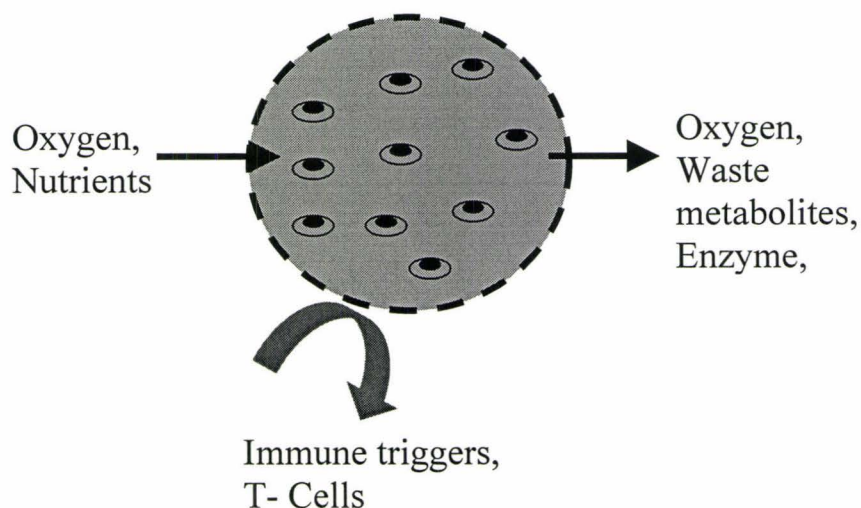


Figure 1.1: A schematic representation of the basic principle of artificial cells.

Hormone or protein secreting cells could be enclosed within a wide range of polymeric matrices and used to treat diseases caused by failure of secretory cell function. The concept is based on the protection of allo- and xenogenic transplanted cells within the confines of semi-permeable matrices or membranes that are ultimately designed to be implanted into the intraperitoneal cavity or other suitable transplant sites in a patient. The cells may be genetically engineered to express certain enzymes missing in the patient, such as lysozymes for patients suffering from one of about 40 identified lysosomal storage disorders (LSD's). The encapsulating membranes have to be designed to keep high molecular weight antibodies (~250 kDa) out, while allowing exchange of oxygen, nutrients and metabolites including the specific enzymes needed by the patient (Figure 1.1). The metabolic requirements of various cell types are different and, hence, optimal membrane permeability is expected to depend on the choice of cells. The membrane must be biocompatible with regards to the host and to the cells it surrounds. It must be

physically strong enough to protect cells during handling, and transplantation, and to shield them from mechanical and biochemical stresses inside the host for about one year. This thesis aims to develop capsules that can protect encapsulated cells for one year or longer, using covalent cross-linking to reinforce the outer capsule shells or the core.

1.3 Brief History of Cell Encapsulation

Bisceglie gave the earliest demonstration of cell encapsulation in 1933, enclosing tumor cells in a polymer membrane and transplanting them into a pig's abdominal cavity. The results showed that the cells survived for at least 21 days, and were not destroyed by the immune system.⁴ Thirty years later, Chang introduced the idea of using encapsulation for the immunoprotection of transplanted therapeutic cells, and coined the term 'artificial cells' for this concept.¹ The breakthrough in applying Chang's principles of bioencapsulation came with the work of Lim and Sun.⁵ In 1980; they successfully implemented Chang's idea to immobilize xenograft islet cells to aid in glucose control for diabetes in mice and other small animals. Since then, enormous efforts have been made to understand the biology, genetics, polymer and pharmaceutical science for the development of novel microencapsulations. As a consequence, Chang applied cell encapsulation for the therapeutic treatment of renal failure⁶, and Sun used it for the treatment of diabetes.⁷ Those results have provided the scientific basis for several clinical trials. Calafiore et al⁸ initiated a clinical trial where microencapsulated human islets were implanted into non-immunosuppressed patients with type 1 diabetes. An alginate based encapsulation system was developed by Emerich et al⁹ where choroid plexus bodies were immobilized in an effort to achieve an appropriate delivery of neurotrophic factors to the

brain in a primate model of Huntington's disease. Moran et al¹⁰ studied the microencapsulation of engineered cells to deliver sustained levels of interleukin-6 in an animal model for the treatment of hepatocellular carcinoma. Dvir-Ginzberg et al¹¹ developed an interesting gene therapy strategy where retroviral vector producer cells were entrapped in three dimensional alginate matrixes for potential use in cancer. Recently, a myocardial infarction rat model was evaluated by Zhang et al¹² using microencapsulated Chinese hamster ovary cells for the treatment of cardiovascular disorders.

Cell microencapsulation is a technology with enormous clinical potential for the treatment of a wide range of diseases.¹³ The last three decades have seen tremendous advances in the field of cell encapsulation.^{14, 15} However, despite very promising and encouraging results we are still far from clinical application of cell based constructs due to many difficulties, some of which will certainly challenge our scientific ingenuity. One of the main reasons is the lack of reproducibility. However, in the last few years, the strategy in the field has changed, applying a stepwise analysis of the essential obstacles instead of an approach via trial and error. Coupled with increased international collaboration, this approach should move the technology forward in a careful and controlled way and bring it much closer to clinical reality.^{16, 17, 18, 19} This has renewed the excitement and hopes surrounding this cell-based technology.

1.4 Encapsulation Technique

The general cell encapsulation processes can be broadly divided into two groups:

1.4.1 Macroencapsulation:

Macroencapsulation allows the implantation of large groups of living cells into the host without immune rejection (Figure 1.2a). These systems can be in the form of a flat disk, hollow fiber or tube, and follow planar or cylindrical geometry that isolate the cells from the body. They are much larger in size compared to microcapsules. Unlike the hydrogel membranes of microcapsules, the membranes of macrocapsules are typically composed of thermoplastic materials that vary in their structural, functional, and mechanical properties. The main advantage of macrocapsules is that they can be implanted and retrieved with minimal risk. However, the main drawback is the limitation of oxygen diffusion and nutrient transport, which reduces cell function and viability.

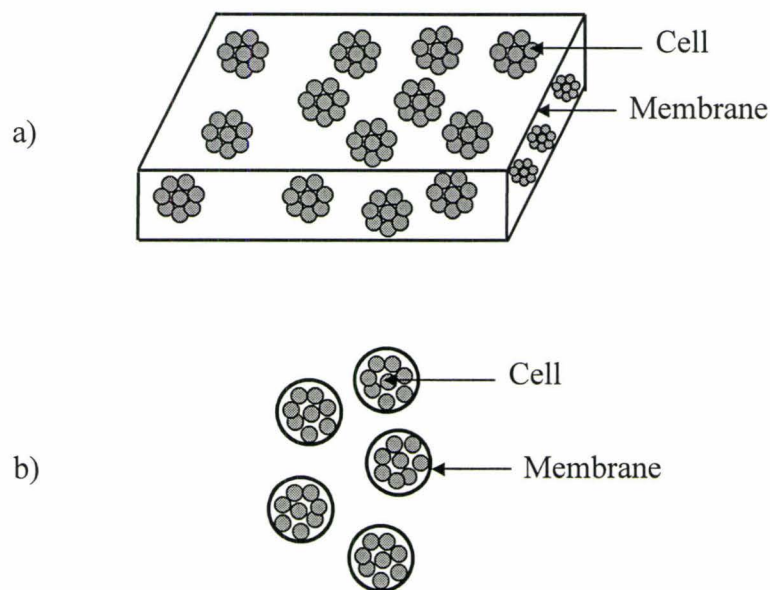


Figure 1.2: Schematic representation of cell encapsulation process: a) Macroencapsulation, b) Microencapsulation

1.4.2 Microencapsulation:

The objective of microencapsulation is to entrap smaller groups of typically 100 cells into a semi permeable membrane (Figure 1.2b). These microcapsules are usually spherical in shape,¹ and capsule diameter is usually 50 μm to 1.5 mm in range,²⁰ with the upper limit determined by passive oxygen diffusion. Microcapsules can be stronger and more durable than macrocapsules and difficult to mechanically disrupt, and their spherical shape results in large surface/volume ratios, which increased oxygen, nutrient and metabolic exchange. However, the main drawback of microencapsulation is the difficulty in removing the implants if necessary. To construct the spherical geometry, microcapsules are almost exclusively produced from hydrogels. These hydrogel capsules have a number of appealing features. Firstly, the hydrogel reduces mechanical and frictional irritation of surrounding tissue. Secondly, hydrogels by nature are hydrophilic, which reduces their interfacial tension with surrounding fluids and tissues and helps to minimize protein adsorption and cell adhesion. Thirdly, hydrogels are permeable to low-molecular-mass nutrients and metabolites. Some of the most popular biomaterials, which have been applied to microencapsulations, are hence based on alginate, carboxymethyl cellulose, carrageenan, chitosan, and agarose.

The debate of the relative benefits of macro versus microencapsulation is ongoing, and neither technique has demonstrated clear superiority over the other. Above

all, the success of any encapsulation technique will ultimately rely on a systematic evaluation of capsule properties and encapsulated cell performance.

1.5 Present Methods of Microcapsule Preparation

In cell encapsulation system, cells are usually surrounded by liquid. One of the most important general goals for coating cells or tissues is to achieve isolation from their environment. Microcapsules can be formulated by many different methods.

1.5.1 Dropping Method:

The most often described microencapsulation system is based on the calcium gellation of polyanions, as shown in Figure 1.3 in which cell containing alginate solution is extruded through a needle with concentric air flow to drop into the gellation bath which contains a solution of a cross-linking agent such as calcium chloride.

The major advantage of this method is the rapid gelation at ambient temperature. However, in order to control the droplet size, many parameters such as viscosity, wettability, molecular weight and concentration of the polymer solution, as well as the diameter and geometry of the nozzle, need to be considered.

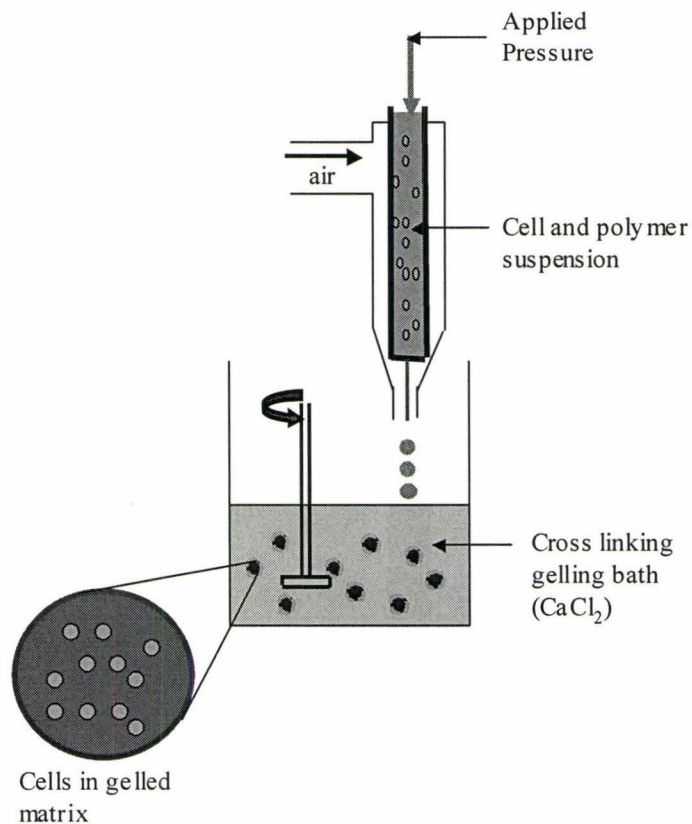


Figure 1.3: Schematic representation of entrapment of cells in gel beads using the dropping method.

1.5.2 Simple Coacervation Method:

The coacervation (often called co-extrusion) method is generally used as an encapsulation process. This method is based on dispensing a suspension of the cells through the inner needle and the polymeric wall-forming solution through the outer needle of a concentric needle assembly, into a precipitation bath. The polymer solution gels upon entering the precipitation bath. A schematic representation of encapsulation of cells using the coacervation method is shown in Figure 1.4.

The major advantage of the final product is that it enables the cells to have some degree of freedom, and the gel matrix is present only as external shell.

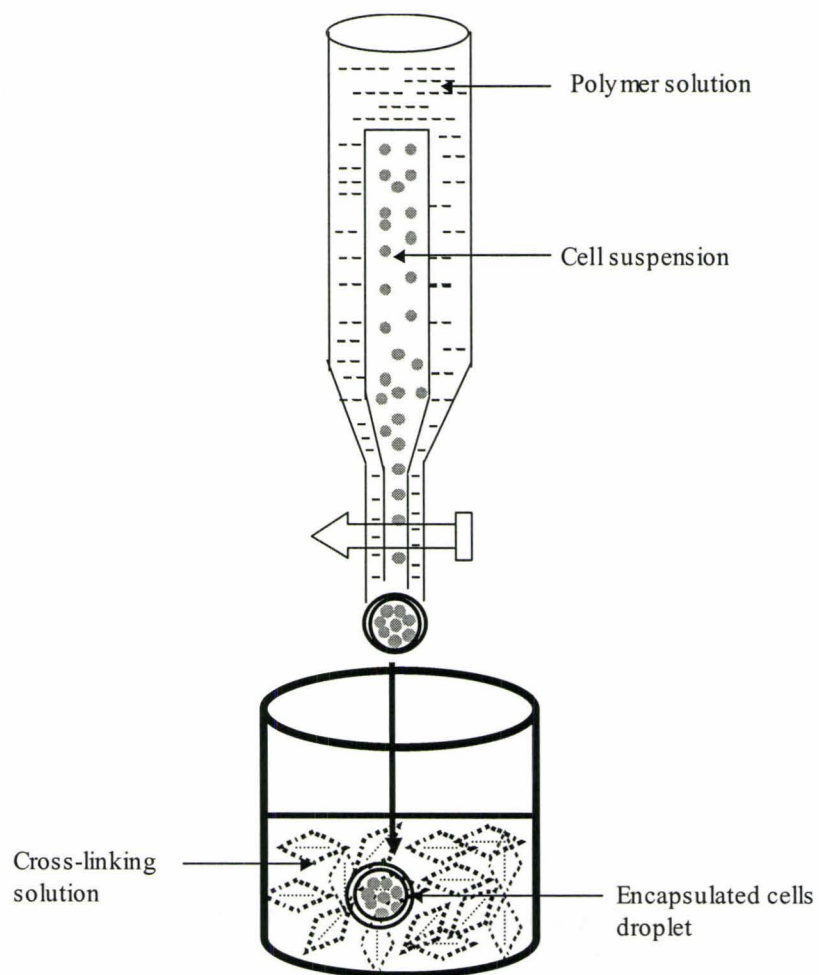


Figure 1.4: Schematic representation of encapsulation of cells using the coacervation technique.

1.5.3 Complex Coacervation Method:

There is a similar technique as described in section 1.5.2, called complex coacervation, which involves the interaction between two oppositely charged polyelectrolytes to form a film. This technique was used to encapsulate somatic embryos for producing artificial vegetative seeds, although with limited success.²¹ This method is mainly used for coating oil droplets in i.e. perfume industry. Coating consists typically of gum acacia/gelatin, and is cross-linked using small reactive molecules such as formaldehyde or glutaraldehyde.

1.5.4 Spraying Method:

Spraying also can be used for producing matrix type microcapsules.²² During the free fall of cell/polymer suspension droplets, a rapid interfacial reaction can be initiated by spraying an aerosol cross-linking solution towards it, as shown in Figure 1.5.

The cross-linking reaction stops when the falling drop encounters buffered wash bath. An inverted method can involve spraying a charged polymer solution on drops of a suspension of cells in a cross-linking solution. The advantage of this method is that it can be used to form relatively thin films around cell containing droplets, and it also enables the production of dry encapsulates using hot-air blowers. However, gelation depends upon the droplet exposure time and nature to the cross-linking aerosol along the spraying path.

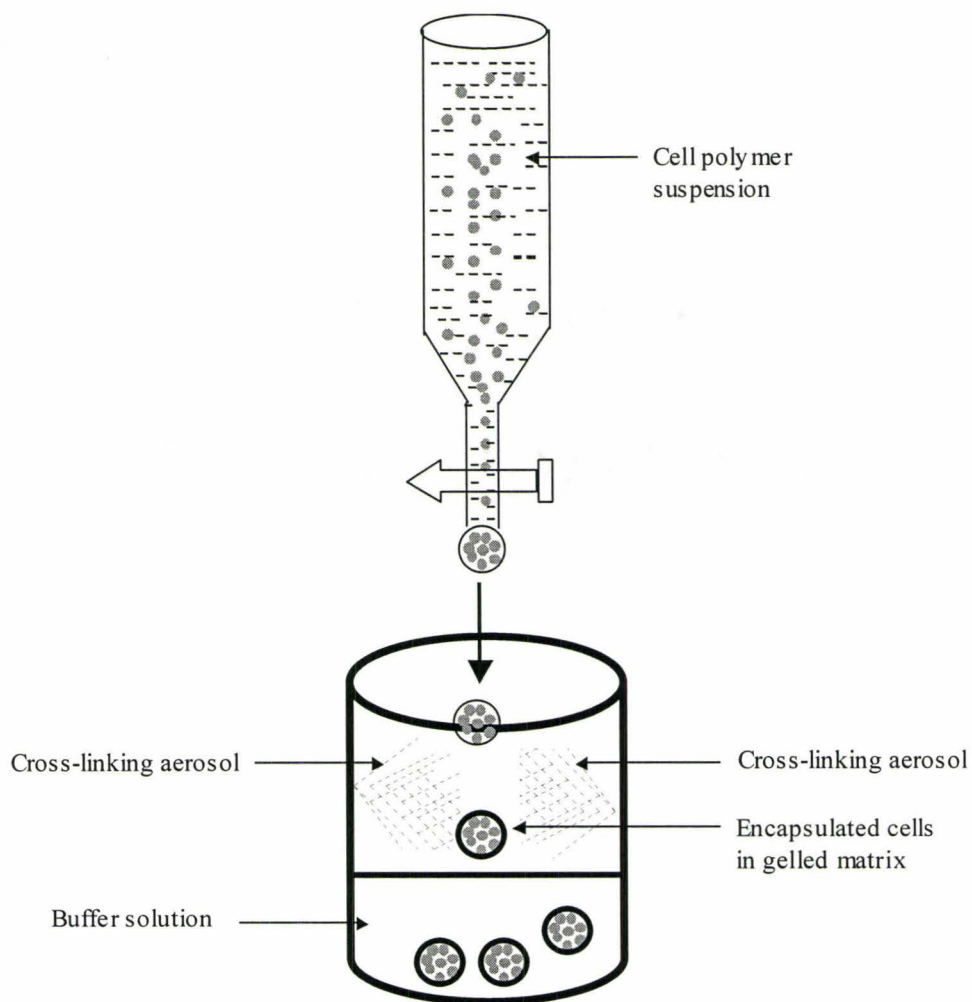


Figure 1.5: Schematic representation of encapsulation of cells using the spraying method.

1.5.5 Interfacial Reaction:

Interfacial reactions between polymers have been explored for cell encapsulation. Dautzenberg et al²³ described a method of microcapsule preparation by interfacial reaction that can be potentially used for microencapsulation of biological material. In this system, the aqueous solution of anionic polyelectrolyte is interfacially reacted with the

aqueous solution of cationic polyelectrolytes. The principle of microcapsules preparation by interfacial reaction is demonstrated in the following Figure 1.6.

This process often involves extruding the anionic polyelectrolyte/cell solution through a needle, and forms droplets. These droplets are then reacted in a precipitation bath with a suitable cationic polyelectrolyte, and form a microcapsule with a liquid core containing the cell. Several research groups successfully immobilized living cells and enzymes by this method without losing their biological activity.^{24, 25}

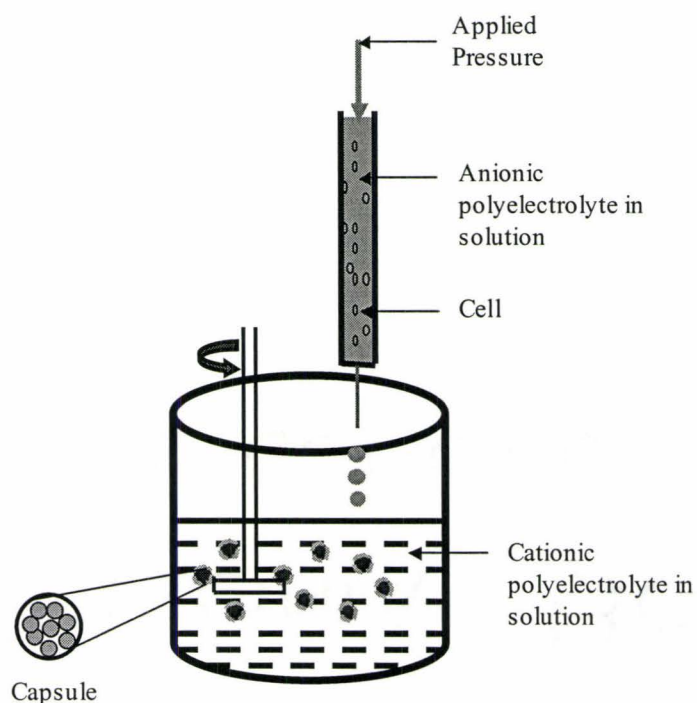


Figure 1.6: Schematic representation of microcapsule preparation by interfacial reaction.

Other methods can involve photosensitive polymers whereby cross-linking occurs and forms polymeric networks by exposure to UV light.²⁶ In interfacial photopolymerization method, photoinitiators are previously adsorbed onto the surface of

interest such as cells, tissue and polymeric surfaces, which is then exposed to the photo-polymerizable mixture and successively irradiated. This polymerization method can be used to form a thin layer or barrier of photo-polymerized materials around cells or groups of cells,^{26, 27} and has been used in drug delivery,²⁸ tissue engineering^{29, 30} and cell encapsulation.^{26, 31, 32, 33}

1.5.6 Layer- by- layer Method:

The layer-by-layer method of depositing polyelectrolytes on a range of surfaces, involves several sequential deposition steps of polyanions and polycations from dilute solution.^{34, 35} In this process, the cell suspensions are dipped into an oppositely charged polyelectrolyte for a certain period, and then washed with saline to remove untreated polyelectrolyte, followed by the oppositely charged polyelectrolyte.³⁶ The process is continued until the desired properties (capsules with well-controlled size and shape, finely tuned capsule wall thickness and variable wall compositions) are achieved. The schematic representation of the preparation process is shown in Figure 1.7.

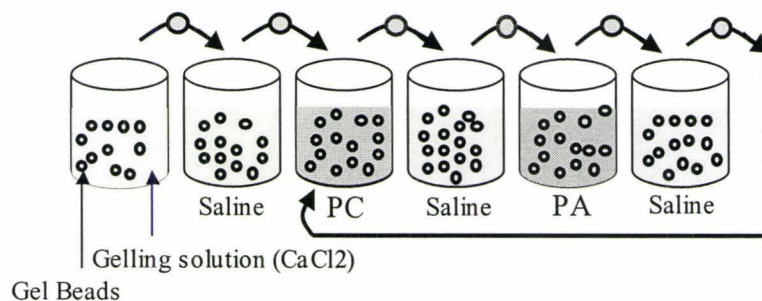


Figure 1.7: Schematic representation of the preparation process of layer-by-layer microcapsules. PC represents polycation; PA represents polyanion

Abstract

Polyelectrolyte complexes between poly(methacrylic acid, sodium salt) (PMAANa) and poly(diallyldimethylammonium chloride) (PDADMAC) or poly([2-(methacryloyloxy)ethyl] trimethylammonium chloride) (PMOETAC) are found to form gels, liquid phases or soluble complexes, depending on charge ratio, total polymer loading, polymer molecular weight, and ionic strength. Increasing the ionic strength of the medium led most polyelectrolyte pairs to transition from gel through liquid complexes (complex coacervate) to soluble complexes. These transitions shift to higher ionic strengths for higher molecular weight polymers, as well as for PMOETAC compared to PDADMAC. The complex phases swelled with increasing polymer loading, ultimately merging with the supernatant phase at a critical polymer loading. The isolated liquid complex phases below and above this critical loading were temperature sensitive, showing cloud points followed by macroscopic phase separation upon heating. Incorporating 5-mol% lauryl methacrylate (LMA) into the polyanion led to increased complex yield with PDADMAC, and increased resistance to ionic strength. In contrast, incorporating 30 mol% of oligo(ethylene glycol) methacrylate (PEGMA) into the polyanion led to decreased complex yield, and to lower resistance to ionic strength. Two polyelectrolyte systems that produced liquid complexes were used to encapsulate hydrophobic oils, and in one case were used to demonstrate the feasibility of cross-linking the resulting capsule walls.

2.1 Introduction

The interaction of oppositely charged polyelectrolytes to form polyelectrolyte complexes (PECs) is a topic of considerable interest^{1,2,3,4,5} stemming in part from the potential to use PECs in a wide variety of applications, including separation membranes,^{6,7} immobilization of enzymes⁸ or cells,⁹ drug carriers,¹⁰ gene delivery tools,^{11,12} and protein purification.¹³ PECs can come in the form of layer-by-layer (LBL) assemblies^{5,14,15,16,17,18,19,20,21} soluble complexes^{1,2, 22, 23} solid precipitates^{24, 25, 26} and liquid coacervates.^{27, 28, 29} Both the nature of the interactions and the nature of the PECs formed depend on variables such as charge ratio, ionic strength, pH, temperature, polymer concentration, charge density, molecular weight and polymer structure.^{1,2,3,4,5,27,28}

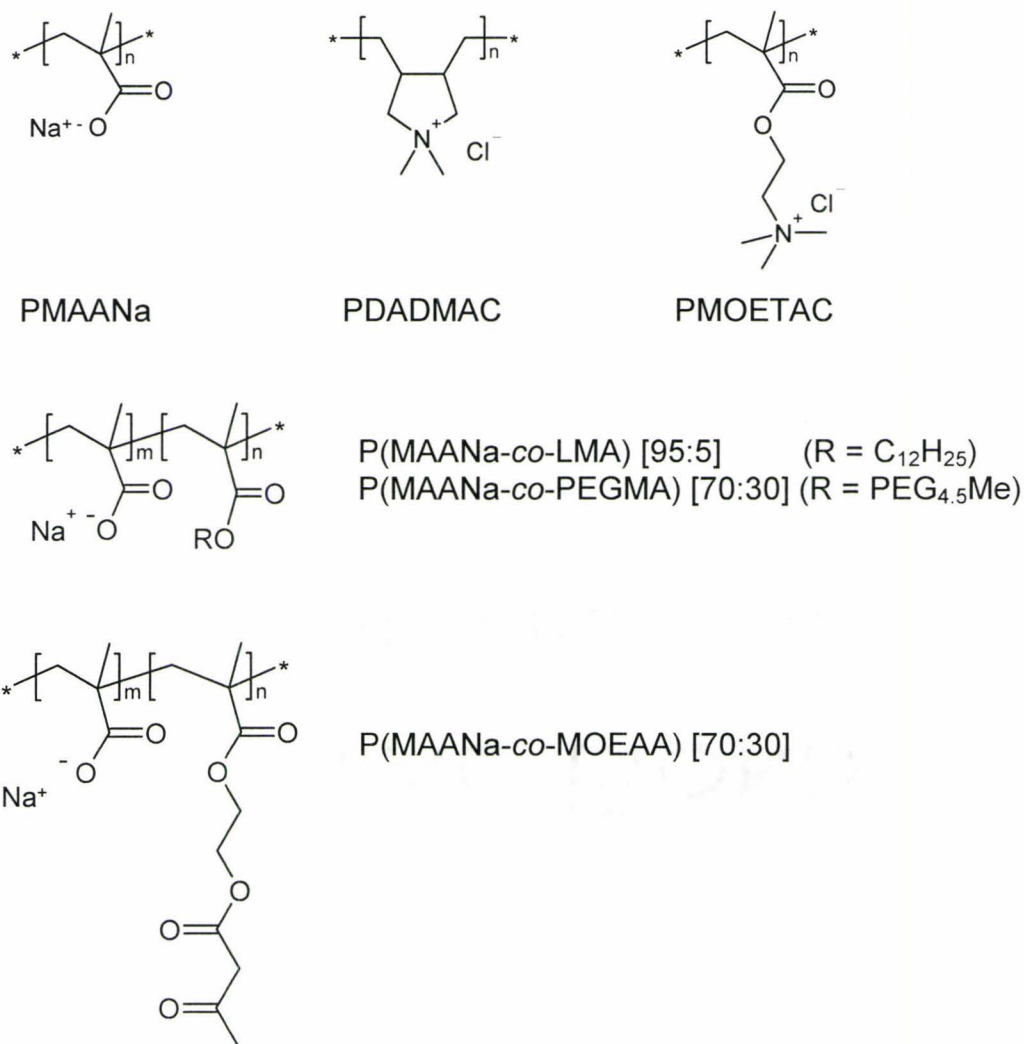
The deposition of PECs onto preformed particles or droplets often results in capsules where the polyelectrolyte coating may modify colloidal behaviour, protect the fill and control its release. Encapsulation with PECs is typically achieved by either LBL assembly or complex coacervation. LBL assembly, introduced by Decher,¹⁴ involves sequential deposition of polyanions and polycations, and allows excellent control of the thickness and composition of the layers.^{5, 21} Complex coacervation is a liquid-liquid phase separation brought about by charge neutralization between oppositely charged polyelectrolytes that yields two immiscible aqueous liquid phases. The denser, polymer-rich coacervate phase can deposit onto dispersed oils, solids or cells in a single step.^{30,31} The thickness of the resulting capsule walls depends on the ratio of coacervate to available surface area rather than on the number of layers deposited, and can reach several microns. A well-known example is the liquid complex coacervate formed upon

mixing aqueous solutions of gum acacia, a negatively charged polysaccharide derived from the acacia tree, with pig-skin derived gelatin, at pH = 4-5 and above the gel point of gelatin at 50 °C.^{32,33}

In some instances, especially liquid coacervates, it can be necessary to further harden the PECs to withstand chemical or mechanical challenges in subsequent use. In the case of gelatin/acacia, the liquid complex formed at 50 °C is initially gelled by cooling below 35 °C and often hardened by chemical cross-linking with glutaraldehyde or formaldehyde. Other PECs have been cross-linked by the addition of small-molecule crosslinkers,^{10,32,34} although this often links only one of the two polyelectrolytes. Reaction of polymer bound functional groups promoted by heating³⁵ or reagents such as carbodiimides,^{36,37,38} or by photochemical approaches^{39,40,41,42} have also been used. In some cases it might be desirable to employ polyelectrolytes bearing complementary functional groups for cross-linking, as this would lead to covalent incorporation of both polyelectrolytes, avoids exposure of the capsule fill to small-molecule additives, heat or light, and might reduce environmental risks associated with the use of small-molecule crosslinkers such as formaldehyde and glutaraldehyde.

Complex coacervates are most often based on natural polymers including gum acacia and gelatin, with source- dependent variation in their properties. We here choose synthetic methacrylates and DADMAC because of their easy of synthesis, stability, and the large body of existing knowledge regarding possible co-monomers, molecular weight control, and biomedical uses. Synthetic polyelectrolytes offer the ability to fine-tune key properties such as charge density, hydrophobic/hydrophilic balance, and molecular weights, and can introduce additional functionality through appropriate co-monomers.

We have previously investigated synthetic polymers including polyelectrolytes that undergo coacervation.⁴³ This paper describes our initial studies of such complexation, using three model polyelectrolytes, shown in Scheme 2.1, based on methacrylic acid (MAA), diallyldimethylammonium chloride (DADMAC) and [2-(methacryloyloxy)ethyl] trimethylammonium chloride (MOETAC). We examine how the physical nature of the complexes and the efficiency of complex formation are affected by ionic strength, charge ratio, polymer loading, polymer molecular weight, and hydrophobic or hydrophilic comonomers such as lauryl methacrylate (LMA) and poly(ethylene glycol) methyl ether methacrylate (PEGMA)]. Conditions under which liquid complex coacervates are formed are identified and some of the resulting complex coacervates are used to encapsulate hydrophobic oils. As well, the feasibility of cross-linking the resulting coacervate capsule walls via complementary polymer-bound reactive groups is investigated.⁴³ In the present work, polymer-bound acetoacetate groups, introduced via copolymerization of MAA with 2-(methacryloyloxy)ethyl acetoacetate (MOEAA), are used to react with polymer-bound amine groups in polyethyleneimine (PEI).



Scheme 2.1. Polyelectrolytes used in this study.

2.2 Experimental

2.2.1 Materials:

Methacrylic acid (MAA, 99%), 2-(methacryloyloxy)ethyltrimethylammonium chloride (MOETAC, 75 wt% solution), 2-(methacryloyloxy)ethyl acetoacetate (MOEAA,

95%), poly(ethylene glycol) monomethyl ether methacrylate (PEGMA, $M_n = 300$ Da), lauryl methacrylate (LMA, 96%), 2,2'-azobis(2-methylpropionamide) dihydrochloride (Vazo-56), methyl isobromobutyrate (MeiBrB, 99⁺%), cuprous chloride (99%), 2,2'-dipyridyl (99⁺%) and polyethyleneimine (PEI, $M_w = 2000$ Da) were purchased from Sigma-Aldrich Co. (Oakville, ON) and used as received. Azobis(isobutyronitrile) (AIBN) was received as a gift from Dupont and used as received. Poly(methacrylic acid, sodium salt) (PMAANa, $M_n = 5400$ Da; 30 wt% solution) and poly(diallyldimethylammonium chloride) (PDADMAC) with very low (40 wt% solution), low ($M_w \sim 100 - 200$ kDa; 20 wt% solution), and high ($M_w \sim 400 - 500$ kDa; 20 wt% solution) molecular weights were purchased from Aldrich and used as received. Ethyl ether, methanol, acetone, sodium chloride (Caledon Laboratories, Georgetown, ON), sodium sulfate (BDH, Toronto, ON) and ethanol (Commercial Alcohols, Brampton, ON) were used as received. Tetrahydrofuran (THF, Caledon Laboratories) was distilled over Na/K amalgam before use. HCl and NaOH solutions were prepared by diluting standard volumetric concentrates (Anachemia, Rouses Point, NY) with deionized water.

2.2.2 Low MW P(MOETAC):

Low MW PMOETAC was prepared by atom transfer radical polymerization using a method described in the literature.⁴⁴ CuCl (99 mg, 1.0 mmol) and 2,2'-bipyridine (390 mg, 2.5 mmol) were placed in a flask, which was sealed and flushed with nitrogen. MOETAC (8.3 g of 75 wt% solution, 6.22 g, 30 mmol), deionized water (2.1 mL) and isopropanol (3.7 mL) were mixed, bubbled with nitrogen for 20-30 min and then transferred via a double-tipped needle to the flask containing CuCl and bipyridine. The

mixture was stirred for 10 min to allow catalyst formation. Methyl isobromobutyrate (181 mg, 1.0 mmol) was dissolved in isopropanol (0.5 mL), and the mixture was bubbled with nitrogen for 5 min before being transferred via a double-tipped needle to the reaction flask. An exotherm was detected upon the addition of the initiator and within one hour, the reaction mixture had become a viscous slurry. The reaction was stopped after two hours by exposing it to air. A small sample was removed, dried under a stream of air, dissolved in D₂O and analyzed by ¹H NMR to determine monomer conversion. Water (~10 mL) was added to the remainder of the reaction mixture to produce a homogeneous solution. The reaction mixture was then dialyzed against deionized water using cellulose tubing with a 3.5 kDa MW cut-off and freeze-dried. Yield: 5.42 g (85%).

2.2.3 PMOETAC-770:

MOETAC (10.00 g, 48.1 mmol) and Vazo-56 (0.131 g, 0.48 mmol) were dissolved in 90 mL water in a 125 mL HDPE bottle. The solution was bubbled with nitrogen for several minutes before the bottle was sealed. The bottle was placed in an oven and heated from 25 to 60 °C during 1 h, and then maintained at 60 °C for 23 h. The bottles were slowly rotated (4 rpm) in the oven to provide mixing. The polymer was isolated and purified by precipitation in acetone or by dialysis (3.5 kDa MW cut-off) followed by freeze-drying. The purified polymer was then dried to a constant weight in a vacuum oven at 50 °C. Yield: 9.1 g (91 %).

2.2.4 PMOETAC-300:

PMOETAC-300 was prepared in a similar fashion except that 2 mol% of Vaso-56 was used.

2.2.5 P(MAA-co-LMA):

MAA (8.65 g, 100.5 mmol), LMA (1.35 g, 5.29 mmol) and AIBN (174 mg, 1.1 mmol, 1 mol%) were dissolved in THF/EtOH (1:1, 90 mL) in a 125 mL HDPE bottle. The solution was degassed and heated as described above for PMOETAC-770. The polymer was precipitated in ether (1 L), washed with ether and then dried to a constant weight in a vacuum oven at 50 °C. P(MAA-co-LMA)[95:5] was obtained as a white powder in a yield of 9.63 g (96 %).

2.2.6 P(MAA-co-PEGMA):

Polymerization and isolation were conducted in a similar fashion. MAA (4.01 g, 46.6 mmol), PEGMA (5.99 g, 20.0 mmol) and AIBN (109 mg, 0.67 mmol, 1 mol%) were heated in THF/ethanol (1:1, 90 mL), followed by precipitation in ether, to give 8.36 g (84%) P(MAA-co-PEGMA)[70:30].

2.2.7 P(MAA-co-MOEAA):

Polymerization and isolation were conducted in a similar fashion. MAA (4.84 g, 56.2 mmol), MOEAA (5.43 g, 24.1 mmol) and AIBN (132 mg, 0.80 mmol, 1 mol%) were heated in ethanol (100 mL), followed by precipitation in ether, to give 8.74 g (87%) P(MAA-co-MOEAA)[70:30].

2.2.8 Characterization:

The composition of the P(MAA-*co*-MOEAA), P(MAA-*co*-PEGMA) and P(MAA-*co*-LMA) polymers was determined by ^1H nuclear magnetic resonance (NMR) spectroscopy using a Bruker AV 200 spectrometer for polymers dissolved in DMSO- d_6 .

Size exclusion chromatography (SEC) was conducted with a system consisting of a Waters 515 HPLC pump, Waters 717 plus Autosampler, three columns (Waters Ultrahydrogel-120, -250, -500; 30 cm \times 7.8 mm; 6 μm particles) and a Waters 2414 refractive index detector, and was calibrated with narrow molecular weight poly(ethylene glycol) standards (Waters). The P(MAA-*co*-MOEAA) and P(MAA-*co*-LMA) samples were neutralized with 1 M NaOH prior to SEC analysis with 0.3 M NaNO_3 in 0.1 M phosphate buffer at pH 7 as the eluent.

Viscometry, conducted with an Ubbelohde viscometer (viscometer constant: 0.00314 cSt/s), was used to measure molecular weights of PMOETAC samples dissolved in 1 M NaCl at 20 ± 0.1 $^\circ\text{C}$. All solutions were passed through 0.45 μm Acrodisc (Supor membrane, Pall Corp.) filters before measurement. The intrinsic viscosity $[\eta]$ was calculated by a double extrapolation of the Huggins plot (η_{sp}/c vs. c) to infinite dilution. The polymer molecular weights were calculated from the intrinsic viscosity using values for K and a found in the literature.⁴⁵

Optical microscope images of complexes and capsules were taken using an Olympus BX51 optical microscope fitted with a Q-Imaging Retiga EXi digital camera and ImagePro software or an Olympus BH-2 optical microscope fitted with Kodak DC120 digital camera and software.

2.2.9 Coacervation Efficiency:

Solutions (typically 15.00 g) of PMAANa, PDADMAC, or PMOETAC at the appropriate concentration and ionic strength were mixed in a pre-weighed 50 mL polyethylene centrifuge tube. The solutions were mixed several times on a vortex mixer and allowed to stand. The mixture was centrifuged and the supernatant decanted or transferred by pipette to a pre-weighed, polystyrene weighing-dish. The centrifuge tube was weighed to determine the wet complex yield, and then both the complex and supernatant were dried to constant weight by heating at 65 °C. The dried complex and dried supernatant were weighed to determine the polymer content in the two phases.

2.2.10 Encapsulation:

An oil-in-water emulsion was prepared by dispersing methyl benzoate (0.5 mL) in 10 mL of 1.31 % w/v PMOETAC-300 containing 325 mM NaCl with an overhead stirrer (800 rpm) for 30 minutes at room temperature (20 °C). To this mixture, an aqueous solution of PMAANa (10 mL, 0.69 % w/v, 325 mM NaCl) was added drop-wise, and the mixture was stirred for an additional 30 minutes before a sample was removed for examination by optical microscopy.

2.2.11 Encapsulation and Crosslinking:

An oil-in-water emulsion was prepared by dispersing paraffin oil (0.5 mL) in 10 mL of 1.31 % w/v PMOETAC-300 containing 375 mM NaCl (pH 7) with an overhead stirrer (800 rpm) for 30 minutes at room temperature (20 °C). To this mixture, 10 mL of a

1.32% w/v solution of P(MAANa-co-MOEAA)[70:30] (1.05 eq of anions) containing 375 mM NaCl (pH 7) was added drop-wise. The mixture was stirred for an additional 30 minutes before 1.4 g of a 2 wt% PEI solution (pH 10.5) was added and stirring was continued for 3 h at room temperature.

2.3 Results and Discussion

Complexation studies were focused on interactions between pairs of homopolymers, PMAANa / PDADMAC and PMAANa/PMOETAC. The PMAANa employed in this work had a molecular weight (M_n) of 5.4 kDa. Three types of commercial PDADMAC from Aldrich were used. Two of these have molecular weights described by Aldrich as low ($M_w \sim 150$ kDa), and high ($M_w \sim 450$ kDa), and are denoted as PDADMAC-150, and -450, respectively, in this article. The molecular weight of the third PDADMAC sample (PDADMAC-20) has been determined to be 20 kDa by viscometry.⁴³

Two PMOETAC samples, PMOETAC-770 and PMOETAC-300, were prepared by free radical polymerization in water initiated with 1 and 2 mol% Vazo-56. Their molecular weights were measured by viscometry, using 1 M NaCl to suppress coil-expansion with dilution,⁴⁶ and were found to be $M_n = 770$ and 300 kDa, respectively. A third sample, PMOETAC-13, was prepared by atom transfer radical polymerization (ATRP) initiated with methyl isobromobutyrate (Me*i*BrB) in isopropanol/water (1:1 v/v).⁴⁴ After 2 hours polymerization time, the conversion was determined to be 98% by ¹H NMR. Both ¹H NMR and viscometry were used to determine the molecular weight of the purified polymer. Comparison of the peak area of the signal due to the methoxy

group, derived from the Me₂BrB initiator, with those due to MOETAC in the ¹H NMR spectrum, gave a number-average molecular weight of $M_n = 6$ kDa. Viscometry in 1 M NaCl gave a viscosity-average molecular weight of $M_\eta = 13$ kDa.

Copolymers of MAA with MOEAA, PEGMA or LMA were prepared by AIBN-initiated free radical polymerization in ethanol or THF/ethanol mixtures. P(MAA-*co*-MOEAA)[70:30], P(MAA-*co*-PEGMA)[70:30], P(MAA-*co*-LMA)[95:5] were determined to have compositions of [67:33], [68:32] and [93:7], respectively, by ¹H NMR. Thus, the compositions closely mirrored the co-monomer feed ratios. This included samples removed at lower conversions (~30%) indicating that there is no drift in copolymer composition during polymerization. P(MAA-*co*-MOEAA) and P(MAA-*co*-LMA) were found to have molecular weights (M_n) of 42 and 7.1 kDa, respectively, by aqueous SEC. Polyanion solutions were prepared from the MAA copolymers by the addition of stoichiometric amounts of a 1.000 M NaOH solution.

2.3.1 Nature of the Complexes of PMAANa with PDADMAC-20, PDADMAC-450 and PMOETAC-300:

Aqueous solutions of PMAANa were combined with solutions of PDADMAC-20, PDADMAC-450 or PMOETAC-300 to obtain mixtures with a 1:1 charge ratio and a total polymer concentration of 1 wt%. In each case, phase separation occurred immediately to form polyelectrolyte complexes (PECs). The PMAANa / PDADMAC-20 complex formed a separate liquid complex coacervate layer, which could be easily redispersed by shaking (Figure 2.1a).

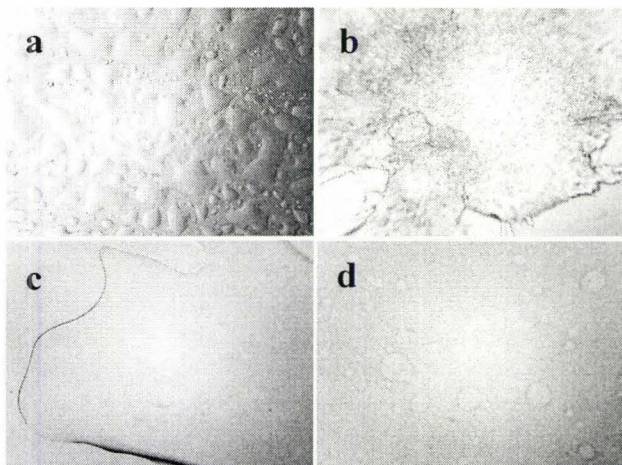


Figure 2.1: Optical microscope images of polyelectrolyte complexes: a) liquid complex coacervate PMAANa/PDADMAC-20 (no added NaCl). b) – d) PMAANa / PMOETAC-300, in presence of b) 200 mM, c) 300 mM and d) 400 mM added NaCl. All complexes were formed by combining the polyelectrolytes in ratios that result in 1 wt% total polymer loading with 1:1 charge ratios. Width of each image is 5 mm.

The analogous PMAANa complex with the higher molecular weight PDADMAC-450 formed a stiff gel, which turned into a liquid coacervate in presence of 300 mM NaCl due to partial shielding of the electrostatic interactions. Similar behaviour is seen for the PMAANa / PMOETAC-300 complex (Fig. 2.1, b-d), which is transformed from an opaque gel to a liquid complex coacervate as the salt concentration was increased from 200 mM (Fig. 2.1b) to 300 mM (Fig. 2.1c) to 400 mM NaCl (Fig. 2.1d). The coacervate phase disappears entirely in the presence of 500 mM NaCl.

2.3.2 Factors Affecting Complexation Efficiency:

As the above results illustrate, polyelectrolyte complexation may be effected by polymer properties and complexation conditions.^{22,27,28,47,48,49} Therefore, a quantitative

study was undertaken to examine the role of polymer concentration, charge ratio, ionic strength and polymer molecular weight on the complexation of PMAANa with either PDADMAC or PMOETAC. Polyanion and polycation solutions were combined to give polyelectrolyte complexes over a range of polymer concentration, charge ratio and ionic strength. The phase-separated complexes were isolated from the supernatant and immediately weighed to determine the yield of the hydrated complex. Both the supernatant and the complex were then dried to determine the amount of polymer (and NaCl) present in each phase. The relative amounts of polymer and water within the complex were obtained by comparison of the weights before and after drying. The expressions used to describe complex formation are shown below:

$$\text{Complex yield} = \frac{\text{wt. of complex} \times 100\%}{\text{total wt. of solution}}$$

$$\text{Complexation efficiency} = \frac{\text{wt. of dry complex} \times 100\%}{\text{total polymer loading}}$$

$$\text{Polymer fraction in complex} = \frac{\text{wt. of dry complex} \times 100\%}{\text{wt. of complex}}$$

The recovery of material was quantitative in all experiments: $103 \pm 3\%$ for PMAANa/PDADMAC-20 samples and $98 \pm 3\%$ for PMAANa/PMOETAC-300 samples,

for example. For samples containing added NaCl, the values measured for complexation efficiency and polymer fraction have been corrected for the presence of the added NaCl in the complex, with the assumption that the NaCl is equally distributed between the complex and supernatant phases.

2.3.3 Charge ratio:

The formation of PECs is normally maximized at a 1:1 ratio of anionic to cationic groups. Indeed, the yield and efficiency of complexation between PMAANa and either PDADMAC-20 or PMOETAC-300 were greatest at a 1:1 charge ratio (Figures 2.2 and 2.3).

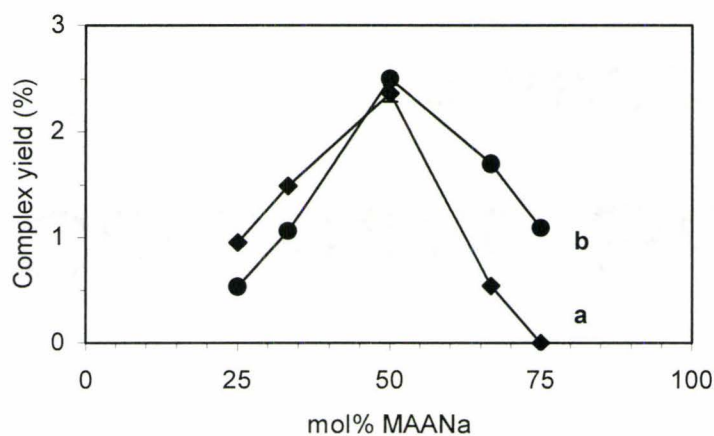


Figure 2.2: Complex yield as a function of the charge ratio, for complexes formed between PMAANa and a) PDADMAC-20 or b) PMOETAC-300. Total polymer loading is 1 wt%, with no added NaCl.

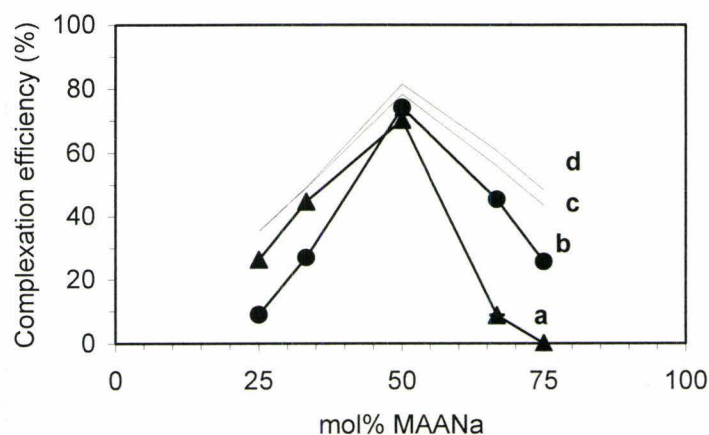


Figure 2.3: Complexation efficiency as a function of the charge ratio for complexes formed between PMAANa and a) PDADMAC-20 or b) PMOETAC-300. Total polymer loading was 1 wt%, with no added NaCl. Also shown are the two curves for efficiency, expected if there were quantitative formation of a 1:1 complex and complete loss of associated Na^+ and Cl^- ions – c) PDADMAC-20 and d) PMOETAC-300.

At 1:1 charge ratio, the observed complexation efficiencies of 70 % for PDADMAC-20 and 74 % for PMOETAC-300, correspond reasonably well to the values expected after accounting for the loss to the supernatant of up to 21.7 wt% (PDADMAC) and 18.5 wt% (PMOETAC) of the total polyelectrolyte weights as NaCl generated during complexation. Figure 2.3 shows that the complexation efficiency falls further below the theoretical at non-stoichiometric charge ratios, especially in presence of excess polyanion. This is likely due to the formation of some fraction of colloiddally stable complex.

2.3.4 Ionic Strength:

Ionic strength is known to strongly affect polyelectrolyte complexation.^{22,27,28,47,48} For soluble complexes, typically formed at low polyelectrolyte concentrations and a non-stoichiometric mixing ratio, small increases in ionic strength often cause a reduction in hydrodynamic radius due to shielding of the charges of the excess polyelectrolyte within individual complex particles. This can also reduce repulsive interactions between colloidal particles, and hence facilitate aggregation and macroscopic phase separation. On the other hand, large increases in ionic strength can lead to shielding of opposite charges within the complexes, causing swelling and even dissolution of the complex. For example, the coacervation efficiency of gum acacia / gelatin complexes at a 1:1 charge ratio and 0.5%(w/v) total polymer loading was zero in the absence of added salt, increased to >80% upon addition of ~1mM NaCl and then returned to zero as the ionic strength reached 10 mM.²⁸

Thus, it is possible to control both the efficiency of complexation and the physical nature of the complex (solid, gel, liquid, soluble) by varying the ionic strength. The systems studied in this work lie at different points along the continuum between solid and soluble complexes, and the ability to use ionic strength to shift between solid and liquid complex may be of significant use in encapsulation. Indeed, as shown in Figure 2.1 above, raising the ionic strength from 0 to 400 mM caused the PMAANa/PMOETAC-300 complex to change from a gel to a liquid, while the PMAANa/PDADMAC-20 complex was converted from a liquid to a soluble complex. Below we explore the effect on complexation and complex properties, by varying the ionic strength through added salt and polymer loading.

The effect of added NaCl on the yield of complexes between PMAANa and PDADMAC-20, -150, -450 and PMOETAC-13 and -300 is displayed in Figure 2.4. The complex yield for 1 wt% total polymer loading in the absence of added NaCl is nearly identical ($2.40 \pm 0.05\%$) for four of the systems, while that for PMAANa/PMOETAC-13 (curve d, Figure 2.4) is slightly lower (2.1%). The complex yield increases as NaCl is added for all of the systems, and is most pronounced for the higher MW polycations. The complex yield for PDADMAC-450, the polycation with the highest MW, more than doubles in 350 mM NaCl. In each case, the yield reaches a maximum and then drops sharply to zero as the complex phase dissolves. The ionic strength required to dissolve the complexes is higher for polymers with higher MW (compare curves a and c, or d and e). For polymers with comparable MWs, it is higher for PMOETAC than PDADMAC (compare curves a and d, or c and e). It has been reported that PMAANa/PDADMAC complexes made from polymers with MWs of 114 and 250 kDa, respectively, underwent dissolution at about 500 mM NaCl consistent with the results in the present work for a PMAANa with a much lower MW.⁴⁷

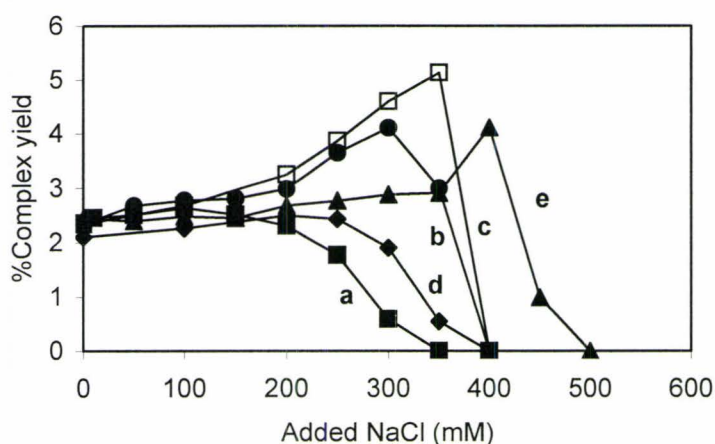


Figure 2.4: Complex yield as a function of ionic strength for PMAANa complexation with a) PDADMAC-20 or b) PDADMAC-150, c) PDADMAC-450 d) PMOETAC-13 or e) PMOETAC-300. 1:1 Charge ratio, 1 wt% polymer loading.

At low ionic strengths, all five of the PECs show complexation efficiencies (Figure 2.5), i.e. the fraction of the initial polyelectrolyte loading contained within the complex, near the values expected for complete polyanion/polycation complexation and loss of associated Na^+ and Cl^- counter ions. Unlike the complex yield, the complexation efficiency does not rise appreciably with ionic strength, and even decreases at ionic strengths corresponding to maximum yields. The complexation efficiency results also show the greater resistance to ionic strength of complexes made from higher MW polymers, or from PMOETAC rather than PDADMAC.

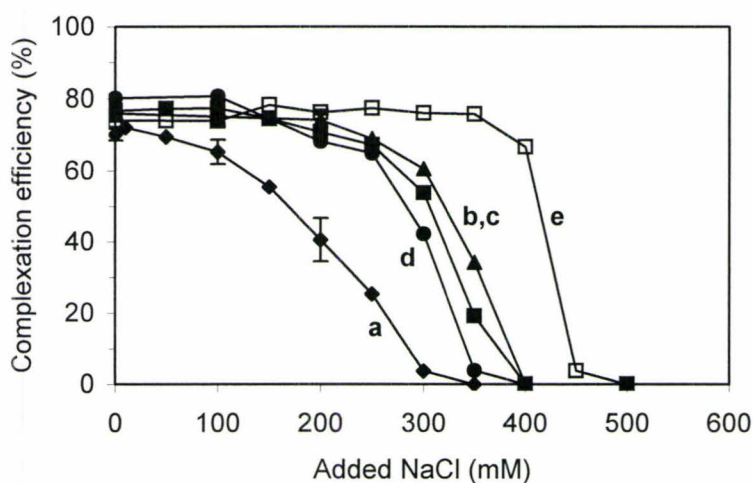


Figure 2.5: Complexation efficiency as a function of ionic strength for complexation of PMAANa with a) PDADMAC-20 or b) PDADMAC-150, c) PDADMAC-450, d) PMOETAC-13 or e) PMOETAC-300. 1:1 Charge ratio, 1 wt% polymer loading.

The effect of ionic strength on the polymer weight fraction in the complex phases is shown in Figure 2.6. In the absence of added NaCl, four of the complex phases have polymer fractions close to 30%, while PMOETAC-13 (Fig. 2.6d) surprisingly shows the highest polymer fraction (38%). Increasing ionic strength causes a weakening of the electrostatic interactions between the chains and allows the complexes to swell. This swelling increases the complex yield but decreases the polymer fraction in the complex phase. All of the complexes show a steady decrease in polymer fraction as the ionic strength is increased. The complex made with PDADMAC-20 shows little change in complex yield between 0 and 150 mM NaCl, while the complexation efficiency and polymer fraction are steadily dropping in this range. This reveals that any swelling of this complex with increasing ionic strength is offset by the dissolution of some of the chains, plausibly those of lower molecular weight. The complexes made with polycations of higher MW have more electrostatic interactions per chain and thus higher ionic strength is needed to dissolve the complexes. The greater resistance to dissolution of the PMAANa/PMOETAC complexes may be a result of more efficient complexation due to the greater accessibility of the ammonium ions borne on the side chain in PMOETAC compared to the main chain of PDADMAC.

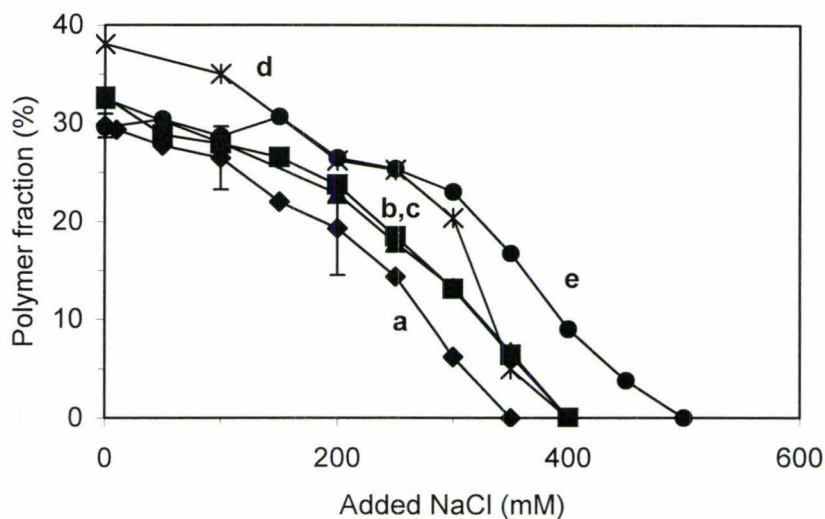


Figure 2.6: Polymer fraction in the complex phase as a function of ionic strength for complexation of PMAANa with a) PDADMAC-20 or b) PDADMAC-150, c) PDADMAC-450, d) PMOETAC-13 or e) PMOETAC-300. 1:1 Charge ratio, 1 wt% polymer loading.

The effect of ionic strength on complexes formed at non-stoichiometric charge ratios was also examined. The complexation efficiency for a PMAANa/PMOETAC-300 complex prepared at a 1:1 charge ratio (50 mol% MAANa) rose only slightly when the ionic strength was raised from 0 to 300 mM (curve e, Figure 2.5). However, there is a more dramatic increase in efficiency for non-stoichiometric mixing ratios (Figure 2.7). For example, the efficiency at a 3:1 ratio (75 mol% MAANa) is doubled from 23.8% at 0 mM to 49-51% in the presence of 100 to 300 mM NaCl. For all non-stoichiometric ratios at $I = 300$ mM, the efficiency nears or exceeds the value expected for quantitative formation of a 1:1 complex and loss of the associated small ions (NaCl). As mentioned, increased ionic strength can allow rearrangement of non-stoichiometric soluble

complexes and reduction of the colloidal stability of the initially formed complexes, both of which can lead to greater amounts of macroscopic phase separation. Complexation efficiencies slightly in excess of the “maximum” line in Figure 2.7 may result from the presence of small ions and/or more than one equivalent of the excess polyelectrolyte within the complexes. The complex yield and complexation efficiency for non-stoichiometric PMAANa/PDADMAC-20 complexes was also found to increase in the presence of 100 mM NaCl (data not shown).

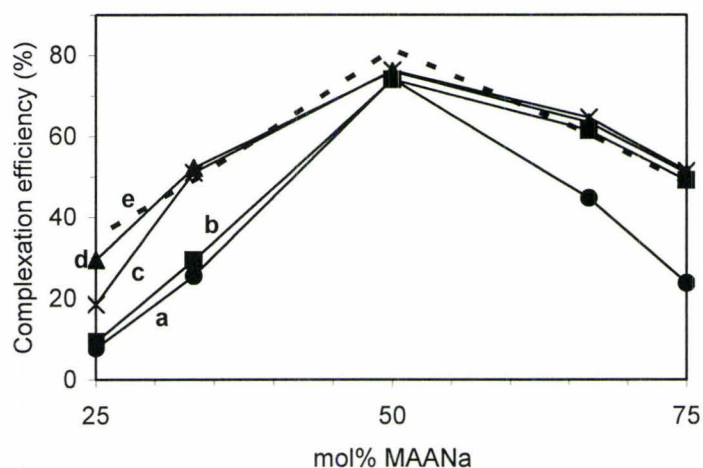


Figure 2.7: The effect of ionic strength on PMAANa/PMOETAC-300 complexation efficiency at various charge ratios for 1 wt% polymer loading. Added NaCl: a) 0 mM, b) 100 mM, c) 200 mM and d) 300 mM. Also shown is the curve (e) for “maximum” efficiency if there were quantitative formation of 1:1 complex and loss of associated small ions (NaCl).

2.3.5 Polymer loading:

The total polyelectrolyte concentration also plays an important role in complexation. Low polyelectrolyte loadings often result in soluble complexes with little or no macroscopic phase separation. Phase separation becomes dominant at higher concentrations, but at still higher polymer concentrations, phase separation can disappear. The range of polymer concentrations in which phase separation is observed, depends on factors such as the nature and MW of the polyelectrolytes, temperature and the contribution to ionic strength, I , due to small ions. For gelatin/acacia at a 1:1 charge ratio and $I = 0$, coacervation was observed only when the total polyelectrolyte concentration was between 0.5 and 14% (w/v).²⁸ In a study closely related to the present one, the complexation of PDADMAC and poly(acrylic acid, sodium salt) was examined as a function of mixing ratio, total polymer concentration and polymer MW.^{50,51} For most of the MWs studied, phase separation was observed at polymer concentrations up to about 13.2%, and then disappeared to give a macroscopically homogeneous one-phase system. The transition to a one-phase system was thought to be due to reaching a critical ionic strength for this polyelectrolyte pair.

The effect of polymer loading was explored here for complexes formed by PMAANa with PDADMAC or PMOETAC of different MW. At lower polymer loadings (<5% wt%), the complex yields increase with loading and were independent of polycations (Figure 2.8). Each of the systems exhibited upward curvature of the yield versus loading plot, without a corresponding increase in complexation efficiency (data not shown). For PDADMAC-20 and -450, an increase in loading from 1 to 8% causes 11- and 20-fold increases in complex yield, respectively, while the complexation efficiency

either drops (from 70 to 57% for PDADMAC-20) or shows only a small increase (76 to 82% for PDADMAC-450). Thus, the dramatic increase in complex yield at higher loading is due to swelling of the complexes. The most pronounced increase in complex yield with loading is seen for the PMAANa/PDADMAC- 450 system, the system that had shown the greatest swelling in response to added NaCl (Figure 2.4).

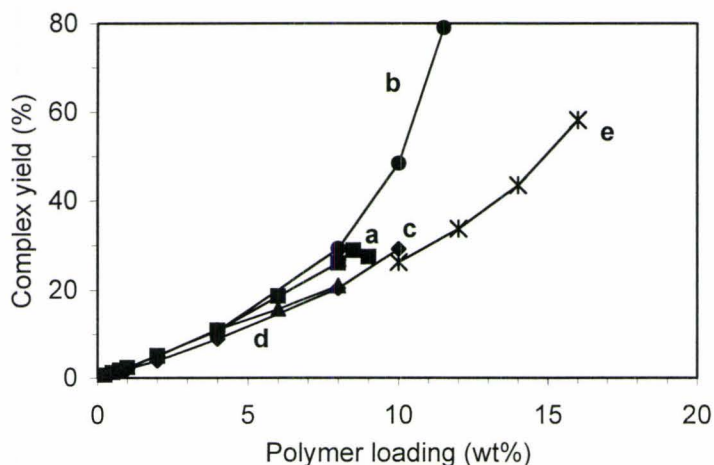


Figure 2.8: Complex yield as a function of total polymer loading for complexation of PMAANa with a) PDADMAC-20, b) PDADMAC-450, c) PMOETAC-13, d) PMOETAC-300 and e) PMOETAC-770. Charge ratio = 1:1, no added NaCl.

Figure 2.9 shows that polymer content in the complex and supernatant phases rapidly converges as the total polymer loading approaches the critical value of 9.5 wt% for PMAANa / PDADMAC-20, or 12 wt% for PMAANa / PDADMAC-450, where visible phase separation disappears (dashed line, Figure 2.9). These critical polymer concentrations for transition to a macroscopic one-phase system are somewhat lower than the 13.2 wt% observed for the closely related poly(acrylic acid, sodium salt)/PDADMAC system^{50,51} likely because of the low MW of PMAANa (5.4 kDa). In approaching the critical loading, the PDADMAC- 450 complex yields continues to increase while the

complex yield for the PDADMAC-20 complex plateaus, as it more easily dissolves in the supernatant. At 9 and 11.5 wt% loading, the highest loadings to show phase separation for PDADMAC-20 and -450, respectively, both complex phases have polymer fractions of 14%. However, only 44% of the total polymer, most likely the higher MW fraction, is in the PDADMAC-20 complex compared to 92% for PDADMAC-450. Similar behavior was observed for these two systems in response to added salt (Figures 2.4-2.6). The curves for PMOETAC (Fig. 2.9, curves c, d, e) suggest the presence of a critical polymer loading closer to 20 wt%.

The decreasing polymer fraction in the complex leads to a corresponding decrease in the viscosity of the complex phase, similar to the effects seen for addition of NaCl. For example, the PMAANa/PDADMAC- 450 complexes gradually change from a gel to a free flowing liquid coacervate as the loading is increased from 1 to 11.5 wt%.

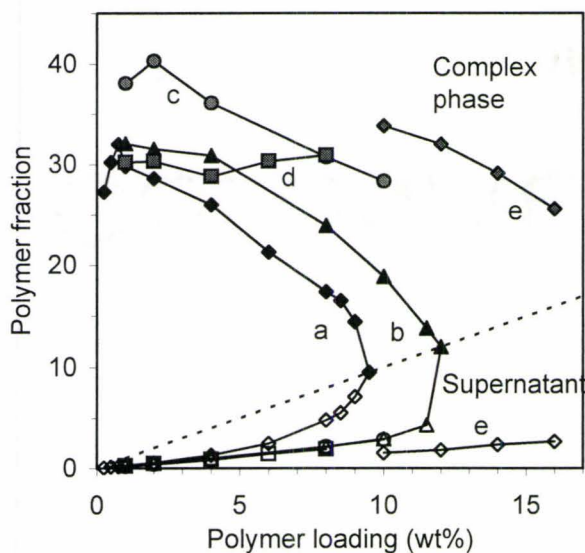


Figure 2.9: The polymer fraction in the complex (closed symbols) and the supernatant (open symbols) as a function of the total polymer loading for complexation of PMAANa

with a) PDADMAC-20, b) PDADMAC-450, c) PMOETAC-13, d) PMOETAC-300 and e) PMOETAC-770. Charge ratio = 1:1.

Complex phases near their critical loading were also found to exhibit a dramatic temperature sensitivity. For instance, the PMAANa/PDADMAC-450 complex phase formed at 20 °C and 11.5 wt% total polymer loading was separated from the supernatant and then heated in a sealed tube. The clear liquid complex turned cloudy nearly immediately and when left overnight at 62 °C, separated into two layers with relative volumes of complex: supernatant ~ 60:40. The more concentrated complex phase was noticeably more viscous even at 62 °C than the initial complex at 20 °C. Similarly, the PMAANa/PDADMAC-20 solution formed at 9.5 wt% loading showed no phase separation at room temperature but separated into two phases with relative volumes of complex:supernatant of approximately 25:75 when heated to 62 °C. Figure 2.10 below illustrates the increasing phase separation upon heating of solutions containing 11.5 and 12 wt% PMAANa/PDADMAC-450, respectively.

Dissolution or hydration of the complexes exposes more hydrophobic portions of the polymer chains to water. The entropic penalty associated with hydrating these hydrophobic portions is greater at higher temperatures and the system responds by undergoing phase separation and dehydration, presumably to allow some of the hydrophobic groups to associate with each other. Temperature has been seen to affect complexation in other studies but the nature of this effect depends strongly on the system being studied. The yield of gelatin/albumin coacervation was increased at lower temperatures presumably because higher temperatures caused the loss of some electrostatic interactions.²⁸ Conversely, soluble complexes made from PDADMAC and

PMAANa where the polyelectrolytes bore poly(ethylene glycol) grafts or blocks exhibited cloud points, and in some cases macroscopic phase separation, when heated.⁵² The temperature induced phase separation of the polyelectrolyte complexes examined in the present work might be useful in applications such as encapsulation, or purification via complexation.

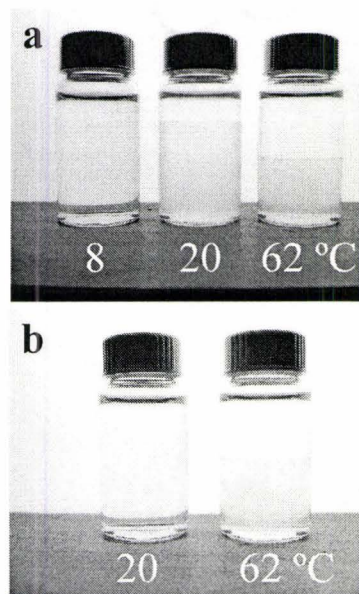


Figure 2.10: The effect of temperature on the PMAANa/PDADMAC-400 complexes formed at a) 11.5 wt% and b) 12 wt% total polymer loading.

2.3.6 The Effect of Co-Monomers:

The nature of the complex and the efficiency of complexation are also influenced by the composition of the polyelectrolytes. Polymer properties such as charge density, hydrophobic/hydrophilic balance and molecular weight can all be controlled through the selection of co-monomers and polymerization conditions. In addition, it may be possible

to adjust complex properties such as the colloidal stability or binding to surfaces through the introduction of appropriate chemical groups.

Two polyanions of differing hydrophobic/hydrophilic balance were prepared by free radical copolymerization of methacrylic acid (MAA) with either 5 mol% lauryl methacrylate (LMA) or 30 mol% poly(ethylene glycol) methyl ether methacrylate (PEGMA). Following isolation and characterization of the copolymers, the MAA in the copolymers was neutralized by the addition of NaOH to give the two polyanions, P(MAANa-co-LMA)[95:5] and P(MAANa-co-PEGMA)[70:30]. In Figures 2.11 and 2.12, the complex yields and complexation efficiencies of these copolymers is compared with those of the parent polyanion, PMAANa. The polyanion containing 5 mol% of the hydrophobic LMA shows slightly higher yield and efficiency than the parent PMAANa over the range of ionic strengths and polymer loadings investigated. The polyanion that bears the uncharged, hydrophilic PEG groups shows much lower efficiency than the other two polyanions and no complex is formed when the ionic strength is increased by the addition of 100 mM NaCl or by raising the polymer loading to 4 wt%. The presence of PEG side chains has been shown previously to enhance the colloidal stability of soluble polyelectrolyte complexes and hinder macroscopic phase separation.^{52,53,54}

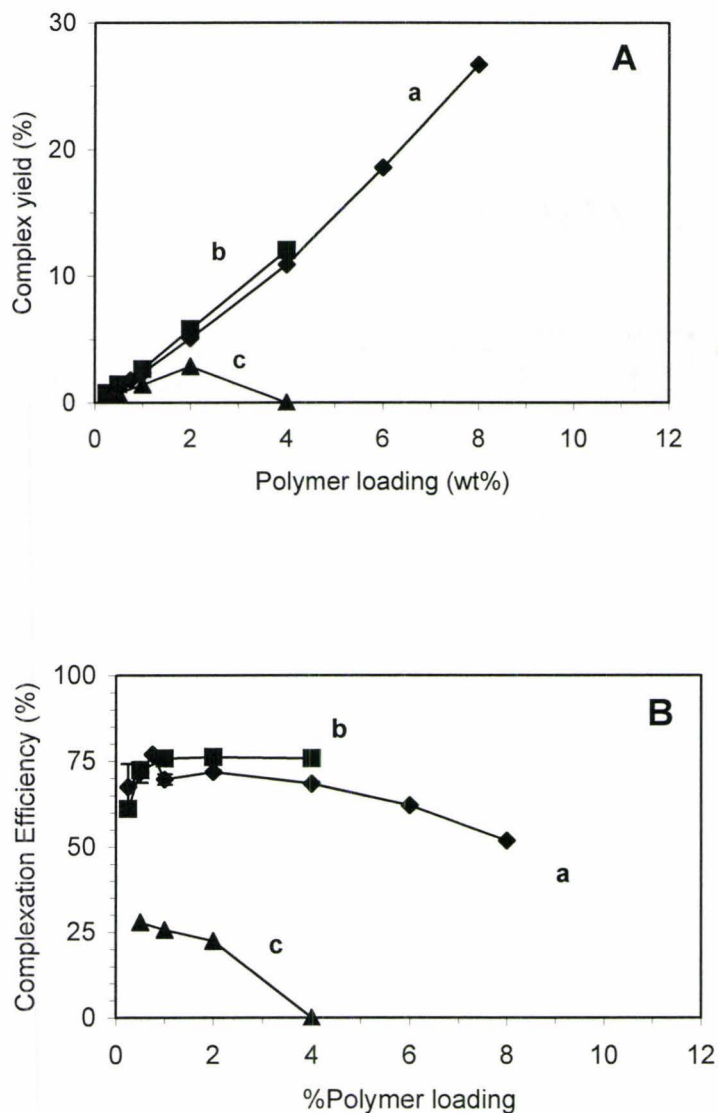


Figure 2.11: The effect of total polymer loading (wt%) on the A) complex yield and B) complexation efficiency for the complex formed between PDADMAC-20 and a) PMAANa, b) P(MAANa-LMA)[95:5] and c) P(MAANa-PEGMA)[70:30]. Charge ratio = 1:1.

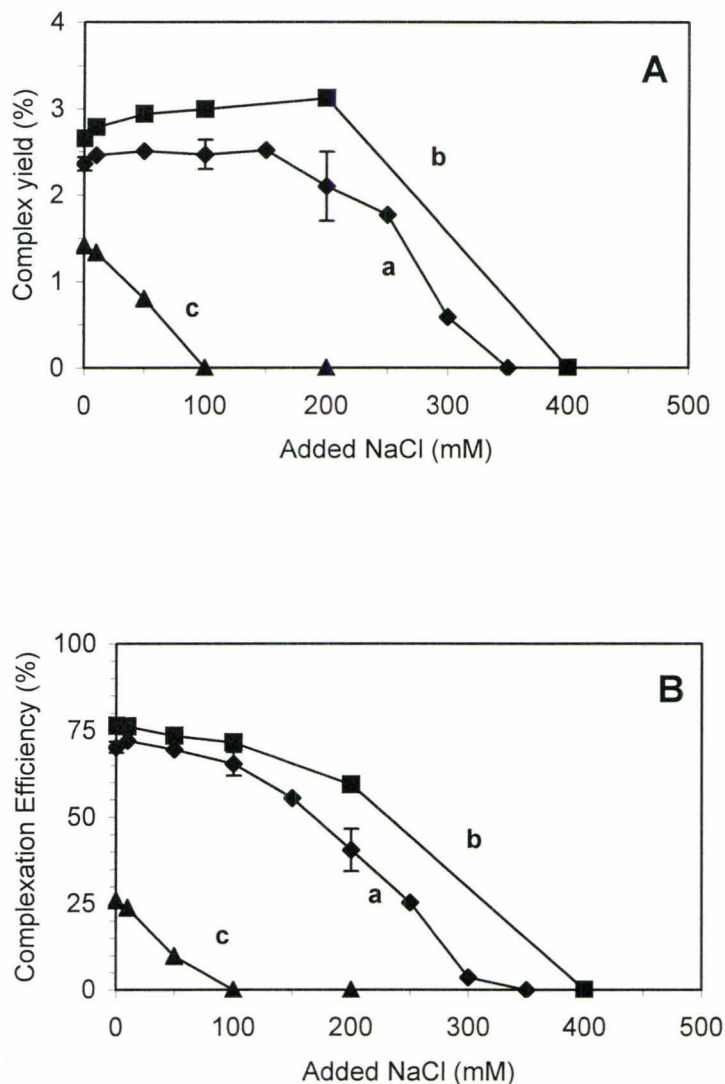


Figure 2.12: The effect of ionic strength on A) complex yield and B) complexation efficiency for the complex formed between PDADMAC-20 and a) PMAANa, b)P(MAANa-LMA)[95:5] and c) P(MAANa-PEGMA)[70:30]. Charge ratio = 1:1.

As well as influencing the efficiency of complexation, these groups can alter the nature of the complex. Complexes made from the PEGMA-containing polymer had higher water content. At 1 % polymer loading the complex formed from P(MAANa-co-PEGMA) had a polymer fraction of 18%, while the complexes made from the other two

polyanions had polymer fractions of 29-30%. The introduction of a hydrophilic comonomer such as PEGMA might be used to obtain a coacervate under conditions where the parent polyelectrolytes would give a gel or solid complex.

2.3.7 Encapsulation of Oils with Complex Coacervates:

Bungenberg De Jong ²⁷ was the first to encapsulate hydrophobic liquid droplets with a coacervate, and complex coacervates have now been used to encapsulate oils or solids for a number of applications. The polar coacervate walls can protect volatile oils from evaporation. Consequently, model experiments were undertaken to examine whether coacervates of the type studied in this work could be used to coat the surface of hydrophobic oils.

Methyl benzoate was dispersed with an overhead stirrer in a PMOETAC-300 solution before PMAANa was added. The mixture contained 325 mM added NaCl at which ionic strength the PMAANa/PMOETAC complex exists as a liquid coacervate. Optical microscopy showed the presence of coacervate droplets and capsules where the coacervate coats both methyl benzoate droplets and air bubbles (Figure 2.13). To be useful for encapsulation, the coacervate coating would need to be gelled, either physically or chemically. One means of gelling the PMAANa/PMOETAC capsule would be to reduce the ionic strength following encapsulation by diluting the solution. At reduced ionic strength (200 mM or lower, for example), the complex would become a gel (see Figure 2.1b).

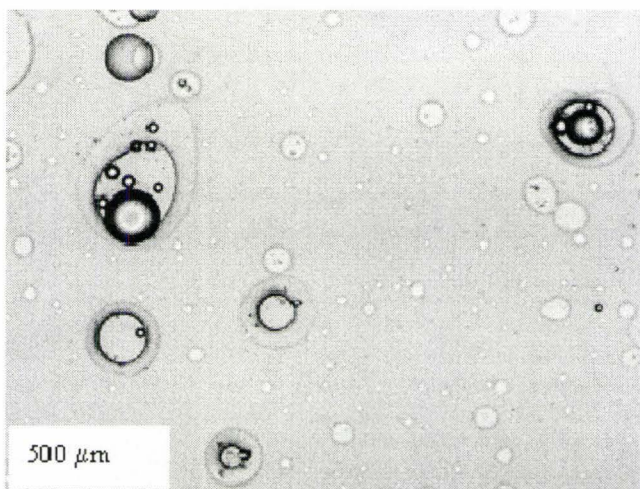


Figure 2.13: Optical microscopic image of methyl benzoate encapsulated with a complex made from PMAANa/PMOETAC-300 at a 1:1 charge ratio. Polymer loading: 1%, ionic strength: 325 mM.

2.3.8 Encapsulation and Crosslinking of the Capsule Walls:

The use of synthetic polyelectrolytes allows the introduction of reactive groups that may be used to crosslink the polyelectrolyte complex during or after encapsulation.⁴³ Towards this end, a polyanion containing acetoacetate groups, P(MAANa-co-MOEAA)[70:30], was combined with PMOETAC-300 (1.05:1 mixing ratio) and used to encapsulate paraffin oil giving capsules similar to those shown in Figure 2.13. There was no appreciable change in the appearance of the capsules when a small amount of 2 wt% aqueous poly(ethyleneimine) (PEI) was added to the stirred capsule suspension (Figure 2.14a). PEI is a branched polyamine with a net cationic charge that would be attracted to the anionic complex. The free amine groups of PEI may react with acetoacetate groups on the polyanion chains to form covalent cross-links as shown in Scheme 2.2. The capsules formed before PEI treatment disappeared when exposed to a 4 wt% NaCl

solution since the complex is held together by electrostatic interactions only. The PEI-treated capsule walls survived the NaCl challenge (Figure 2.14b) showing that the walls were chemically cross-linked.

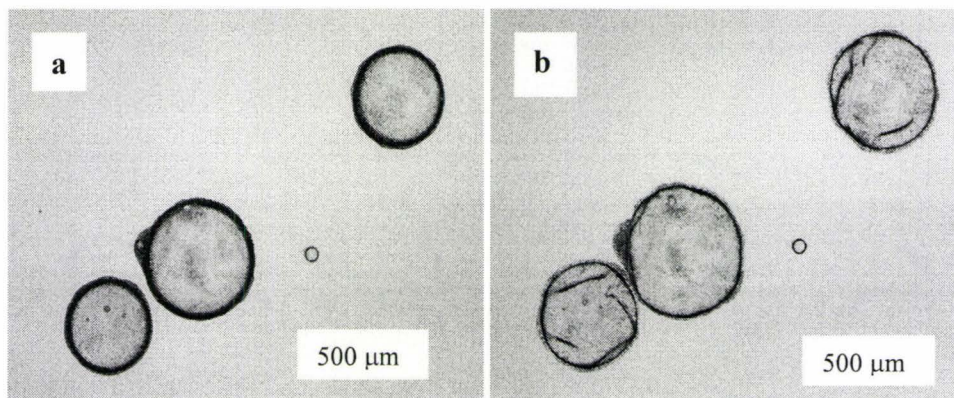
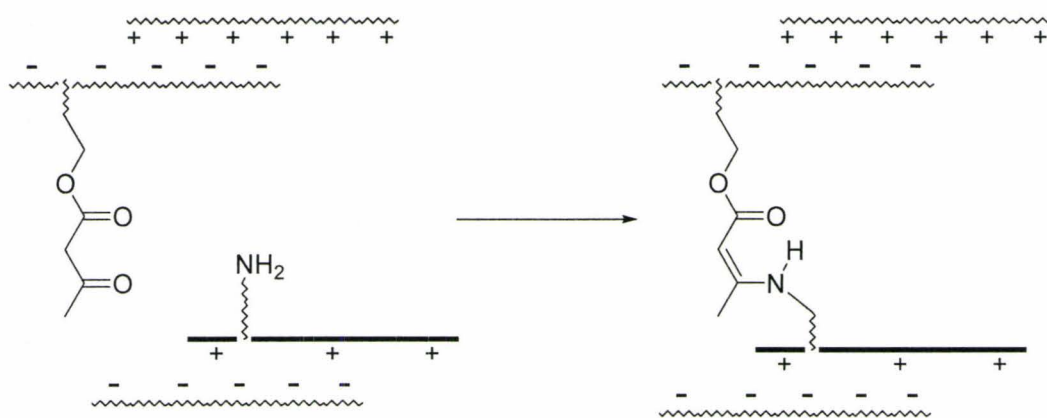


Figure 2.14: Optical microscopic image of paraffin oil encapsulated with a complex made from P(MAANa-co-MOEAA)/PMOETAC-300 at a 1.05:1 charge ratio and an ionic strength of 375 mM: a) after cross-linking with PEI, and b) after addition of excess 4% NaCl (684 mM).



Scheme 2.2: Reaction between acetoacetate and amine groups to form crosslinked polyelectrolyte complex.

The polyelectrolyte complexes formed between PMAANa and PDADMAC or PMOETAC may prove useful for LBL assembly, encapsulation, protein purification, or other applications because of the ability to a) vary the complex nature by changing polymer properties and/or complexation conditions, and b) covalently crosslink the complexes. We are planning to use these and similar approaches for the encapsulation of live cells used in enzyme-replacement therapy.

2.4 Conclusion

Polyelectrolyte complexes formed between poly(methacrylic acid, sodium salt) (PMAANa) and poly(diallyldimethylammonium chloride) (PDADMAC) or poly([2-(methacryloyloxy)ethyl]trimethylammonium chloride) (PMOETAC) were shown to form gels, liquids or soluble complexes, depending on the conditions used. Liquid coacervates were favoured by higher ionic strength, whether from added NaCl or from higher polymer loading, and by using polyelectrolytes of lower molecular weight.

Complex yield was greatest when 1:1 charge ratios were used. In the absence of added salt, all of the complexes formed at 1 wt% polymer loading had similar yields, efficiencies and polymer fractions. As the ionic strength of the solutions was increased, the complexes underwent swelling and eventually dissolved. The ionic strength at which dissolution occurred was greater for polyelectrolytes of higher molecular weight, and for PMOETAC compared to PDADMAC. Likewise, when polymer loading was increased, the complexes became more swollen and above a critical loading, no macroscopic phase separation was observed for the complexes made with PDADMAC. The polyelectrolyte

complexes formed near the critical loading were found to be temperature sensitive, exhibiting cloud points or de-swelling when heated.

When some of the carboxylate groups of PMAANa were replaced with hydrophobic lauryl (dodecyl) groups, the complex with PDADMAC was formed in a slightly higher yield and showed greater resistance to increasing ionic strength. When some of the carboxylates were replaced with hydrophilic but neutral poly(ethylene glycol) side-chains, the complex with PDADMAC was formed in much lower yield and showed much lower resistance to ionic strength. Two polyelectrolyte systems that gave liquid complexes (coacervates) were used to encapsulate hydrophobic oils and, in one case, the cross-linking of the resulting capsule walls was demonstrated. The ability to vary the nature of the complex by varying ionic strength, polymer MW, polymer loading or temperature might be useful in encapsulation, protein purification, or other applications.

2.5 References

- ¹ Tsuchida, E.; Abe, K. *Adv Polym Sci* **1982**, *45*, 1-119.
- ² Kabanov, V. A. In *Macromolecular Complexes in Chemistry and Biology*; Dubin, P.; Bock, J.; Davis, R.; Schulz, D. N.; Thies, C., Eds.; Springer-Verlag: Berlin, 1994; Chapter 10, pp 151-174.
- ³ Philipp, B.; Dautzenberg, H.; Linow, K.-J.; Kötz, J.; Dawydoff, W. *Prog Polym Sci* **1989**, *14*, 91-172.
- ⁴ Thünemann, A.F.; Müller, M.; Dautzenberg, H.; Joanny, J.-F.; Löwen, H. *Adv Polym Sci.*, **2004**, *166*, 113-171.
- ⁵ Sukhishvili, S. A.; Kharlampieva, E.; Izumrudov, V. *Macromolecules* **2006**, *39*, 8873-8881.
- ⁶ Iwatsubo, T.; Kusumocahyo, S.P.; Shinbo, T. *J Appl Polym Sci* **2002**, *86*, 265-271.
- ⁷ Kim, S.-G.; Lim, G.-T.; Jegal, J.; Lee, K. H. *J Membr Sci* **2000**, *174*, 1-15.
- ⁸ Dumitriu, S.; Chornet, E. *Biotechnol Prog* **1997**, *13*, 539-545.
- ⁹ Chu, C.H.; Kumagai, H.; Nakamura, K. *J Appl Polym Sci* **1996**, *60*, 1041-1047.
- ¹⁰ Mi, F. L.; Sung, H. W.; Shyu, S. S. *Carbohydr Polym* **2002**, *48*, 61-72.
- ¹¹ Liu, W.G.; Yao, K.D.; Liu, Q. G. *J Appl Polym Sci* **2001**, *82*, 3391-3395.
- ¹² Makita, N.; Yoshikawa, K. *Biophys Chem* **2002**, *99*, 43-53.
- ¹³ Wang, Y.; Gao, J. Y.; Dubin, P. L. *Biotechnol Progr* **1996**, *12*, 356-362.
- ¹⁴ Decher, G.; Hong, J. D. *Makromol Chem Macromol Symp* **1991**, *46*, 321-327.
- ¹⁵ Decher, G. *Science* **1997**, *277*, 1232-1237.
- ¹⁶ Sukhorukov, G.B.; Mohwald, H.; Decher, G.; Lvov, Y.M. *Thin Solid Films* **1996**, *284-285*, 220-223.

-
- ¹⁷ Schlenoff, J.B.; Dubas, S.T. *Macromolecules* **2001**, *34*, 592-598.
- ¹⁸ Mermut, O.; Barrett, C. J. *J Phys Chem B* **2003**, *107*, 2525-2530.
- ¹⁹ Choi, J.; Rubner, M. F. *Macromolecules* **2005**, *38*, 116-124.
- ²⁰ Glinel, K.; Moussa, A.; Jonas, A.M.; Laschewsky, A. *Langmuir* **2002**, *18*, 1408-1412.
- ²¹ Sukhishvili, S. A. *Curr Opin Colloid Interface Sci* **2005**, *10*, 37-44.
- ²² Kabanov, V. A.; Zezin, A. B. *Pure Appl Chem* **1984**, *56*, 343-354.
- ²³ Kabanov, V.A.; Zezin, A.B.; Rogacheva, V.B.; Gulyaeva, Z.G.; Zansochova, M.F.; Joosten, J.G.H.; Brackman, J. *Macromolecules* **1999**, *32*, 1904-1909.
- ²⁴ Fredheim, G. E.; Christensen, B. E. *Biomacromolecules* **2003**, *4*, 232-239.
- ²⁵ Paneva, D.; Mespouille, L.; Manolova, N.; Degee, P.; Rashkov, I.; Dubois, P. *J Polym Sci A: Polym Chem* **2006**, *44*, 5468-5479.
- ²⁶ Michaels, A. S.; Miekka, R. G.; *J Phys Chem* **1961**, *65*, 1765-1773.
- ²⁷ Bungenberg De Jong, H. G. In *Colloid Science*; Kruyt, H., Ed.; Elsevier: New York, 1949; vol. II, pp 335-432.
- ²⁸ Burgess, D. J. *J Colloid Interface Sci* **1990**, *140*, 227-238.
- ²⁹ Vanerek, A.; van de Ven, T. G. M. *Colloids Surfaces A: Physicochem Eng Aspects* **2006**, *273*, 55-62.
- ³⁰ Arshady, R. *Polym Eng Sci* **1990**, *30*, 905-914
- ³¹ Burgess, D. J. In *Macromolecular Complexes in Chemistry and Biology*; Dubin, P.; Bock, J.; Davis, R.; Schulz, D. N.; Thies, C., Eds.; Springer-Verlag: Berlin, 1994; Chapter 17, pp 285- 300.
- ³² Fubao, X.; Cheng, G.; Bingxing, Y.; Ma, L. *J Appl Polym Sci* **2004**, *91*, 2669-2675.
- ³³ Burgess, D. J.; Singh, O. N. *J Pharm Pharmacol* **1993**, *45*, 586-591.

-
- ³⁴ Tong, W.; Gao, C.; Möhwald, H. *Macromolecules* **2006**, *39*, 335-340.
- ³⁵ Stair, J. L.; Harris, J. J.; Bruening, M. L. *Chem Mater* **2001**, *13*, 2641-2648.
- ³⁶ Schuetz, P.; Caruso, F. *Adv Funct Mater* **2003**, *13*, 929-937.
- ³⁷ Schneider, A.; Vodouhê, C.; Richert, L.; Francius, G.; Guen, E. L.; Schaaf, P.; Voegel, J.-C.; Frisch, B.; Picart, C. *Biomacromolecules* **2006**, *8*, 139-145.
- ³⁸ Mauser, T.; Déjugnat, C.; Sukhorukov, G. B. *Macromol Rapid Commun* **2004**, *25*, 1781-1785.
- ³⁹ Pastoriza-Santos, I.; Scholer, B.; Caruso, F. *Adv Funct Mater* **2001**, *11*, 122-128.
- ⁴⁰ Olugebefola, S. C.; Ryu, S.-W.; Nolte, A. J.; Rubner, M. F.; Mayes, A. M. *Langmuir* **2006**, *22*, 5958-5962.
- ⁴¹ Vuillaume, P. Y.; Jonas, A. M.; Laschewsky, A. *Macromolecules* **2002**, *35*, 5004-5012.
- ⁴² Wang, J.; Jia, X.; Zhong, H.; Luo, Y.; Zhao, X.; Cao, W.; Li, M.; Wei, Y. *Chem Mater* **2002**, *14*, 2854-2858.
- ⁴³ Yin, X.; Stover, H. D. H. *Macromolecules* **2003**, *36*, 8773-8779.
- ⁴⁴ Li, Y.; Armes, S. P.; Jin, X.; Zhu, S. *Macromolecules* **2003**, *36*, 8268-8275.
- ⁴⁵ Griebel, Th.; Kulicke, W.-M.; Hashemzadeh, A. *Colloid Polym Sci* **1991**, *269*, 113-120.
- ⁴⁶ Mazumder, M. A. J.; Umar, Y.; Ali, S. A. *Polymer* **2004**, *45*, 125-132.
- ⁴⁷ Dautzenberg, H.; Karibyants, N. *Macromol Chem Phys* **1999**, *200*, 118-125.
- ⁴⁸ Dautzenberg, H.; Kriz, J. *Langmuir* **2003**, *19*, 5204-5211.
- ⁴⁹ Dautzenberg, H. *Macromolecules* **1997**, *30*, 7810-7815.
- ⁵⁰ Koetz, J.; Kosmella, S. *Nuovo Cimento* **1994**, *16D*, 865-871.

-
- ⁵¹ Kötzt, J; Beitz, T. *Trends Polym Sci* **1997**, *5*, 86-90.
- ⁵² Andersson, T.; Holappa, S.; Aseyev, V.; Tenhu, H. *J Polym Sci A: Polym Chem* **2003**, *41*, 1904-1914.
- ⁵³ Dautzenberg, H. *Macromol Chem Phys* **2000**, *201*, 1765-1773.
- ⁵⁴ Holappa, S.; Andersson, T.; Kantonen, L.; Plattner, P.; Tenhu, H. *Polymer* **2003**, *44*, 7907-7916.

Chapter 3: Self- cross- linking polyelectrolytes complexes for therapeutic cell encapsulation

Mazumder, M. A. J.; Shen, F.; Burke, N. A. D.; Potter, M. A.; Stöver, H. D. H.

Published in *Biomacromolecules*, **2008**, *9(9)*, 2292-2300

This chapter has been reproduced with permission from *Biomacromolecules*. Copyright
2008 American Chemical Society.

Contributions:

I performed all the experiments except for the encapsulations and subsequent studies involving cells which were carried out by Dr. Feng Shen, Research Associate in Dr. Murray A. Potter's Group, our collaborators in the Faculty of Health Sciences, McMaster University. The manuscript was written by myself with edits by Drs. Burke and Stöver.

Abstract

Self-cross-linking polyelectrolytes are used to strengthen the surface of calcium alginate beads for cell encapsulation. Poly([2-(methacryloyloxy)ethyl] trimethyl ammonium chloride) containing 30 mol% 2-aminoethyl methacrylate, and poly(sodium methacrylate) containing 30 mol% 2-(methacryloyloxy)ethyl acetoacetate, were prepared by free radical polymerization. Sequential deposition of these polyelectrolytes on calcium alginate films or beads led to a shell consisting of covalently crosslinked polyelectrolyte complex that resisted osmotic pressure changes as well as challenges with citrate and high ionic strength. Confocal laser fluorescence microscopy revealed that both polyelectrolytes were concentrated in the outer 7 to 25 micrometer of the calcium alginate beads. The thickness of this crosslinked shell increased with exposure time. GPC studies of solutions permeating through analogous flat model membranes showed molecular weight cut-offs between 150 and 200 kg/mol for poly(ethylene glycol), suitable for cell encapsulation. C₂C₁₂ mouse cells were shown to be viable within calcium alginate capsules coated with the new polyelectrolytes, even though some of the capsules showed fibroid overcoats when implanted in mice, due to an immune response.

3.1 Introduction

Cell encapsulation is a process by which live cells are entrapped within semi-permeable matrices or membranes for biomedical applications.^{1,2,3,4,5,6} Cells to be encapsulated can be designed to express therapeutic proteins.^{7,8} As their use involves implantation into the host's body, often the peritoneal cavity, non-autologous cells require encapsulation that isolates them from the host's immune system, while permitting metabolic exchange and release of therapeutic proteins.⁹ These capsules need to be compatible with both host and implanted cells and should not degrade *in vivo*. This requires capsule walls with molecular weight (MW) cut-offs of about 150 kDa, and ideally some form of crosslinking to strengthen the shell against biochemical and mechanical degradation.

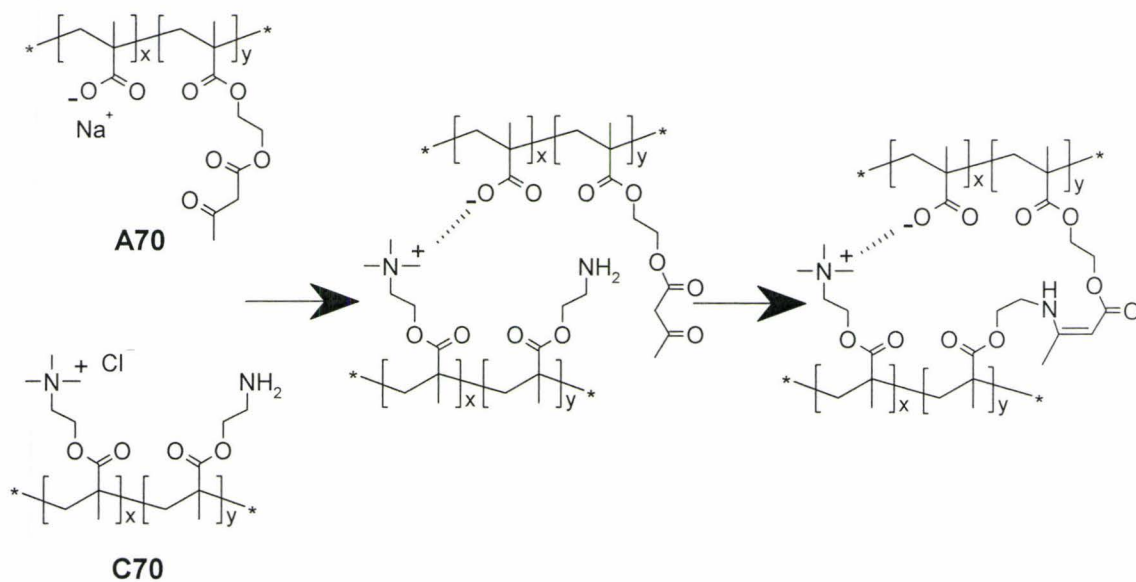
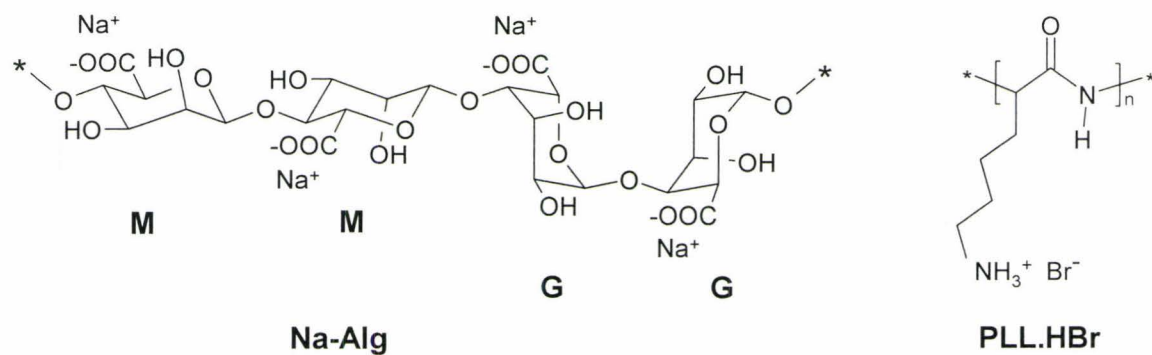
The most common approach to such cell-encapsulation for immuno-isolation involves alginate-poly(L-lysine)-alginate (APA) microcapsules as first described by Lim and Sun.⁹ Alginate is a natural polysaccharide consisting of β -D-mannuronic acid (M) and α -L-guluronic acid (G) residues (Scheme 3.1) that can be ionically crosslinked by calcium ions through the G-rich regions of the alginate chains. These beads are coated with poly(L-lysine) (PLL) in order to strengthen the outer bead surface and control permeability,¹⁰ followed by coating with a final layer of alginate to hide the cationic PLL from the host⁴ and thus make the capsules biocompatible. While these APA capsules meet many of the requirements for immuno-isolation of cells implanted into mice,¹¹ they have shown insufficient strength when implanted into larger animals such as dogs, and presumably, humans.¹² This may be due to slow loss of calcium or the polyelectrolyte overcoats.

Approaches to strengthen these microcapsules include the use of barium ions, which results in stronger microcapsules¹³ though at the possible cost of some neurotoxicity.¹⁴ A range of other alginate-based systems have been explored, including ultrahigh viscosity alginate,¹⁵ (Alg-cellulose sulfate)-poly(methylene-*co*-guanidine),¹⁶ Alg-chitosan,¹⁷ Alg-PLL-poly(acrylic acid),¹⁸ Alg-poly(L-ornithine)-Alg,¹⁹ Alg-PLL-poly(ethylene glycol), Alg-chitosan-poly(ethylene glycol), and Alg-PLL-poly(ethylene glycol)-Alg.²⁰

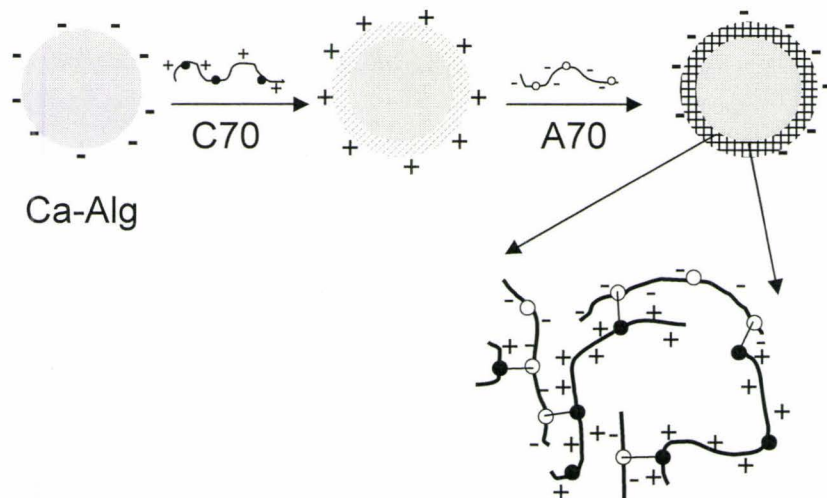
Fully synthetic systems such as poly(hydroxyethyl methacrylate-*co*-methyl methacrylate) (p(HEMA-*co*-MMA)),²¹ and polyphosphazene,² have been used as wall formers as well, though there are no *in vivo* results available for p(HEMA-*co*-MMA) capsules, and polyphosphazenes have been shown to elicit an immune response.²²

Crosslinking of Alg-chitosan capsules with glutaraldehyde or carbodiimide was shown to improve their mechanical strength,²³ though these small-molecule crosslinkers raise serious toxicity issues. Photopolymerization of monomer-functionalized alginate,^{24, 25, 26, 27, 28} or of monomers within the alginate core,^{29, 30} was used to strengthen the capsules, though irradiation and the presence of photoinitiator and monomers again posed challenges to the encapsulated cells. Recently, Hallé and coworkers^{31, 32} studied APA microcapsules in which a photoactivated crosslinker was used to covalently link the PLL chains with other PLL chains and with adjacent alginate chains, in both the surface of the core and the outer coating. These capsules displayed greatly improved mechanical stability while maintaining the cell viability and permeability of standard APA capsules.

In this paper, formation of a self-crosslinked polyelectrolyte skin on flat calcium alginate (Ca-Alg) model gels and around Ca-Alg beads is examined. This approach is based on crosslinking through complementary reactive groups attached to two oppositely charged polyelectrolytes. Being polymer-bound, these reactive groups should not pose a toxicity concern to either cells or host. The reactive polyelectrolytes used here are based on commonly used methacrylates.^{21,33,34} Their structures, along with those of sodium alginate (Na-Alg) and PLL, are shown in Scheme 3.1. The polycation p(MOETAC-co-AEMA) (C70, a 70/30 mole ratio copolymer of [2-(methacryloyloxy)ethyl] trimethyl ammonium chloride and 2-aminoethyl methacrylate) and polyanion p(MAANa-co-MOEAA) (A70, a 70/30 mol ratio copolymer of sodium methacrylate and 2-(methacryloyloxy)ethyl acetoacetate) bear amino and acetoacetate groups, respectively, that undergo a rapid covalent crosslinking reaction³⁵ once the polyelectrolytes are brought together by electrostatic interactions as shown in Scheme 3.1. Sequential coating of Ca-Alg beads with these polyelectrolytes (Scheme 3.2) should lead to a permanently crosslinked yet permeable polyelectrolyte skin.



Scheme 3.1: Natural and synthetic polyelectrolytes used to prepare coated capsules.



Scheme 3.2: Formation of crosslinked shells on Ca-Alg capsules by sequential coating with self-crosslinking polyelectrolytes having complementary reactive groups, amino (C70) and acetoacetate (A70).

3.2 Experimental

3.2.1 Materials:

Na-Alg (Keltone LV, 428 kg/mol²⁹) was a gift from the Nutrasweet Kelco Company (San Diego, CA). MOETAC (75 wt% solution in water), AEMA (90%, as HCl salt), methacrylic acid (MAA, 99%), MOEAA (95%), PLL (hydrobromide salt, $M_n = 15$ -30 kg/mol), 2,2'-azobis(2-methylpropionamide) dihydrochloride (97%), fluorescein isothiocyanate (FITC, 90%), 2-(cyclohexylamino)ethanesulfonic acid (CHES), sodium chloride, sodium citrate, calcium chloride, sodium nitrate and trypan blue stain (0.4% in 0.85% saline) were purchased from Sigma-Aldrich (Oakville, ON), and were used as received. 2,2'-Azobis(isobutyronitrile) (AIBN) was received as a gift from Dupont (Mississauga, ON) and used as received. Ethanol, acetone, N,N-dimethylformamide

(DMF) and anhydrous ethyl ether from Caledon Laboratories (Caledon, ON), sodium dihydrogen orthophosphate from BDH (Toronto, ON), ethylenediaminetetraacetic acid, disodium salt (EDTA) from Anachemia (Montreal, QC) and serum free media (SFM) from Gibco (Mississauga, ON) were used as received. Sodium hydroxide and hydrochloric acid solutions were purchased as concentrates from Anachemia Chemical, and were prepared by diluting to 1.000 or 0.100 M with deionized water.

3.2.2 *p*(MOETAC)(C100) and (*p*(MOETAC-co-AEMA)[70:30],(C70):

The preparation of C100 (M_w 300 kg/mol) was described previously.³⁶ C70 was prepared in a similar fashion. MOETAC (5.59 g, 26.9 mmol), AEMA hydrochloride (2.13 g, 12.8 mmol) and 2,2'-azobis(2-methylpropionamide) dihydrochloride (0.209 g, 0.77 mmol, 2 mol% relative to monomer) were dissolved in 75 mL deionized water in a 125 mL high-density polyethylene (HDPE) screw-cap bottle. The solution was bubbled with nitrogen for several minutes, the bottle sealed and heated at 60 °C for 24 hours while being rotated (15 rpm) to provide mixing. The polymer was isolated by precipitation in acetone (1 L) and then dried to a constant weight in a vacuum oven at 50 °C. Yield: 6.35 g (83%). Alternatively, the polymer was purified by dialysis in cellulose tubing (12 kg/mol MW cut-off, Spectrum Laboratories) with deionized water maintained at pH 5 by the addition of HCl followed by freeze-drying. Yield: 6.88 g (90 %). The C70 purified by dialysis was used in the permeability study and for any capsules that included cells or were implanted.

3.2.3 *p(MAANa) (A100) and p(MAANa-co-MOEAA)[70:30] (A70):*

The preparation of A70 has been described³⁶ and A100 was prepared in a similar manner. MAA (5.00 g; 58 mmol) and AIBN (95 mg; 0.58 mmol) were dissolved in ethanol (45 mL) in a 60 mL HDPE bottle, bubbled with nitrogen, and then heated at 60 °C for 24 h while the bottle was rotated at 4 rpm to provide mixing. PMAA was isolated by precipitation in ether (500 mL), washed with ether and dried to constant weight at 50 °C in a vacuum oven. Yield: 4.81 g (96%). A70 and A100 solutions were prepared by neutralizing the MAA-based polymers with a stoichiometric amount of 1M NaOH and then diluting to the desired polymer concentration.

3.2.4 *FITC-labelled polymers, C70f and A70f:*

C70 (0.108 g, 0.17 mmol AEMA) was dissolved in 10 mL water in a 20 mL glass vial. The pH was adjusted to 9 by adding 0.1M NaOH. FITC (0.010 g, 0.026 mmol) dissolved in 1 mL DMF was added to the polymer solution under stirring. The mixture was stirred for 1 hour at room temperature (20 °C). The FITC-labelled copolymer C70f was dialysed against deionized water using cellulose membranes (3.5 kg/mol MW cut-off, Spectrum Laboratories). The resulting polymer solution was freeze-dried, and the polymer dried further to constant weight in a vacuum oven at 50 °C. A70f, FITC-labelled A70, was prepared in a similar fashion by treating 0.118 g of A70 (0.26 mmol MOEAA) with 0.010 g FITC (0.026 mmol) for 24 h at 20 °C. Final label contents were determined by UV/Vis spectroscopy, and were 1.7 and 0.3 mol% of the total monomer units for C70f and A70f, respectively.

3.2.5 Characterization:

The compositions and/or pK_a values of C70, A100 and A70 were determined by potentiometric titration. Accurately weighed samples were dissolved in about 30 mL of deionized water for C70 and PMAA, or 1:1 methanol/water for p(MAA-co-MOEAA). A small volume (0.5-1 mL) of 0.1 M HCl was added to the solution to ensure complete protonation of the primary amine or carboxylic acid groups before titration with 0.100 M NaOH in a PC Titrate automatic titrator (Man Tech Associates). The titration curves showed two endpoints, one for excess HCl and one for the polymer-bound groups. The pK_a was taken as the pH at the midpoint (0.5 eq NaOH) of the titration curve for the polymer-bound groups.

The degree of labelling with FITC was measured by UV-Vis spectrophotometry, using a Varian Cary 50 BIO UV-Vis Spectrophotometer.

Optical microscope images of complexes, capsules and microspheres were taken using an Olympus BX51 optical microscope fitted with a Q-Imaging Retiga EXi digital camera and ImagePro software. Phase contrast microscope images were taken using a Wild M40 microscope.

A Confocal laser scanning imaging system equipped with an Argon-ion laser and a Nikon microscope using EZ-C1 software, version 1.50, was used to investigate the distribution of FITC labeled polycation and polyanion in the microcapsules.

3.2.6 MW Determination:

The MW of A100 was determined with a gel permeation chromatography system consisting of a Waters 515 HPLC pump, Waters 717 plus Autosampler, three columns

(Waters Ultrahydrogel-120, -250, -500; 30 cm × 7.8 mm; 6 μm particles) and a Waters 2414 refractive index detector. The columns were maintained at 35 °C and the system was calibrated with narrow-dispersed PEG standards (Waters, Mississauga, ON). Samples were eluted at a flow rate of 0.80 mL/min with a mobile phase consisting of 0.3 M sodium nitrate in phosphate buffer (pH 7) prepared by dissolving 27.6 g monosodium phosphate, 101.98 g sodium nitrate, and 4.66 g sodium hydroxide in 4.0 L of HPLC grade water. The pH was adjusted to 7 with 1 M NaOH. The A100 solution (1%) for analysis was prepared by adding a stoichiometric amount of 1 M NaOH to the PMAA precursor followed by dilution with the mobile phase.

An Ubbelohde viscometer (viscometer constant: 0.00314 cSt/s), was used to determine the MW of C70 dissolved in 1 M NaCl at 20.0 ± 0.1 °C. Prior to the measurements, all stock solutions were filtered through a 0.45 μm membrane filter. The intrinsic viscosity $[\eta]$ was calculated by extrapolation of the Huggins plot (η_{sp}/c vs. c) to zero concentration. The polymer MW was calculated from the intrinsic viscosity using the relationship $[\eta] = KM^a$ with values for K and a found in the literature.³⁷

3.2.7 Spin Coating:

Planar films of Na-Alg, Ca-Alg and polyelectrolyte-coated Ca-Alg were prepared with a spin coater (Model EC101, Headway Research Inc.). 1 mL of 1.5 %(w/v) Na-Alg was placed onto a pre-weighed glass cover slide (2.5 cm × 2.5 cm), and spun for 30 seconds at 400 RPM. The resulting Na-Alg films were immediately coated with 1 mL of 1.1% calcium chloride, and allowed to gel for different lengths of time before the excess solution was again removed by spinning at 400 RPM for 30 seconds. The resulting Ca-

Alg film was washed by placing 1 mL of saline on the film for 30 seconds and then spinning at 400 rpm for 30 seconds. Subsequently, 1 mL of 1w% C70 was placed on the Ca-Alg film for 10 seconds, followed by spinning (400 RPM, 30 s) and then a saline wash as described above. An A70 coating was added in analogous fashion using 1w% A70. The cover glass was weighed within 10 ± 5 seconds of each coating step to determine the weight of the film.

3.2.8 Preparation and Coating of Ca-Alg Beads:

Ca-Alg beads were prepared and coated as described previously.^{8,12} A 1.5% aqueous solution of Na-Alg was filtered through sterile 0.45 μm Acrodisc syringe filters (Pall Corp., USA). A modified Sage syringe pump (Orion/Thermo Electron) was used to extrude the alginate solution at a rate of 99.9 mL/hr through a 27-gauge blunt needle (Popper and Sons), with a concentric airflow (4 L/min) used to induce droplet formation. The droplets were collected in gelling bath ($10\times$ alginate volume) consisting of 1.1% calcium chloride and 0.45% NaCl causing the formation of Ca-Alg beads. These beads were washed in sequence with four-fold volumes, relative to the concentrated bead suspension, of a) 1.1% CaCl_2 , 0.45% NaCl for 2 minutes; b) 0.55% CaCl_2 , 0.68% NaCl for 2 minutes; c) 0.28% CaCl_2 , 0.78% NaCl for 2 minutes; d) 0.1% CHES, 1.1% CaCl_2 , 0.45% NaCl for 3 minutes; e) 0.9% NaCl for 2 minutes and then stored in saline.

APA capsules were prepared by exposing Ca-Alg beads (3 mL) to 0.05% PLL in saline (10 mL) for 6 minutes and washing them in sequence with 12 mL of wash solutions d), a) and e) above. The beads were then coated with 0.03% (w/v) Na-Alg (10 mL) in saline for 4 minutes followed by three washes with 0.9% saline (12 mL). Coating

with C70 and A70 was performed in a similar fashion except that a variety of concentrations and exposure times were explored. Unless otherwise specified, standard C70 and A70 coatings were prepared with 0.5% solutions of C70 and A70 and exposure times of 10 min.

3.2.9 Mechanical Stability:

The mechanical stability of capsules and beads was tested by agitating the beads in the presence of hypotonic or calcium chelating solutions. The osmotic pressure test (OPT)³⁸ utilized six hypotonic solutions containing 0.52%, 0.78%, 1.19%, 1.52%, 3.25% and 6.50% SFM in water, with corresponding osmolarities of 1.9, 2.8, 4.2, 5.6, 11.1, 21.3 mOsm, respectively. 100 μ L of capsule suspension (~200 microcapsules) and 10 mL of hypotonic solution were placed in a 15 mL polypropylene conical tube, and then agitated for 3 hrs on an orbital mixer at 30 rpm. The capsules were stained with trypan blue and transferred to glass Petri dishes on a light box. The percentage of intact capsules was determined by direct visual inspection or from an image taken with a digital camera. Experiments were conducted in triplicate. In the calcium chelation test, the 100 μ L capsule suspension was exposed to 10 mL of water or 0.03% EDTA solution while being agitated for 15 min before analysis as described for the OPT.

3.2.10 Permeability Studies:

Permeabilities of flat model APA and AC70A70 films were determined using a two-compartment Teflon diffusion cell where the compartments were separated by an APA film, or by a C70/A70 coated calcium alginate film, supported on a porous,

polypropylene support membrane (a gift from 3M Centre, St. Paul, MN; 4×4 cm, average pore size - 5µm). The base calcium alginate membrane was prepared by immersing the support membrane in 1.5% Na-Alg, then 1.1% CaCl₂ for 10 min followed by three saline washes. The membrane was then mounted in the diffusion cell and coated on one side by exposure to 1) polycation solution (0.05% PLL or 0.5% C70) for 6 min, 2) three saline washes, 3) polyanion solution (0.03% Na-Alg or 0.5% A70) for 4 min, and 4) three saline washes. A mixture of poly(ethylene glycol) samples with viscosity-average MWs of 100, 200 and 300 kg/mol (Sigma-Aldrich, 0.1% w/v each in saline) was placed into the source compartment, with an equal volume of saline loaded into the sink compartment. The assembly was maintained at room temperature (23 ± 2 °C) with stirring in both compartments for 24 hrs. Samples were taken from each sink side and analyzed by gel permeation chromatography (GPC) as described above except that the mobile phase was 0.1 M NaNO₃. The samples from the sink compartments were concentrated by evaporation prior to analysis.

3.2.11 Cell Culture:

The cell line used was a murine C₂C₁₂ myoblast cell line (American Type Culture Collection [ATCC], Rockville, MD, USA; Catalogue No. CRL-1772). The cells were maintained in Dulbecco's Modified Eagle's Medium (DMEM) supplemented with 10% fetal bovine serum (Gibco, Grand Island, NY, USA) and 100 U/mL penicillin and 100 µg/mL streptomycin (Gibco, Grand Island, NY, USA) at 37 °C in a water-jacket incubator (5% CO₂, 100% humidity).

3.2.12 Encapsulation of Cells:

The cells were harvested, counted and centrifuged at 1000 rpm for 10 min at 4 °C. The supernatant was aspirated and the cells were re-suspended in ice cold normal saline. A known number of cells were centrifuged and resuspended in 50 µL of cold normal saline. Pre-filtered (0.45 µm) Na-Alg solution (1.5%, 5-20 mL) was added to the cells to produce a cell loading of 2 million cells/mL of solution. The cell suspension was mixed well and then transferred to a syringe for capsule preparation as described above. Polyelectrolyte solutions used for coating were filtered through 0.45 µm syringe filters prior to use.

3.2.13 Cell Viability:

The number of viable cells per capsule was determined with an Alamar Blue assay.³⁹ 100 µL of capsules were loaded in a 24-well plate with 500 µL media. 50 µL of Alamar Blue was added to each sample and the plate was incubated at 37 °C for 4 hours. After incubation, 100 µL of solution was taken from each well and placed in a microtiter plate. The fluorescence of each sample was read with a Cytofluor II fluorimeter, with an excitation wavelength of 530 nm and an emission wavelength of 590 nm. The number of viable cells was determined by comparing fluorescence values with a standard curve generated from a known number of cells.

3.2.14 Implantation:

Animals were treated in accordance with the Canadian Council on Animal Care Guide to the Care and Use of Experimental Animals. Freshly made capsules were kept in

the supplemented DMEM described above at 37 °C for 3 days before implantation in mice as described previously.⁸ Briefly, the mice were anaesthetized with isoflurane (Anaquest, Mississauga, ON, Canada) using a small-animal anaesthetic machine (Med-Vet, Toronto, ON, Canada). Three mL of capsules suspended in normal saline (4 mL total) were implanted into the abdominal cavity of mice with an 18-gauge catheter (Angiocath, Mississauga, ON). For microcapsule recovery after implantation, mice were euthanized, the peritoneal cavity was opened and the capsules were scooped out with a spatula. The capsules were washed several times with normal saline before testing.

3.3 Results and Discussion

The use of the oppositely charged reactive polyelectrolytes C70 and A70 (Scheme 3.1) to strengthen Ca-Alg microcapsules was examined, and compared with the more commonly used non-covalent coatings based on PLL / Na-Alg. The polyelectrolytes C70 and A70, and their non-reactive analogs C100 and A100, were prepared by conventional free-radical copolymerization (Table 3.1).

Table 3.1: Polyelectrolyte properties.

Polyelectrolyte	Composition	MW (kg/mol)	pK _a
Na-Alg	G: M = 40:60 ^a	428 ^d	3.20/3.38 (G/M) ^g
A70	MAA: MOEAA 70:30 (± 4) ^b	42 ^b	7.1 ^h
A100	--	40 ^e	7.2 ^h /6.3 ⁱ
PLL	--	15-30 ^a	10.5 ^j
C70	MOETAC: AEMA 70:30 (± 4) ^c	167 ^f	7.3 ⁱ
C100	--	300 ^b	--

a) given by supplier, b) ref³⁶, c) MOETAC: AEMA determined by titration, d) ref²⁹, e) M_n obtained from gel permeation chromatography data, f) M_w obtained from viscometry data, g) ref⁴⁰, h) from titration in 50% methanol, i) from titration in water, j) ref⁴¹.

Polyelectrolyte complexes formed with the non-reactive analogs, C100 and A100, were shown earlier to dissolve when exposed to $[\text{NaCl}] > \sim 500 \text{ mM}$.³⁶ Complexes that included C100 or A100 dissolved rapidly in 2 M NaCl. In contrast, the C70/A70 gel complex formed by combining solutions of A70 and C70 in a 1:1 mole ratio swelled slightly in 2 M NaCl but did not dissolve. The survival of this complex at high ionic strength, where the electrostatic interactions are broken, is attributed to the formation of covalent cross-links. The C70/A70 complex survives with little change when challenged with 2 M NaCl within 1 min of formation, showing that the reaction between amine and acetoacetate groups in the complex is rapid at room temperature. Sequential deposition of C70 and A70 on the surface of Ca-Alg model films and microcapsules should lead to a covalently crosslinked complex that is better able to resist environmental stresses.

3.3.1 Ca-Alg Model Films Coated with C70/A70:

Flat Ca-Alg model films prepared by spin coating were sequentially coated with C70/A70 (multi) layers (Scheme 3.3) in order to better understand the polyelectrolyte interactions involved. The weights and thicknesses of these films at different stages of coating are shown in Table 3.2.

During the process oppositely charged polyelectrolytes served as the counter ion to build up the multilayer polyelectrolyte membrane.

1.5.7 Moulding Method:

In the moulding method, a warm (37 °C) solution of cells and a thermotropic polymer is cast into moulds with the desired shape, which is shown in Figure 1.8. After cooling, the gels can be removed and transferred to an appropriate buffer solution. The advantage of this method is the possibility of producing other shapes of gels than round beads, but it suffers from low efficiency and temperature limitations. However, in order to get suitable cell containing gel beads, the sensitivity of cells to heat should be taken into account.

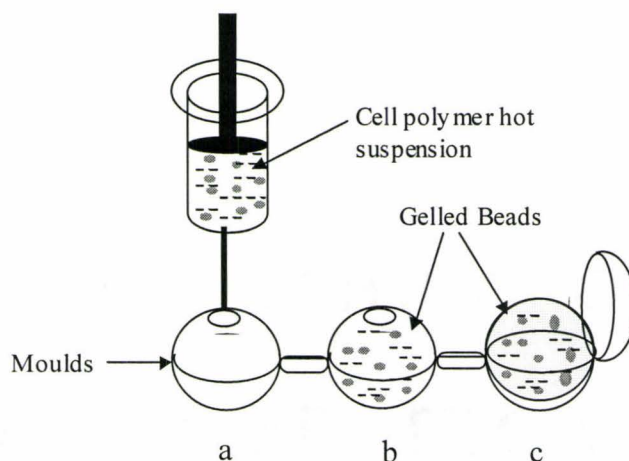


Figure 1.8: Schematic representation of entrapment of cells using moulds. a) The warm polymer-cell suspension solution is cast into moulds, b) after the gel setting time, c) entrapped cells are carefully taken out of the moulds, and then stored in a buffer solution.

1.6 Polyelectrolyte Complex:

Polyelectrolytes are macromolecules that have charged or chargeable groups when dissolved in polar solvents like water. They dissociate into a macromolecular ion and small counter ions, similar to their cross linked analogs that have found much uses as ion exchange resins. Combining solutions of oppositely charged polyelectrolytes can lead to formation of layer- by-layer assemblies,^{34, 35, 37, 38} soluble,³⁹ liquid coacervate,⁴⁰ gel-like⁴¹ and even solid^{42, 43} polyelectrolyte complexes (PEC's) that in the latter three cases phase-separate from solution. Polyelectrolyte complexes have been widely used for a number of applications such as separation membranes, immobilization of enzymes or cells, drug carriers, gene delivery tools and protein purification.

This complexation is driven by the gain of entropy of the small counter ions upon PEC formation. The resulting complex can be insoluble in water, organic or common solvents. In general, the stoichiometric composition of these polyelectrolyte complexes depends on the degree of dissociation of the two polyelectrolytes. The equilibrium water content can vary from 30 to 90% by weight.⁴⁴ Possible combinations of polyelectrolyte complexes are strong polyacids-strong polybases, strong polyacids-weak polybases, weak polyacids-strong polybases, and weak polyacids-weak polybases. In general, the nature of the interactions, the properties of the polyelectrolyte complexes and the efficiency of complexation formed, depend on variables such as charge ratio, ionic strength, polymer concentration, pH, charge density, molecular weight, temperature and polymer structure.^{37, 45}

The layer-by-layer assembly, introduced by Decher et al in the early nineties,^{34, 35} involves the alternating immersion of substrates into dilute solutions of oppositely

charged polyelectrolytes (polyanions and polycations), produces multilayers on surfaces. It allows excellent control of the thickness and composition of the layers (roughness, wettability, and swelling behavior), by varying the conditions used to assemble the layers such as pH, ionic strength, polymer functionality, and polymer concentration.³⁷ Although layer-by-layer assembly is normally applied to a wide variety of substrates differing in size, composition, and geometry,⁴⁶ it has potential for applications on hydrogel substrates.

The formation of polyelectrolyte complexes is depicted in Figure 1.9. Strong polymer-polymer interactions can lead to precipitation of the complex. On the other hand, if the interaction is weak, the complexes often remain soluble. In between these two interactions, the solution can separate into two immiscible liquid phases, in a process called liquid coacervation (from latin, coacere: heaping together). One of the phases, the polymer-rich phase is called the coacervate phase, and the second, polymer-lean phase, is called the supernatant or equilibrium phase.⁴⁷

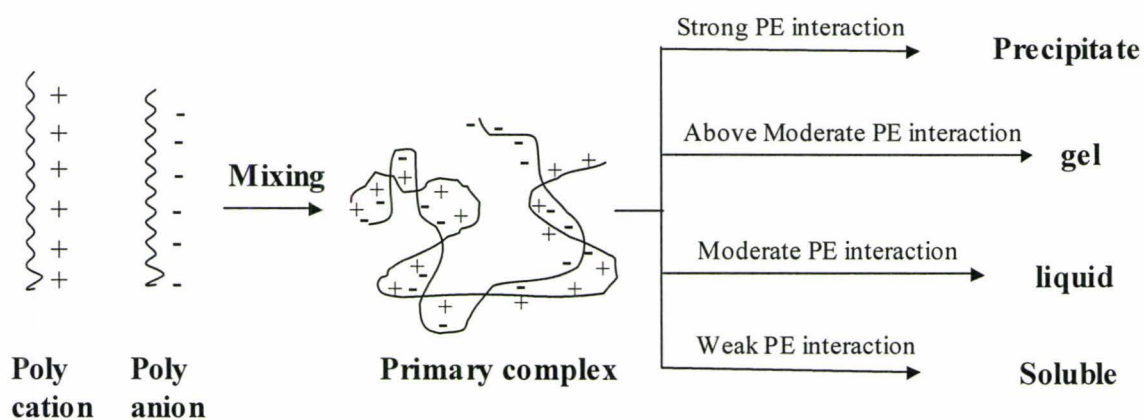


Figure 1.9: Schematic representation of formation of polyelectrolyte complexes.

Coacervation can occur with a single polymeric species, and is then called simple coacervation. This is a liquid-liquid phase separation to form a condensed droplet rich in a single polymer species. It involves only one macromolecule and may result from the addition of a dehydrating agent that promotes polymer- polymer interactions over polymer solvent interactions. This polymer solvent interaction can be brought about by changes in temperature or solvent composition (pH, ionic strength, non-solvents). For example, the addition of alcohol to an aqueous solution of gelatin causes dehydration of the gelatin, leading to the formation of a simple coacervate consisting of a separate phase rich in gelatin.⁴⁸

Complex coacervation involves the interactions of two oppositely charged polyelectrolytes in aqueous media, where the charges are sufficiently large to activate interaction, but not large enough to cause precipitation.⁴⁷ For this case, Piculill and Lindman⁴⁹ have recommended the term “associative phase separation” to replace “complex coacervation”. One of the best-studied examples of complex coacervation is the gelatin-gum arabic system.⁵⁰ At pH around 4.6, gelatin has a net cationic charge due to its high lysine contents, and can hence form a PEC with the anionic gum acacia. These PECs are often covalently cross-linked with formaldehyde or glutaraldehyde. Complex coacervation is dependent on the molecular weight, charge density, concentration, hydrophobic/hydrophilic content of the polymer, and on the nature of the medium such as temperature, pH, ionic strength or the presence of non-solvents. Both coacervation processes have been extensively applied in the field of encapsulation, as well as for protein separations.^{51, 52, 53, 54}

Several examples of synthetic and natural coacervate systems are illustrated below:

Synthetic polyelectrolytes:

Non-ionic thermo-responsive copolymers of 2-hydroxyethyl methacrylate and 2-hydroxyethyl acrylate undergo a liquid-liquid phase separation above the lower critical solution temperature in aqueous solutions, and have potential applications in ophthalmology.⁵⁵ Similar liquid-liquid phase separation was observed by Miyazaki et al⁵⁶ for copolymers of *N,N*-dimethylamide-co-*N*-phenylacrylamide. Yin and Stöver⁵⁷ studied for *N,N*-dimethylacrylamide-co-glycidyl methacrylate, Maeda et al⁵⁸ studied for *N*-isopropylacrylamide-co-2-hydroxyisopropylacrylamide, and potentially they can be used in protein separation processes.

Anionic polyphosphazenes can form micro droplets by NaCl induced simple aqueous coacervation. These micro droplets can be stabilized by the addition of CaCl₂ to form hydrogel microspheres. This method is especially appealing for protein encapsulation. However, these hydrogel microspheres were not stable at very high or very low salt concentrations.⁵⁹

Cationic polyacrylamide copolymers (cPAM) above a certain MW can form coacervate complexes with anionic sulfonated Kraft lignin (SKL). Coacervation efficiency increases with increasing MW of cPAM. Below the cPAM critical molar mass, colloidal complexes form instead.⁶⁰

Recently Wang et al⁶¹ prepared microcapsules by an *in-situ* coacervation method in which polyallylamine was adsorbed onto the polystyrene sulfonate doped CaCO₃ microparticles, followed by cross-linking of the polyallylamine hydrochloride with glutaraldehyde and core removal in a solution of EDTA with or without polyallylamine.

Natural and mixed polyelectrolytes:

Gelatin and gum arabic form a complex coacervate that can be covalently cross-linked with formaldehyde or glutaraldehyde to make stable microcapsules.⁵⁰

Ca-alginate gel beads can be coated with positively charged polymers such as poly-L-lysine, chitosan and others. However, the resulting electrostatically linked alginate/poly-L-lysine complex can be weakened by interactions with other charged molecules in the environment.⁶² Alginate and chitosan, like other polysaccharides, are furthermore vulnerable to a variety of degradation mechanisms, including redox degradation, and acid, alkaline and enzyme- catalyzed degradation.⁶³

Bovine serum albumin and cationic poly (diallyldimethyl ammonium chloride) (PDADMAC) can form coacervate complexes in specific pH region (6.5-7), depending on their stoichiometry as well as on the salinity.⁵³ On the other hand, bovine serum albumin can form coacervates in presence of anionic polyelectrolytes such as sodium polystyrene sulfonate below pH 4 irrespective of varying ionic strength and protein polyelectrolyte ratio. However, this coacervation system is not efficient since a large fraction (~50%) of the protein-polyelectrolyte complex is present in the supernatant after the coacervation.⁶⁴

One goal of this thesis is to study the coacervation as well as layer-by-layer encapsulation using of synthetic polymers that combine electrostatic interactions and covalent cross-linking.

1.7 Materials in Cell Encapsulation

The materials used in cell encapsulation must be of constant quality and be biocompatible with the host and the enclosed cells. The capsules membrane must have reasonable mechanical strength to survive handling, implantation, and the mechanical, biochemical and biological stresses imposed by the host, and allow the exchange of oxygen, nutrients and metabolites, while obscuring the encapsulated cells from the host's immune system (Figure 1.1). Moreover, rough surfaces of the microcapsules must also be avoided because they can elicit inflammatory responses.

In the search for a better microencapsulation design (single and multilayer), many types of natural and synthetic polymers are being explored since polymers are playing an important role in the encapsulation of cells. These polymeric materials often will not provoke an immune response, and the diversified and adjustable properties of polymers enable their use in cell encapsulation.⁶⁵ In addition, their ability to exist as liquids, gels or solids, enables them to meet a large range of mechanical and physical demands. There is a large variety of polymers that can be used in these systems, including synthetic, semi-synthetic (chemically modified natural polymers) and natural polymer and recent reviews described their utilization in these systems in detail.^{66, 67, 68}

Among them, alginates are the most widely studied and characterized material for cell encapsulation.⁶⁹ Alginate is a naturally occurring anionic polysaccharide obtained by extraction from marine brown algae. It is a linear binary copolymer composed of β -D-mannuronic acid (M) and α -L-guluronic acid (G) residues (Figure 1.10).

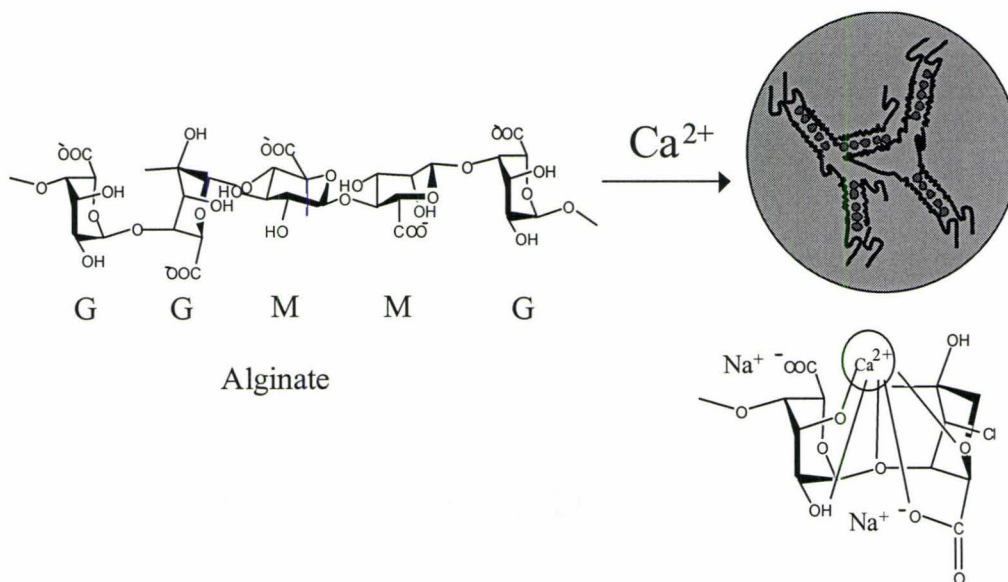


Figure 1.10: Calcium cross-linking of Alginate bead formation in Calcium Chloride bath.

Conceptually, non-autologous recombinant cells are encapsulated within a biocompatible polymer, and microcapsules can be formed by many different methods. One of the most widely studied microencapsulation system involves the alginate-poly-L-lysine-alginate (APA) microcapsules derived from the protocol of Lim and Sun.⁵

This encapsulation process involves three different steps. The first step involves dispersing an alginate solution containing cells in droplet form into a calcium chloride gelation bath. When these droplets are immersed in the calcium gelation bath, calcium ionically cross-links the guluronic residue of the alginate chains (Figure 1.10), which leads to the formation of firm calcium alginate hydrogel beads. This process often involves extruding the alginate/cell solution through a needle with continuous annular airflow, and is illustrated in Figure 1.3.

The second step in encapsulation is the coating of the alginate hydrogel beads with poly-L-lysine (PLL) in order to strengthen the outer bead surface. PLL interacts with

the alginate through ionic interactions and the resulting alginate/PLL polyelectrolyte complex on the bead surface serves to increase the structural stability of the microcapsules, and defines permeability.

The third step involves coating the outside of the resulting capsule with a layer of alginate, in order to hide the inflammatory PLL⁷⁰ from the host and make the final capsules biocompatible. While these APA capsules meet many of the requirements for immuno-isolation of cells implanted into mice (intact for 6 months), they still show insufficient strength when implanted into larger animals such as dogs, where they collapse within 2 weeks.⁷¹ This may be due to the destabilization of the alginate core matrix through slow exchange of calcium ions with other physiological ions and/or the loss or degradation of the polyelectrolyte overcoats.^{72, 73} The membrane instability caused undesirable leakage of encapsulated cells. This could severely damage the whole process, and raise many safety issues. Moreover, due to PLL, APA microcapsules show inflammatory reactions *in vivo*, and the amount of PLL needs to be carefully considered for long-term transplantation based applications.⁷⁰

In addition to the standard APA microcapsules, several other alginate-based microcapsules have been used for the purpose of immuno-isolation. Since barium ions have a higher affinity for alginate than calcium ions, barium has been used instead of calcium, and found to create mechanically stronger microcapsules.⁷⁴ Despite promising results, the clinical use of barium cross-linked microcapsules may be limited by reports that barium ions are neurotoxic.⁷⁵

A number of studies have attempted to address the challenge of long-term mechanical stability by varying the molecular weight⁷⁶ or G/M ratio of the alginate,^{75,77}

using uncoated alginate microcapsules,⁷⁸ and varying the cross-linking ion⁷⁴ and/or use of polyelectrolytes to coat the alginate based capsule that includes Alg-chitosan-Alg,⁷⁹ Alg-PLL-poly(acrylic acid),⁸⁰ Alg-PLL-poly(ethylene glycol), Alg-chitosan-poly(ethylene glycol), and Alg-PLL-poly(ethylene glycol)-Alg,⁸¹ Alg-poly-L-ornithine-Alg,^{82,83} Alg-poly(allylamine)-Alg,⁸⁴ Alg-PEI-poly(acrylic acid)-PEI-Alg, and Alg-PEI-carboxymethylcellulose-PEI-Alg.⁸⁵ Some alginate-based microcapsules have also been tried for targeted applications based on immuno-isolation, which are listed in the following Table 1.1.

Table 1.1: Cell encapsulation approaches based on alginate matrices:

Material	Modification	Application
Alginate	-	Bone and cartilage engineering, diabetes and cancer ^{11,86, 87, 88}
Alginate	With RGD	Bone regeneration and muscle regeneration ^{89, 90}
Alginate	Enzymatic modification	Increased stability ⁹¹
Alginate	Photo reactive liposomes	Substrates containing cells immobilized in precise locations ⁹²
Alginate	Phenol moieties	Increased stability ⁹³
Alginate-PLL-alginate	-	Bone repair and regeneration, chronic neuropathic pain and anemia ^{94, 95, 96}
Alginate-PLL-alginate	Covalent cross links between membrane	Increased stability ^{97, 98}
Alginate-PLL-alginate	Polymerization	Increased stability ⁹⁹
Alginate-Agarose	-	Sub sieve (less than 100 μm) size capsules ¹⁰⁰
Alginate-chitosan	Lactose modified chitosan	Increased mechanical properties ^{101, 102}
Alginate-PLO-alginate	-	Diabetes and neuroprotection ^{103, 104}

While alginate microcapsules are appealing because they are well characterized and reasonably biocompatible, their usefulness may be limited by the presently limited stability. Consequently, new types of microcapsules have been made from synthetic polymers that will potentially yield stronger microcapsules. Till to date few synthetic system, such as poly(hydroxyethyl methacrylate-*co*-methyl methacrylate), p(HEMA-*co*-MMA)¹⁰⁵, poly(hydroxyethyl methacrylate-*co*-ethyl methacrylate), p(HEMA-*co*-EMA)¹⁰⁶ and polyphosphazene (PPP)¹⁰⁷ have been studied as biomaterials for microencapsulation. The major difference between water-soluble polymers such as alginate and water insoluble polymers such as poly(HEMA-*co*-MMA) is that water insoluble polymers are assumed to be more stable than water-soluble polymers after implantation, but do require the use of somewhat cytotoxic solvents during their formation.¹⁰⁸ The p(HEMA-*co*-MMA) microcapsules were predicted to be biocompatible since poly(MMA) and poly(HEMA) constituents have been successfully used for biomedical purposes.¹⁰⁹ To date, there are no published results available for *in vivo* delivery of therapeutic proteins from cells in p(HEMA-*co*-MMA) microcapsules. On the other hand, p(HEMA-*co*-EMA) has shown to elicit an immune reaction to the host.¹⁰⁶

Polyphosphazene is a synthetic polymer composed of alternating nitrogen and phosphorus atoms. While there are relatively few studies on the delivery of protein using polyphosphazene microcapsules, cells remain viable when encapsulated in an ionically cross linkable polyphosphazene and it has been shown that secretion of protein does occur *in vitro*.¹⁰⁷ However, *in vivo* biocompatibility of polyphosphazene microcapsules may be limited since the use of polyphosphazene elicited an immune response.¹¹⁰

Finally, Agarose (natural polymer) has been investigated for the microencapsulation of pancreatic islets and treatment of diabetes.¹¹¹ *In vivo* the microcapsule mechanical strength was increased. However, when pancreatic islets were encapsulated in agarose and implanted into mice, a cellular immune response was observed.¹¹²

Thus calcium alginate remains a promising matrix for cell encapsulations, but it would be desirable to improve the mechanical strength through biocompatible cross-linking. A number of alginate composite materials have also been explored for cell encapsulation.¹¹³ Compounds added to the alginate forming the bead core were designed to be thermally (agarose¹⁰⁰), ionically (carrageenan¹¹⁴) or photochemically gelled,¹¹⁵ or designed to modify viscosity or water content (carboxymethylcellulose¹¹⁶), act as wall forming materials (heparin,¹¹⁶ cellulose sulphate¹¹⁷), control permeability or provide an improved environment for cell growth (chitlac - lactitol-functionalized chitosan¹⁰²). For example, capsules designed for longer-term cell implantation have been prepared with alginate-cellulose sulfate composite cores where the cellulose sulfate acted as a viscosity modifier and was thought to be a better wall builder than alginate when forming polyelectrolyte complexes with the polycations used to coat the capsules.¹¹⁷

Still other composite cores have been formed by the in-diffusion of polymeric or monomeric species followed, in some cases, by cross-linking or polymerization. To study the properties like controlled release and swelling, physical interpenetrating networks were reported using alginate and chitosan¹¹⁸ or acrylic acid.¹¹⁹ Gaserod et al¹²⁰ found that the in-diffusion of low MW chitosan into CaAlg beads resulted in the formation of an alginate-chitosan gel in the core of the capsule that was able to withstand the loss of

calcium. Smeds et al¹²¹ introduced methacrylate groups to alginate to study the degree of methacrylate modification and covalent affect mechanical properties like swelling, compression, and creep compliance of alginate based hydrogel.

Several groups have tried to improve the strength of alginate-based materials via the photo polymerization of (meth)acrylate-functionalized alginate^{121,122,123,124,125} or of other monomers within the alginate core.^{126,127} Childs and coworkers formed a capsule composed of alginate and poly(sodium acrylate-*co*-N-vinylpyrrolidone) formed by UV-photo polymerization of vinyl monomers allowed to diffuse into the CaAlg beads.¹²⁶ This approach worked reasonably well; through the presence of photoinitiator and added sodium acrylate did pose some toxicity challenge to the encapsulated cells. Recently, Hallé and coworkers^{128,129} studied APA microcapsules in which a photoactivatable cross-linker was used to covalently link the PLL layer with the adjacent alginate in both the core and the outer coating. These capsules displayed greatly improved mechanical stability while maintaining the cell viability and permeability of standard APA capsules. In addition, these covalently cross linked capsules prevents malignant cells to escape and proliferate into the body of recipients.¹³⁰

This thesis proposes to use synthetic polymers to strengthen Ca-alginate capsules. In particular, I plan to employ self-cross linking polyelectrolytes to form a tough “skin” around or to reinforce the core of Ca alginate microcapsules. In contrast to photochemical cross-linking, the key to this approach is that the ultimate cross-linking groups are already attached to the polyelectrolytes, such that they are not very bioavailable to the cells and hence should not pose a toxicity concern during encapsulation.

Copolymers of methacryloyl oxyethyl trimethyl ammonium hydrochloride with zero to 100% of amino ethyl methacrylate and the homopolymer of N-(3-aminopropyl) methacrylamide hydrochloride (APM), will be used as polycations, symbolically denoted as C100-C0, and PAPM, respectively. Copolymers of methacrylic acid sodium salts with 0 to 70% methacryloyloxy ethyl acetoacetate will be used as polyanions that are symbolically denoted as A100-A70 in this thesis. Methacrylate has been known as biocompatible materials, and many methacrylates are available.^{109, 131} Methacrylate has also been successfully used for medical purposes for long time. More over, the monomer pairs have approximately similar reactivity ratios.

It is well known that cells can be entrapped in calcium alginate gel beads by extruding cell containing alginate solution with a concentric airflow into the calcium chloride gelling bath. In the following steps calcium alginate or Ca (Alginate/A70) beads can be coated with polycation and polyanion by following the classical APA encapsulation protocol.⁵ During coating, in the first step, the quaternary amine group of the polycation will ionically cross-link with the carboxylate group of the polyanion. In the second step, the primary amine group of the polycation will covalently cross-link with the acetoacetate group of the polyanion. It is well understood that synthetic polymers offer the advantage of controlled synthesis, and one can easily modify the properties of the polyelectrolytes like hydrophobicity, charge density, cross linker content, and molecular weight. As the system contains ionic as well as covalent cross-links, we expect to be able to balance these two factors to achieve semipermeable shells or matrix with improved mechanical and biochemical resistance that would allow for longer-term protection of the encapsulated cells.

1.8 Research Objectives

The objectives of this thesis are:

1. To design, prepare and characterize self-cross-linking polyelectrolytes to be used to strengthen cell-containing calcium alginate capsules.
2. To study their polyelectrolyte properties, especially their ability to form polyelectrolyte complexes (PEC's) with each other, as well as with alginate and calcium.
3. To study their use in coating calcium alginate microcapsules, including the effects of polyelectrolyte composition and concentration on morphology, strength, permeability and cell viability (*in vitro* and *in vivo*) of the coated capsules
4. To study their use in the formation of multilayer Ca alginate capsules, including the effects of polyelectrolyte composition and concentration on morphology, strength, permeability and cell viability (*in vitro* and *in vivo*) of the coated capsules.
5. To examine the feasibility of using self-cross-linkable synthetic polycations as an alternative of poly-L-lysine as coating for alginate based microcapsules.
6. To study the feasibility of using synthetic polyelectrolytes to augment the core material of Ca alginate microcapsules, and to study the interaction of the anionic polyelectrolyte with calcium, diffusion of these polyanions within calcium alginate hydrogel matrices and interaction with polycations at the capsule surface or within the matrix.

1.9 References

- ¹ Chang, T. M. S. *Science*, **1964**, *146*, 524-525
- ² Chang, T. M. S.; MacIntosh, F. C.; Mason, S. G. *Can. J. Physiol. Pharmacol.* **1966**, *44*, 115-128
- ³ Sefton, M. V.; Stevenson, W. T. K. *Adv. Polym. Sci.* **1993**, *107*, 143-197
- ⁴ Bisceglie V. *Ztschr. Krebsforsch*, **1933**, *40*, 122-140
- ⁵ Lim, F.; Sun, A. M. *Science*, **1980**, *210*, 908-910
- ⁶ Prakash, S.; Chang, T. M. S. *Nat. Med.*, **1996**, *2*, 883-887
- ⁷ Sun, Y. L.; Ma, X. J.; Zhou, D. B.; Vacek, I.; Sun, A. M. *J. Clin. Invest*, **1996**, *98*, 1417-1422
- ⁸ Calafiore, R.; Basta, G.; Luca, G.; Lemmi, A.; Montanucci, M. P.; Calabrese, G.; Racanicchi, L.; Mancuso, F.; Brunetti, P. *Diabetes Care*, **2006**, *29*, 137-138
- ⁹ Emerich, D. F.; Thanos, C. G.; Goddard, M.; Skinner, S. J. M.; Geany, M. S.; Bell, W. J.; Bintz, B.; Schneider, P.; Chu, Y.; Babu, R. S.; Borlongan, C. V.; Boekelheide, K.; Hall, S.; Bryant, B.; Kordower, J. H. *Neurobiol. Dis.*, **2006**, *23*, 471-480
- ¹⁰ Moran, D. M.; Koniaris, L. G.; Jablonski, E. M.; Cahill, P. A.; Halberstadt, C. R.; McKillop, I. H. *Cell Transplant.* **2006**, *15*, 785-798
- ¹¹ Dvir-Ginzberg, M.; Konson, A.; Cohen, S.; Agbaria, R. J. *Biomed. Mater. Res. B Appl. Biomater.* **2007**, *80*, 59-66
- ¹² Zhang, H.; Zhu, S.-J.; Wang, W.; Wei, Y.-J.; Hu, S.-S. *Gene Ther.* **2008**, *15*, 40-48
- ¹³ Dove, A. *Nature Biotechnol.* **2002**, *20*, 339-343
- ¹⁴ Karp, J. M.; Langer, R. *Curr. Opin. Biotechnol.* **2007**, *18*, 454-459
- ¹⁵ Zimmermann, H.; Ehrhart, F.; Zimmermann, D.; Muller, K.; Globa, A. K.; Behringer,

-
- M.; Feilen, P. J.; Gessner, P.; Zimmermann, G.; Shirley, S. G.; Weber, M. M.; Metze, J.; Zimmermann, U. *Appl. Phys. A. Mater. Sci. pros.* **2007**, *89*, 909-922
- ¹⁶ Dominguez, D. C.; Lopes, R.; Torres, M. L.; *Clin. Lab. Sci.* **2007**, *20*, 245-248
- ¹⁷ Yasuhara, T.; Date, I. *Cell Transplant.*, **2007**, *16*, 125-132
- ¹⁸ Benny, O.; Kim, S. K.; Gvili, K.; Radzishovsky, I. S.; Mor, A.; Verduzco, L.; Menon, L. G.; Black, P. M.; Machluf, M.; Carroll, R. S. *FASEB J.* **2008**, *22*, 488-499
- ¹⁹ Calafiore, R.; Basta, G.; Luca, G.; Lemmi, A.; Montanucci, M. P.; Calabrese, G.; Racanicchi, L.; Mancuso, F.; Brunetti, P. *Transplant. Proc.* **2006**, *38*, 1156-1157
- ²⁰ Uludag, H.; De Vos, P.; Tresco, P. A. *Adv. Drug Deliv. Rev.* **2000**, *42*, 29-64
- ²¹ Redenbaugh, K.; Paasch, B. D.; Nichol, J. W.; Kossler, M. E.; Viss, P. R.; Walker, K. *A. Biotechnol.*, **1986**, *4*, 797-801
- ²² King, C. J. *Chem. Eng. Prog.* **1990**, *June*, 33-39
- ²³ Stamberg, J.; Dautzenberg, H.; Loth, F.; Benes, M.; Kuhn, A. D.D.R. Patent. 218 372, C08 B 15/06, 16.7.83/6.2.85.
- ²⁴ Li, W.; Nicol, F.; Szoka, F. C. *Adv. Drug Del. Rev.*, **2004**, *56*, 967-985
- ²⁵ Lukas, J.; Palaeckova, V.; Mokry, J.; Karbanova, J.; Dvorankova, B. *Macromol. Symp.* **2001**, *172*, 157-165
- ²⁶ Desmangles, A. I.; Jordan, O.; Marquis- Weible, F. *Biotechnol. Bioeng.* **2001**, *72(6)*, 634-641
- ²⁷ Hubbell, J. A. *J. Control. Rel.*, **1996**, *39*, 305-313
- ²⁸ Missirlis, D.; Tirelli, N.; Hubbell, J. A. *Langmuir*, **2005**, *21*, 2605-2513
- ²⁹ DeLong, S. A.; Moon, J. J.; West, J. L. *Biomaterials*, **2005**, *26*, 3227-3234
- ³⁰ Yang, F.; Williams, C. G.; Wang, D. A.; Lee, H. *Biomaterials*, **2005**, *26*, 5991-5998

-
- ³¹ Cruise, G. M.; Heggre, O. D.; Lamberti, F. V.; Hager, S. R.; Hill, R.; Scharp, D. S.; Hubbell, J. A. *Cell Transplant.*, **2000**, *8*, 293-306
- ³² Williams, C. G.; Malik, A. N.; Kim, T. K.; Manson, P. N.; Elisseeff, J. H. *Biomaterials*, **2005**, *26*, 1211-1218
- ³³ Dusseault, J.; Leblond, F. A.; Robitaille, R.; Joudan, G.; Tessier, J.; Menard, M.; Henly, N.; Halle, J. -P. *Biomaterials*, **2005**, *26*, 1515-1522
- ³⁴ Decher, G.; Hong, J. D. *Makromol. Chem. Macromol. Symp.* **1991**, *46*, 321-327
- ³⁵ Decher, G. *Science*, **1997**, *277*, 1232-1237
- ³⁶ Leung, A.; Trau, M.; Nielsen, L. K. *J. Biomed. Mater. Res. A*, **2009**, *88*, 226-237
- ³⁷ Sukhishvili, S. A.; Kharlampieva, E.; Izumrudov, V. *Macromolecules*, **2006**, *39*, 8873-8881
- ³⁸ Choi, J.; Rubner, M. F. *Macromolecules*, **2005**, *38*, 116-124
- ³⁹ Kabanov, V. A.; Zezin, A. B.; Rogacheva, V. B.; Gulyaeva, Z. G.; Zansochova, M. F.; Joosten, J. G. H.; Brackman, J. *Macromolecules*, **1999**, *32*, 1904-1909
- ⁴⁰ Vanerek, A.; van de Ven, T. G. M. *Colloids Surf Part A: Physicochem. Eng. Aspects* **2006**, *273*, 55-62
- ⁴¹ Martinez- Ruvalcaba, A.; Chornet, E.; Rodrigue, D. *Carbohydr. Polym.* **2007**, *67*, 586-595
- ⁴² Paneva, D.; Mespouille, L.; Manolova, N.; Degee, P.; Rashkov, I.; Dubois, P. *J. Polym. Sci. Part A: Polym. Chem.* **2006**, *44*, 5468-5479
- ⁴³ Fredheim, G. E.; Christensen, B. E. *Biomacromolecules*, **2003**, *4*, 232-239
- ⁴⁴ Vogel, M. K.; Cross, R. A.; Bixler, H. J. *J. Macromol. Sci. Chem A*, **1970**, *4(3)*, 675-692

-
- ⁴⁵ Thunemann, A. F.; Muller, M.; Dautzenberg, H.; Joanny, J. -F.; Lowen, H. *Adv. Polym. Sci.* **2004**, *166*, 113-171
- ⁴⁶ Kato, N.; Schuetz, P.; Fery, A.; Caruso, F. *Macromolecules*, **2002**, *35*, 9780-9787
- ⁴⁷ Burgess, D. J. *J. Colloid Interface Sci.*, **1990**, *140*, 227-238
- ⁴⁸ Mohanty, B.; Bohidar, H. B. *Biomacromolecules*, **2003**, *4*, 1080-1086
- ⁴⁹ Piculell, L.; Lindman, B. *Adv. Colloid Interface Sci.* **1992**, *41*, 149-178
- ⁵⁰ Leclercq, S.; Milo, C.; Reineccius, G. A. *J. Agric. Food Chem.*, **2009**, *57*, 1426-1432
- ⁵¹ Wen, Y.; Dubin, P. L. *Macromolecules*, **1997**, *30*, 7856-7861
- ⁵² Arshady, R. *Polym. Eng. Sci.* **1990**, *30*, 905-914
- ⁵³ Kaibara, K.; Okazaki, T.; Bohidar, H. B.; Dubin, P. L. *Biomacromolecules*, **2000**, *1*, 100-107
- ⁵⁴ Prokop, A.; Hunkeler, D.; DiMari, S.; Haralson, M.; Wang, T. G. *Adv. Polym. Sci.*, **1998**, *136*, 1-51
- ⁵⁵ Khutoryanskaya, O. V.; Mayeva, Z. A.; Mun, G. A.; Khutoryanskiy, V. V. *Biomacromolecules*, **2008**, *9*, 3353-3361
- ⁵⁶ Miyazaki, H.; Kataoka, K. *Polymer*, **1996**, *37(4)*, 681-685
- ⁵⁷ Yin, X.; Stöver, H. D. H. *Macromolecules*, **2003**, *36*, 9817-9822
- ⁵⁸ Maeda, T.; Kanda, T.; Yonekura, Y.; Yamamoto, K.; Aoyagi, T. *Biomacromolecules*, **2006**, *7*, 545-549
- ⁵⁹ Andrianov, A. K. J. *Inorg. Organometallic. Polym. Mater.* **2006**, *16*, 397-406
- ⁶⁰ Vanerek, A.; Van de Ven, T. G. M. *Colloids and Surfaces A*, **2006**, *273*, 55-62
- ⁶¹ Wang, F.; Tong, W.; Li, J.; Gao, C. *Macromol. Chem. Phys.* **2008**, *209*, 957-966
- ⁶² Dusseault, J.; Langlois, G.; Meunier, M.-C.; Menard, M.; Perreault, C.; Halle, J.-P.

Biomaterials, **2008**, *29*, 917-924

⁶³ Holme, H. K.; Davidsen, L.; Kristiansen, A.; Smidsrod, O. *Carbohydr. Polym.* **2008**, *73*, 656-664

⁶⁴ Chodankar, S.; Aswal, V. K.; Kohlbrecher, J.; Vavrin, R. Wagh, A. G. *Phys. Rev. E* **2008**, *78*, 319131-319138

⁶⁵ Lacik, I. *Aust. J. Chem.* **2006**, *59*, 508-524

⁶⁶ Nastruzzi, C.; Luca, G.; Basta, G.; Calafiore, R., in focus on biotechnology: Applications of cell immobilization biotechnology (Eds V. Nedovic, R. Willaert, Springer: Berlin) **2005**, P1, pp. 17-37

⁶⁷ Ghosh, S. K., in focus on Functional Coatings by Polymer Microencapsulation (Ed Swapan Kumar Ghosh Wiley-VCH), **2006**

⁶⁸ Orive, G.; Hernandez, R. M.; Gascon, A. R.; Pedraz, J. L. microencapsulation for Disease Treatment (Eds V. Nedovic, R. Willaert, Springer: Berlin) **2005**, P2, pp. 185-196

⁶⁹ Zimmermann, H.; Shirley, S. G.; Zimmermann, U. *Curr. Diabet. Rep.* **2007**, *7*, 314-320

⁷⁰ Strand, B. L.; Ryan, L.; Veld, P. I.; Kulseng, B.; Rokstad, A. M.; Skjak-Braek, G.; Espevik, T. *Cell Transplant.*, **2001**, *10*, 263-275

⁷¹ Peirone, M.; Ross, C. J. D.; Hortelano, G.; Brash, J. L.; Chang P. L. *J. Biomed Mater Res*, **1998**, *42*, 587-596

⁷² Van Raamsdonk, J. M.; Cornelius, R. M.; Brash, J. L.; Chang, P. L. *J. Biomater. Sci. Polym. Ed.*, **2002**, *13*, 863-884

⁷³ Rokstad, A. M.; Holton, S.; Strand, B.; Steinkjer, B.; Ryan, L.; Kulseng, B.; Skjak-

-
- Braek, G.; Espevik, T. *Cell Transplant.*, **2002**, *11*, 313-324
- ⁷⁴ Mørch, Y. A.; Donati, I.; Strand, B. L.; Skjåk-Bræk, G. *Biomacromolecules*, **2006**, *7*, 1471-1480.
- ⁷⁵ Zekorn T.; Siebers, U.; Horcher, A.; Schnettler, R.; Klock, G.; Bretzel, R. G.; Zimmerman, U.; Federlin, K. *Transplant. Proc.*, **1992**, *24(3)*, 937-939
- ⁷⁶ Zimmermann, H.; Zimmermann, D.; Reuss, R. *J. Mater. Sci., Mater. Med.* **2005**, *16*, 491-501
- ⁷⁷ Darrabie, M. D.; Kendall, W. F.; Opara, E. C. *J. Microencapsul.*, **2006**, *23*, 613-621
- ⁷⁸ Lanza, R. P.; Kuhlreiber, W. M.; Ecker, D.; Staruk, J. K.; Chick, W. L.; *Transplantation*, **1995**, *59(10)*, 1377-1384
- ⁷⁹ Gaserod, O.; Smidsrod, O.; Skjak-Braek, G. *Biomaterials*, **1998**, *19*, 1815-1825
- ⁸⁰ Bunger, C. M.; Gerlach, C.; Freier, T.; Schmitz, K. P.; Pilz, M.; Werner, C.; Jonas, L.; Schareck, W.; Hopt, U. T.; De Vos, P. J. *J. Biomed. Mater. Res.* **2003**, *67A*, 1219-1227
- ⁸¹ Haque, T.; Chen, H.; Ouyang, W.; Martini, C.; Lawuyi, B.; Urbanska, A. M.; Prakash, S. *Mol. Pharmaceutics*, **2005**, *2*, 29-36
- ⁸² Darrabie, M. D.; Kendall Jr, W. F.; Opara, E. C. *Biomaterials* **2005**, *26*, 6846-6852
- ⁸³ Leung, A.; Lawrie, G.; Nielson, L. K.; Trau, M. *J. Microencapsul.*, **2008**, *25*, 387-398
- ⁸⁴ Wang, Y. *J. Mater. Sci. Eng C*, **2000**, *13*, 59-63
- ⁸⁵ Schneider, S.; Feilen, P. J.; Sloty, V.; Kampfner, D.; Preuss, S.; Berger, S.; Beyer, J.; Pommersheim, R. *Biomaterials*, **2001**, *22*, 1961-1970
- ⁸⁶ Dufrane, D.; Van Steenberghe, M.; Goebbels, R. M.; Saliez, A.; Guiot, Y.; Gianello, P. *Biomaterials*, **2006**, *27*, 3201-3208

-
- ⁸⁷ Cai, X.; Lin, Y.; Ou, G.; Luo, E.; Man, Y.; Yuan, Q.; Gong, P. *Cell Biol. Int.* **2007**, *31*, 776-783
- ⁸⁸ Dean, S. K.; Yulyana, Y.; Williams, G.; Sidhu, K. S.; Tuch, B. E. *Transplantation*, **2006**, *82*, 1175-1184
- ⁸⁹ Evangelista, M. B.; Hsiong, S. X.; Fernandes, R.; Sampaio, P.; Kong, H. J.; Barrias, C. C.; Salema, R.; Barbosa, M. A.; Mooney, D. J.; Granja, P. L. *Biomaterials*, **2007**, *28*, 3644-3655
- ⁹⁰ Hill, E.; Boontheekul, T.; Mooney, D. J. *Proc. Natl. Acad. Sci. U. S. A.* **2006**, *103*, 2494-2499
- ⁹¹ Morch, Y. A.; Donati, I.; Strand, B. L.; Skjak-Braek, G. *Biomacromolecules*, **2007**, *8*, 2809-2814
- ⁹² Smith, A. M.; Harris, J. J.; Shelton, R. M.; Perrie, Y. *J. Control. Release* **2007**, *119*, 94-101
- ⁹³ Sakai, S.; Hashimoto, I.; Ogushi, Y.; Kawakami, K. *Biomacromolecules*, **2007**, *8*, 2622-2626
- ⁹⁴ Ding, H. F.; Liu, R.; Li, B. G.; Lou, J. R.; Dai, K. R.; Tang, T. T. *Biochem. Biophys. Res. Commun.* **2007**, *362*, 923-927
- ⁹⁵ Murua, A.; de Castro, M.; Orive, G.; Hernandez, R. M.; Pedraz, J. L. *Biomacromolecules*, **2007**, *8*, 3302-3307
- ⁹⁶ Wang, X.; Wang, W.; Ma, J.; Guo X.; Yu, X.; Ma, X. *Biotechnol. Prog.* **2006**, *22*, 791-800
- ⁹⁷ Dusseault, J.; Langlois, G.; Meunier, M.; Menard, M.; Perrault, C.; Hallé, J. -P. *Biomaterials*, **2008**, *29*, 917-924

-
- ⁹⁸ Yim, E. K. F.; Wan, A. C. A.; Le Visage, C.; Liao, I. C.; Leong, K. W. *Biomaterials*, **2006**, *27*, 6111- 6122
- ⁹⁹ Wilson, J. T.; Cui, W.; Sun, X.; Tucker-Burden, C.; Weber, C. J. Chaikof, E. L. *Biomaterials*, **2007**, *28*, 609-617
- ¹⁰⁰ Sakai, S.; Hashimoto, I.; Kawakami, K. *Biochem. Eng. J.* **2006**, *30*, 76-81
- ¹⁰¹ Marsich, E.; Borgogna, M.; Donati, I.; Mozetic, P.; Strand, B. L.; Salvador, S. G.; Vittur, F.; Paoletti, S. *J. Biomed. Mater. Res. A* **2008**, *84*, 364-376
- ¹⁰² Donati, I.; Haug, I. J.; Scarpa, T.; Borgogna, M.; Draget, K. I.; Skjak-Braek, G.; Paoletti, S. *Biomacromolecules*, **2007**, *8*, 957-962
- ¹⁰³ Thanos, C. G.; Calafiore, R.; Basta, G.; Bintz, B. E.; Bell, W. J.; Hudak, J.; Vasconcellos, A.; Schneider, P.; Skinner, S. J. M.; Geaney, M.; Tan, P.; Elliot, R. B.; Tatnell, M.; Escobar, L.; Qian, H.; Mathiowitz, E.; Emerich, D. F. *J. Biomed. Mater. Res. A* **2007**, *83*, 216-224
- ¹⁰⁴ Elliot, R. B.; Escobar, L.; Tan, P. L. J.; Garkavenko, O.; Calafiore, R.; Basta, P.; Vasconcellos, A. V.; Emerich, D. F.; Thanos, C.; Bamba, C. *Transplant. Proc.* **2005**, *37*, 3505-3508
- ¹⁰⁵ Vallbacka, J. J.; Sefton, M. V. *Tissue Eng.* **2007**, *13(9)*, 2259-2269
- ¹⁰⁶ Mokry, J.; Karbanova, J.; Lukas, J.; Paleckova, V.; Dvorankova, B. *Biotechnol. Prog.* **2000**, *16*, 897-904
- ¹⁰⁷ Bano, M. C.; Chen, S.; Visscher, K. B.; Allock, H. R.; Langer, R. *Nat. Biotechnol.*, **1991**, *9*, 468-471
- ¹⁰⁸ Sefton M.V.; *Biomaterials*, **1993**, *14*, 1127-1134
- ¹⁰⁹ Crooks, C. C.; Douglas, J. A.; Broughton, R. L.; Sefton, M.V. *J. Biomed. Mater. Res.*,

-
- 1990, 24, 1241-1262
- ¹¹⁰ De Scheerder, I. K.; Wilczek, K. L.; Verbeken, E.V.; Vandorpe, J.; Lan P.N.; Schacht E.; De Geest, H.; Piessens, J. *Atherosclerosis*, **1995**, *114(1)*, 105-114
- ¹¹¹ Orive, G.; Hernandez, R. M.; Gascon, A. R.; Igartua, M.; Rojas, A.; Pedraz, J. L. *Biotechnol Bioeng*, **2001**, *76*, 285-294
- ¹¹² Kobayashi, T.; Aomatsu, Y.; Iwata, H.; Kin, T.; Kanehiro, H.; Hisanaga, M.; Ko, S.; Nagao, M.; Nakajima, Y. *Transplant*. **2003**, *75*, 619-624
- ¹¹³ Prokop, A.; Hunkeler, D.; Powers, A. C.; Whitesell, R.; Wang, T. G. *Adv. Polym. Sci.*, **1998**, *136*, 53-73.
- ¹¹⁴ Prakash, S.; Martoni, C. *Appl. Biochem. Biotechnol.*, **2006**, *128*, 1-21
- ¹¹⁵ Hertzberg, S.; Moen, E.; Vogelsang, C.; Østgaard, K. *Appl. Microbiol. Biotechnol.*, **1995**, *43*, 10-17
- ¹¹⁶ Prokop. A.; Hunkeler, D.; Dimari, S.; Haralson, M. A.; Wang, T. G. *Adv. Polym. Sci.*, **1998**, *136*, 1-51
- ¹¹⁷ Wang. T.; Lacik, T.; Brissova, M.; Anilkumar, A. V.; Prokop, A.; Hunkeler, D.; Green, R.; Shahrokhi, K.; Powers, A. C. *Nat. Biotechnol.*, **1997**, *15*, 358-362
- ¹¹⁸ Chandy, T.; Mooradian, D. L.; Rao, G. H. R. *J. Appl. Polym. Sci.* **1998**, *70*, 2143-2153
- ¹¹⁹ Yuk, S. H.; Cho, S. H.; Shin, B. C.; Lee, H. B. *Eur. Polym. J.* **1996**, *32*, 101-104
- ¹²⁰ Gaserod, O.; Sannes, A.; Skjak-Braek, G. *Biomaterials*, **1999**, *20*, 773-783
- ¹²¹ Smeds, K. A.; Grinstaff, M. W. *J. Biomed. Mater. Res.* **2001**, *54*, 115-121
- ¹²² Hubbell, J. A.; Pathak, C. P.; Sawhney, A. S.; Desai, N. P.; Hossainy, S. F. A. Gels for encapsulation of biological materials US Patent 5, 529,914, 1996
- ¹²³ Soon-Shiong, P.; Heintz, R. A.; Skjak-Braek, G. Microencapsulation of cells US

Patent 5, 762,959, 1998

- ¹²⁴ Soon-Shiong, P.; Desai, N. P.; Sandford, P. A.; Heintz, R. A.; Sojomihardjo, S.
Crosslinkable polysaccharides, polycations and lipids useful for encapsulation and drug release US Patent 5, 837,747, 1998
- ¹²⁵ Rokstad, A. M.; Donati, I.; Borgogna, M.; Oberholzer, J.; Strand, B. L.; Espevik, T.; Skjåk-Braek, G. *Biomaterials*, **2006**, *27*, 4726-4737
- ¹²⁶ Wang, M.; Childs, R. F.; Chang, P. L. *J. Biomater. Sci. Polym. Edn.* **2005**, *16*, 91-113
- ¹²⁷ Araki, T.; Hitchcock, A. P.; Shen, F.; Chang, P. L.; Wang, M.; Childs, R. F. *J. Biomater. Sci. Polym. Edn.* **2005**, *16*, 611-627
- ¹²⁸ Dusseault, J.; Leblond, F. A.; Robitaille, R.; Jourdan, G.; Tessier, J.; Menard, M.; Henly, N.; Hallé, J.-P. *Biomaterials*, **2005**, *26*, 1515-1522
- ¹²⁹ Leblond, F. A.; Hallé, J. -P. Semi-permeable microcapsule with covalently linked layers and method for producing the same US Patent 7128931, 2006
- ¹³⁰ Dusseault, J.; Langlois, G.; Meunier, M. -C.; Menard, M.; Perreault, C.; Halle, J.-P. *Biomaterials*, **2008**, *29*, 917-924
- ¹³¹ Scranton, A. B.; Rangarajan, B.; Klier, J. *Adv. Polym. Sci.*, **1995**, *122*, 1-54

Chapter 2: Polyelectrolyte Complexation between Poly(methacrylic acid, sodium salt) and Poly(diallyldimethylammonium chloride) or Poly[2-(methacryloyloxyethyl) trimethyl ammonium chloride]

Burke, N. A. D.; Mazumder, M. A. J.; Hanna, M.; Stöver, H. D. H.

Published in *Journal of Polymer Science: Part A: Polymer Chemistry*, **2007**, *45*, 4129-4143.

This chapter has been reproduced with permission from *J. Polym. Sci., Part A: Polym. Chem.* Copyright 2007 John Wiley & Sons, Inc.

Contributions:

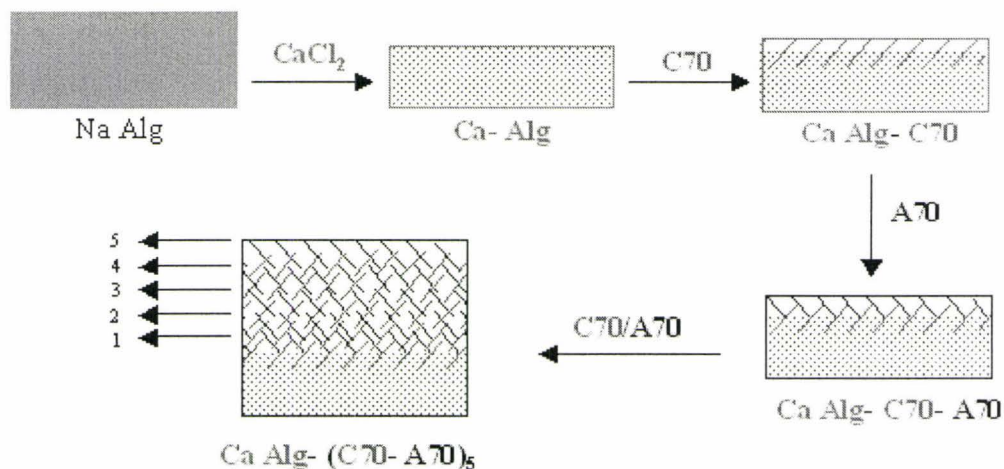
I performed all the experiments except for some of the complexation studies, in particular those between PDADMAC and p(MAANa-co-LMA) or p(MAANa-co-PEGMA) which were carried out by Dr Nicholas A. D. Burke. Mark Hanna prepared low molecular weight PMOETAC. The manuscript was written by Dr Nicholas A. D. Burke and edited by Dr Harald D. H. Stöver and myself.

Table 3.2: Weight and thickness of hydrogel films prepared on glass cover slides.

Film	Weight of film (mg)		Thickness of wet film (μm)	
	Wet film	Dry film	From film wt ^a	From OM ^b
Na-Alg	54 ± 5	1.0 ± 0.1	86 ± 8	80 ± 8
Ca-Alg	19 ± 5	1.2 ± 0.1	31 ± 8	26 ± 3
Ca-Alg-C70	19 ± 5	1.5 ± 0.1	30 ± 8	25 ± 3
Ca-Alg-C70-A70	23 ± 5	1.7 ± 0.1	37 ± 8	31 ± 3
Ca-Alg-(C70-A70) ₁₀	54 ± 5	2.9 ± 0.1	86 ± 8	80 ± 8

a. assuming a film density of 1.0 g/cm^3 ; b. Optical microscopy

The original Na-Alg hydrogel film had a water content of about 98%, which decreased to about 94% after gelling with calcium chloride for three minutes or longer. Except for the first C70 layer, each polyelectrolyte exposure caused gains in weight and thickness (Figure 3.1), a typical trend for layer-by-layer assembly.^{42,43} The average incremental thickness of each bilayer is $\sim 5 \mu\text{m}$, similar to results obtained by Goosen *et al* for a single bilayer.⁴⁴ This large incremental layer thickness is partly due to the porous, swellable nature of the Ca-Alg gel. Polycations such as C70 may diffuse into this porous gel, complexing with alginate and displacing Ca to a certain depth. Subsequent exposure to A70 should lead to charge reversal and formation of a crosslinked layer of C70A70.



Scheme 3.3: Formation of C70A70 bilayer or multilayers films by sequential coating of Ca-Alg hydrogel films on glass slides.

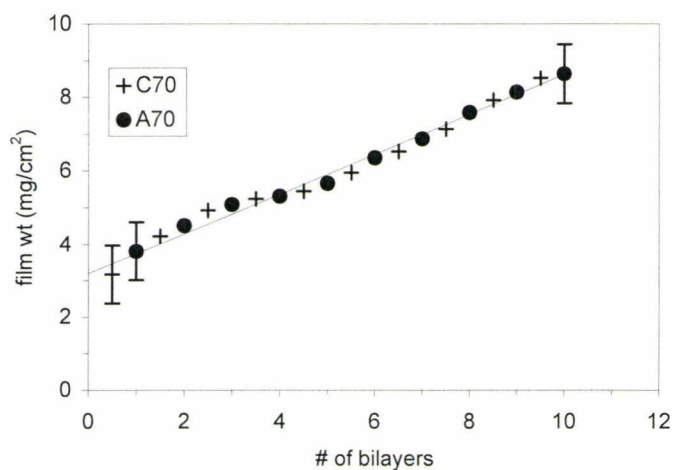


Figure 3.1: Film weights during formation of Ca-Alg-(C70-A70)₁₀ multilayer film on a glass cover slide.

Exposure of the Ca-AlgC70A70 film to sodium citrate (170 mM) to extract the calcium led to isolation of a thin crosslinked C70A70 film. This film was stable in NaCl

(2 M), confirming its crosslinked nature. In the following section, this approach is used to coat Ca-Alg beads.

3.3.2 Polyelectrolyte Coating of Ca-Alg Microcapsules:

The nature of the coating formed by interaction of polycations with Ca-Alg beads depends on factors such as polycation concentration and MW, and exposure time.^{4,44,45,46} The work by Bysell and Malmsten⁴¹ on the interaction of PLL with poly(acrylic acid) micro gels provides a good model for the present systems: at pH 7, they found low MW PLL (1-10 kg/mol) throughout the particle, together with significant but uniform shrinkage of the micro gel. Medium MW PLL (28-84 kg/mol) gave less shrinkage, while high MW PLL (84-170 kg/mol) gave the least shrinkage, but a wrinkled and dense outer layer. It was believed that the intermediate MW PLL could redistribute itself at the hydrogel surface during deswelling, while the high MW PLL formed a strong surface polyelectrolyte complex that could not redistribute itself, hence leading to a wrinkled surface layer.

In our case, Ca-Alg beads exposed to PLL or C70 appeared unchanged when examined by optical microscopy (OM) but trypan blue staining, as well as phase contrast OM (Figure 3.2a and 3.2c) indicated that the polycations were confined to the surface region. This is consistent with other studies that showed that polycations with MW greater than about 15 kg/mol are restricted to the surface region of Ca-Alg beads.^{44,46,47} Longer exposure times caused only slight increases in shell thickness as seen in phase contrast microscopy (Fig 3.2d vs. 3.2c), however, in a number of cases the beads became wrinkled (Fig 3.2b).

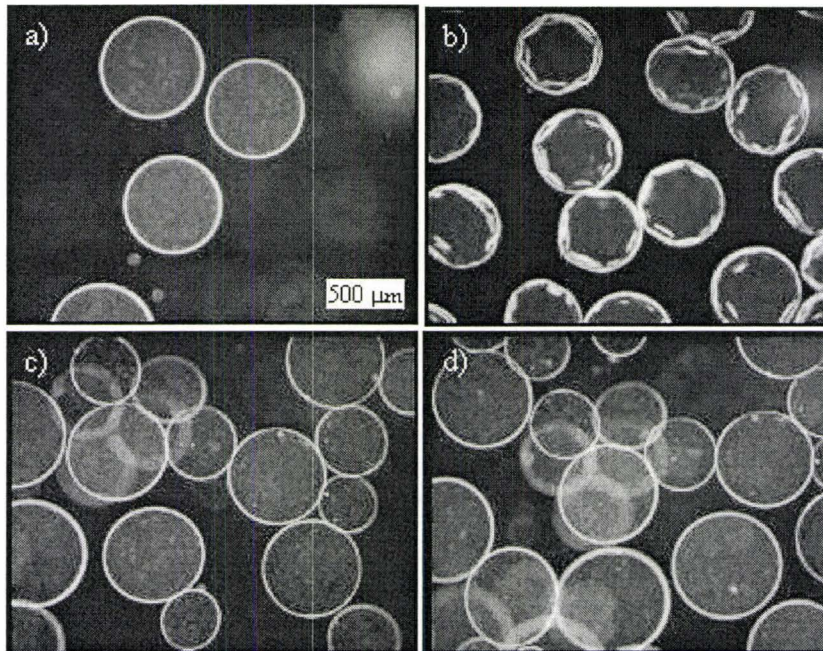


Figure 3.2: Phase contrast microscope images of Ca-Alg beads exposed to a 0.05% solution of PLL for a) 10 minutes, b) 30 minutes, or to a 0.05% solution of C70 for c) 10 minutes, d) 30 minutes, followed by saline washing.

Ca-Alg beads were coated with C70 concentrations ranging from 0.001 to 1%. Capsules coated at the lowest concentrations had incomplete or very thin shells and fared poorly in subsequent stability tests. Intermediate concentrations (0.01-0.1%) often led to capsule aggregation during coating. When coating was done at higher concentrations (0.5-1%), no aggregation occurred although wrinkling of the capsules was more likely as the concentration and, presumably, the osmotic pressure increased. Most subsequent experiments were performed using 0.5% C70 for coating since this avoided capsule aggregation and wrinkling. The C70 concentration is higher than the standard 0.05% PLL concentration but it does not produce shells that are significantly thicker (*vide infra*)

because penetration of the high MW C70 is limited. In the future, the coating process can likely be optimized (i.e., by addition of CaCl_2 or a surface stabilizer) to allow coating at lower C70 concentrations.

The C70 solutions used during coating acquired free calcium ions, revealed by the precipitation as CaCO_3 following treatment with NaOH and Na_2CO_3 . In addition to binding with free charges on alginate, C70 displaces some Ca^{2+} from the hydrogel. The displacement of calcium by the polycation has been mapped in detail using Scanning Transmission X-ray Microscopy, and will be reported separately.

Penetration depth of the polycation was further studied using Confocal Laser Scanning Microscopy (CLSM)^{41,48,49,50} and the fluorescein-labelled polycation C70f. Ca-Alg beads exposed to a 0.5% C70f solution showed a shell increasing from a few microns in thickness after 30 sec exposure (image not shown) to approximately $25 \pm 2 \mu\text{m}$ after 10 min exposure (Figure 3.3a). Continued exposure to 120 min leads to a wrinkled surface but no significant further increase in skin thickness or penetration (Figure 3.3b).

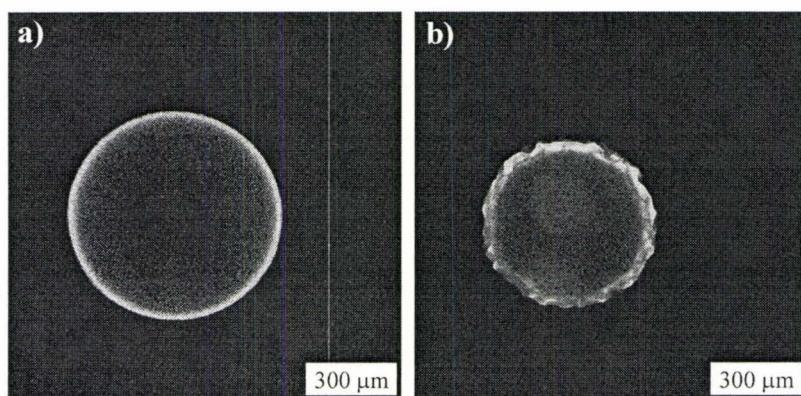


Figure 3.3: Confocal laser scanning microscopy image showing an equatorial section of representative Ca-Alg capsules exposed to a 0.5% solution of C70f for a) 10 minutes, and b) 120 minutes.

The coating process was further studied using A70f, a fluorescein-labelled version of A70. Capsules exposed to C70f and then A70f, each for 30 sec, showed a fluorescent shell approximately $7 \pm 1 \mu\text{m}$ thick (Figure 3.4a) that grew to approximately $26 \pm 2 \mu\text{m}$ thick when each exposure was increased to 10 min (Figure 3.4b). The thickness of the fluorescent layer was similar to that formed by C70f alone (Figure 3.3a) or to that formed when only one of the two polyelectrolytes was fluorescently labelled (Figures 3.4c and 3.4d), indicating that the A70f is approximately coincident with the C70f (Figure 3.4e).

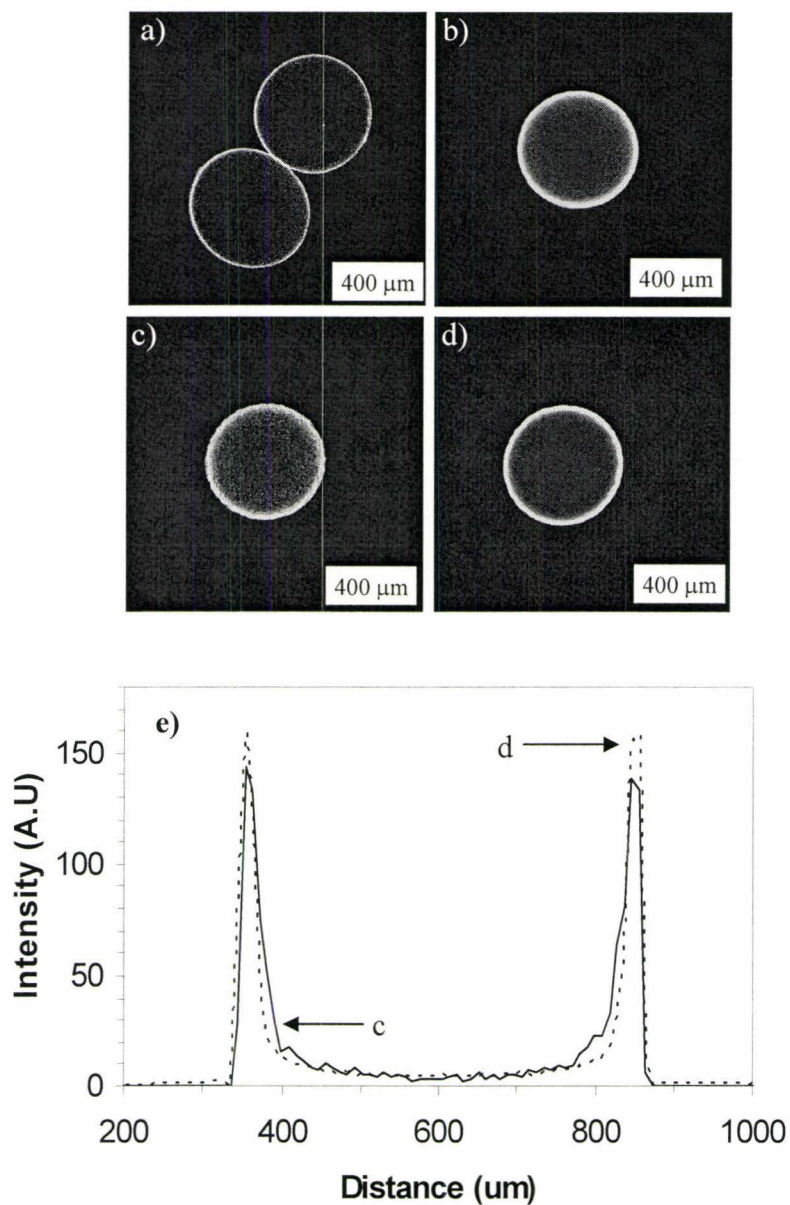


Figure 3.4: CLSM optical sections in the equatorial region of Ca-Alg beads exposed to 0.5% solution of polycation and polyanion for a) C70f and A70f; 30 sec each, b) C70f and A70f; 10 min each, c) C70f and A70; 10 min each d) C70 and A70f; 10 min each, e) intensity line profile of microcapsules c and d showing the distribution of C70f and A70f.

3.3.3 *Microcapsule Stability:*

The physicochemical stability of the Ca-Alg microcapsules was probed in several ways. As described earlier, a measure of the resistance to chemical degradation can be obtained by challenging the capsules with sodium citrate and high ionic strengths, which can lead to dissolution of the capsule core, and of the surface coating. Uncoated Ca-Alg beads are stiff gels at physiological salt concentrations. Upon treatment with 170 mM sodium citrate, the beads rapidly dissolved, as the Ca^{2+} was lost. When APA, AC70A70 or AC70A100 capsules (Figure 3.5, left column) were treated with citrate to liquefy the cores, the capsules swelled but the polyelectrolyte shells survived (Figure 3.5, centre column). The shells of APA and AC70A100, which are held together by ionic interactions alone, disappeared when further exposed to 2 M NaCl (Figure 3.5, right column, top/bottom), while the covalently crosslinked shell present in the AC70A70 capsules resisted this challenge unless punctured (Figure 3.5, right column, middle).

Mechanical stability was examined by exposing the capsules to osmotic pressure in a test developed by Chang and co-workers³⁸ or to the gradual loss of Ca^{2+} using an EDTA solution. Microcapsules were tumbled in hypotonic or EDTA solutions and the fraction of intact capsules was determined. APA and AC70A70 capsules that were empty (containing no cells) were subjected to the tests and the results are shown in Table 3.3. All of the capsules survive tumbling in SFM but the standard APA capsules are largely broken in the hypotonic or EDTA solutions after tumbling. APA capsules prepared with a 10x higher PLL concentration (0.5%) proved to be stable in distilled water (0% SFM) but 40% were broken in the EDTA solution. This higher PLL concentration would likely create a thicker Alg/PLL polyelectrolyte complex shell since at least a fraction of the 15-

30 kg/mol PLL will be able to penetrate into the Ca-Alg gel. In contrast, capsules made with 0.5% C100 showed similar stability to the standard APA capsules. C100, which has a considerably higher MW than PLL, will be restricted to the surface of the Ca-Alg gel and the shell that is formed is no stronger than that formed by 0.05% PLL. Similarly, C70 is restricted to the surface due to its high molecular weight, and the greater stability in the hypotonic and EDTA solutions compared to APA capsules is attributed to the formation of covalently crosslinked shells around the AC70A70 capsules.

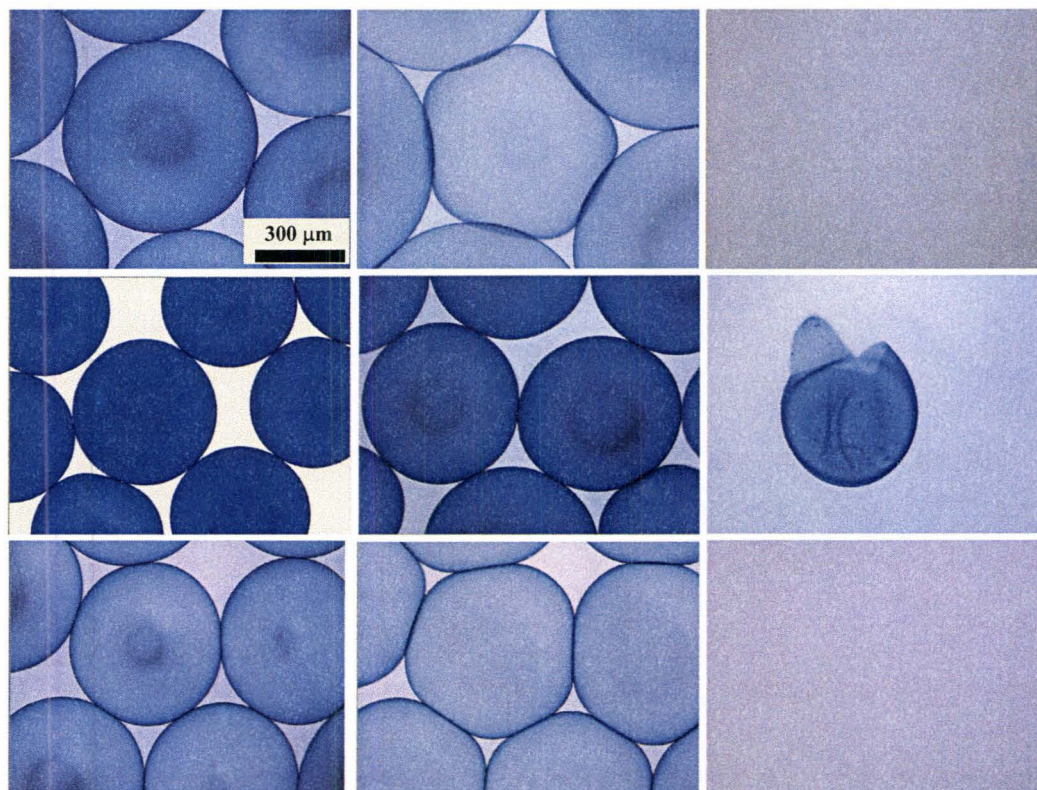


Figure 3.5: Optical microscope image of APA(0.05/0.03) (top row), AC70A70(0.5/0.5) (middle row) and AC70A100(0.5/0.5) (bottom row) microcapsules in: saline (left column), after exposure to 170 mM sodium citrate (centre column) and then 2 M NaCl (right column). Concentrations of polyelectrolytes (wt%) used to coat the capsules are

shown in brackets. Capsules were stained with trypan blue to facilitate observation. Size bar = 300 μm .

Table 3.3: Performance of empty APA and AC70A70 microcapsules in the OPT and calcium chelation test.

Microcapsules ^a	Percent intact capsules ^b			
	100% SFM	0.52% SFM	water	0.03% EDTA
APA (0.05/0.03)	99 \pm 1	15 \pm 10	0	0
APA (0.5/0.03)	--	--	100	60
AC100A (0.5/0.03)	99 \pm 1	15 \pm 10	--	--
AC70A70 (0.5/0.5)	100	100	100	100

a. Concentrations in brackets refer to polyelectrolyte concentrations (%w/v) used for coating. b. Capsules were tumbled for 3h in SFM solutions or 15 min in water or EDTA solution.

The OPT was used to examine the stability of capsules containing cells. APA(0.05/0.03) and AC70A70(0.5/0.5) capsules containing myoblast C₂C₁₂ cells were prepared and then incubated for times ranging from 4 to 72 h before the OPT (Figure 3.6). Both types of capsules showed reduced stability in comparison to the analogous empty capsules (Table 3.3). This effect of encapsulated cells on mechanical stability has been observed previously and was attributed to the interruption of the Ca-Alg gel by the cells.³⁸ The fraction of intact APA capsules decreased on moving from 6.5 to 0.52% SFM, with no effect observed for varying the duration of storage before the OPT. The AC70A70 capsules again performed better than the APA control capsules (Figure 3.6). In addition, the fraction of intact AC70A70 capsules increased with increasing storage time before the OPT, suggesting that the crosslinking reaction continues for several days after

coating. While the reaction between amine and acetoacetate groups is rapid in freely diffusing systems, it will slow as the movement of the polyelectrolytes becomes restricted. The change in the extent of crosslinking is probably not substantial after the first few hours because the polyelectrolytes become locked in place by electrostatic and covalent interactions. However, it appears that the additional curing time can lead to noticeable changes in the capsule strength. This extended curing reaction was not considered in our initial tests of capsule stability, which were typically conducted within 4 to 24 h of capsule preparation. The AC70A70 capsules might have shown even greater strength in these tests, had they been allowed to cure for a longer period of time.

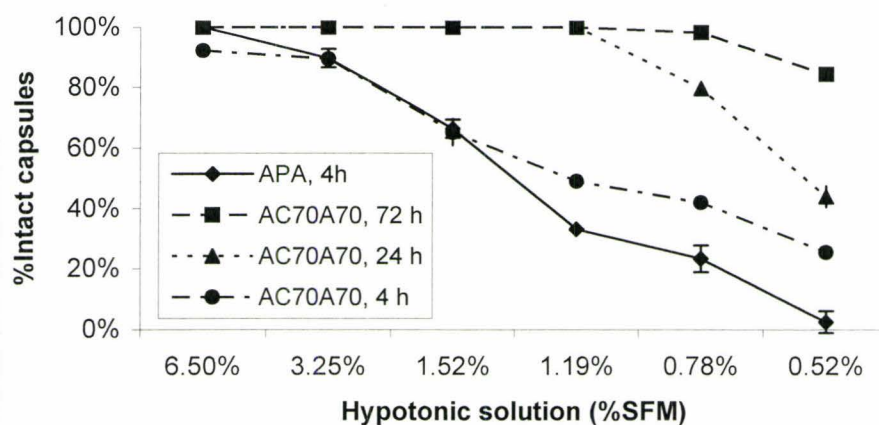


Figure 3.6: Percentage of intact cell-containing APA(0.05/0.03) and AC70A70(0.5/0.5) capsules after osmotic pressure test. Values in brackets denote polyelectrolyte concentrations (%w/v) used during coating. AC70A70 capsules were stored in saline for 4, 24 or 72 hours between coating and the OPT.

3.3.4 Permeability of AC70A70 Capsules:

Capsules used for immuno-isolation of non-autologous cells must have well-defined wall permeabilities, capable of preventing in-diffusion of immune modulators, but permitting any therapeutic protein to escape the capsule. This usually requires MW cut-offs for diffusion through the capsule shell of about 150 kg/mol.⁸ The size exclusion properties of the covalently cross linked membranes were tested by allowing a poly(ethylene glycol) mixture to diffuse through flat APA or AC70A70 model membranes made by coating one side of a Ca-Alg gel held in a porous, polypropylene support.²⁹ Figure 3.7 shows the GPC traces for the original PEG mixture and for concentrated samples from sink compartments for both membranes after 24 hrs of equilibration. It clearly shows that in both cases the high MW fraction of the PEG remains excluded from the sink, while the low MW fraction (<~20 kg/mol) can diffuse through the membrane. Above ~20 kg/mol, the PEG permeates the membrane more slowly and above ~170 kg/mol (vertical line in Figure 3.7) little or no PEG has passed through the membrane. These results indicate that the cross-linked AC70A70 capsule walls have MW cut-offs similar to those of APA control capsules, and are hence suitable for encapsulation of therapeutic non-autologous cells. Both sink solutions were concentrated by evaporation, and the higher intensity of curve b may be due to differing degrees of evaporation rather than greater diffusion.

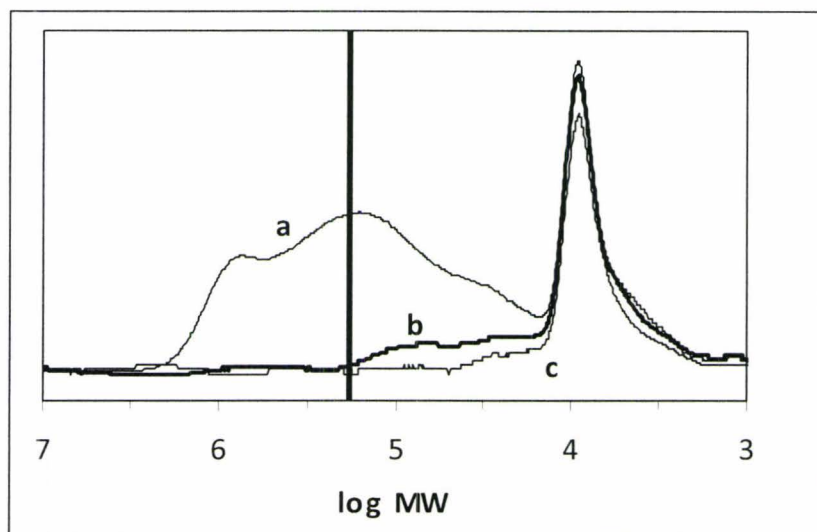


Figure 3.7: GPC traces of a) the original PEG mixture and the solution in the sink compartment of the stirred diffusion cell(s) separated by b) AC70A70(0.5/0.5), and c) APA(0.05/0.03) membranes after 24 h at room temperature (23 ± 2 °C). The sink samples were concentrated prior to analysis. The approximate MW cut-off is indicated by the vertical line at about 170 kg/mol.

3.3.5 Cell Viability in Microcapsules with Cross-linked Shells:

The viability of myoblast C_2C_{12} cells in APA and AC70A70 capsules was examined. Cell-containing AC70A70 capsules incubated for 1 week are shown in Figure 3.8 and were similar in appearance to APA capsules. The number of living cells per capsule was monitored vs. time of *in vitro* incubation (Figure 3.9). APA capsules contained about 90 living cells each after incubation for 1 day, rising to 240 cells/capsule after 7 days. Capsules coated with C70 and A70 contained significantly fewer living cells/capsule after incubation for 1 day. As the incubation continued, the number of cells/capsule rose in each case but the rise was most rapid for the capsules exposed to the

lower C70/A70 concentrations. This trend continued when still lower C70/A70 concentrations of 0.1% were used, though the data are not shown in Figure 3.9 because some capsule aggregation occurred making the capsules tested less representative of the whole sample. The reduced viability and proliferation, scaling with polyelectrolyte concentration, could be due to sub-optimal ionic strength or osmotic pressure during coating. While low MW impurities were removed from C70 by dialysis, the C70 likely contains shorter chains able to diffuse into the capsule interior where they may prove to be cytotoxic. Alternately, the formation of a coating that inhibits the in-diffusion of nutrients to the cells could be responsible. Although coating with C70/A70 has an initially negative impact on cell viability, the cells that survive the coating process remain viable and do begin to proliferate. The coating process with C70/A70 remains to be optimized further, and it should be possible to find conditions that are less harmful to the cells while still forming a robust coating and avoiding capsule aggregation.

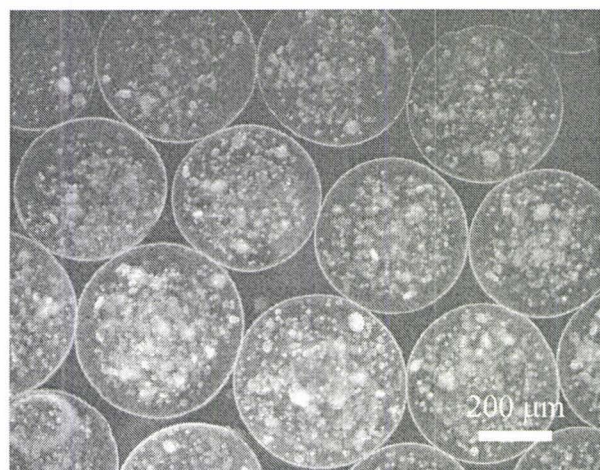


Figure 3.8: Phase contrast microscope image of C_2C_{12} cells encapsulated in AC70A70 after *in vitro* incubation for 1 week. Polyelectrolyte coatings prepared with 0.5% solutions and 10 min exposure times.

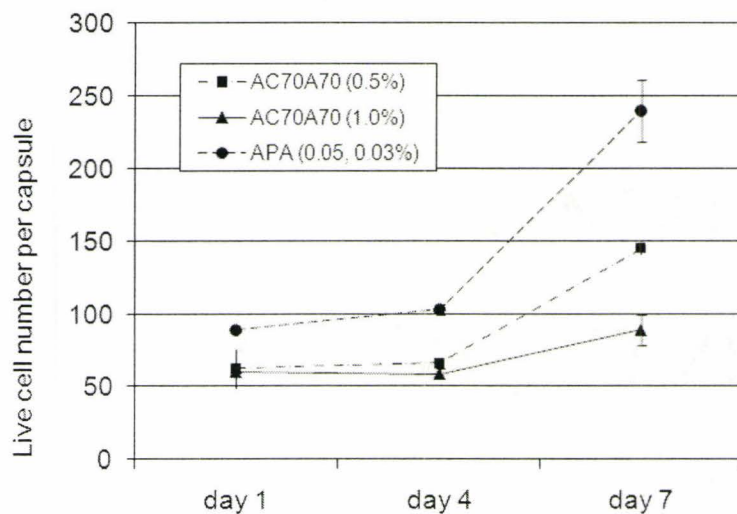


Figure 3.9: *In vitro* cell viability for C_2C_{12} cells encapsulated in APA and AC70A70 microcapsules. Values in parentheses refer to C70/A70 or PLL/Na-Alg concentrations used to coat the capsules.

Initial results with cell-containing AC70A70(0.5/0.5) capsules indicated significant fibroid over-coating on many capsules after implantation in mice for 1 to 2 weeks. This over-coating indicates an immune response of the host, and would limit viability of the encapsulated cells. The immune response appears to be related to the coating since cell-containing APA capsules prepared from the same Na-Alg do not show this immune response. Further experiments are currently underway to study the causes of this response, and to improve the *in vivo* performance of the new capsules.⁵¹

3.4 Conclusion

We have shown that covalently crosslinked shells can be formed around Ca-Alg capsules by coating with oppositely charged polyelectrolytes bearing complementary amine and acetoacetate reactive groups. Use of fluorescently labelled analogs of these polyelectrolytes indicates that they are concentrated near the surface of the Ca-Alg bead. Fluorescent layers of similar thickness are observed irrespective of which polyelectrolyte is labelled, indicating the presence of a homogeneous mixture of the two polyelectrolytes near the surface of the alginate bead. The thickness of this crosslinked shell increases moderately from about 7 to 25 micron upon increasing the exposure time, but appears to be ultimately limited by diffusion. The crosslinked nature of this outer shell was demonstrated by its resistance to citrate and 2 M sodium chloride. These capsules with crosslinked shells have greater resistance to osmotic pressure changes, and to mechanical stress tests, compared to APA control capsules. The crosslinked polyelectrolyte coating was found to have a MW cut-off of about 170 kg/mol, similar to that of an APA membrane and a value suitable for cell encapsulation. C₂C₁₂ cells were viable within Ca-Alg capsules coated with the new polyelectrolytes. The number of live cells within the capsules was somewhat lower than in APA capsules, but the number of live cells remained stable or increased with extended incubation. Preliminary implantation studies in mice revealed a fibroid overgrowth on many capsules. This immune response is related to the presence of the new polyelectrolytes and current studies are focused on reducing or eliminating the response.

In summary, these results describe a promising new approach to cell encapsulation. We believe that covalent reinforcement through use of self-crosslinking

polyelectrolytes provides a fundamental advantage in the long-term strengthening of Ca-Alg beads, combining the inherently low toxicity of polymer-bound reactive groups with the ability to modify coating thickness and possibly permeability, through changes in the polyelectrolytes or the coating process. Further studies of the *in vivo* use of these and related capsules are being conducted and will be reported shortly.

3.5 References

- ¹ Chang, T.M.S. *Science*, **1964**, *146*, 524-525.
- ² Bañó, M. C.; Cohen, S.; Visscher, K.B.; Allcock, H. R.; Langer, R. *Nat. Biotechnol.*, **1991**, *9*, 468-471.
- ³ Uludag, H.; Sefton, M. V. *Biotechnol. Bioeng.*, **1992**, *39*, 672-678
- ⁴ Thu, B.; Bruheim, P.; Espevik, T.; Smidsrød, O.; Soon-Shiong, P.; Skjåk-Bræk, G. *Biomaterials*, **1996**, *17*, 1031-1040.
- ⁵ Hübner, H. *Meth. Biotechnol.*, **2007**, *24*, 179-191.
- ⁶ Torre, M. L.; Faustini, M.; Attilio, K. M. E.; Vigo, D. *Rec. Patents Drug Deliv. Formul.*, **2007**, *1*, 81-85
- ⁷ Cirone, P.; Bourgeois, J. M.; Chang, P. L. *Hum. Gene Ther.*, **2003**, *14*, 1065-1077
- ⁸ Shen, F.; Li, A. A.; Gong, Y- K.; Somers, S.; Potter, M. A.; Winnik, F. M.; Chang, P. *L. Hum. Gene Ther.*, **2005**, *16*, 971-984
- ⁹ Lim, F.; Sun, A. M. *Science*, **1980**, *210*, 908-910
- ¹⁰ Vandenbossche, G.M.R.; Van Oostveldt, P.V.; Demeester, J.; Remon, J.-P. *Biotechnol. Bioeng.*, **1993**, *42*, 381-386.
- ¹¹ Schneider, S.; Feilen, P.J.; Brunnenmeier, F. *Diabetes*, **2005**, *54*, 687-693.
- ¹² Peirone, M. A.; Delaney, K.; Kwiecin, J.; Fletch, A.; Chang, P. L. *Hum. Gene Ther.*, **1998**, *9*, 195-206
- ¹³ Smidsrød O, Skjåk-Bræk G, *Trends Biotechnol.* **1990**, *8*, 71-78; Mørch, Y.A.; Donati, I.; Strand, B.L.; Skjåk-Bræk, G. *Biomacromolecules*, **2006**, *7*, 1471-1480.
- ¹⁴ Zekorn, T.; Siebers, U.; Horcher, A.; Schnettler, R.; Klock, G.; Bretzel, R. G.;

-
- Zimmerman, U.; Federlin, K. *Transplant. Proc.*, **1992**, *24*, 937-939.
- ¹⁵ Zimmermann, H.; Zimmermann, D.; Reuss, R. *J. Mater. Sci., Mater. Med.*, **2005**, *16*, 491-501.
- ¹⁶ Wang, T.; Lacik, I.; Brissova, M.; Anilkumar, A.V.; Prokop, A.; Hunkeler, D.; Green, R.; Shahrokhi, K. *Nat. Biotechnol.* **1997**, *15*, 358-362
- ¹⁷ Chandy, T.; Mooradian, D. L.; Rao, G. H. R. *J. Appl. Polym. Sci.*, **1998**, *70*, 2143-2153.
- ¹⁸ Bünger, C. M.; Gerlach, C.; Freier, T.; Schmitz, K. P.; Pilz, M.; Werner, C. Jonas, L.; Schareck, W.; Hopt, U. T.; De Vos, P. *J. Biomed. Mater. Res.*, **2003**, *67A*, 1219-1227
- ¹⁹ Darrabie, M. D.; Kendall Jr, W. F.; Opara, E. C. *Biomaterials*, **2005**, *26*, 6846-6852.
- ²⁰ Haque, T.; Chen, H.; Ouyang, W.; Martini, C.; Lawuyi, B.; Urbanska, A. M.; Prakash, S. *Mol. Pharmaceut.*, **2005**, *2*, 29-36.
- ²¹ Crooks, C. A.; Douglas, J. A.; Broughton, R. L.; Sefton, M. V. *J. Biomed. Mater. Res.*, **1990**, *24*, 1241-1262.
- ²² De Scheerder, I. K.; Wilczek, K. L.; Verbeken, E. V.; Vandorpe, J.; Lan, P. N.; Schacht, E.; De Geest, H.; Piessens, J. *Atherosclerosis*, **1995**, *114*, 105-114
- ²³ Chandy, T.; Mooradian, D. L.; Rao, G. H. R. *Artific. Organs*, **1999**, *23*, 894-903.
- ²⁴ Hubbell, J. A.; Pathak, C. P.; Sawhney, A. S.; Desai, N. P.; Hossainy, S. F. A. Gels for encapsulation of biological materials. US Patent 5529914, 1996.
- ²⁵ Soon-Shiong, P.; Heintz, R. A.; Skjåk-Bræk, G. Microencapsulation of cells. US Patent 5762959, 1998.
- ²⁶ Soon-Shiong, P.; Desai, N. P.; Sandford, P. A.; Heintz, R. A.; Sojomihardjo, S. Crosslinkable polysaccharides, polycations and lipids useful for encapsulation and

-
- drug release. US Patent 5837747, 1998.
- ²⁷ Smeds, K. A.; Grinstaff, M. W. *J. Biomed. Mater. Res.*, **2001**, *54*, 115-121
- ²⁸ Rokstad, A. M.; Donati, I.; Borgogna, M.; Oberholzer, J.; Strand, B. L.; Espevik, T.; Skjåk-Bræk, G. *Biomaterials*, **2006**, *27*, 4726-4737.
- ²⁹ Wang, M.; Childs, R. F.; Chang, P. L. *J. Biomater. Sci. Polym. Ed.*, **2005**, *16*, 91-113.
- ³⁰ Araki, T.; Hitchcock, A. P.; Shen, F.; Chang, P. L.; Wang, M.; Childs, R. F. *J. Biomater. Sci. Polym. Ed.*, **2005**, *16*, 611-627
- ³¹ Dusseault, J.; Leblond, F. A.; Robitaille, R.; Joudan, G.; Tessier, J.; Menard, M.; Henly, N.; Halle, J. -P. *Biomaterials*, **2005**, *26*, 1515-1522.
- ³² Leblond, F. A.; Halle, J.-P. Semi-permeable microcapsule with covalently linked layers and method for producing the same. US Patent 7128931, 2006.
- ³³ Scranton, A. B.; Rangarajan, B.; Klier, J. *Adv. Polym. Sci.*, **1995**, *122*, 1-54
- ³⁴ Petrak, K. *J. Bioact. Compat. Polym.*, **1986**, *1*, 202-219.
- ³⁵ Yu, Z.; Alesso, S.; Pears, D.; Worthington, P. A.; Luke, R. W. A.; Breadly, M. *Tetrahed. Lett.*, **2000**, *41*, 8963-8967.
- ³⁶ Burke, N. A. D.; Mazumder, M. A. J.; Hanna, M.; Stover, H. D. H. *J. Polym. Sci. A: Polym. Chem.*, **2007**, *45*, 4129-4143.
- ³⁷ Griebel, T.; Kulicke, W.-M.; Hashemzadeh, A. *Colloid Polym. Sci.*, **1991**, *269*, 113-120.
- ³⁸ Van Raamsdonk, J. M.; Chang, P.L. *J. Biomed. Mater. Res.*, **2001**, *54*, 264- 271.
- ³⁹ Li, A. A.; McDonald, N. C.; Chang P.L. *J. Biomater. Sci. Polym. Ed.*, **2003**, *14*, 533-549.
- ⁴⁰ Martinsen, A.; Storro, I.; Skjåk-Bræk, G. *Biotechnol. Bioeng.*, **1992**, *39*, 186-194.

-
- ⁴¹ Bysell, H.; Malmsten, M. *Langmuir*, **2006**, *22*, 5476-5484.
- ⁴² Olugebefola, S. C.; Ryu, S.-W.; Nolte, A. J.; Rubner, M. F.; Mayes, A. M. *Langmuir*, **2006**, *22*, 5958-5962.
- ⁴³ Xie, A. F.; Granick, S. *J. Am. Chem. Soc.*, **2001**, *123*, 3175-3176.
- ⁴⁴ Goosen, M. F. A.; O'Shea, G. M.; Gharapetian, H. M.; Chou, S.; Sun, A. M. *Biotechnol. Bioeng.*, **1985**, *27*, 146-150.
- ⁴⁵ Thu, B.; Bruheim, P.; Espevik, T.; Smidsrød, O.; Soon- Shiong, P.; Skjåk-Bræk, G. *Biomaterials*, **1996**, *17*, 1069-1079.
- ⁴⁶ King, G. A.; Daugulis, A. J.; Faulkner, P.; Goosen, M. F. A. *Biotechnol. Prog.*, **1987**, *3*, 231-240.
- ⁴⁷ Gåserød, O.; Smidsrød, O.; Skjåk-Bræk, G. *Biomaterials*, **1998**, *19*, 1815-1825.
- ⁴⁸ Mauser, T.; Dejugnat, C.; Mohwald, H.; Sukhorukov, G. B. *Langmuir*, **2006**, *22*, 5888- 5893.
- ⁴⁹ Lapitsky, Y.; Kaler, E. W. *Colloid. Surf. A: Physicochem. Eng. Aspects*, **2006**, *282-283*, 118-128.
- ⁵⁰ Zhu, H.; McShane, M. J. *Chem. Commun.*, **2006**, 153-155.
- ⁵¹ Shen, F.; Mazumder, M. A. J.; Burke, N. A. D.; Stöver, H. D. H.; Potter, M. A. *J. Biomed. Mater. Res. B: Appl. Biomater.* **2009**, *90B(1)*, 350-361.

Chapter 4: Mechanically Enhanced Microencapsulated Cellular Gene Therapy

Shen, F.; Mazumder, M. A. J.; Burke, N. A. D.; Stöver, H. D. H.; Potter, M. A.

Published in *Journal of Biomedical Material Research, Part B. Applied Biomaterials*,

2009, *90B(1)*, 350-361

This chapter has been reproduced with permission from J. Biomed. Mater. Res., Part B:

Appl. Biomater. Copyright 2009 John Wiley & Sons, Inc.

Contributions:

I prepared and characterized the synthetic polyelectrolytes and their fluorescent analogs used in this study. I studied the cross-linking nature of the microcapsules as well as the binding of BSA-FITC to different capsules. Dr. Nicholas Burke and I carried out the permeability measurements. Dr Feng Shen, Research Associate in Dr Murray A. Potter's Group, Health Sciences, McMaster University carried out the encapsulations and subsequent capsule and cell tests. . The manuscript was written by Dr. Feng Shen, with edits by Drs. Burke, Stöver, Potter and myself.

Abstract

Microcapsules bearing a covalently cross-linked coating have been developed for cellular gene therapy as an improvement on alginate–poly(L-lysine)–alginate (APA) microcapsules that only have ionic cross-linking. In this study, two mutually reactive polyelectrolytes, a polycation (designated C70), poly([2-(methacryloyloxy)ethyl] trimethylammonium chloride-*co*-2-aminoethyl methacrylate hydrochloride) and a polyanion (designated A70), poly(sodium methacrylate-*co*-2-(methacryloyloxy)ethyl acetoacetate), were used during the microcapsule fabrication. Ca-alginate beads were sequentially laminated with C70, A70, poly(L-lysine) (PLL), and alginate. The A70 reacts with both C70 and PLL to form a ~30 μm thick covalently cross-linked interpenetrating polymer network on the surface of the capsules. Confocal images confirmed the location of the C70/A70/PLL network and the stability of the network after 4 weeks implantation in mice. The mechanical and chemical resistance of the capsules was tested with a “stress test” where microcapsules were gently shaken in 0.003% EDTA for 15 minutes. APA capsules disappeared during this treatment while the modified capsules, even those that had been retrieved from mice after 4 weeks implantation, remained intact. Analysis of solutions passing through model flat membranes showed that the molecular weight cut-off of alginate-C70-A70-PLL-alginate is similar to that of alginate-PLL-alginate. Recombinant cells encapsulated in APA and modified capsules were able to secrete luciferase into culture media. The modified capsules were found to capture some components of regular culture media used during preparation, causing an immune reaction in implanted mice, but use of Ultra Culture serum free medium was

found to prevent this immune reaction. *In vivo* biocompatibility of the new capsules was similar to the APA capsules, with no sign of clinical toxicity on complete blood counts and liver function tests. The increased stability of the covalently modified microcapsules coupled with the acceptable biocompatibility and permeability demonstrated their potential for use as immuno-isolation devices in gene therapy.

4.1 Introduction

Microencapsulated cells engineered to secrete therapeutic proteins have been effectively applied in treating mouse models of genetic disorders such as dwarfism,¹ lysosomal storage diseases,^{2,3} hemophilia,⁴ and cancer.⁵⁻⁹ The semi-permeable microcapsules allow non-autologous cells to be implanted into the host animal by protecting the cells from immune mediators yet still allowing the therapeutic protein to leave the microcapsule. The design of the microcapsules has to be optimized for permeability, stability and biocompatibility. One of the most commonly used and studied microcapsules is the alginate–poly(L-lysine)–alginate (APA) capsule. Alginate is a natural polysaccharide composed of β -D-mannuronic acid (M) and α -L-guluronic acid (G) residues. Divalent cations, such as Ca^{2+} , can be used to cross-link G-rich regions to form a hydrogel calcium-alginate (Ca-alginate) bead. The M/G ratio, molecular weight, polydispersity index, and the ratio of homologous to heterologous chains dominate the properties of the Ca-alginate beads.¹⁰⁻¹² APA capsules are made by further layering Ca-alginate beads with poly(L-lysine) (PLL) and then alginate to give suitable biocompatibility and permeability for implantation.¹³⁻¹⁵ A concern with APA microcapsules is loss of structural integrity during long-term implantation due to

disruption of ionic cross-linking.^{13,16} In our previous study, APA capsules that were successfully maintained in mice for over six months totally collapse after 14 days implantation in dogs.¹³

A number of synthetic polymers have been used to augment or replace Ca-alginate or the PLL/alginate coatings in attempts to improve long-term mechanical stability of the capsules. Polymers such as poly(hydroxyethyl methacrylate-*co*-methyl methacrylate), polyphosphazene, and poly(N-vinylpyrrolidone-*co*-sodium acrylate) have been employed during the capsule fabrication. However, there are still few formulations that greatly improve the mechanical properties while maintaining the high biocompatibility and optimal permeability characteristics of APA capsules. Our objective was to prepare a capsule with improved stability, yet similar biocompatibility and permeability to the APA capsule by forming a covalently cross-linked coating on the capsule.

In this study, two mutually reactive polyelectrolytes were used: a polycation, poly([2-(methacryloyloxy)ethyl]trimethyl ammonium chloride-*co*-2-aminoethyl methacrylate hydrochloride), designated C70, and a polyanion, poly(sodium methacrylate-*co*-2-(methacryloyloxy)ethyl acetoacetate), designated A70.¹⁷ During fabrication of the modified microcapsules (designated as “4-layer” capsules), Ca-alginate beads were sequentially laminated with C70, A70, PLL, and finally alginate. Four-layer capsules were designed to improve the biocompatibility of previously described 2-layer modified capsules, avoiding the surface overgrowth seen in *in vivo* pilot studies employing Ca-alginate coated with C70 and A70 alone.¹⁷

The acetoacetate groups of A70 are able to react with amino groups from both C70 and PLL to form a ~30 μm thick covalently cross-linked interpenetrating polymer network coating on the surface of the capsules. *In vitro* and *in vivo* tests for stability, permeability and biocompatibility were undertaken, which showed the 4-layer capsules to have permeability and biocompatibility similar to APA capsules, along with an increased stability.

4.2 Materials & Methods

4.2.1 Chemicals:

Sodium alginate (Keltone LV, 428kDa) was a gift from the International Specialty Products (ISP) Co. (San Diego, CA). Poly-L-lysine (PLL, $M_n = 15\text{-}30$ kDa), poly(ethylene glycol) (PEG, $M_v = 10\text{k}, 100\text{k}, 200\text{k}, \text{ and } 300\text{k}$), 2-(*N*-cyclohexylamino) ethanesulfonic acid (CHES), EDTA (ethylenediaminetetraacetic acid, disodium salt, dihydrate), sodium chloride, calcium chloride, sodium nitrate and FITC labelled Bovine serum albumin (BSA_f) were purchased from Sigma Aldrich Chemical Company Inc. (St. Louis, MO), and were used as received. Narrow-dispersed PEG standards for GPC calibration were purchased from Waters (Mississauga, ON). Sodium dihydrogen orthophosphate was obtained from BDH, ON. DMEM (Dulbecco's Modified Eagle's Medium), Trypan blue solution, Fetal Bovine Serum (FBS), UltraCulture serum free media (SFM) were purchased from Gibco (Mississauga, ON), and were used as received. Sodium hydroxide and hydrochloric acid were purchased as concentrates from Anachemia Chemical Inc, NY, and were prepared by diluting to 0.100 M with deionized water.

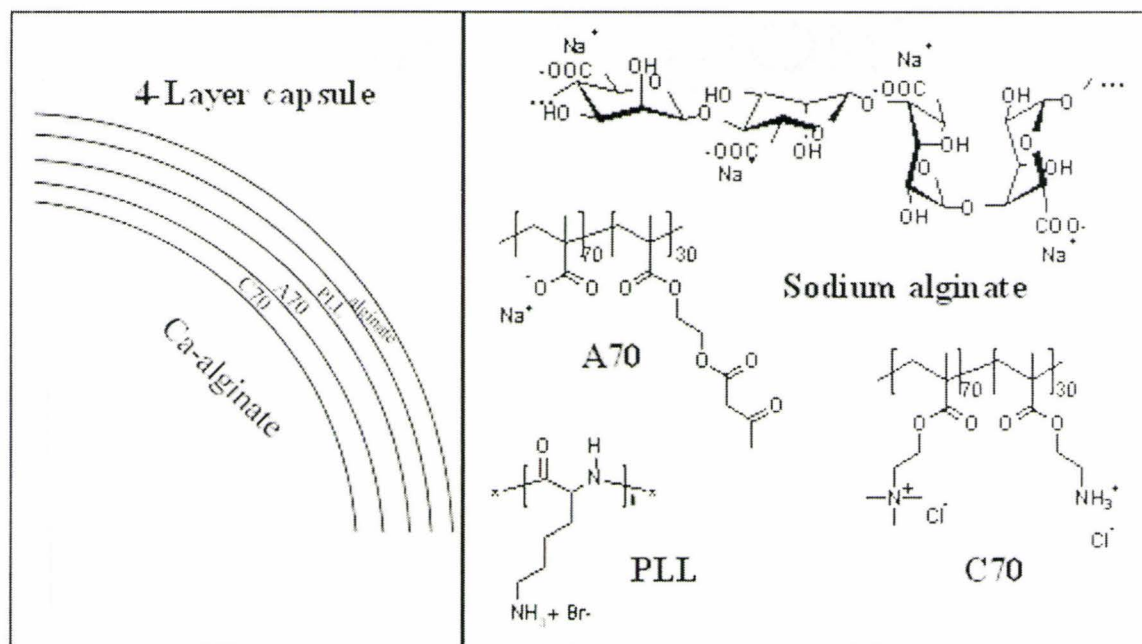


Figure 4.1. Construction of 4-layer-capsule.

4.2.2 Polymer synthesis:

The synthesis of A70 (42 kDa), A100 (40 kDa) and C70 (167 kDa) polymers and a fluorescein-labelled analog of C70 (C70f) is described fully in our previous publication.¹⁷

4.2.3 Encapsulation:

The APA microcapsules were fabricated as previously described,¹⁸ and the preparation of 4-layer capsules followed a similar procedure. Briefly, 1.5(w/v)% sodium alginate in 0.9% NaCl was sterile filtered, extruded through a 27 gauge needle with concentric airflow into a 1.1(w/v)% CaCl₂ bath. For the 4-layer capsules, these beads were then coated with 0.5(w/v)% C70 and 0.5(w/v)% A70 for 3 minutes each. The Ca-alginate-C70-A70 capsules or Ca-alginate beads were then laminated with 0.05(w/v)%

PLL for 6 min, and then with 0.03(w/v)% alginate for 4 min, to form the 4-layer capsules or APA capsules, respectively (Figure 4.1). Each layering step was followed by two 0.9% NaCl washes (2 minutes each). For some 4-layer capsules, C70 was replaced with C70f.

For microcapsules containing cells, a C₂C₁₂ myoblast cell suspension was mixed with the sterile alginate solution to a final cell concentration of 2 millions cells/mL of alginate. Following the final wash step, the microcapsules with cells were cultured in DMEM medium (with 10% FBS and 1% penicillin/streptomycin) in a tissue culture incubator at 37 °C, while empty microcapsules were left in normal saline for incubation.

4.2.4 Luciferase activity assay *in vitro*:

The expression and release of recombinant proteins from encapsulated cells was demonstrated with Luciferase vector pC3B.Luci transfected MDCK (Madin-Darby canine kidney) cells constructed in this lab.¹⁹ The cells were encapsulated and incubated as described above for 24h before samples of the media was removed. Luciferase expression by the encapsulated cells was assayed using the Luciferase activity kit (Promega, Madison, WI) using the protocol provided by the manufacturer. Approximately 100 capsules were cultured in 1 mL of media for 24 hours, and 20 µL of the media was loaded into a 96 well plate. An automated injector added 50 uL of luciferase substrate mixture to each well at specified time intervals and luciferase activity in relative light units (RLUs) was measured with an automated luminometer using a total integration time of 10 s.

4.2.5 Pore size measurement:

Permeability through uncoated and coated Ca-alginate membranes was measured using a two-compartment plastic permeation cell separated by an alginate-based membrane on a porous polypropylene support membrane (a gift from 3M, St. Paul, MN; average pore size = 5 μm). The Ca-alginate membrane was prepared by immersing the polypropylene support in 1.5% sodium alginate, then 1.1% CaCl_2 for 6 min, followed by three 0.9% NaCl washes. The supported Ca-alginate membrane was mounted in the diffusion cell and then coated on one side by exposing to polycation (6 min) or polyanion (4 min) solutions to build-up layers analogous to the microcapsule coatings. To create an APA-like membrane, the Ca-alginate was coated with 0.05% PLL and then 0.03% alginate. For the 4-layer capsule membrane the Ca-alginate was coated with 0.5% C70, followed by 0.5% A70, 0.05% PLL and finally 0.03% alginate. After each round of coating the membrane was washed three times with 0.9% sodium chloride for 2 minutes. The diffusion cells containing the uncoated Ca-alginate membrane, APA membrane or 4-layer membrane, were loaded with a mixture of PEG samples (0.2(w/v)% each of 10, 100, 200, and 300 kDa PEG in 0.9% sodium chloride) in the source compartment, and an equal amount of saline in the sink compartment. The assembly was maintained at room temperature with stirring in both compartments for 24 hrs.

Samples were taken from each side and analyzed by a Gel Permeation Chromatography (GPC) system consisting of a Waters 515 HPLC pump, Waters 717 plus Autosampler, three columns (Waters Ultrahydrogel -120, -250, -500; 30cm \times 7.8mm; 6 μm particles) and a Waters 2414 refractive index detector. The columns were maintained at 35 $^\circ\text{C}$ and the system was calibrated with molecular weight standards.

Samples were eluted at a flow rate of 0.8 mL/min with a mobile phase consisting of 0.1M NaNO₃ in 0.05 M phosphate buffer (pH 7).

4.2.6 Bovine serum albumin (BSA) uptake:

FITC-labeled BSA (BSAf) was dissolved in 0.9% NaCl to form a 0.01% solution. Capsules (4-layer or APA) containing C₂C₁₂ cells were kept in an incubator at 37 °C for 3 days, and then 5 mL of BSAf solution, 2 mL capsules and 10 mL medium were added to a culture dish. After 24 hours at 37 °C, the capsules were then washed six times with 0.9% NaCl before examination by confocal microscopy.

4.2.7 Confocal microscopy:

Confocal microscopy was performed with a MRC 1024 confocal laser-scanning microscope (Bio-Rad, Hemel Hempstead, United Kingdom) attached to a Microphot SA microscope (Nikon, Tokyo, Japan) equipped with a 10×, 0.3 NA (Nikon) lens. Images were analyzed with Image J1.34S (<http://fbs.info.nih.gov/ij>).

4.2.8 Stress test:

100 µL of microcapsules and 10 mL of 0.003% sodium-EDTA solution were loaded into a conical polypropylene tube and then agitated with an orbital mixer at 30 rpm for 15 minutes at room temperature. The capsules were then stained with trypan blue and transferred to glass dishes to determine the percentage of intact capsules. Each test was performed in triplicate.

4.2.9 Cell Viability:

The viable cell number per capsule was determined using an Alamar Blue Assay (Trek Diagnostic Systems, Inc. Cleveland, OH).²⁰ Briefly, a known number of capsules (in 100 μL suspension) were loaded in a 24-well plate containing 500 μL medium and 50 μL Alamar Blue. The plate was incubated at 37 $^{\circ}\text{C}$ for 4h. After the incubation, 100 μL of the supernatant was transferred to a 96-well plate and checked for fluorescence ($\lambda_{\text{ex}}/\lambda_{\text{em}} = 535/590 \text{ nm}$) with a TECAN GENios plate reader (Australia). The number of viable cells was determined by comparing fluorescence values with a standard curve generated from a known number of un-encapsulated cells.

4.2.10 In vivo assessment of capsules:

The animals were treated in accordance with Canadian Institutional Animal Care guidelines. C57BL/6 mice (Charles River, Montreal QC) were anaesthetized with isoflurane (Anaquest, Mississauga, Ontario) before a suspension of 3 mL microcapsules in normal saline (total volume 5 mL) was implanted into the intraperitoneal cavity of mice under sterile conditions using a 20 gauge catheter (BD, Oakville, ON). Blood samples from mice implanted with capsules for 1 and 4 weeks were collected by orbital bleeding. Hematological and biochemical liver function tests were performed by VITA-TECH Canada Inc. (Mississauga, ON). At the end of the experiment mice were sacrificed and the capsules retrieved as previously described.²¹ Three mice were tested for each kind of capsules at each time point.

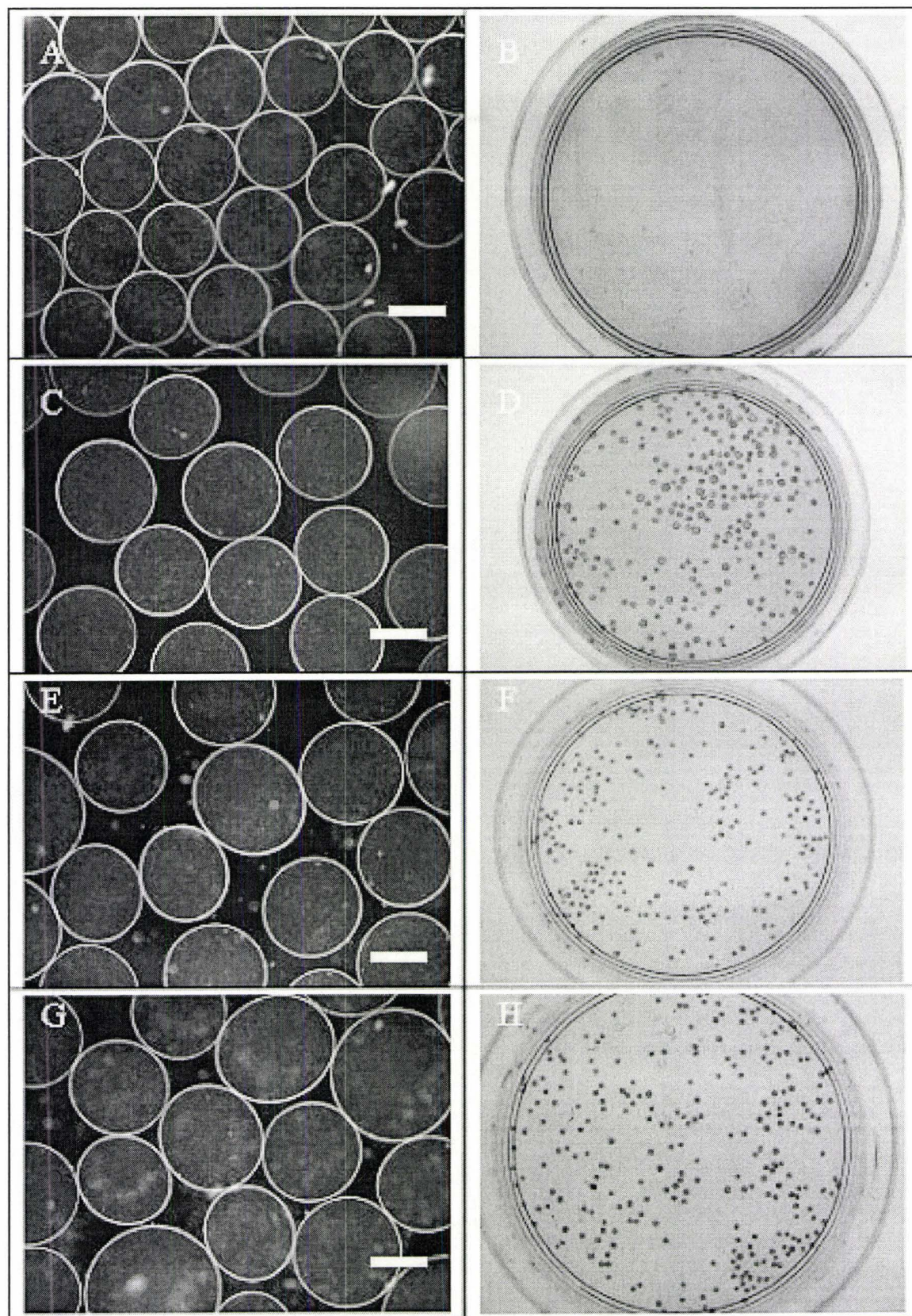


Figure 4.2. Light microscopy phase contrast images (A, C, E, G) of capsules before stress test, and optical pictures (B, D, F, H) of Petri dishes containing the same capsules shaken in 0.003% EDTA solution for 15 min and then stained with trypan blue. (A, B) Empty APA capsules, stored in saline for 3 days. (C, D) Empty 4-layer capsules, stored in saline for 3 days. (E, F) Empty 4-layer capsules, retrieved from mice after 1- week implantation. (G, H) Empty 4-layer capsules, retrieved from mice after 4- weeks implantation.

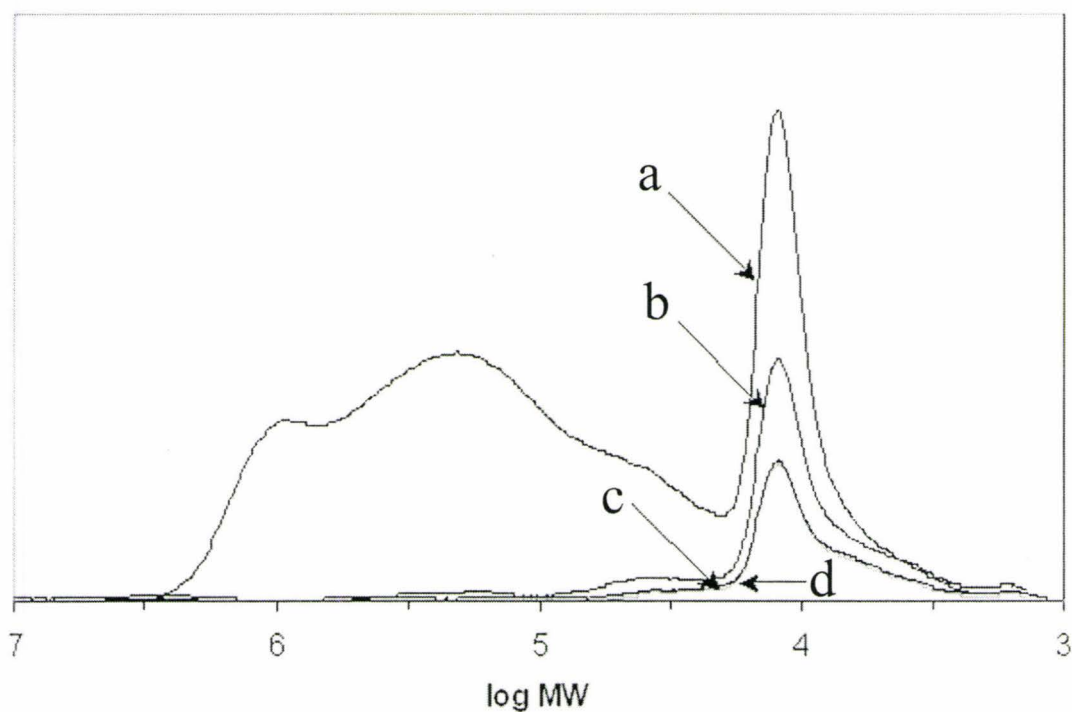


Figure 4.3. GPC traces of: (a) the original PEG solution; and the solutions in the receptor compartments at $t = 24$ h for (b) Ca-alginate membrane; (c) Ca-alginate-PLL-alginate membrane; and (d) Ca-alginate-C70-A70-PLL-alginate membrane.

4.3 Results

4.3.1 Capsule structure and strength testing:

Empty capsules (without cells) were kept in saline in an incubator at 37 °C for 3 days and then implanted into mice. Optical images of the capsules before implantation and those retrieved after implantation for one or four weeks are shown in Figures 4.2c, 4.2e and 4.2g. The capsules were subjected to the stress test. After shaking in EDTA, all of the APA capsules were dissolved or broken (Figure 4.2b). However, most (>95%) of the 4-layer capsules were intact (Figure 4.2d). 4-Layer capsules retrieved from mice after one week (Figure 4.2f) and four weeks (Figure 4.2h) showed similar results where the majority of the capsules remained intact after the EDTA test. Previous studies^{22,23} have shown that the strength of APA capsules decreases after mouse implantation.

The molecular weight cut-off of Ca-alginate, APA, and 4-layer membranes was tested by PEG diffusion across model flat membranes. Free diffusion through the membrane would result in source and receptor compartments with half the concentration of the original PEG mixture. The GPC spectrum in Figure 4.3 shows that higher MW PEG is excluded from the receptor compartments, while the 10 kDa PEG (log MW = 4) shows up in all receptor compartments. The transfer of intermediate MW PEG was partially retarded by all membranes, with an apparent pore-size order of Ca-alginate > APA \approx 4-layer. The apparent MW cut-off for the APA and 4-layer membranes is approximately 70 kDa.

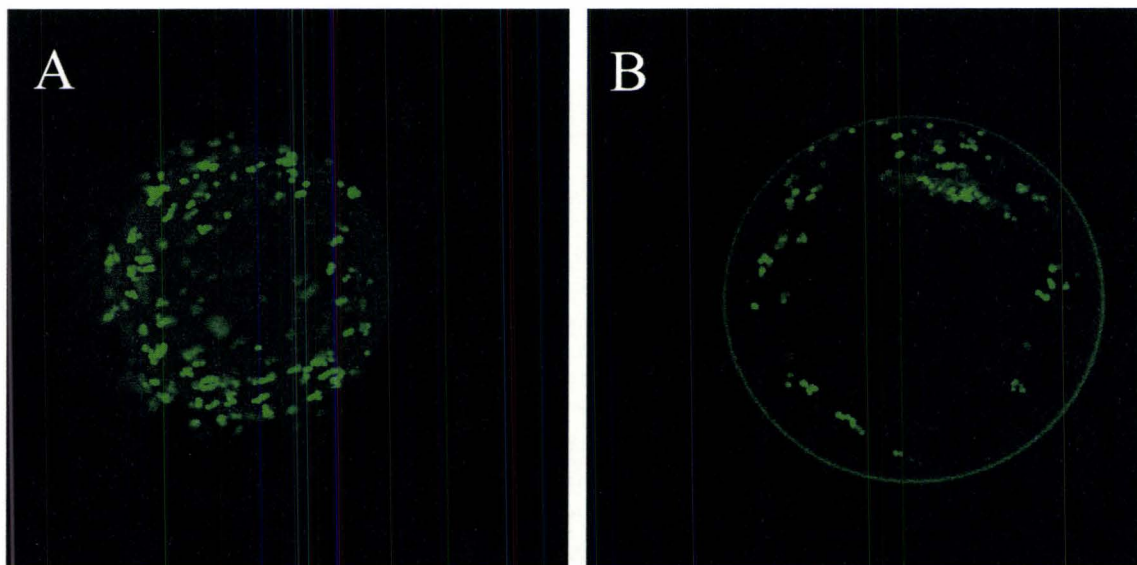


Figure 4.4. Confocal images of APA (A) and 4-layer (B) capsules containing C_2C_{12} cells that were incubated with fluorescently labelled BSA at $37\text{ }^{\circ}\text{C}$ for 24 h.

From the above data it appears that the pores for the APA and 4-layer membranes are close in size. A similar result was observed when the diffusion of BSAf into microcapsules was examined (Figure 4.4). Confocal images for 4-layer capsules or APA capsules incubated with BSAf (MW 67 kDa) showed that both kinds of capsules allowed BSAf through the surface membrane to interact with the encapsulated C_2C_{12} cells. After 24 h incubation there are less fluorescent cells in the core of the 4-layer capsules, suggesting the rate of diffusion into the 4-layer capsules is less than that of the APA capsules.

The *in vivo* stability of the 4-layer capsule was assessed by fluorescently labelling the capsules with C70f. After incubation for three days, the labelled 4-layer capsules were implanted into six mice. Capsules were retrieved from three mice one week after

implantation and from the remaining 3 mice after 4 weeks and were examined with confocal microscopy. Figures 4.5A and B show typical confocal images of labelled 4-layer capsules before and 4 weeks after implantation (1 week data, not shown, was similar). The integrated fluorescence intensity per capsule, which reflects the density of C70f on the capsule, remained stable after one or four weeks' implantation in mice (Figure 4.5C).

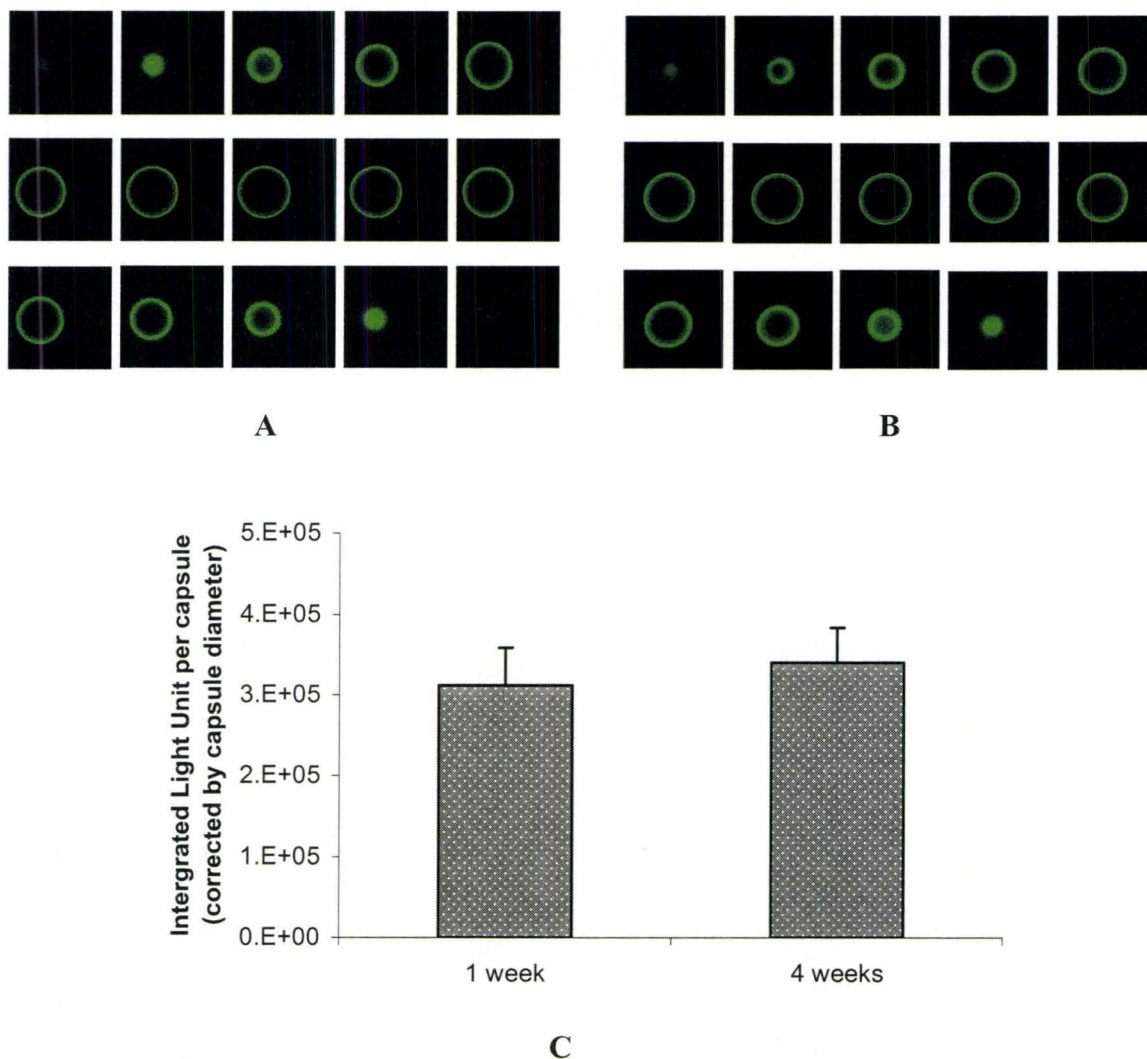


Figure 4.5: A series of optical slices taken with a confocal microscope from the top to the bottom of a 4-layer-capsule labelled with C70 before (A) and after (B) four weeks

implantation in mice. The fluorescence intensity (corrected for capsule diameter) of capsules retrieved from mice after implantation for one and four weeks (C).

4.3.2 Biocompatibility tests:

The use of C70 and A70 and the presence of the cross-linked shell formed by C70/A70/PLL might impact the viability of encapsulated cells. Figure 4.6 shows the cell number per capsule in either 4-layer capsules or in APA capsules after 1, 7, or 14 days of *in vitro* incubation at 37 °C. On the day after the capsule fabrication, the average cell number in 4-layer capsules was about 85% of that in APA capsules indicating some disadvantage in survival during the 4-layer capsule fabrication. The cell density in the 4-layer capsules increased at the same rate as in the APA capsules after one or two week's *in vitro* incubation, which confirms the suitability of the internal environment of the modified capsules for cell growth.

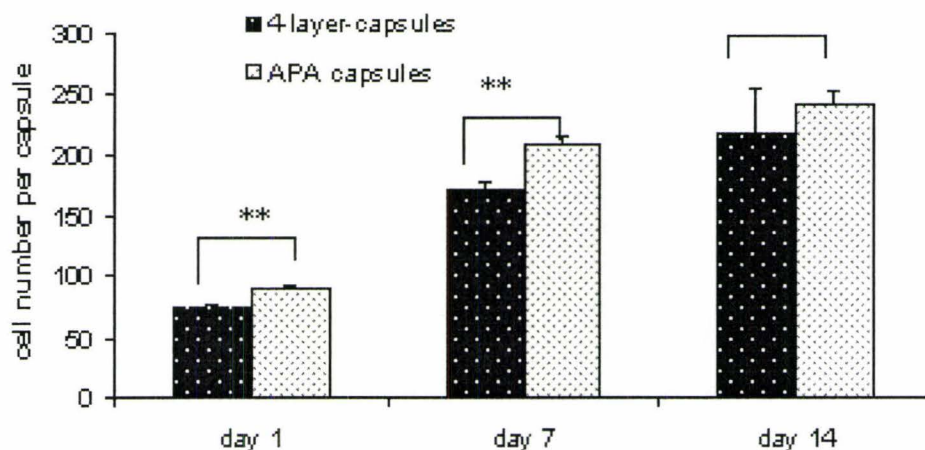


Figure 4.6. Effect of the C70 and A70 coating on survival of encapsulated cells. C₂C₁₂ myoblasts were encapsulated in 4-layer-capsules or APA capsules. The viable cell number per capsule was assayed after incubation for up to 14 days. (**p<0.01; no statistical difference between the two kinds of capsules at day 14).

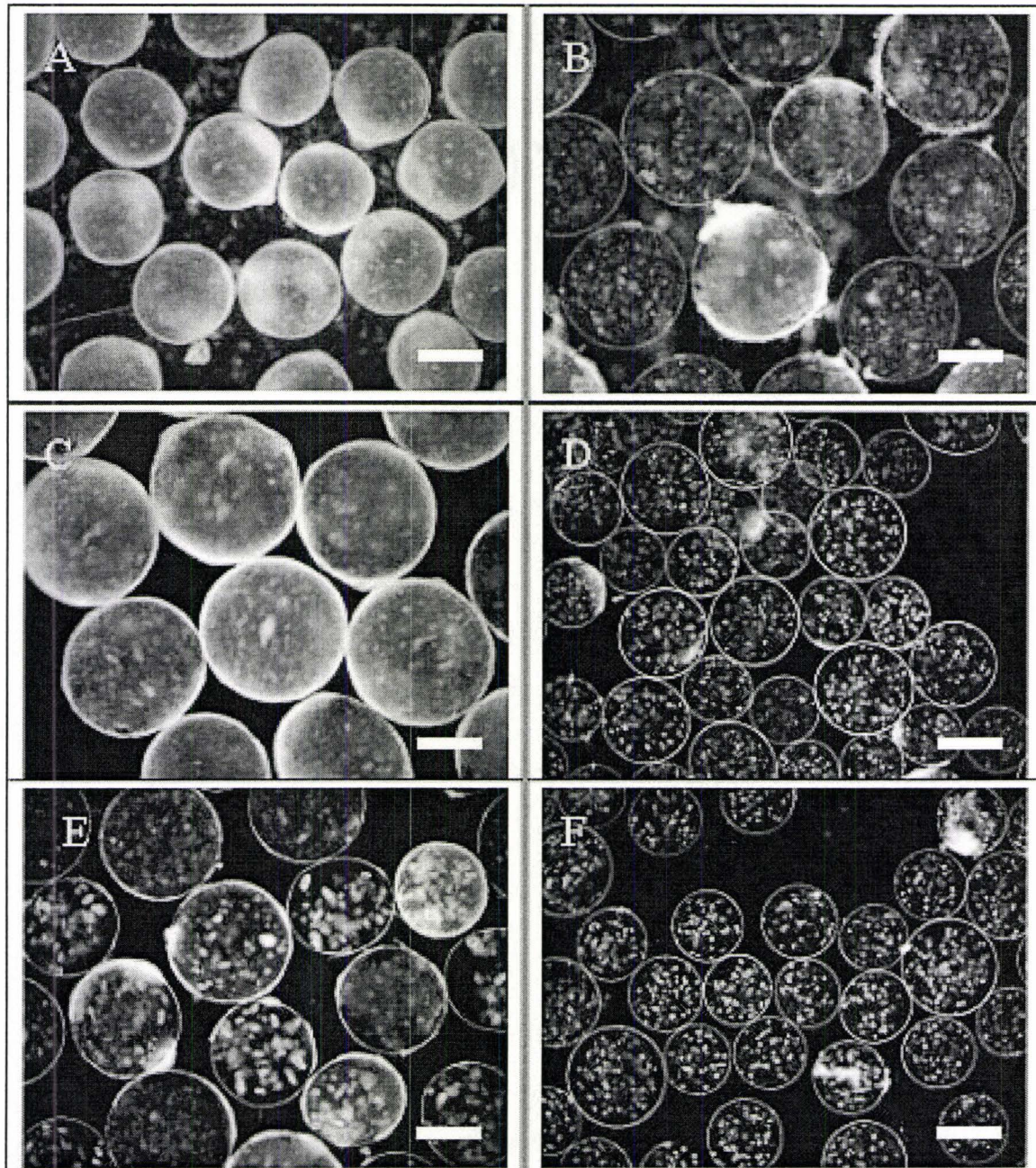
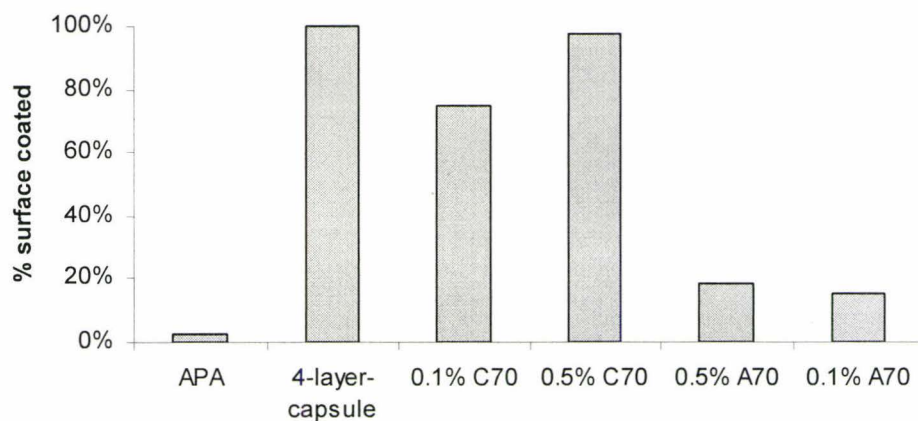


Figure 4.7. Phase contrast images of capsules retrieved from mice after one-week implantation. (A) 4-layer capsules (Ca-alginate beads sequentially coated with 0.5% C70, 0.5% A70, 0.05% PLL, 0.03% alginate). (B) “0.50% C70” capsules (Ca-alginate beads sequentially coated with 0.50% C70, 0.03% alginate). (C) “0.10% C70” capsules (Ca-alginate beads sequentially coated with 0.10% C70, 0.03% alginate). (D) “0.50% A70” capsules (Ca-alginate beads sequentially coated with 0.05% PLL, 0.50% A70, 0.05% PLL, 0.03% alginate). (E) “0.10% A70” capsules (Ca-alginate beads sequentially coated with 0.05% PLL, 0.10% A70, 0.05% PLL, 0.03% alginate). (F) “0.05% A70” capsules (Ca-alginate beads sequentially coated with 0.05% PLL, 0.05% A70, 0.05% PLL, 0.03% alginate). Data for “0.05% C70” capsules (Ca-alginate beads sequentially coated with 0.05% C70, 0.03% alginate) is absent because C70 concentrations lower than 0.1% cause the beads to clump together. Bar = 200 μm .

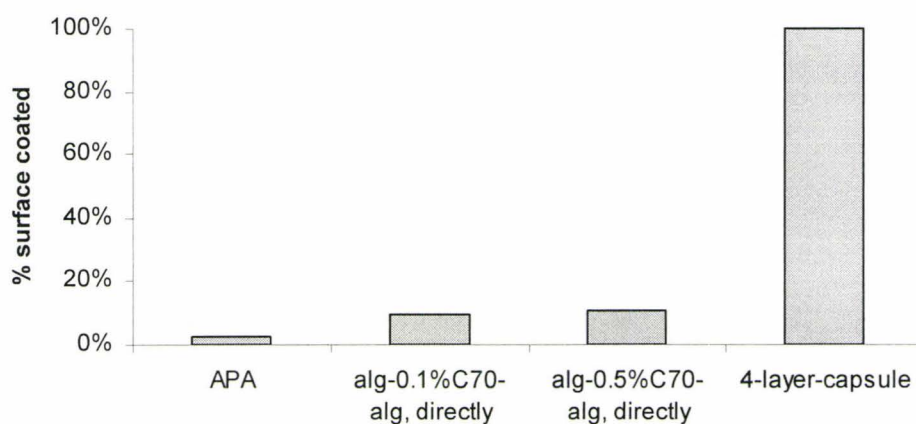
In contrast to the empty 4-layer capsules (Figure 4.2e-h), the *in vivo* performance of these capsules with cells was sub-optimal. One week after implantation, the modified capsules were opaque in appearance (Figure 4.7a) likely indicating an inflammatory or immune reaction. It was surmised that this reaction was related to the A70 or C70, since in previous work with APA capsules containing the same concentration of C₂C₁₂ cells showed excellent biocompatibility in mice in *in vivo* tests.²¹

The effect of A70 and C70 and their respective concentrations was examined by fabrication of microcapsules in which only A70 or C70 was present. The images of these capsules retrieved from mice after 1-week implantation are shown in Figure 4.7b-f. From

these images, it is clear that 0.5% C70 or A70 alone are sufficient to initiate a host reaction that leads to the coating on the capsule surface. It appears that presence of C70 is more important than A70 for initiating the host response. A semi-quantitative scoring was devised for the retrieved capsules: 200 capsules from each experiment were evaluated under microscopy, and the approximate percentage of the capsule surface covered by growth was recorded. This data, summarized in Figure 4.8a, agrees with the initial impression from the images shown in Figure 4.7.



(A)



(B)

Figure 4.8: Summary of the surface analysis of capsules retrieved from mice that were implanted after 3-days in culture media (A) or implanted directly after manufacture (B). Capsules (~200) were randomly selected and the percentage of visible surface area coated by opaque materials was visually determined by light microscopy and the mean values are shown. 4-layer-capsules: Ca-alginate beads sequentially coated with 0.5% C70, 0.5% A70, 0.05% PLL, 0.03% alginate. “0.50% C70” capsules: Ca-alginate beads sequentially coated with 0.50% C70, 0.03% alginate. “0.10% C70” capsules: Ca-alginate beads sequentially coated with 0.10% C70, 0.03% alginate. “0.50% A70” capsules: Ca-alginate beads sequentially coated with 0.05% PLL, 0.50% A70, 0.05% PLL, 0.03% alginate. “0.10% A70” capsules: Ca-alginate beads sequentially coated with 0.05% PLL, 0.10% A70, 0.05% PLL, 0.03% alginate. “0.05% A70” capsules: Ca-alginate beads sequentially coated with 0.05% PLL, 0.05% A70, 0.05% PLL, 0.03% alginate

A critical difference between the empty capsules and those containing cells was the culture conditions. Capsules with cells were kept in culture medium containing 10% FBS in an incubator for 3 days while empty capsules were incubated in normal saline for the same time period. Capsules implanted directly after manufacture (Figure 4.8b) showed less overgrowth. To examine the possibility that the C70 or A70 on the capsule surface absorbed proteins from the culture medium or from cell debris from the encapsulation procedure, empty capsules were incubated with BSAf immediately after fabrication. The 4-layer capsules have a fluorescent layer of BSAf on the surface, whose

thickness depends on the amount of C70 and A70 used (Figure 4.9a-b). This layer was absent in APA capsules (Figure 4.9c).

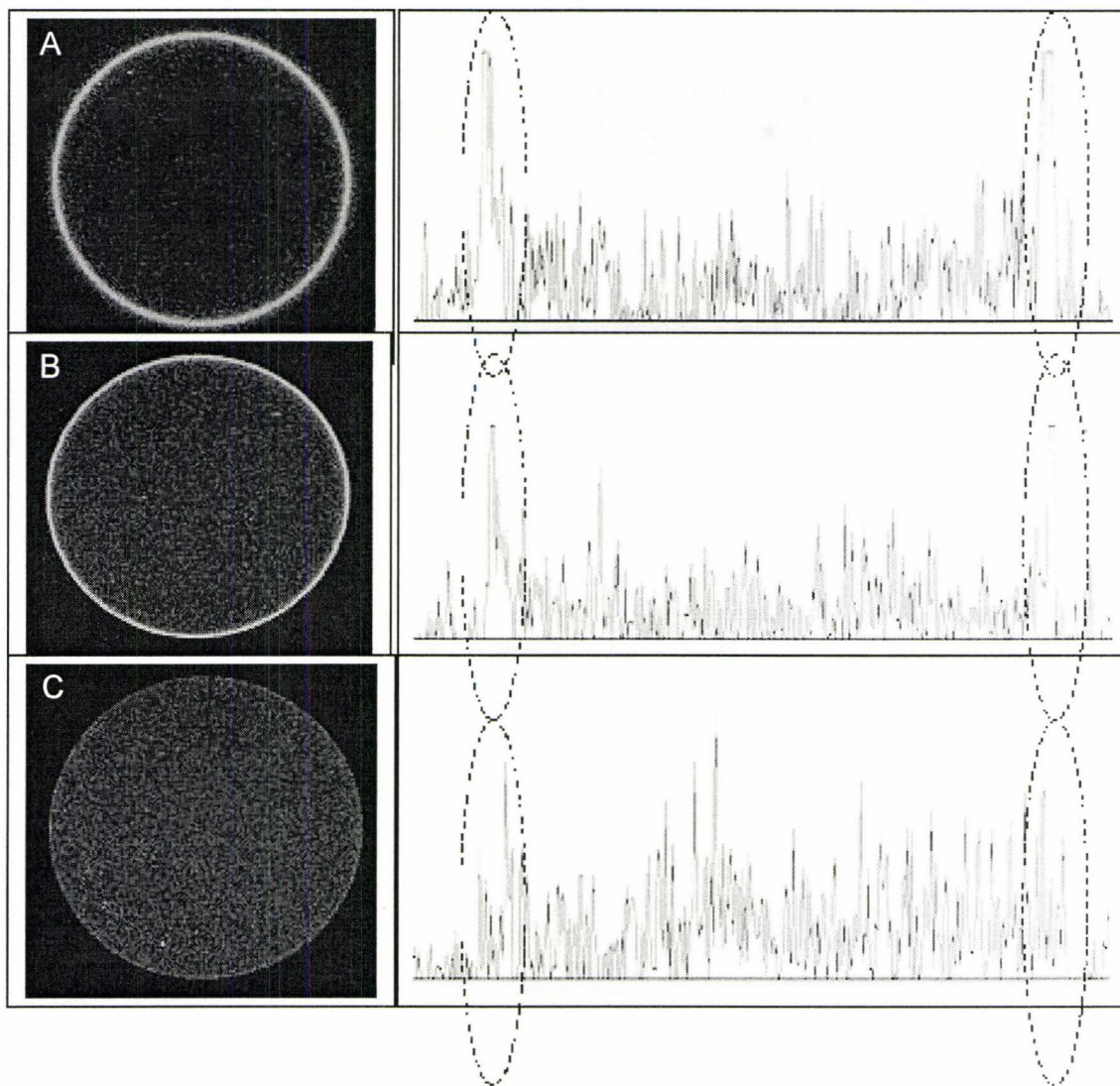


Figure 4.9: Confocal image through middle of capsules incubated in 0.05% FITC labelled BSA solution at 37 °C for 24 h. Line profiles are shown to the right for each kind of capsule. (A) 4-layer-capsules (Ca-alginate bead sequentially coated with 0.50% C70, 0.50% A70, 0.05% PLL, 0.03% alginate). (B) Reduced C70/A70 4-layer-capsules (Ca-

alginate bead sequentially coated with 0.10% C70, 0.10% A70, 0.05% PLL, 0.03% alginate). (C) APA capsules.

The dependence of BSAf binding on C70 and/or A70 was probed by preparing 4-layer capsules in which C70 was replaced by PLL and/or A70 was replaced by A100 (poly(methacrylic acid, sodium salt)), an analog of A70 that lacks acetoacetate groups. The capsules were exposed to 0.05% BSAf for 24h at 20 °C, washed five times with saline and then examined by confocal microscopy. The APA capsule (Figure 4.10a) shows a weak and uniform distribution of BSAf throughout. A similar intensity and distribution is seen for a 4-layer capsule when the C70/A70 layers were replaced by PLL/A100 (Figure 4.10b). When A70 is present, some trapping of BSAf at the surface is observed (Figure 4.10c). A capsule containing C70 but lacking A70 showed very strong BSAf binding (Figure 4.10d), similar to that exhibited by the 4-layer capsule (Figure 4.10e).

In order to further confirm the role of culture medium, serum free medium (SFM) was used to replace the regular DMEM medium (containing FBS) for culture of the 4-layer capsules after fabrication. Figure 4.11 shows the resulting C₂C₁₂-containing 4-layer capsules retrieved from mice after one-week implantation. Exclusion of FBS from the process eliminates the reaction of the host against the 4-layer capsules, with the capsule surface remaining optically transparent. Further, the average cell number per capsule increased from 120 immediately after fabrication to 850 after one-week *in vivo*.

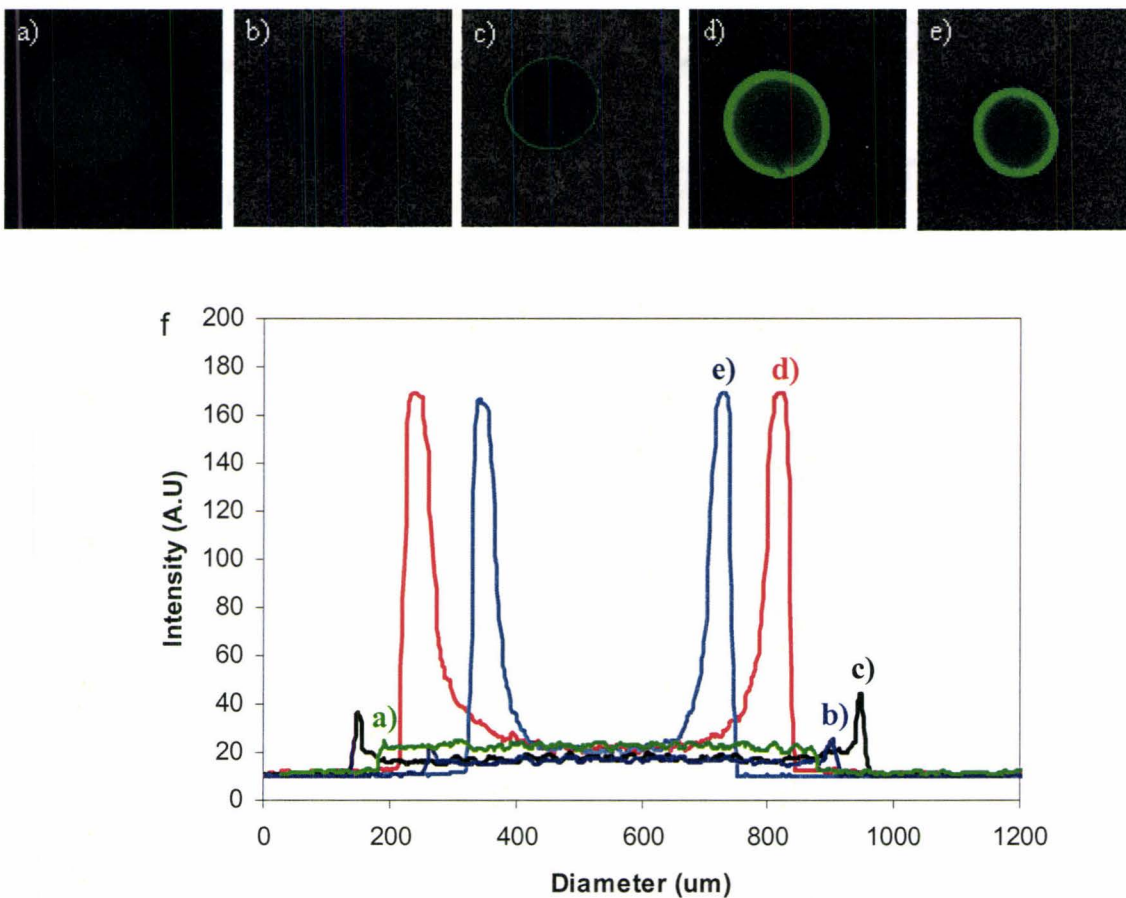


Figure 4.10: Top – Confocal images through the middle of a) APA, b) APA100PA, c) APA70PA, d) AC70A100PA and e) 4-layer (AC70A70PA) microcapsules exposed to 0.05 w/v% BSA-FITC at 20 °C for 24 h. Bottom f) Line profiles of microcapsules shown at top.

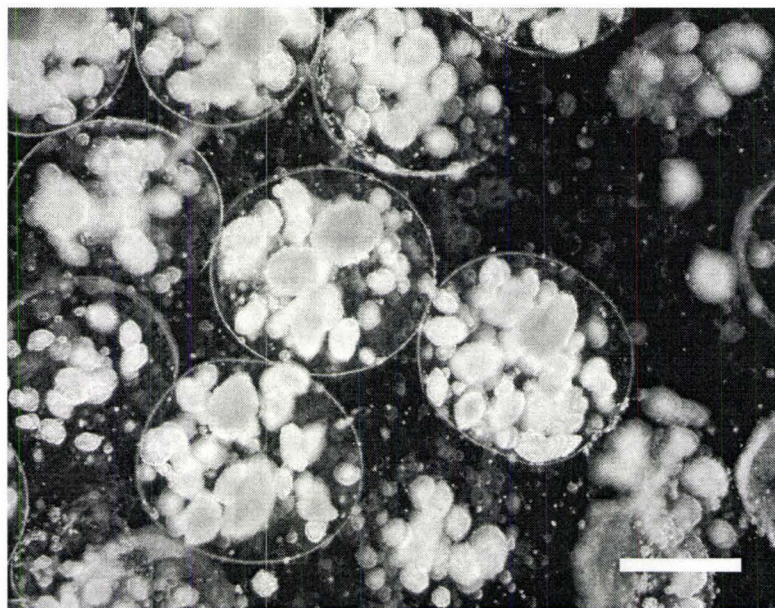


Figure 4.11: Four layer-capsules (cultured in serum-free medium for 72 hours in advance of implantation) were retrieved after one week of mouse implantation. The average cell number per capsule was 850. Bar = 200 μm .

4.3.3 Protein Expression and Release from Encapsulated Cells:

pC3B.Luci transfected MDCK cells were encapsulated in APA and 4-layer capsules. Encapsulated cells were then cultured and the growth medium was collected for a luciferase assay 24 h after capsule fabrication. There was secretion and release of luciferase from pC3B. Luci transfected cells in both kind of capsules, but significantly less luciferase was released by the 4-layer capsules (27 ± 5 RLU/thousand cells for APA capsules; 13.4 ± 0.2 for 4-layer capsules, $p < 0.01$). As a control, untransfected MDCK cells were encapsulated and tested in the same way, and no luciferase activity was detected.

4.4 Discussion

Cellular microencapsulation based on Ca-alginate beads typically requires several coating layers to confer the desired characteristics for *in vivo* implantation. These characteristics pertain to three areas: stability, permeability, and biocompatibility. Most applications require the highest stability possible without compromising the other two areas. In Ca-alginate beads, guluronate residues can be bound with divalent cations (i.e. Ca^{2+} , Ba^{2+}) and form chain-chain associations²⁴ allowing formation of the hydrogel core. However, leaching of calcium from the capsules can cause capsule failure. *In vivo*, this may happen by equilibration of calcium in the capsule with the large body pool of calcium that is bound by proteins (i.e. albumin) and tightly regulated by hormone systems. Covalently linked coatings may be able to resist dissolution and survive the loss of the underlying Ca-alginate gel leading to improve capsule stability. However, it is important to test the effects of capsule modifications on permeability, and biocompatibility in addition to stability.

4.4.1 Stability:

In the 4-layer capsules, a reaction between C70 and A70 builds up a covalently linked network on the surface of Ca-alginate. The beads are then coated with PLL to further strengthen the capsule and to control the permeability, and finally with alginate to “hide” the other polymers and maximize biocompatibility (Figure 4.1). An *in vitro* assay, which we have called the stress test, mimics the *in vivo* effect of calcium leaching from the capsules at the same time as exposing the capsules to osmotic and mechanical stress.

Figure 4.2 shows that the 4-layer capsules can survive the stress test while APA capsules are totally destroyed. This is true of microcapsules maintained *in vitro* or *in vivo* in mice for up to 4 weeks before the stress test. Additionally, studies with fluorescently labelled C70f (Figure 4.5) showed that the fluorescence intensity of the capsule did not diminish after 4 weeks' implantation in mice, indicating the stability of the C70 component of the 4-layer capsules.

4.4.2 Permeability:

There is a wide range reported for the permeability of alginate-based capsules.^{21,25} One advantage of the typical APA capsule is that the PLL layer can be manipulated to provide a desired permeability. This allows the permeability to be selected to block immune mediators while still allowing the therapeutic secretion of recombinant proteins. The permeability of the chemically modified capsules was probed by PEG diffusion, fluorescently labelled protein (BSAf) uptake and luciferase secretion from encapsulated cells. PEG diffusion analysis showed that the pore size of the 4-layer membrane was shown to be much smaller than Ca-alginate but similar to that of the alginate-PLL-alginate (Figure 4.3). This method is able to test the permeability to a large MW range, but is not able to detect small differences between capsule permeability. Protein/enzyme uptake and secretion, however, allow a more detailed examination of the permeability to a mono-dispersed MW molecule. Using these methods, the 4-layer capsule appears to have slightly smaller pore size than the APA capsule, as indicated by reduced fluorescence of encapsulated cells during BSAf uptake (Figure 4.4) and reduced amount of luciferase detected in media from encapsulated recombinant cells. Both of these latter

tests examine permeability characteristics for proteins with MW near 65 kDa, and the luciferase experiment, in particular, provides proof of principle for encapsulated cellular therapy applications. Varying the molecular weight, concentration, and exposure time of PLL and/or the C70/A70 would allow further modifications of the pore size in the modified capsule in order to “fine-tune” the capsule for a particular application.

4.4.3 Biocompatibility:

There are two considerations for microencapsulated cells that we include under “biocompatibility”: first is the survival of the encapsulated cells within the microcapsule, and second is the reaction of the host to the microcapsules / microencapsulated cells after implantation.

The first is relatively easy to quantify by measuring cell survival after the encapsulation process and after a period of time *in vitro* or *in vivo*. Survival during the encapsulation process can be affected by many factors, such as exposure to reactive/harmful chemicals and length of time spent in sub-optimal tissue culture conditions (i.e. sub-optimal nutrient, gas and/or temperature levels). Our results show that the 4-layer capsules have a slightly negative effect on the cells, but that this seems to be mostly related to the encapsulation process itself. Survival and expansion of cells after the initial encapsulation is robust (Figures 4.6, 4.10).

It is more complex to measure the host reaction to the microcapsules and the encapsulated cells. Liver function and CBC tests (data not shown) suggest that capsule implantation, regardless of capsule type or whether the capsules contain cells or not, did

not produce systemic toxicity to the mice. Another gross estimate of biocompatibility is to examine the microcapsules after implantation. Clearly the 4-layer capsules had greatly decreased biocompatibility when compared to the APA capsules, as evidenced by what appears to be a fibrotic coating on the surface of the retrieved microcapsules containing cells. Yet, 4-layer capsules without cells and APA microcapsules with or without cells did not show the same reaction.

These findings made us suspect the A70 and/or C70 were binding to cell debris from cells that died during encapsulation or to components of the culture media. Culturing the microcapsules before implantation is intended to allow the encapsulated cells to recover from the fabrication process and to reduce the load of necrotic and marginally surviving cells implanted. However, if cell debris or foreign proteins are trapped on the microcapsule surface, they would have an immune-stimulating effect upon implantation. By varying the nature or the concentration of the polymers used to make the coating (Figures 4.7, 4.8, 4.10), it was determined that the C70 was the major contributor to binding of media proteins to the microcapsule surface, while A70 had less effect. The binding of media proteins was lessened by reducing the concentration of C70 or A70, but was eliminated by using serum-free media to culture the microcapsules post-fabrication. This suggests that the media components had the largest effect on inducing a fibrotic reaction. We postulate that a covalent linkage between the acetoacetate groups of A70 and amine groups on media proteins or a polyelectrolyte complex between C70 and negatively charged proteins (e.g. albumin) was formed, fixing the proteins on the capsule surface (supported by the BSAf results, Figure 4.9). Fortunately, the relatively simple

measure of replacing the regular medium with serum free medium for incubation after fabrication eliminated the host reaction as shown in Figure 4.11.

In summary, we have constructed an alginate-based microcapsule with a covalently cross-linked shell that shows improved stability on chemical testing. The 4-layer capsule maintained good biocompatibility characteristics and had permeability similar to APA capsules.

4.5 References

1. al-Hendy A, Hortelano G, Tannenbaum G. S, Chang P. L. Correction of the growth defect in dwarf mice with nonautologous microencapsulated myoblasts-- an alternate approach to somatic gene therapy. *Hum Gene Ther* **1995**;6(2):165-75.
2. Ross C. J, Bastedo L, Maier S. A, Sands M. S, Chang P. L. Treatment of a lysosomal storage disease, mucopolysaccharidosis VII, with microencapsulated recombinant cells. *Hum Gene Ther* **2000**;11(15):2117-27.
3. Ross C. J, Ralph M, Chang P. L. Somatic gene therapy for a neurodegenerative disease using microencapsulated recombinant cells. *Exp Neurol* **2000**;166(2):276-86.
4. Van Raamsdonk J. M, Ross C. J, Potter M. A, Kurachi S, Kurachi K, Stafford D. W, Chang P. L. Treatment of hemophilia B in mice with nonautologous somatic gene therapeutics. *J Lab Clin Med* **2002**;139(1):35-42.
5. Cirone P, Bourgeois J. M, Chang P. L. Antiangiogenic cancer therapy with microencapsulated cells. *Hum Gene Ther* **2003**;14(11):1065-77.
6. Cirone P, Bourgeois J. M, Shen F, Chang P. L. Combined immunotherapy and antiangiogenic therapy of cancer with microencapsulated cells. *Hum Gene Ther* **2004**;15(10):945-59.
7. Joki T, Machluf M, Atala A, Zhu J, Seyfried N. T, Dunn I. F, Abe T, Carroll R. S, Black P. M. Continuous release of endostatin from microencapsulated engineered cells for tumor therapy. *Nat Biotechnol* **2001**;19(1):35-9.
8. Lohr M, Muller P, Karle P, Stange J, Mitzner S, Jesnowski R, Nizze H, Nebe B, Liebe S, Salmons B. Targeted chemotherapy by intratumour injection of

- encapsulated cells engineered to produce CYP2B1, an ifosfamide activating cytochrome P450. *Gene Ther* **1998**;5(8):1070-8.
9. Muller P, Jesnowski R, Karle P, Renz R, Saller R, Stein H, Puschel K, von Rombs K, Nizze H, Liebe S. Injection of encapsulated cells producing an ifosfamide-activating cytochrome P450 for targeted chemotherapy to pancreatic tumors. *Ann N Y Acad Sci* **1999**;880:337-51.
 10. Zimmermann H, Hillgartner M, Manz B, Feilen P, Brunnenmeier F, Leinfelder U, Weber M, Cramer H, Schneider S, Hendrich C. Fabrication of homogeneously cross-linked, functional alginate microcapsules validated by NMR, CLSM and AFM-imaging. *Biomaterials* **2003**;24(12):2083-96.
 11. Zimmermann H, Shirley SG, Zimmermann U. Alginate-based encapsulation of cells: past, present, and future. *Curr Diab Rep* **2007**;7(4):314-20.
 12. Zimmermann H, Zimmermann D, Reuss R, Feilen P. J, Manz B, Katsen A, Weber M, Ihmig F. R, Ehrhart F, Gessner P. Towards a medically approved technology for alginate-based microcapsules allowing long-term immunoisolated transplantation. *J Mater Sci Mater Med* **2005**;16(6):491-501.
 13. Peirone M. A, Delaney K, Kwiecin J, Fletch A, Chang P. L. Delivery of recombinant gene product to canines with nonautologous microencapsulated cells. *Hum Gene Ther* **1998**;9(2):195-206.
 14. Soon-Shiong P, Heintz R. E, Merideth N, Yao Q. X, Yao Z, Zheng T, Murphy M, Moloney MK, Schmehl M, Harris M and. Insulin independence in a type 1 diabetic patient after encapsulated islet transplantation. *Lancet* **1994**;343(8903):950-1.

15. Xue Y. L, Wang Z. F, Zhong D. G, Cui X, Li X. J, Ma X. J, Wang L. N, Zhu K, Sun A. M. Xenotransplantation of microencapsulated bovine chromaffin cells into hemiparkinsonian monkeys. *Artif Cells Blood Substit Immobil Biotechnol* **2000**;28(4):337-45.
16. Wang M. S, Childs R. F, Chang P. L. A novel method to enhance the stability of alginate-poly-L-lysine-alginate microcapsules. *J Biomater Sci Polym Edn* **2005**;16:91-113.
17. Mazumder. M. A. Jafar Shen F, Burke Nicholas A. D., Potter Murray A., Stöver Harald D. H. Self-crosslinking Polyelectrolyte Complexes for Therapeutic Cell Encapsulation. *Biomacromolecules* **2008**, 9(9), 2292-2300
18. Li A. A, Shen F, Zhang T, Cirone P, Potter M, Chang P. L. Enhancement of myoblast microencapsulation for gene therapy. *J Biomed Mater Res B Appl Biomater* **2006**;77(2):296-306.
19. Li A. A, Hou D.Y, Shen F, Seidlitz E. P, Potter M. A. Luciferase Therapeutic Microcapsules for Gene Therapy. Submitted to Biomaterials.
20. Li A. A, MacDonald N. C, Chang P. L. Effect of growth factors and extracellular matrix materials on the proliferation and differentiation of microencapsulated myoblasts. *J Biomater Sci Polym Edn* **2003**;14(6):533-49.
21. Shen F, Li A. A, Gong Y. K, Somers S, Potter M. A, Winnik F. M, Chang P. L. Encapsulation of recombinant cells with a novel magnetized alginate for magnetic resonance imaging. *Hum Gene Ther* **2005**;16(8):971-84.

22. Shen F, Li A. A, Cornelius R. M, Cirone P, Childs R. F, Brash J. L, Chang P. L. Biological properties of photocrosslinked alginate microcapsules. *J Biomed Mater Res B Appl Biomater* **2005**;75(2):425-34.
23. Van Raamsdonk J. M, Chang P. L. Osmotic pressure test: a simple, quantitative method to assess the mechanical stability of alginate microcapsules. *J Biomed Mater Res* **2001**;54(2):264-71.
24. Chang P. L. Non-autologous somatic gene therapy. in somatic Gene Therapy. Florida: CRC; **1995**. Chap.12 p.
25. Awrey D. E, Tse M, Hortelano G, Chang P. L. Permeability of alginate microcapsules to secretory recombinant gene products. *Biotechnol. Bioeng* **1996**; 52(4):472-484.

Chapter 5: Primary amine based polyelectrolytes for cell Encapsulation

Mazumder, M. A. J.; Burke, N. A. D.; Shen, F.; Potter, M. A.; Stöver, H. D. H.

To be submitted

Contributions:

I performed all the experiments except for the cell encapsulation and cell viability work, which was carried out by Dr. Feng Shen, Research Associate in Dr Murray A. Potter's Group, Health Sciences, McMaster University. I wrote the manuscript edits by Drs. Burke and Stöver.

Abstract

The formation of a covalently crosslinked shell around calcium alginate beads by reaction of a reactive polyanion, poly[(methacrylic acid, sodium salt)-co-2-(methacryloyloxy)ethyl acetoacetate] (70:30, A70) with four different polyamines, poly(L-lysine) (PLL), poly[(2-(methacryloyloxy)ethyl trimethylammonium chloride)-co-2-aminoethylmethacrylate] (70:30, C70), poly(2-aminoethyl methacrylate) (C0) and poly(N-(3-aminopropyl)methacrylamide) (PAPM) was studied, using a range of stability tests. PAPM and PLL were found to form the strongest shells. Coating with PAPM required the presence of calcium chloride in the coating bath to prevent aggregation of the hydrogel beads during coating. Viability of encapsulated C₂C₁₂ cells, and resistance to protein binding using fluorescently labeled bovine serum albumin, were found to be comparable to those of alginate / poly-L-lysine / alginate (APA) control capsules.

5.1 Introduction

Microencapsulation of cells and enzymes has a number of promising bioindustrial¹ and biomedical applications² and is likely to play a major role in cell and transplantation therapies.³ Cell encapsulation technologies are currently being developed for the treatment of several human diseases such as lysosomal storage disease (LSD)⁴, diabetes⁵, Parkinson's disease⁶ and certain cancers⁷. To avoid rejection by the host, the transplanted cells are often protected by a semi-permeable matrix, which permits the passage of smaller molecules (nutrients and therapeutic proteins), while obscuring the encapsulated cells from the host's immune system.^{8,9}

In a typical cell encapsulation process, cells are suspended in an alginate solution, which is then dropped into a gelling bath containing multivalent ions (Ca^{2+} , Ba^{2+}), followed by coating with polyelectrolytes. The most widely studied capsule type is the APA capsule in which the calcium alginate gel is coated with poly(L-lysine) and then alginate. The main concern with APA microcapsules is loss of structural integrity during long term implantation due to disruption of ionic cross-linking.¹⁰ In some cases, capsules that are held together by ionic interactions have been further reinforced by covalent crosslinking of the core or coating layer, either photochemically^{11,12} or by using a small-molecule crosslinker (i.e., glutaraldehyde or carbodiimide).¹³

We recently described the formation of a covalently self-cross-linked coating from polyelectrolytes bearing complementary reactive groups.¹⁴ Unlike small-molecule cross-linkers, these polymer-bound reactive groups should be less bioavailable and should not pose a toxicity concern to either cells or host. The polyanion, A70 (a 70/30 mole ratio copolymer of methacrylic acid and 2-[methacryloyloxy]ethyl acetoacetate)),

has shown good biocompatibility with encapsulated cells and after implantation into mice.¹⁵ However, the polycation C70 (a 70/30 mole ratio copolymer of [2-(methacryloyloxy)ethyl] trimethylammonium chloride and 2-aminoethyl methacrylate) was found to bind proteins from the growth medium causing an immune response when implanted in mice.¹⁶ In addition, C70 coated capsules are more prone to aggregation during the coating process than PLL-coated capsules and preliminary studies have shown that C70 undergoes intra/intermolecular amidation under some conditions leading to cross linked gels that cannot be used for capsule coating.

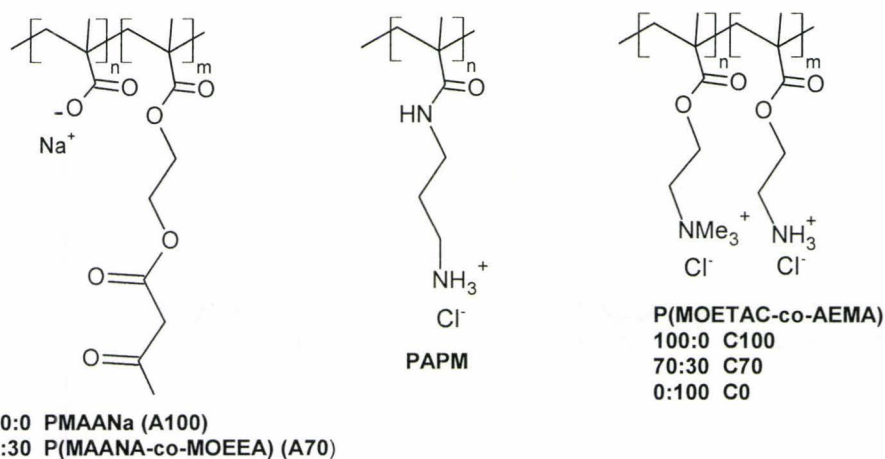
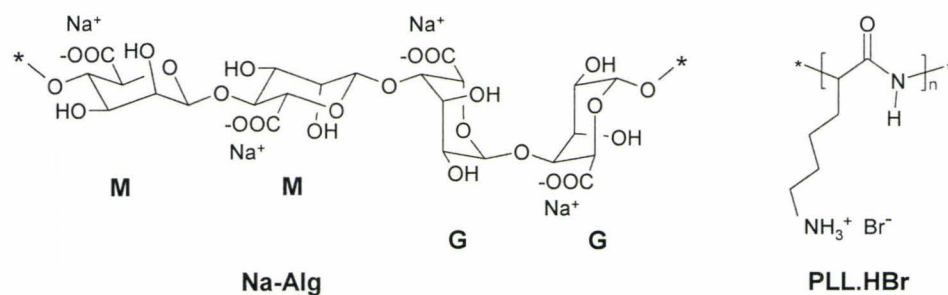
Thus, it was desirable to identify other polycations with primary amine groups capable of replacing C70 as a component in the self-cross-linking coatings. Ideally, the polycations would be available in a variety of molecular weights (MWs) and have a composition that was easily modified to vary properties such as charge density, hydrophobicity, H-bonding ability, etc. Primary amine-containing polycations¹⁷ of both natural and synthetic origin, such as poly(L-lysine) (PLL)⁸, chitosan, poly(ethyleneimine)¹⁸, poly(L-ornithine)¹⁹, poly(L-arginine)²⁰, poly(allylamine)^{21,22}, poly(methylene-co-guanidine)²³ and poly(vinylamine)^{21,24,25} have been used to coat calcium alginate beads for cell encapsulation. In addition, Prokop et al have screened a number of polycations, including some with primary amines, and identified some with promise for use in cell encapsulation.²⁶ While many of these polycations formed stable coatings on the alginate surface, there are some limitations for their use in this particular application. For example, poly(L-arginine) is expensive and has a high pKa that may not be ideal for the cross-linking reaction with A70 where it is desirable to have a portion of the amine groups in their non-protonated state. PLL, the most widely used polycation is

expensive, has been shown to induce inflammation,²⁷ and also has a pKa (10.5)²⁸ well above physiological pH.

Thus, we chose to investigate amine-bearing acrylic polymers containing either 2-aminoethyl methacrylate (AEMA) or N-(3-aminopropyl)methacrylamide (APM), two commercially available monomers. The homopolymers produced from these two monomers (PAEMA (or C0) and PAPM) have some structural similarities to PLL, but also some important differences, in terms of charge spacing, side chain length and the nature of the functional groups (Scheme 5.1). A number of copolymers that contain either AEMA³⁰ or APM^{29,33} are known, indicating that polymer properties and functionality could be further tuned through copolymerization of APM or AEMA with the wide range of acrylic monomers available. This stands in contrast to poly(allylamine) and poly(vinylamine), which are made from low reactivity monomers that copolymerize poorly with most other monomers. In addition, controlled polymerization techniques such as atom transfer radical polymerization (ATRP) and reversible addition-fragmentation chain transfer (RAFT) polymerization have been used to polymerize AEMA^{30,31} and APM^{32,33} and thus it should be possible to prepare (co)polymers with well controlled MWs and architectures.

In this paper, the feasibility of using C0 and PAPM as coatings for alginate capsules is examined and compared with that of C70, poly(2-(methacryloyloxy)ethyl)trimethylammonium chloride) (C100) and the widely used PLL. Polyelectrolyte complexes formed from these polycations and alginate, poly(methacrylic acid, sodium salt) (A100) or A70 were studied and some of these polyelectrolyte pairs were used to coat Ca-Alg beads. The structures of these polyelectrolytes are shown in

Scheme 5.1. In particular, the resistance of the complexes to ionic strength, their ability to form a covalently cross-linked complex, and the viability of cells in Ca-Alg capsules coated with the complexes were explored with the goal of forming a self-cross-linked polyelectrolyte skin without sacrificing biocompatibility.



Scheme 5.1. Polyelectrolytes used in this study.

5.2 Experimental

5.2.1 Materials:

Sodium alginate (Keltone LV) was a gift from the Nutrasweet Kelco Company (San Diego, CA) and sodium alginate (Pronova UP, MVG) was purchased from NovaMatrix

(Sandvika, Norway). N-(3-Aminopropyl)methacrylamide hydrochloride (APM) was purchased from Polysciences (Warrington, PA) and used as received. 2-Aminoethyl methacrylate (AEMA, 90%, as HCl salt), [2-(methacryloyloxy)ethyl] trimethylammonium chloride (MOETAC, 75 wt% solution in water), 2,2'-azobis(2-methylpropionamide) dihydrochloride (97%), poly(methacrylic acid, sodium salt) (PMAANa, $M_n = 5400$ g/mol; 30 wt% solution), poly(L-lysine) hydrobromide (PLL, $M_n = 15-30$ kg/mol), fluorescein isothiocyanate (FITC)-conjugated bovine serum albumin ($M_n = 66$ kDa) (BSA_f), and trypan blue stain (0.4% in 0.85% saline) were purchased from Sigma-Aldrich Co. (Oakville, ON) and used as received. Sodium chloride (Caledon Laboratories, Georgetown, ON), calcium chloride (Fisher), ethylenediaminetetraacetic acid, disodium salt (EDTA) (Anachemia, Montreal, QC) and trisodium citrate dihydrate (Analar, EMD Chemicals, Gibbstown, NJ) were used as received. Sodium hydroxide and hydrochloric acid solutions were prepared from concentrates (Anachemia Chemical, Rouses Point, NY) by diluting to 0.100 M or 1.000 M with deionized water.

The preparations of A70 (M_n 42 kg/mol),³⁴ C70 (M_w 167 kg/mol),¹⁴ C100 (M_w 300 kg/mol)³⁴ and C100-13k (M_w 13 kg/mol)³⁴ were described elsewhere.

5.2.2 Synthesis of Poly(N-(3-aminopropyl)methacrylamide hydrochloride), PAPM and Poly(2-aminoethyl methacrylate), C0:

The polymers were prepared as described previously for C70.¹⁴ APM (5.24 g, 29.3 mmol) and 2,2'-azobis(2-methylpropionamide) dihydrochloride (0.159 g, 0.59 mmol, 2 mol% relative to monomer) were dissolved in 50 mL deionized water in a 60 mL high-density polyethylene bottle. The solution was bubbled with nitrogen for several minutes before the bottle was sealed and then heated in an UVP HB-1000 Hybridizer at 60 °C for 24 h while being rotated (15 rpm) to provide mixing. PAPM was purified by dialysis with cellulose tubing (12 kDa MW

cut-off, Spectrum Laboratories, USA) in deionized water and then isolated by freeze-drying. Yield: 4.29 g (82 %).

In a similar fashion, C0 was prepared using AEMA hydrochloride (5 g, 30.2 mmol) and 2,2'-azobis(2-methylpropionamidine) dihydrochloride (81 mg, 0.30 mmol, 1 mol% relative to monomer). During dialysis the solutions were maintained at pH 5 to avoid intra- and intermolecular amidation reactions. Yield: 3.41 g (68 %).

5.2.3 Molecular Weight Determination:

Viscometric measurements on PAPM and C0 solutions in 1 M NaCl at pH 5 were performed with an Ubbelohde viscometer (viscometer constant: 0.00314 cSt/s) at 20.0 ± 0.1 °C. Prior to measurement, all solutions were filtered through a 0.45 μm Acrodisc sterile membrane filters. The intrinsic viscosity $[\eta]$ calculated from the Huggins plot (η_{sp}/c vs. c) was used to calculate the polymer molecular weight using values for K and a found in the literature for PMOETAC.³⁵

5.2.4 Determination of pK_a :

The pK_a values of PAPM and C0 were determined by potentiometric titration (PC Titrator automatic titrator, Man Tech Associates Inc.) of the hydrochloride salts with 0.100 M NaOH. The pK_a was taken as the midpoint of the neutralization curve.

5.2.5 Preparation and coating of Ca-Alg Beads:

The Ca-Alg beads and polyelectrolyte-coated capsules were prepared as described by Mazumder et al.¹⁴ A syringe pump (Razel Scientific Instruments Inc., Model A-99) was used to deliver an aqueous sodium alginate solution (1.5%(w/v) Keltone LV or Pronova UP MVG) through a 27-gauge blunt needle (Popper & Sons, New York) at a rate of 30.1 mL/h into a

gelling bath (1.1% CaCl₂, 0.45% NaCl) with a concentric airflow used to shear the drops. These resulting spherical beads were ca.500-600 μm diameter. Capsules were coated as described previously except that the effect of variables such as pH, calcium chloride concentration, and ionic strength in the coating solution was examined. Unless otherwise indicated, the coating was done at approximately pH 7.5 with exposures of 6 min for PLL and 10 min for any of the synthetic polycations.

5.2.6 Characterization:

The physical appearance of capsules and polyelectrolyte complexes were examined with an Olympus BX51 optical microscope fitted with a Q-Imaging Retiga EXi digital camera and Image Pro software. The average diameters of the beads and capsules were determined by analyzing three batches of approximately 50-100 beads or capsules each. Phase contrast microscope images were taken using a Wild M40 microscope. A confocal laser scanning imaging system comprised of an air-cooled Argon-ion laser and a Nikon microscope using EZ-C1 software, version 1.50, was used to investigate the distribution of BSA_f in the microcapsules.

5.2.7 Chemical and Mechanical stress test:

Concentrated capsule suspensions in saline (100 μL) were placed in 15 mL polypropylene conical tubes and exposed to 5% w/v (170 mM, 5 mL) sodium citrate for 5 min. The capsules were allowed to settle before the supernatant was removed, and replaced by 5 mL of 2 M sodium chloride. The tubes were attached to a wheel tilted 30° from horizontal and rotated at 30 rpm for 15 min at room temperature. The beads were allowed to settle, washed once with 5 mL distilled water, and treated with 0.06 mL of a 0.4% solution of trypan blue in 0.85% saline followed by 2-3 ml distilled water. After 5 minutes the supernatant was removed, and the

beads washed once with 5 mL distilled water. The samples were then examined by optical microscopy.

5.2.8 Mechanical Stability:

The mechanical stability of capsules was tested by agitating the capsules while they were exposed to hypotonic solution (the osmotic pressure test (OPT)),³⁶ or by using a Ca chelation test.^{14,16} Briefly, in the OPT, 100 μ L of sedimented capsules (~200 capsules) and 10 ml of distilled water were placed in a 15 mL polypropylene conical tube and then agitated for 3 h on an orbital mixer (REAX 3, Caframo Ltd, Warton, ON) at 30 rpm. The capsules were then stained by adding 0.12 mL of a 0.4% solution of trypan blue in 0.85% saline, and transferred to glass petri dishes on a light box. The percentage of intact capsules was determined by direct visual inspection, or from an image taken with a digital camera. In the calcium chelation test, 100 μ L of sedimented capsules were exposed to 0.003% (0.1 mM, 10 mL) EDTA solution in distilled water while being agitated for 15 min on an orbital mixer at 30 rpm, before analysis, as described for the OPT. Experiments were conducted in triplicate.

5.2.9 Encapsulation of Cells:

The C₂C₁₂ myoblast cell line (American Type Culture Collection [ATCC]) was used and the cells were cultured and encapsulated as described previously.¹⁴

5.2.10 Cell Viability:

The number of viable cells per capsule was determined with an Alamar Blue assay.³⁷ A 100 μ L sample of capsules was loaded in a 24-well plate with 500 μ L media. Alamar Blue reagent (50 μ L) was added to each sample and the plate was incubated at 37 °C for 4 hours. After incubation, 100 μ L of solution was taken from each well and placed in a microtiter plate. The

fluorescence of each sample was read with a Cytofluor II fluorimeter, with an excitation wavelength of 530 nm and an emission wavelength of 590 nm. The number of viable cells was determined by comparing fluorescence values with a standard curve generated from a known number of unencapsulated cells.

5.2.11 Bovine serum albumin (BSA) uptake by capsules:

FITC-labeled BSA (BSA_f) was dissolved in 0.9% NaCl to form a 0.05% solution, and the pH was adjusted to 7.1. A concentrated capsule suspension (0.3 mL) was equilibrated with 3 mL of BSA_f for 24 h at 20 °C. The capsules were then washed 4 times with 3 mL of 0.9% NaCl before examination by confocal microscopy.

5.3 Results and Discussion

The aim of the present work is to evaluate the ability of several polycations to form cross linked coatings on Ca-Alg capsules, in conjunction with the reactive polyanion A70 described earlier.^{14,15,16} In particular, the aim is to reduce protein binding and capsule aggregation observed previously with the quaternary ammonium ion-rich C70. The properties of the polycations are shown in Table 5.1.

Table 5.1: Properties of polycations:

Polycation	MW (kg/mol) ^a	pKa ^b	[NaCl], mM at which polycation complex with A100-5.4k dissolves
PLL	15-30 ^c	10.5 ²⁸	400
C100-13k	13	--	400
C100	300	--	500
C70	167	7.0 ± 0.2	650
C0	299	7.6	700
PAPM	260	8.6	800

^aM_w obtained from viscometry data. ^bFrom titration in water. ^cgiven by supplier.

With the exception of C100-13k, the synthetic polymers have MWs considerably higher than PLL (>150k vs. 15-30k) and this might be expected to affect the nature of the complex formed on the Ca-Alg beads. However, 15-30k PLL has been shown to be trapped at the surface of Ca-Alg beads and thus all of the polycations, except perhaps C100-13k, would also be expected to be captured at or near the surface of the Ca-Alg beads.

The synthetic polymers that contain primary amine groups have pKa values considerably lower than PLL, which should afford more free amines during coating and hence more efficient covalent cross-linking. Three of the polycations (PLL, PAPM, C0) bear only primary ammonium ions but have pKa values ranging from of 10.5 to 7.6, likely caused by changes in the spacing of the ammonium ions along the backbone. The value measured for C0 agrees well with pKa values found in the literature for C0 (7.6)³⁰ or a C0 block in a block copolymer (7.1).³¹ C70 had the lowest pKa of all reflecting the high charge density present at half-neutralization due to the quaternary ammonium ions.

One concern with the use of C0 is that, like C70, it will be sensitive to intra- and intermolecular amidation reactions or hydrolysis. He et al. studied these reactions and found that C0 was stable for several days at 20 °C in an aqueous solution at pH 9 but that degradation

reactions were detected within a few hours at pH 10 or greater.³⁰ For this reason, C0 solutions were kept at pH 7.5 or lower during this work.

Polyelectrolyte complexation between any polyanion (Alg, A100, A70) and any polycation (PLL, C0, C70, C100, PAPM) at 1% total polymer concentration and pH 7 all gave phase-separated materials, but only the polyelectrolyte complexes (PECs) made between primary amine-containing polymers and A70 survived when exposed to 2 M NaCl, demonstrating that these complexes had become covalently cross linked.

5.3.1 Coating of Ca-Alg Beads:

Ca-Alg beads were coated with the different polycations (C0, C70, C100, PAPM, and PLL), using concentrations from 0.01-0.5% w/v in saline at pH 7.5. The C100 and PLL-coated capsules were well dispersed for all polycation concentrations. In contrast, Ca-Alg beads exposed to C70 or C0 aggregated at polycation concentrations from 0.01 to 0.1wt%, but stayed dispersed at 0.5wt%. Ca-Alg beads exposed to PAPM in saline aggregated (Figure 5.1) at all PAPM concentrations examined (0.01-0.5%). This aggregation at low and intermediate polycation concentration is likely due to bridging flocculation, and is may be exacerbated by the high molecular weight of some of the polycations used.

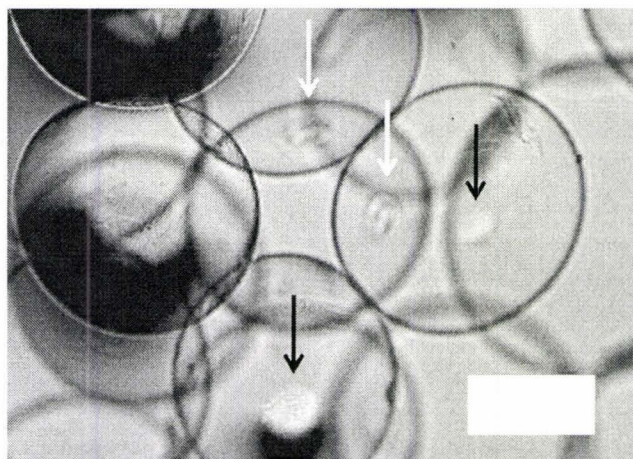


Figure 5.1: Optical microscope image of aggregated Ca-Alg-PAPM capsules formed by exposure of Ca-Alg beads to 0.5wt% PAPM solution in saline for 10 min. Points of contact (white arrows) between capsules and detached patches (black arrows) are visible. Scale bar is 300 μm .

The effects of varying the pH or ionic strength of the coating solution were also investigated. Aggregation occurred at all pH values between 5.5 and 8.5 for Ca-Alg beads coated with 0.5% PAPM in saline. Similarly, aggregation was observed for NaCl concentrations ranging from 0-374 mM (Figure 5.2). However, when CaCl_2 was used instead of NaCl aggregation was suppressed for concentrations ≥ 70 mM as shown in Figure 5.2. This is not simply an effect of ionic strength since the final two data points of the CaCl_2 curve (70 and 125 mM) have the same ionic strengths as the final two points of the NaCl curve (210 and 374 mM). This points to specific interactions between the divalent Ca^{2+} , PAPM and the Ca-Alg bead and is consistent with a number of studies showing that the presence of CaCl_2 in chitosan solutions has a strong effect on chitosan binding to Ca-Alg beads.^{38,39,40}

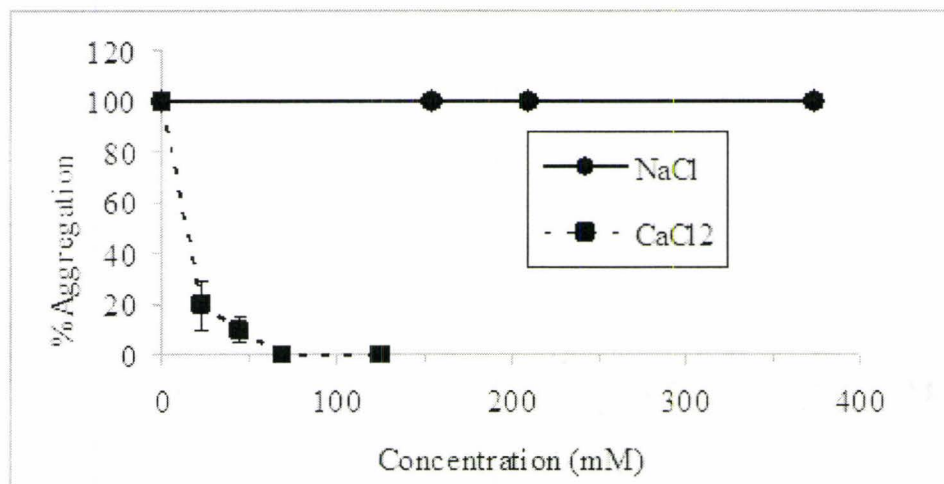


Figure 5.2: Effect of $[\text{NaCl}]$ and $[\text{CaCl}_2]$ on capsule aggregation during coating with 0.5% PAPM.

For all subsequent polycation coatings, a solution containing 1.1% (100 mM) CaCl_2 and 0.45% (77 mM) NaCl solution was used. This solution is known to be reasonably well tolerated by the capsules and any encapsulated cells since it is commonly used as a gelling bath. With this solution, aggregation was suppressed during coating of Ca-Alg beads with C70, C0 and PAPM solutions at polycation concentrations ranging from 0.01 to 0.5%, leading to well dispersed and smooth capsules that were easily stained with the dianionic dye Trypan blue (Figure 5.3) showing that the polycation had been bound to the surface of the bead.

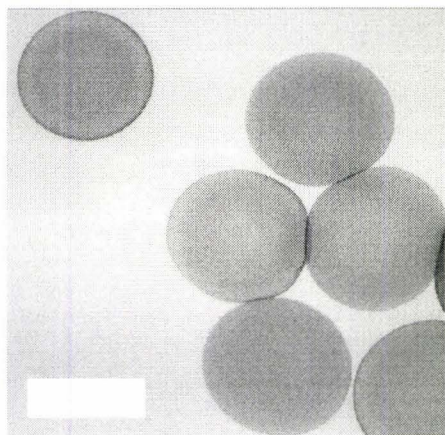


Figure 5.3: Optical microscope image of Ca-Alg beads exposed for 10 minutes to 0.5% PAPM in 1.1% CaCl_2 /0.45% NaCl, followed by washing and trypan blue staining. Scale bar 500 μm .

In some instances the capsules became wrinkled during coating with polycations. This has been observed previously^{14,41} and is presumably caused of osmotic pressure induced shrinkage of the Ca-Alg beads where the surface layer is unable to undergo a corresponding shrinkage. The wrinkling of hydrogel beads such as Ca-Alg is known to depend on the type, MW

and concentration of the polycation, exposure time, the size of the Ca-Alg beads, as well as the nature of the solutions used to wash the beads prior to coating.^{14,28,41}

In the present work, one batch of CaAlg beads that had been stored at 4 °C in saline for several weeks prior to coating with the polycations was found to be particularly prone to wrinkling, likely due to some loss of Ca^{2+} or breakdown of alginate,⁴² resulting in weakening of the hydrogel core. Coating of this batch of Ca-Alg beads with higher molecular weight polycations resulted in different types of wrinkling, depending on polymer composition. Figure 5.4 shows a representative Ca-Alg capsule coated with 0.5 wt% C70 for 10 min. Appearance of such wrinkling is hence an indicator for loss of gel strength, high osmotic pressure or the formation of an inflexible shell.

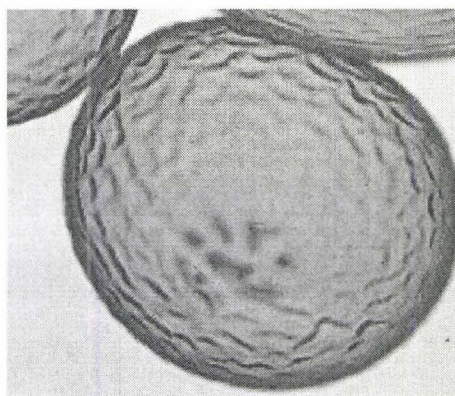


Figure 5.4: Ca-Alg beads, coated with 0.5 wt% C70 for 10 min, followed by washing and trypan blue staining.

The primary amine-containing polycations, C0, PAPM and PLL, as well as C70 were used in subsequent encapsulation experiments. Coating with these polycations was conducted such that no wrinkling of Ca-Alg beads was observed by using freshly prepared Ca-Alg beads and polycation concentrations and exposure times of no more than 0.5% and 10 min,

respectively. Each type of polycation-coated bead was then coated with either sodium alginate or A70 before being evaluated further.

5.3.2 Capsule stability:

Ca-Alg capsules coated with C0, PAPM or PLL, followed by either alginate or A70, were evaluated for stability, by challenging them with a) citrate and 2 M NaCl, b) water or c) a dilute EDTA solution.

Exposure of coated Ca-Alg beads to sodium citrate (170 mM) caused the Ca-Alg core to dissolve while the PEC shells survived. When the resulting hollow shells were challenged with 2 M NaCl, those from the non-cross linked APA, A-PAPM-A and A-C0-A capsules (Figure 5.5a, b, d) disappeared as the ionic interactions within the PECs were screened. In contrast, the shells from the A-PAPM-A70 and A-C0-A70 capsules remained intact (Figure 5.5c, e inset) as they were maintained by covalent cross-linking, in addition to the ionic interactions.

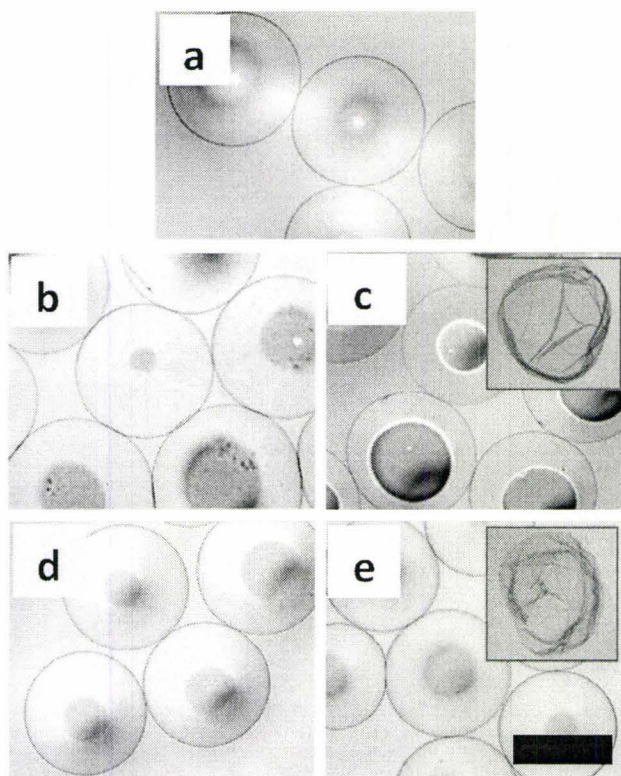


Figure 5.5: Optical microscope images of a) APA (0.05/0.03), b) A-PAPM-A (0.5/0.03), c) A-PAPM-A70 (0.5/0.5), d) A-C0-A (0.5/0.03), and e) A-C0-A70 (0.5/0.5) capsules. After treatment with 170 mM sodium citrate and then 2 M NaCl, followed by trypan blue staining a, b, d have dissolved, while c and e shells survive and are shown in insets. Polycation/polyanion concentrations (wt%) are shown in brackets. Scale bar: 500 μm . The dark circular features within the capsules are caused by contact with the slide or the air/liquid interface.

The capsules were also challenged with an osmotic pressure test (OPT),³⁶ and with a related EDTA test involving removal of Ca^{2+} using a dilute EDTA solution. Capsules were tumbled in distilled water for 3 hours, or in EDTA solution for 15 minutes, before the fraction of intact capsules was determined (Table 5.2). Standard APA capsules prepared with 0.05% PLL were completely broken in both tests. APA capsules formed with 0.5% PLL survive the OPT but nearly half were broken in the EDTA test. In contrast, all of the capsules prepared with A70 survive tumbling in either water or EDTA, reflecting the presence of covalently cross linked shells around the capsules, in analogy to the C70/A70 and other A70 reinforced capsules described earlier.^{14,15,16}

Significantly different A70 and alginate concentrations were used (compare 2nd and 3rd entries in Table 5.2) because these concentrations allowed coating without capsule aggregation. If the alginate concentration used for the outer coating was increased to 0.5%, the capsules aggregated and coalesced into larger gels, surrounded by alginate, possibly due to calcium exchange between the bead cores and the coating solution. Capsule aggregation often occurred for A70 concentrations of 0.01-0.1 but not at 0.5%. Experiments with dye-labelled A70 suggested that <10% of the A70 was bound to the capsules at this concentration and thus the amounts of alginate and A70 bound during coating experiments is not significantly different.

Table 5.2: Performance of empty and cell-containing capsules in the OPT and Ca chelation test.

Capsules ^a	% intact ^b			
	OPT		Ca chelation	
	Dist. water (tumbled for 3 hrs)		0.003% EDTA in dist. water (tumbled for 15 min)	
	Empty	With cells	Empty	With cells
APA (0.05/0.03)	0	0	0	0
A-PLL-A (0.5/0.03)	100	0	60	0
A-PLL-A70 (0.5/0.5)	100	100	100	70 ± 5
A-PAPM-A70 (0.5/0.5)	100	100	100	100
A-C0-A70 (0.5/0.5)	100	0	100	5 ± 5

a. Concentrations in brackets refer to polyelectrolyte concentrations (%w/v) used for coating. Capsules were stored in saline (empty) or serum free media (cell- containing) for 24 h between coating and OPT/Ca chelation test.

b. Percent capsules still intact as per optical microscopy after tumbling for 3h in dist. water, or for 15 min in EDTA solution.

The stability of corresponding cell-containing capsules was also examined. Capsules containing myoblast C₂C₁₂ cells were incubated *in vitro* for one day and then tested using the OPT and the EDTA tests (Table 5.2). The cell-containing capsules fared more poorly than the empty capsules, with the exception of the A-PAPM-A70 capsules. Reduced stability for capsules containing cells has been observed previously and was attributed to the disruption of the Ca-Alg gel or the polyelectrolyte complex shell by the cells.³⁶ The use of A70 in conjunction with PAPM or PLL gives capsules that show good strength in these tests. The PAPM-A70 capsules performed better than the previously studied C70-A70 capsules,¹⁴ which remained 100% intact when empty, but were ruptured to some degree if they contained cells.

5.3.3 Cell viability:

The viability of myoblast C₂C₁₂ cells in APA, A-PAPM-A, A-PAPM-A70 and A-C0-A70 capsules, several of which are shown in Figure 5.6, was evaluated using the Alamar Blue assay. The encapsulated cells were incubated *in vitro* and the number of living cells per capsule was monitored over time (Figure 5.7). Immediately after encapsulation there was some reduction (~25%) in cell number for capsules coated with 0.5% PLL or 0.5% C0 compared to APA. The PAPM-coated capsules showed initial cell numbers nearly identical to APA. The cells exhibited similar proliferation rates in all types of capsules such that there were comparable numbers of cells found in each capsule on Day 7. In addition, switching from 0.03% alginate to 0.5% A70 as the outer coating has no noticeable effect on viability, consistent with previous observations of the good cell compatibility of A70.^{14,15} Thus, the capsules coated with PAPM or C0 in combination with A70 provide a good environment for cell growth. These observations reflect the fact that the normally cytotoxic polycations are trapped at the capsule surface away from the cells and findings that polycations that are bound to polyanions (electrostatically, or as here, covalently) do not seem to show much cell toxicity.²⁶

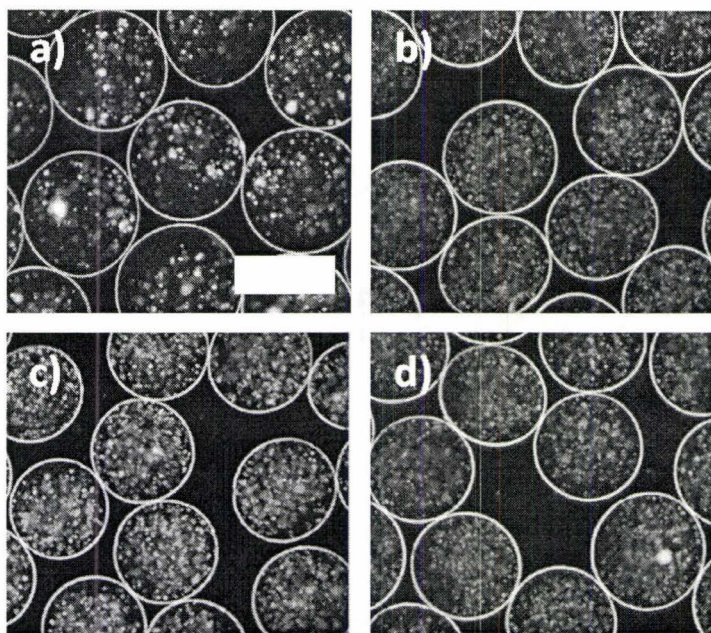


Figure 5.6: Phase contrast microscope image of C_2C_{12} cells encapsulated in a) APA(0.05/0.03), b) A-PAPM-A(0.5/0.03), c) A-PAPM-A70(0.5/0.5), and d) A-C0-A70(0.5/0.5) after *in vitro* incubation for 1 week. Polyelectrolyte concentrations are shown in brackets. Scale bar –500 μm .

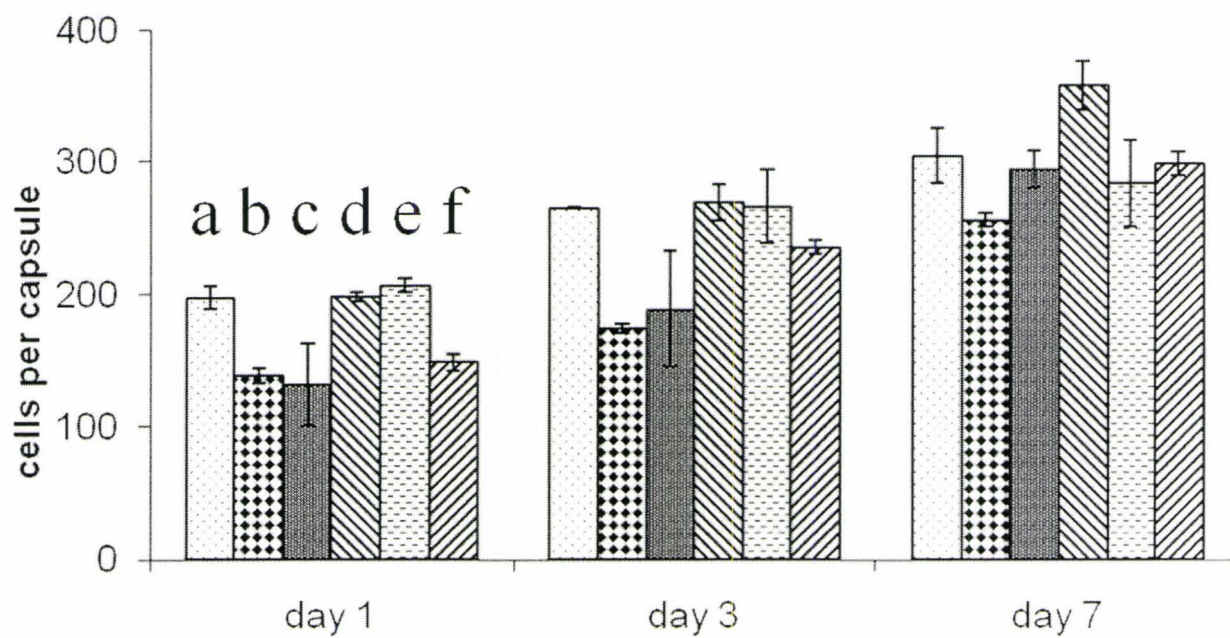


Figure 5.7: *In vitro* cell viability for C₂C₁₂ cells encapsulated in a: APA (0.05/0.03), b: A-PLL-A(0.5/0.03), c: A-PLL-A70(0.5/0.5), d: A-PAPM-A (0.5/0.03), e: A-PAPM-A70(0.5/0.5), and f: A-C0-A70(0.5/0.5) capsules. Polyelectrolyte concentrations are shown in brackets.

5.3.4 Protein Binding:

Protein binding is an important consideration for biomaterials^{43, 44, 45, 46} and is believed to play a key role in the immune response observed upon implantation of capsules coated with C70.¹⁶ In the same work, A70 was shown to only weakly bind BSAf.

In order to examine the ability of polycations on the capsule surface to absorb proteins from the culture medium, potentially leading to an immune response after transplantation into the host, a qualitative protein binding study was undertaken. The test involves determining the relative amounts of BSA bound to capsules coated with the different polycations. It is important to note that these protein-binding experiments were conducted with capsules made from a different alginate than the other experiments described in this paper. It was no longer possible to obtain Keltone LV alginate with same properties as before so the protein binding experiments were conducted with capsules made from a high purity alginate (Pronova UP MVG from NovaMatrix) that is now commonly used in cell encapsulation studies. Since the alginate remained constant while the nature of the polycation was varied, any differences in BSA binding will be due to the polycation.

Empty Ca-Alg beads coated with 0.5% polycation (C70, C0, PAPM or PLL) followed by Alg (0.03%), were incubated with 0.05% BSAf for 24h at 20 °C, washed four times with saline and then examined by confocal microscopy (Figure 5.8). All of the samples show a stronger signal at the capsule surface than in the interior. This is consistent with some binding of BSAf by the polycations which are localized at the surface. The fluorescence is quite weak for A-C0-A,

A-PAPM-A and A-PLL-A capsules (Figure 5.8 b, c, d) indicating minimal binding of BSA f . However, A-C70-A capsules showed very strong BSA f binding (Figure 5.8a), suggesting that the quaternary ammonium ion-containing polymer (C70) is a major contributor to binding proteins to the capsule surface. In contrast, PLL and the primary amine-containing polymers C0 and PAPM showed much less protein binding.

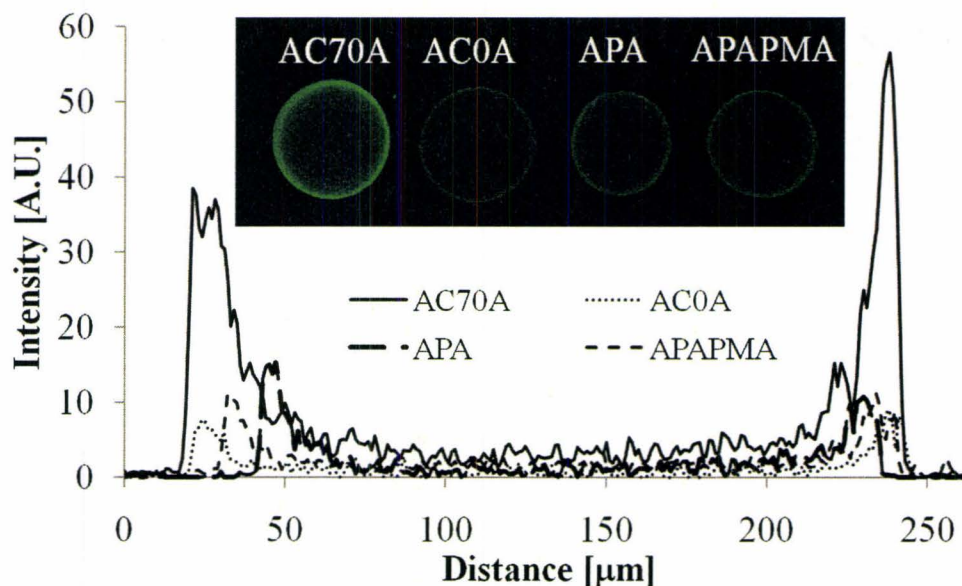


Figure 5.8: Top: Confocal microscopy optical sections in the equatorial region of A-C70-A, A-C0-A, A-PLL-A, and A-PAPM-A capsules, all prepared from Novamatrix alginate, and incubated in 0.05% BSA f at 20 °C for 24h. Bottom: line intensity profiles of capsules shown at top. Concentration of coating solutions: 0.5% polycation, 0.03% alginate. Exposure time: 10 min.

Work is in progress to examine some of these capsules with a more comprehensive protein-binding assay to identify whether there is preferential binding of certain proteins and to test if the BSA f screen provides a useful gauge of overall protein binding.

5.4 Conclusion

These results indicate that PAPM is comparable to PLL in terms of shell strength, cell viability and protein binding, in shell cross-linked Ca-Alg capsules formed with the reactive polyanion A70. Both PAPM and PLL show low BSA_f binding compared to polymers containing quaternary ammonium ions. They also show better capsule strengths compared to C0, the other all-primary amine polymer studied here. Due to the amide linkages near or in their backbone, PAPM as well as PLL are protected from the undesirable hydrolysis and transamidation reactions seen for C70 and for C0.

Addition of calcium chloride to the coating baths was shown to prevent capsule aggregation despite the high molecular weight PAPM used in this study.

This positions PAPM as a promising alternative to PLL in cross-linking coating of Ca-Alg beads. In future we will report on APM homopolymers with controlled molecular weight, and APM copolymers with non-ionic comonomers, currently being developed with the aim of increasing strength while further improving cell and host compatibility compared to PLL.

5.5 References

- ¹ Duff, R. G. *Trends Biotechnol.* **1985**, *3*, 167-170.
- ² Chang, T. M. S. *Biomater. Artif. Cell Artif. Org.* **1987**, *15*, 1-20.
- ³ Berthiaume, F.; Yarmush, M. L. in *The Biomedical Engineering Handbook*, second edition, CRC Press, Boca Raton, 2000, vol. 2, p109-1–109-12.
- ⁴ Shen, F.; Li, A. A.; Gong, Y- K.; Somers, S.; Potter, M. A.; Winnik, F. M.; Chang, P. L. *Hum. Gene Ther.* **2005**, *16*, 971-984.
- ⁵ Weir, G.; Colton, C. K.; O' Sullivan, E.; Lewis, A. Polymer encapsulated pancreatic islet cell products for diabetes treatment. U. S. Patent Application 23760, 2008.
- ⁶ Yasuhara, T.; Date, I. *Cell Transplant.* **2007**, *16*, 125-132.
- ⁷ Pasquale, C.; Shen, F.; Chang, P. L. *Cancer Gene Ther.* **2005**, *12*, 369-380.
- ⁸ Lim, F.; Sun, A. M. *Science* **1980**, *210*, 908-910.
- ⁹ Bañó, M. C.; Cohen, S.; Visscher, K.B.; Allcock, H.R.; Langer, R. *Biotechnology* **1991**, *9*, 468-471.
- ¹⁰ Wang, M. S.; Childs, R. F.; Chang, P. L. *J. Biomater. Sci. Polym. Ed.* **2005**, *16*, 91-113.
- ¹¹ Rokstad, A. M.; Donati, I.; Borgogna, M.; Oberholzer, J.; Strand, B. L.; Espevik, T.; Skjåk-Bræk, G. *Biomaterials* **2006**, *27*, 4726-473.
- ¹² Dusseault, J.; Leblond, F. A.; Robitaille, R.; Jourdan, G.; Tessier, J.; Menard, M.; Henly, N.; Halle, J. -P. *Biomaterials*, **2005**, *26*, 1515-1522.
- ¹³ Chandy, T.; Mooradian, D. L.; Rao, G. H. R. *Artif. Organs* **1999**, *23*, 894-903.
- ¹⁴ Mazumder, M. A. J.; Shen, F.; Burke, N. A. D.; Potter, M. A.; Stöver, H. D. H. *Biomacromolecules* **2008**, *9*, 2292-2300.
- ¹⁵ Mazumder, M. A. J.; Burke, N. A. D.; Shen, F.; Potter, M. A.; Stöver, H. D. H.

-
- Biomacromolecules* **2009**, *10(6)*, 1365-1373.
- ¹⁶ Shen, F.; Mazumder, M. A. J.; Burke, N. A. D.; Stöver, H. D. H.; Potter, M. A. *J. Biomed. Mater. Res. Part B: Appl. Biomater.* **2009**, *90B(1)*, 350-361.
- ¹⁷ Bhatia, S. R.; Khattak, S. F.; Roberts, S. C. *Curr. Opin. Coll. Int. Sci.* **2005**, *10*, 45-51.
- ¹⁸ Tatarkiewicz, K. *Artif. Organs* **1988**, *12*, 446-448.
- ¹⁹ Darrabie, M. D.; Kendall Jr, W. F.; Opara, E. C. *Biomaterials* **2005**, *26*, 6846-6852.
- ²⁰ Wang, S.-B.; Liu, Y.-G.; Weng, L. J.; Ma, X.-J. *Macromol. Biosci.* **2003**, *3*, 347-350.
- ²¹ Wang, Y. *J. Mater Sci. Eng C* **2000**, *13*, 59-63.
- ²² Lu, M. Z.; Lan, H. L.; Wang, F. F.; Chang, S. J.; Wang, Y. J. *Biotechnol. Bioeng.* **2000**, *70*, 479-483.
- ²³ Wang, T.; Lacik, I.; Brissova, M.; Anilkumar, A. V.; Prokop, A.; Hunkeler, D.; Green, R.; Shahrokhi, K.; Powers, A. C. *Nat. Biotechnol.* **1997**, *15*, 358-362.
- ²⁴ Grigorescu, G.; Rehor, A.; Hunkeler, D. *J. Microencapsul.* **2002**, *19*, 245-259.
- ²⁵ Wang, F. F.; Wu, C. R.; Wang, Y. J. *Biotechnol. Bioeng.* **1992**, *40*, 1115-1118.
- ²⁶ Prokop, A.; Hunkeler, D.; DiMari, S.; Haralson, M. A.; Wang, T. G. *Adv. Polym. Sci.* **1998**, *136*, 1-51.
- ²⁷ Strand, B. L.; Ryan, L.; Veld, P. I.; Kulseng, B.; Rokstad, A. M.; Skjak-Braek, G.; Espevik, T. *Cell Transplant.* **2001**, *10*, 263-275. Hobbs, H. A.; Kendall, W. F.; Darrabie, M.; Collins, B.; Bridges, S.; Opara, E. C. *Diabetes* **2000**, *49 (suppl. 1)*, A111
- ²⁸ Bysell, H.; Malmsten, M. *Langmuir* **2006**, *22*, 5476-5484.
- ²⁹ Seiffert, S.; Oppermann, W. *Macromol. Chem. Phys.* **2007**, *208*, 1744-1752.
- ³⁰ He, L.; Read, E. S.; Armes, S. P.; Adams, D. J. *Macromolecules* **2007**, *40*, 4429-4438.
- ³¹ Dufresne, M.-H.; Leroux, J.-C. *Pharm. Res.* **2004**, *21*, 160-169.

-
- ³² Li, Y.; Lokitz, B. S.; McCormick, C. L. *Angew. Chem. Int. Ed.* **2006**, *45*, 5792-5795.
- ³³ Deng, Z.; Boucekif, H.; Babooram, K.; Housni, A.; Choytun, C.; Narain, R. *J. Polym. Sci. Part A: Polym. Chem.* **2008**, *46*, 4984-4996.
- ³⁴ Burke, N. A. D.; Mazumder, M. A. J.; Hanna, M.; Stöver, H. D. H. *J. Polym. Sci., Part A: Polym. Chem.* **2007**, *45*, 4129-4143.
- ³⁵ Griebel, Th.; Kulicke, W. -M.; Hashemzadeh, A. *Colloid Polym. Sci.* **1991**, *269*, 113-120.
- ³⁶ Van Raamsdonk, J. M.; Chang, P.L. *J. Biomed. Mater. Res.* **2001**, *54*, 264- 271.
- ³⁷ Li, A. A.; McDonald, N. C.; Chang P.L. *J. Biomater. Sci. Polym. Ed.* **2003**, *14*, 533-549.
- ³⁸ Gaserod, O.; Sannes, A.; Skjak-Braek, G. *Biomaterials* **1999**, *20*, 773-783.
- ³⁹ Gaserod, O.; Smidsrod, O.; Skjak-Braek, G. *Biomaterials* **1998**, *19*, 1815-1825.
- ⁴⁰ Daly, M. M.; Knorr, D. *Biotechnol. Prog.* **1988**, *4*, 76-81.
- ⁴¹ Strand, B. L.; Gaserod, O.; Kulseng, B.; Espevik, T.; Skjak-Braek, G. *J. Microencapsul.* **2002**, *19*, 615-630.
- ⁴² Holme, H. K.; Davidsen, L.; Kristiansen, A.; Smidsrød, O. *Carbohydr. Polym.* **2008**, *73*, 656-664.
- ⁴³ Freeman, I.; Kedem, A.; Cohen, S. *Biomaterials* **2008**, *29*, 3260-3268.
- ⁴⁴ Coutinho, D. F.; Pashkuleva, I. H.; Alves, C. M.; Marques, A. P.; Neves, N. M.; Reis, R. L. *Biomacromolecules* **2008**, *9*, 1139-1145.
- ⁴⁵ Tzoneva, R.; Seifert, B.; Albrecht, W.; Richau, K.; Lendlein, A.; Groth, T. *J. Biomater. Sci. Polym. Ed.* **2008**, *19*, 837-852.
- ⁴⁶ Unsworth, L. D.; Sheardown, H.; Brash, J. L. *Langmuir* **2008**, *24*, 1924-1929.

Chapter 6: Core Cross-linked Microcapsules for Cell Encapsulation

Mazumder, M. A. J.; Burke, N. A. D.; Shen, F.; Potter, M. A.; Stöver, H. D. H.

Published in *Biomacromolecules*, **2009**, *10(6)*, 1365-1373

This chapter has been reproduced with permission from *Biomacromolecules*. Copyright
2009 American Chemical Society.

Contributions:

I performed all the experiments except the cell related encapsulations and studies which were carried out by Dr Feng Shen, Research Associate in Dr Murray A. Potter's Group, Health Sciences, McMaster University. I wrote the manuscript, with help from Drs. Burke and Stöver.

Abstract

Self-cross-linkable polyelectrolyte pairs comprised of poly(methacrylic acid, sodium salt-*co*-2-[methacryloyloxy]ethyl acetoacetate) (70:30 mol ratio, A70) and poly-L-lysine are incorporated into CaAlg beads to form either a covalently crosslinked shell or a core-cross linked bead. In both cases the reactive polyanion is added to a solution of sodium alginate that may contain live cells, and dropped into a calcium chloride gelling bath. Subsequent exposure to poly-L-lysine (15-30 kDa) leads to formation of a crosslinked shell, while exposure to lower molecular weight poly-L-lysine (4-15 kDa) leads to formation of an interpenetrating matrix of covalently crosslinked polymer within the CaAlg template. The resulting spherical composites are resistant to chemical and mechanical stress yet remain cyto-compatible. This approach to cell-encapsulation may be useful for cell immuno-isolation in therapeutic cell transplants.

6.1 Introduction

Transplantation of encapsulated allogeneic cells expressing therapeutic compounds or peptides is a promising approach for the treatment of diseases such as neurological disorders, dwarfism, hemophilia, lysosomal storage disorders and cancer. To avoid immune rejection by the host, the transplanted cells are typically protected by a semi-permeable membrane, which allows the exchange of oxygen, nutrients and metabolites, while obscuring the encapsulated cells from the host's immune system¹⁻⁵

The most common cell encapsulation system involves the alginate/poly-L-lysine/alginate (APA) microcapsules derived from the original protocol of Lim and Sun.⁵ These capsules are primarily composed of alginate, a naturally occurring polysaccharide composed of β -D-mannuronic acid (M) and α -L-guluronic acid (G) residues. Calcium ions are used to cross-link G-rich regions of the alginate chains, and the resulting calcium alginate (CaAlg) hydrogel beads are coated with poly-L-lysine (PLL) to strengthen the bead surface and control permeability. A final coating with alginate is applied in order to hide the PLL from the host⁴ and make the capsules biocompatible.

While APA capsules meet many of the requirements for immuno-isolation of cells when implanted into mice, they show insufficient strength when implanted into larger animals such as dogs.⁶ This may be due to weakening of the hydrogel core by exchange of calcium with other physiological ions and/or the loss of the protective polyelectrolyte coatings.

A number of studies have attempted to address the challenge of long-term mechanical stability by varying the molecular weight (MW) or G/M ratio of the alginate,^{4,7-9} the cross-linking ion^{9,10}, and/or the polyelectrolytes¹¹⁻¹⁴ used to coat the

capsule. Covalent cross-linking of the coating layer¹⁵⁻¹⁹ or the alginate core²⁰⁻²² have also been investigated.

Another approach has been to examine the use of alternate hydrogel cores,^{2, 23} including those made of composite materials. Reinforcement of the alginate core through the formation of an interpenetrating network or composite may lead to improved mechanical properties while maintaining most of the desirable properties of alginate. In addition, it may be easier to adjust capsule properties such as strength and permeability independently of each other. One requirement would be to maintain the ability of the alginate to form calcium complexes through its extended G blocks.

A number of alginate composite materials have been explored for cell encapsulation.²⁴ Compounds added to the alginate forming the bead core were designed to be thermally (agarose²⁵), ionically (carrageenan²⁶) or photochemically gelled,²⁷ or designed to modify viscosity or water content (carboxymethylcellulose²⁸), act as wall forming materials (cellulose sulphate,²⁹ heparin²⁸), control permeability or provide an improved environment for cell growth (chitlac - lactitol-functionalized chitosan³⁰). For example, capsules designed for longer-term cell implantation have been prepared with alginate-cellulose sulfate composite cores where the cellulose sulfate acted as a viscosity modifier and was thought to be a better wall builder than alginate when forming polyelectrolyte complexes with the polycations used to coat the capsules.²⁹ Still other composite cores have been formed by the in-diffusion of polymeric or monomeric species followed, in some cases, by cross-linking or polymerization. Gaserod et al found that the in-diffusion of low MW chitosan into CaAlg beads resulted in the formation of an alginate-chitosan gel in the core of the capsule that was able to withstand the loss of

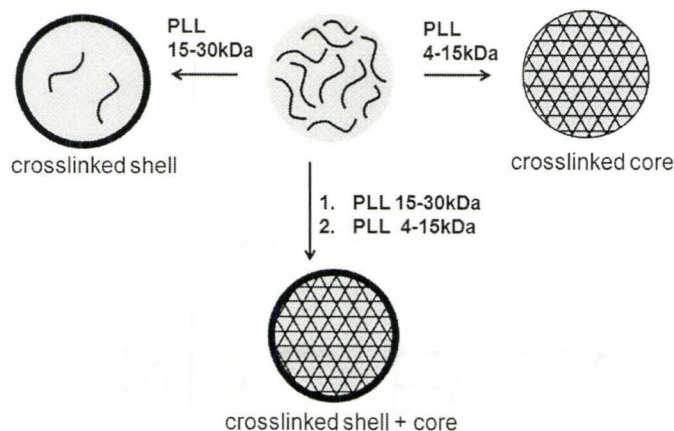
calcium.³¹ Childs and coworkers formed a composite capsule composed of alginate and poly(sodium acrylate-*co*-N-vinylpyrrolidone) formed by photopolymerization of monomers allowed to diffuse into the CaAlg beads.³²

We recently described polyelectrolytes bearing complementary reactive groups that underwent a covalent cross-linking reaction to produce a cross-linked polyelectrolyte complex coating on CaAlg capsules.³³ In contrast to photochemical crosslinking approaches, the described crosslinking by condensation reaction occurs spontaneously upon contact.

These materials and their cross-linking reaction might also be used to reinforce the core of the capsules. This paper describes the addition of the reactive polyanion, poly(methacrylic acid, sodium salt-*co*-2-[methacryloyloxy]ethyl acetoacetate), p(MAANa-*co*-MOEAA), 70:30 A70, to the CaAlg core followed by exposure to PLL. This could lead to two scenarios, depending on the relative ability of the two reactive polyelectrolytes to diffuse through the CaAlg matrix:

1. Larger PLL chains ($MW \geq 15\text{-}30$ kDa) should penetrate no further than 30 μm into the composite bead, the norm for APA-type capsules,³³ covalently crosslinking with the A70 chains that they encounter. If the A70 present in the core has some mobility in the CaAlg, it should diffuse to the capsule surface to further reinforce the shell, which has a thickness largely defined by the penetration depth of the PLL.
2. Smaller PLL chains ($MW < 15$ kDa) should be able to diffuse into the hydrogel bead, and react with A70 at deeper levels. Given appropriate concentrations and stoichiometry of the polyelectrolytes, it might be possible to form a covalently crosslinked network throughout the core.

The potential benefits of this counter-diffusion of the two reactive polyelectrolytes include a different control mechanism over wall thickness and location, compared to the usual sequential layer-by-layer deposition of polyelectrolytes. The first scenario would lead to covalently crosslinked analogs to the conventional APA capsules. The second scenario should lead to covalently core-crosslinked beads, for which loss of alginate due to calcium-sodium exchange or oxidative breakdown³⁴ would be less critical. In both cases the beads would receive a final coat of alginate (Scheme 6.1).



Scheme 6.1: Schematic representation of the capsule morphologies formed when embedding reactive polyanion within the CaAlg capsule, followed by reaction with high MW PLL, low MW PLL, and sequentially with high and low MW PLL.

Interaction of the synthetic polyanion, A70, with calcium, diffusion of these polyanions within CaAlg hydrogel matrices and interaction with polycations at both the capsule surface and within the capsule core were investigated. The internal morphology, mechanical strength, permeability of the capsules, and the viability of encapsulated murine cells are described.

6.2 Experimental

6.2.1 Materials:

Sodium alginate (Keltone LV) was a gift from the Nutrasweet Kelco Company (San Diego, California, USA). Methacrylic acid (MAA, 99%), 2-[methacryloyloxy]ethyl acetoacetate (MOEAA, 95%), fluorescein O-methacrylate (97%), poly-L-lysine hydrobromide (PLL, $M_n = 15\text{-}30$ kDa, 4-15 kDa and 1-4 kDa), fluorescein isothiocyanate (FITC, 90%), FITC-conjugated bovine serum albumin (BSA-FITC, $M_n = 66$ kDa), FITC-conjugated dextran (dextran-FITC, $M_n = 10, 70, 150, 250$ and 500 kDa), Rhodamine B isothiocyanate (RITC, mixed isomers), 2-(*N*-cyclohexylamino)ethanesulfonic acid (CHES, 99%) and trypan blue stain (0.4% in 0.85% saline) were purchased from Sigma-Aldrich, Oakville, ON, and were used as received. 2,2'-Azobis(isobutyronitrile) (AIBN, 99.95%) was purchased from Dupont (Mississauga, ON) and used as received. Sodium chloride (reagent), sodium nitrate (reagent), *N,N*-dimethylformamide (DMF, reagent) and anhydrous ethyl ether were obtained from Caledon Laboratories Ltd (Caledon, ON). Calcium chloride (Fisher), trisodium citrate dihydrate (Analar, EMD Chemicals, Gibbstown, NJ) and sodium dihydrogen orthophosphate (BDH, ON) were used as received. Ethanol from Commercial Alcohols (Brampton, ON) and serum free media (SFM) from Gibco (Mississauga, ON) were used as received. Sodium hydroxide and hydrochloric acid solutions were prepared from concentrates (Anachemia Chemical, Rouses Point, NY) by diluting to 0.100 M or 1.000 M with deionized water. The preparation of A70, its FITC-labelled analog A70*f* and A100 were described previously.³³

6.2.2 Synthesis of Fluorescent version of PMAANa, A100f:

MAA (1.91 g; 22 mmol), fluorescein O-methacrylate (89.7 mg; 0.22 mmol), and AIBN (73.6 mg, 44.7 mmol) were dissolved in 18 mL ethanol and heated at 60 °C for 21 h. The polymer was isolated by precipitation in ethyl ether (200 mL), and washed three times with 50 mL ethyl ether to remove the unreacted fluorescein methacrylate, and dried to a constant weight under vacuum at 50 °C. Yield: 1.36 g (68%). The fluorescence labeling of A100f was determined to be 0.42-mol% based on total monomer groups, by UV-Vis spectroscopy.

6.2.3 Poly(methacrylic acid, sodium salt-co-2-[methacryloyloxy]ethyl acetoacetate) (p(MAA-co-MOEAA), 70:30 (A70) of different molecular weights:

A70 with different MWs were obtained by copolymerization of methacrylic acid (MAA) and 2-(methacryloyloxy)ethyl acetoacetate (MOEAA) in ethanol at 60°C, with isolation by precipitation into ethyl ether, as described previously.³³ Reported reactivity ratios of MOEAA and methylmethacrylate (MMA) in toluene of about 1 and 1³⁵, and of MAA to MMA (in *i*PrOH) of 0.33 and 0.78³⁶ suggest there should not be an unacceptable drift of copolymer composition from the initial comonomer feed ratio, especially given the low percentage of MOEAA of 30%. Monomer to initiator (AIBN) ratios 20:1, 100:1 and 800:1 were used, and resulted in A70 of 22, 42 and 149 kDa, respectively. Fluorescein-labelled versions of A70-22k, A70-42k and A70-149k were prepared using FITC as described,³³ and resulted in degrees of labelling of 0.22, 0.34 and 0.32 mol% of the total monomer units, respectively, determined by UV/Vis spectroscopy. The polymers were neutralized with 1M NaOH to form the sodium salt of A70.

6.2.4 Rhodamine-labelled Poly-L-lysine (PLLr):

PLL with MW of 1-4 kDa, 4-15 kDa, or 15-30 kDa (55.5 mg, 0.265 mmol of lysine units) was dissolved in 5 mL 0.1M NaHCO₃ buffer solution at pH 9 in a 20 mL glass vial. Rhodamine isothiocyanate (2.7 mg, 0.005 mmol) dissolved in 0.5 mL DMF was added to the PLL solution and the mixture was stirred for 1 h at 20 °C. The resulting solution was dialysed against deionized water using a cellulose tubing (Spectrum Laboratories, 3.5 kDa MW cut-off for 4-15 and 15-30 kDa PLL and 1 kDa MW cut-off for 1-4 kDa PLL). The dialysed polymer solution was freeze-dried, and the polymer dried further to constant weight in a vacuum oven at 50 °C. Final yields of isolated, labelled polymer were 10% for the 1-4 kDa, 56% for 4-15 kDa and 40% for the 15-30 kDa PLLr, with degrees of labelling of 0.76, 0.77 and 0.62 mol%, respectively.

6.2.5 Characterization:

Molecular weights of A100f, A70 and dextran-FITC samples were determined by gel permeation chromatography (GPC) with a system consisting of a Waters 515 HPLC pump, Waters 717 plus Autosampler, three Ultrahydrogel columns (0-3 kDa, 0-50 kDa, 2-300 kDa), and a Waters 2414 refractive index detector. Samples were eluted with a flow rate of 0.8 mL/min and the system was calibrated with commercially available narrow dispersed molecular weight polyethylene glycol (PEG) standards (Waters, Mississauga, ON).

Dextran-FITC samples were eluted with 0.1M NaNO₃, while for A100f the mobile phase was 0.3 M NaNO₃ in 0.05 M phosphate buffer (pH 7). A100f was prepared

for GPC analysis by the addition of a stoichiometric amount of 1 M NaOH to the MAA-containing precursor polymer followed by dilution with the mobile phase.

Polymer compositions were determined by ^1H NMR using a Bruker AV 200 spectrometer for samples dissolved in DMSO- d_6 .

6.2.6 Preparation of Ca(A/A70) composite beads:

The Ca(A/A70) beads were prepared following the procedure described by Ross et al.³⁷ Sodium alginate (0.045 g), and A70 or A70f (0.015 g) were dissolved in 3.0 g saline (0.9% NaCl) to form a solution containing 1.5 wt% sodium alginate and 0.5 wt% A70 or A70f. The pH was adjusted to 7 with 0.1M NaOH. The solutions were filtered with sterile filters (0.45 μm , Acrodisc Syringe Filter, Pall Corporation, USA). A syringe pump (Russel Mechanical Inc. pump, model # A-99) was used to extrude this solution through a 27-gauge blunt needle (Popper & Sons, New York) at a rate of 30.1 mL/h. A concentric airflow (4 L/min) passing by the needle tip is used to induce droplet formation. The droplets were collected in 30 mL of 1.1-wt% calcium chloride, 0.45% sodium chloride gelling bath. Twenty minutes after the completion of bead formation, the supernatant was removed, and the resulting concentrated Ca(A/A70) composite bead suspension (about 3 mL) was washed in sequence with four-fold volumes of a) 1.1% CaCl_2 , 0.45% NaCl for 2 minutes; b) 0.55% CaCl_2 , 0.68% NaCl for 2 minutes; c) 0.28% CaCl_2 , 0.78% NaCl for 2 minutes; d) 0.1% CHES, 1.1% CaCl_2 , 0.45% NaCl for 3 minutes; and then e) 0.9% NaCl for 2 minutes and stored in saline.

Analogous cell-containing composite capsules were prepared by preparing a core solution containing 1.5% sodium alginate, 0.5% A70, and 2 million C_2C_{12} cells per mL. This suspension was extruded to form capsules as described above, except for the use of

an Orion sage pump, model # M362 located in a sterile laminar flow hood, and a liquid flow rate of 99.9 mL/hour. The cell containing capsules were washed as above, and stored in serum free media for further use.

6.2.7 Coating of Ca(A/A70) composite beads with poly-L-Lysine and sodium alginate to form (A/A70)PA capsules (typical procedure):

A dense suspension of Ca(A/A70) composite beads (3 mL) was exposed to 10 ml of 0.05% or 0.5% (w/v) PLL (pH = 8, saline) for 6 minutes and washed once each with 12 ml of a) 0.1% CHES, 1.1% CaCl₂, 0.45% NaCl for 3 minutes, b) 1.1% CaCl₂, 0.45% NaCl for 2 minutes and c) 0.9% saline for 2 minutes. The resulting (A/A70)P capsules were then coated with 10 ml of 0.03% (w/v) sodium alginate for 4 minutes, followed by three washes with 12 mL of 0.9% saline. The final (A/A70)PA composite capsules were stored in the last saline solution.

6.2.8 Capsule Characterization:

Capsules and polyelectrolyte complexes were examined with an Olympus BX51 optical microscope fitted with a Q-Imaging Retiga EXi digital camera and ImagePro software. The average diameters of the beads and capsules were determined by analyzing three batches of approximately 50-100 beads or capsules each.

Phase contrast microscope images were taken using a Wild M40 microscope, and confocal images were taken with a confocal laser scanning microscope (CLSM) consisting of air-cooled Argon and HeNe lasers (LASOS; LGK 7628-1), ZEISS LSM 510 and LSM Image browser software (version 3.5).

6.2.9 Chemical and Mechanical Stress Test:

Dense microcapsule suspensions in saline (100 μL) were placed in 15 ml polypropylene conical tubes and exposed to 5% w/v (170 mM, 5 mL) sodium citrate for 5 minutes, followed by exposure to 5 mL of 2M sodium chloride. The tubes were attached to a wheel tilted at 30° from horizontal and rotated at 30 rpm for 15 minutes at room temperature. The capsules were then washed with water, stained with trypan blue and observed by optical microscopy.

6.2.10 Cell culture:

The cell line used was the C_2C_{12} cell line (American Type Culture Collection [ATCC], Rockville, MD; Catalogue No. CRL-1772). The cells were maintained in Dulbecco's Modified Eagle's Medium (DMEM) supplemented with 10% fetal bovine serum (Gibco, Grand Island, NY) and 100 U/mL penicillin-100 $\mu\text{g}/\text{mL}$ streptomycin (Gibco, Grand Island, NY) in the presence of 5% CO_2 with 100% humidity at 37°C in a water-jacketed incubator.

6.2.11 Cell viability:

The number of viable cells per capsule was determined with an Alamar Blue assay.³⁸ 100 μL of capsules were loaded in a 24-well plate with 500 μL media. 50 μL of Alamar Blue reagent was added to each sample and the plate was incubated at 37°C for 4 h. After incubation, 100 μL of supernatant was taken from each well and placed in a microtiter plate. The fluorescence of each sample was read with a Cytofluor II fluorimeter, with an excitation wavelength of 530 nm and an emission wavelength of 590

nm. The number of viable cells per capsule was determined by comparing the fluorescence intensity with a standard curve generated from a known number of cells.

The effect of the encapsulation procedure itself on cell viability has been measured in our lab a number of times for APA capsules, by crushing freshly formed capsules, staining them with trypan blue and counting both live and dead cells. On day 1, the percentage of live cells is consistently above 95%. The number of cells/capsule can be compared to that of APA, assuming similar capsule volumes, to get a measure of the viability in the new capsules.

6.2.12 Permeability Measurements:

Capsule permeability was evaluated using dextran-FITC or BSA-FITC. The procedure with dextran-FITC was a modified version of a published procedure³⁹ and employed samples having nominal MWs of 10, 70, 150, 250 and 500 kDa. In the case of dextran-FITC, the capsules (0.2 g) were suspended in saline (0.2 mL) and exposed to 1.0 mL of 0.0015 or 0.05% dextran-FITC for 24 h at room temperature. When BSA-FITC was employed, the capsules (0.5 g) were suspended in a minimum amount of saline (~0.1 mL), exposed to 5 mL of 0.05% BSA-FITC for 24 h at room temperature, and then washed 5 times with saline (5 mL) to remove free protein.

The microcapsules were then examined by CLSM. A microcapsule suspension (100 μ L) was placed on a microscope slide within a Teflon ring (7 mm diameter, 3 mm depth) and images were obtained at the capsule equator. Intensity profiles were obtained from the CLSM images with a 25-pixel wide line using UTHSCSA Image Tool software (version 3.0).

6.3 Results and Discussion

The aim of this work is to explore covalent reinforcement of CaAlg beads with a crosslinked interpenetrating network formed by reaction between a polyanion present in the core, and a polyamine diffusing in from the outside. We had shown earlier that aqueous solutions of electrophile-containing polyanions such as A70 form crosslinked polyelectrolyte complexes upon contact with polyamines such as PLL, due to the facile reaction between the acetoacetate groups on the polyanion and the primary amines on the polycations.^{33,40,41} We also showed that this reaction can be used to form persistent, cross linked shells around CaAlg beads.^{33,40}

Here, we explore the ability of these polyelectrolytes to form crosslinked networks throughout the bead, leading to formation of a permanent three-dimensional support structure for cell transplantation and other uses.

This involves adding the reactive polyanion, A70, to the sodium alginate solution, prior to gelling with calcium chloride. The resulting primary CaAlg beads thus contain A70 homogeneously distributed throughout. Subsequent exposure of these beads to aqueous solutions of PLL should lead to formation of crosslinked A70 - PLL networks near the bead surface, with thicknesses dependent on the molecular weights and mobilities of the two polyelectrolytes used.

The commonly used 15-30 kDa PLL should not be able to penetrate the CaAlg matrix more than a few tens of micron,^{33,40,42} and hence should result in formation of a thin crosslinked shell similar to those formed in the conventional layer-by-layer approach.^{33,40} On the other hand, use of lower MW PLL should facilitate diffusion into

the beads, resulting in thicker crosslinked layers or even core-crosslinked networks, depending on polyelectrolyte stoichiometry and concentrations.

The MW and mobility of the A70 is similarly expected to play an important role. The mobility of A70 inside the CaAlg should depend both on its molecular weight and on its calcium binding strength. Accordingly, PLL and A70 with a range of molecular weights have been explored.

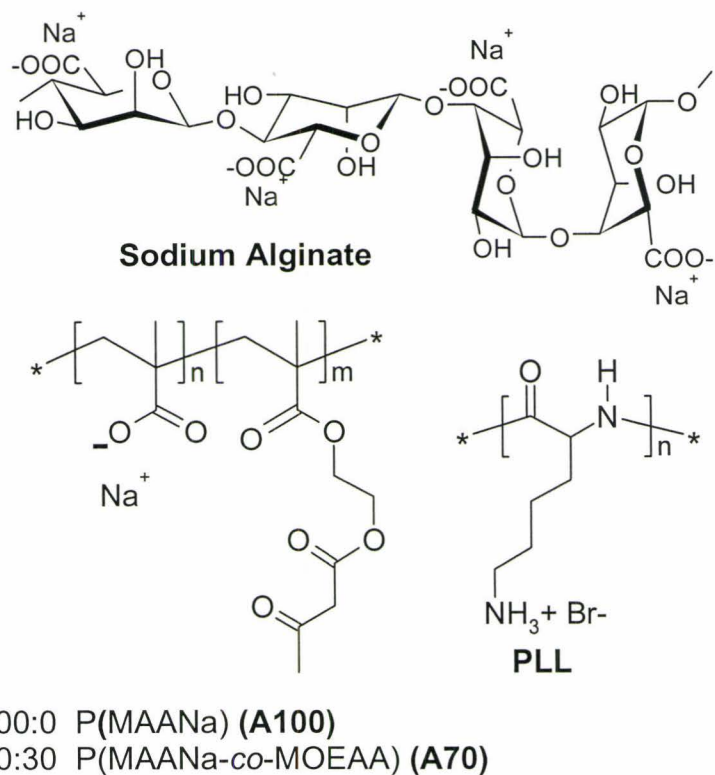
The synthetic polyanions are described in Scheme 6.2 and Table 6.1. Monomer to initiator ratios of 20:1, 100:1 and 800:1 were used to obtain A70 having number average MWs of 22, 42 and 149 kDa, respectively. Attempts to prepare higher MW polymer resulted in gellation, attributed to covalent crosslinking during polymerization. Fluorescently-labelled versions of the polymers were prepared by reaction with FITC (A70*f*) or rhodamine B isothiocyanate (PLL*r*), or via copolymerization with fluorescein O-methacrylate (A100*f*). Unless specifically noted, A70 or A70*f* with a MW of 42 kDa was employed.

Table 6.1: Polymer properties

Polymer	M_n (kDa)/PDI^a	MAA:MOEAA^b
A100	38 / 2.6	-
A100 <i>f</i>	29 / 2.8	-
A70-22k	22 / 3.1	70:30(±3)
A70-42k	42 / 2.4	70:30 (±3)
A70-149k	149 / 1.7	70:30(±5)

a) M_n determined by Gel Permeation Chromatography.

b) Copolymer composition in mol% determined by ¹H NMR.



Scheme 6.2: Natural and synthetic polyelectrolytes used in this study.

6.3.1 (A (1.5%)/A70 (0.5%))PA Composite Capsules, (A/A70)PA:

As the initial step in the capsule formation would be the gellation of the alginate/polyanion mixture in CaCl₂, model experiments were carried out to understand the interaction between CaCl₂ and both A70 and A100.

CaAlg is a solid gel that can resist moderate mechanical stresses, while A100 forms a liquid coacervate in presence of CaCl₂. A70 (22, 42 or 149 kDa) showed no macroscopic phase separation in the presence of CaCl₂, suggesting that these complexes may retain some mobility even within CaAlg beads.

CaAlg beads containing the synthetic polyanions were prepared by dripping saline solutions containing 1.5wt% sodium alginate and 0.5wt% polyanion, adjusted to pH 7, into a CaCl₂ bath.³⁷ The resulting composite beads were exposed to 0.05% PLL (15-30 kDa), washed with saline and then coated with a 0.03% sodium alginate solution. The final capsules had an average diameter of 650 μm and appeared identical to the initial Ca(A/A70) beads but their surface was easily stained by trypan blue indicating the presence of the polycation. In addition, the surface appeared pink when PLL_r was used.

To determine the fraction of A70 trapped in the capsules, the supernatant solutions used during the preparation of capsules containing A70f were analyzed by UV-Vis spectroscopy. This showed that $60 \pm 5\%$ of the original A70f-22k or A70f-42k, and $40 \pm 5\%$ of the A70f-149k were lost from the beads, predominantly to the gelling bath (Figure 6.1). No additional A70f loss was observed during the subsequent PLL coating process. Uncoated Ca(A/A70f) beads stored in a 6-fold excess of saline at 4 °C lost an additional 3% of the original A70f after 2 days, and 16% after 3 months. In contrast, (A/A70f)PA capsules did not lose a significant amount of A70f to the supernatant over 8 months of storage.

Thus, A70f is lost principally in the gellation step during which the droplets were found to shrink to about 60% of their original volume, a value consistent with a number of other studies.^{43,44} Core liquid is expelled from the gelling beads along with any polymer chains that are not physically entangled or ionically bound within the CaAlg gel. Use of higher MW A70 increases the retention of the polymer, possibly due to enhanced entanglement.

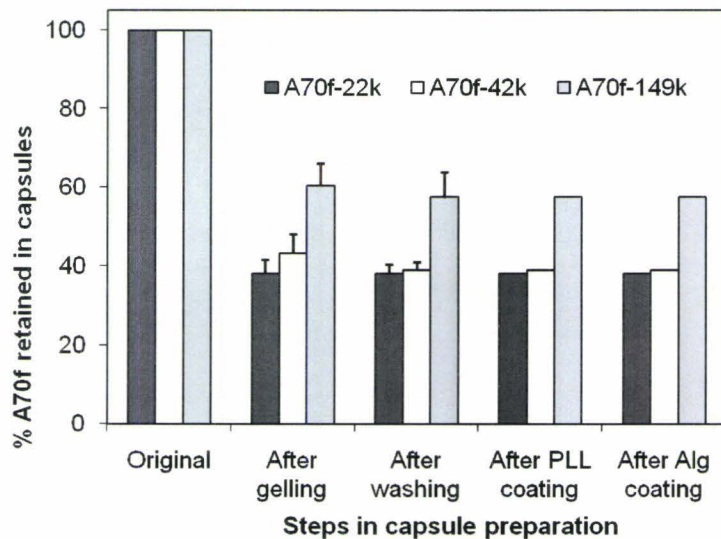


Figure 6.1: Percentage of A70f remaining in the composite microcapsules at different stages of the capsule preparation. Error bars show the standard deviation for select experiments performed in triplicate.

CLSM showed that A70f is initially homogeneously distributed within the Ca(A/A70f) beads (Figure 6.2a). Images obtained 1-2 hours after coating these beads with PLL and sodium alginate (Figure 6.2b), show in addition a very thin outer shell, presumably formed by concentration of some of the A70f in the form of a PLL/A70f cross linked shell.

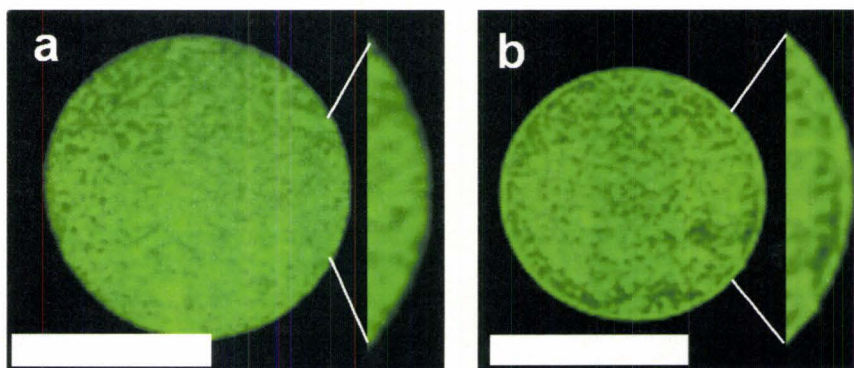


Figure 6.2: CLSM equatorial optical section of Ca(A/A70f) composite capsule: a) uncoated and b) coated with PLL (15-30 kDa) (0.05%, 6 min) and then alginate (0.03%, 4 min). Images were taken within 1-2 h of capsule preparation. The scale bar is 500 μm .

When the coated capsules were treated with excess 170 mM (5% w/v) sodium citrate for 18 h to liquefy the CaAlg core, the capsules retained the fluorescently labelled A70f, but swelled (40-50% diameter increase), indicating the absence of significant core crosslinking. Model studies suggested that formation of a crosslinked A70/PLL network requires equimolar or greater amounts of PLL relative to A70. Accordingly, fluorescently labelled PLL was used to track the in-diffusion of the polycation and determine the fraction that reaches the core of the beads.

CLSM images of capsules coated with 0.05% solutions of PLL_r show that higher MW PLL_r (15 – 30kDa) is concentrated near the capsule surface, while the lowest MW PLL_r (1-4k) is evenly distributed throughout the composite microcapsules (Figure 6.3a and c), in agreement with a number of earlier reports.^{45,46,47,48} The intermediate MW PLL_r (4-15 kDa) showed both formation of a distinct shell, and significant in-diffusion to the core of the bead (Figure 6.3b). The shell formed by 4-15 kDa PLL_r was thicker (36 μm width at half-height of the line-out shown in Figure 6.3d) than that formed by the 15-30 kDa PLL_r, (23 μm), which is consistent with the deeper penetration of expected of this intermediate MW polycation. Hence, reacting Ca(A/A70) beads with PLL of appropriate MW and concentrations, could lead to capsules that are reinforced both internally and externally.

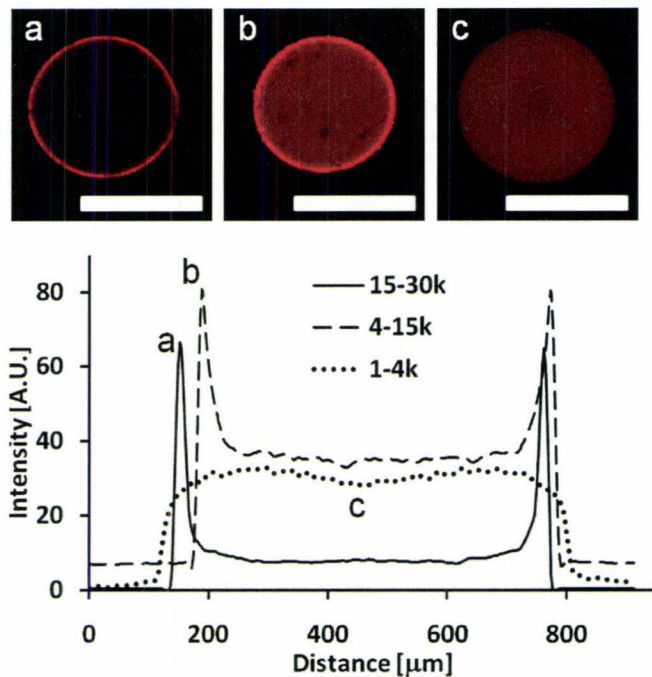


Figure 6.3: *Top*: CLSM equatorial optical sections of (A/A70)PA capsules made with PLLr of a) 15-30 kDa; b) 4-15 kDa; and c) 1-4 kDa. *Bottom*: 25 pixel wide line profiles taken from the images. Coating conditions: PLLr (0.05 %w/v in saline, 6 min); Alg (0.03% w/v, 4 min).

The integrity of uncoated and PLL(15-30k)-coated Ca(A/A70) composite beads in the presence of sodium citrate and sodium chloride was examined by optical microscopy and compared with that of classical APA microcapsules. Uncoated beads composed of Ca(A/A70) or CaAlg dissolve when exposed to 170 mM (5% w/v) sodium citrate, a good calcium chelator. In contrast, addition of sodium citrate to PLL(15-30k)-coated capsules such as APA or Ca(A/A70)PA caused the core of the beads to dissolve, while the shells consisting of the polyelectrolyte complex survived. One test for covalent crosslinking of the shell is to expose citrate-treated capsules to 2 M NaCl while vigorously agitating, which dissolves (in the case of 1-4 and 4-15k PLL) or noticeably weakens (in the case of

15-30k PLL) shells held together by just ionic interactions, compared to their crosslinked analogs. A better test, especially for the higher MW PLL, involves exposing the shells to 0.1 M sodium hydroxide, which neutralizes the ammonium ions of PLL leading to rapid and almost complete dissociation of all electrostatic PECs used here, as described earlier by Dusseault et al.¹⁷

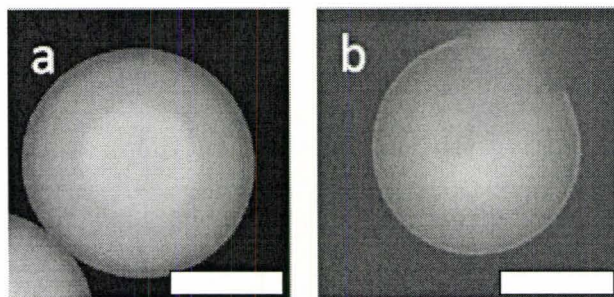


Figure 6.4: Fluorescence microscopy images (greyscale) of (A/A70f)P(4-15 kDa, 0.05%) A(0.03%) capsules; a) as formed, and b) after being exposed to citrate (170 mM) and NaCl (2 M), and manually cut with a micro-knife. Scale bar: 300 μm

Figure 6.4a shows a composite bead coated with 0.05% PLL (4-15kDa). After exposure to sodium citrate followed by 2 M sodium chloride, the capsule was manually cut (Figure 6.4b), revealing both a thin crosslinked shell and A70f diffusing out through the hole in the shell. The shell is self-supporting, but it is clear that the core of the bead is not crosslinked, likely due to the presence of insufficient amounts of PLL. These capsules hence resemble the crosslinked-shell capsules prepared earlier using sequential exposure of CaAlg beads to polycation and A70,^{33,40} except that the reactive A70 is here supplied from the interior of the capsule. The outer surface of the capsule, after coating with alginate, then resembles the conventional APA capsules.

Composite beads coated with low MW PLL (1-4 kDa, 0.05%), which were shown in Figure 6.3c to have PLL_r homogeneously distributed throughout the beads, dissolved within seconds upon exposure to sodium citrate (70 mM). This indicates that although this low MW PLL readily penetrates the interior of the beads, at the present concentration of 0.05% it is unable to crosslink the A70 to the extent necessary to give a crosslinked shell or core. The chains may be too short to effectively bridge between A70 chains. A sodium citrate concentration of 70 mM was found to be sufficient to extract calcium from both CaAlg and composite beads, and was used henceforth.

6.3.2 Core-Crosslinked (A/A70)PA Capsules:

For Ca(A/A70(42 kDa)) beads that retain roughly 40% of their original A70 loading, exposure to 0.05 w% PLL corresponds to a ratio of crosslinking groups (amine/acetoacetate) of about 2:1. UV/Vis analysis of a supernatant PLL (15-30 kDa) solution after coating showed that only half of this PLL was actually absorbed by the capsules and, thus, the PLL-coated beads have an overall amine/acetoacetate ratio of approximately 1:1. However, much of this bound PLL is involved in electrostatic complexation and is concentrated in the dense shell at the surface as shown in Figure 6.3(a). This indicates that the effective amine/acetoacetate ratio in the core is much lower, and explains the absence of core-crosslinking in the resulting capsules.

Analysis of the in-diffusion patterns (Figure 6.3) indicated that the intermediate MW PLL (4-15 kDa) might represent a good compromise between ease of in-diffusion and a MW high enough to crosslink the A70 in the core, provided it is available in sufficiently high concentration to compensate for incomplete capture and preferential binding to the shell.

Accordingly, we explored increasing the PLL (4-15k) concentration from 0.05% to 0.5 and 1%. Coating using 1% PLL solution resulted in wrinkling of the bead surface, while 0.5% PLL (4-15 kDa) resulted in smooth bead surfaces. Figure 6.5a shows (A/A70f)PA capsules coated with 0.5% PLL (4-15k), followed by alginate (0.03%). The resulting capsules were manually cut, and exposed to 70 mM citrate (Figure 6.5b) and then 2 M sodium chloride (Figure 6.5c). The capsules undergo little swelling and there is minimal loss of A70f demonstrating that sufficient PLL has diffused into the core to crosslink the bead throughout. The crosslinked beads also survived subsequent treatment with 0.1M NaOH (not shown).

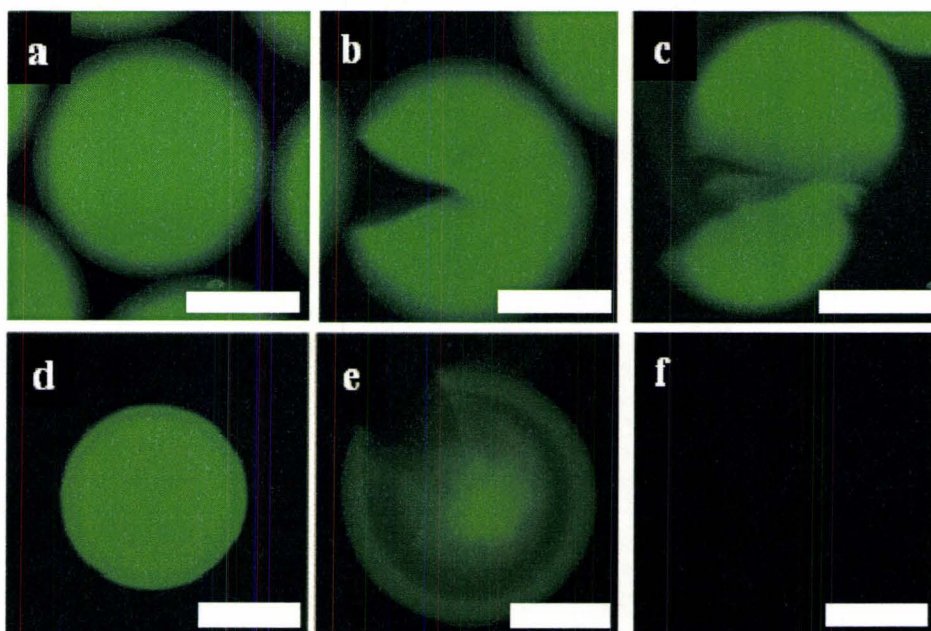


Figure 6.5: Fluorescence microscopy images of a) (A/A70f)P(4-15k, 0.5%)A(0.03%) and d) (A/A100f)P(4-15k, 0.5%)A(0.03%); b, e) the beads were manually cut, and then exposed to excess 70 mM sodium citrate; c, f) after further treatment with 2 M NaCl. The scale bar is 300 μm .

When the A70f (42 kDa) was replaced with A100f (29 kDa), rendering covalent crosslinking impossible, the resulting (A/A100f)P(4-15k, 0.5%)A(0.03%) capsules (Figure 6.5d) swelled considerably when exposed to 70 mM citrate for about 5 min. The outer layer, consisting of an electrostatic complex of PLL with alginate and A100f, appears to swell more than the inner core, revealed when the shell is cut (Figure 6.5e). Subsequent exposure to 2 M sodium chloride completely dissolved both shell and core within three minutes (Figure 6.5f), confirming again that the permanent structure shown in Figure 6.5(a-c) for the A70-containing capsule is indeed based on covalent crosslinking.

As interesting is the location of the PLL, since it will be important for both crosslinking and biocompatibility. Accordingly, Ca(A/A70) beads were coated with 0.5% PLL_r (4-15 kDa) and then examined by fluorescence microscopy and CLSM (Figure 6.6). As observed in Figure 6.5, capsules exposed to citrate and manually crushed; followed by the addition of 2 M NaCl underwent only some swelling and showed minor loss of PLL_r, confirming the role of PLL in the covalent crosslinking of both shell and core. The presence of a distinct PLL_r shell in addition to core crosslinking suggests that the higher MW fraction of PLL_r(4-15kDa) is limited to forming a surface network, while the lower MW fraction can diffuse into the core to crosslink with A70. The presence of the distinct shell in Figure 6.6c, after exposure to 2 M NaCl, indicates that it does not involve electrostatic binding of excess PLL to alginate, but rather covalent bonding, to A70.

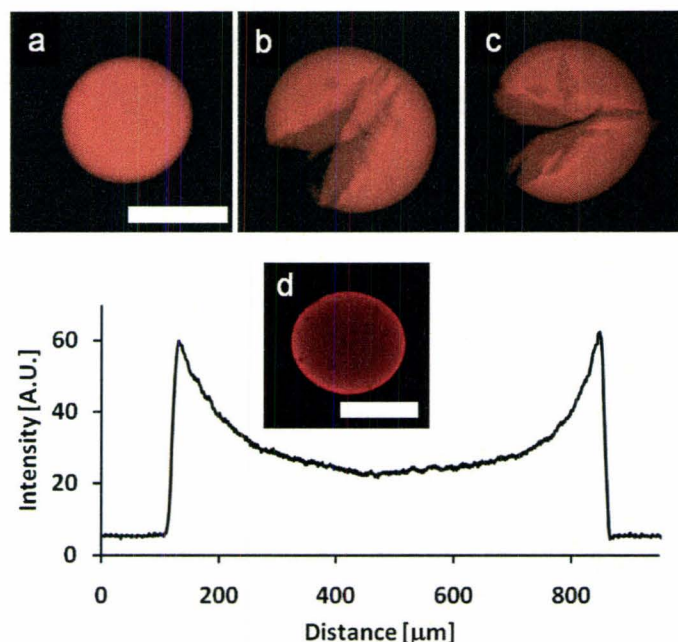


Figure 6.6: Fluorescence microscopy images of core-crosslinked (A/A70)PLLr (4-15k, 0.5%)A (0.03%) composite capsules to show the location of PLLr (4-15 kDa). a) As formed; b) after addition of excess 70 mM sodium citrate and crushing; c) following addition of excess 2 M NaCl. The scale bar is 500 μm . d) CLSM middle optical section, and intensity line profile, of a capsule such as in a).

CLSM analysis of a (A/A70)PLLr (4-15k, 0.5%)A (0.03%) capsule such as that shown in Figure 6.6a shows the concentration of PLL falling more gradually moving from shell to core (Figure 6.6d), compared to the analogous beads coated with 0.05% PLLr (4-15 kDa) shown in Figure 6.3b. The width at half height is now close to 100 micrometer. The confocal image in Figure 6.6d was taken at reduced gain settings compared to Figure 6.3b, to avoid saturating the CCD detector.

Gaserod et al.⁴⁷ had reported that presence of a competing cation such as calcium can enhance in-diffusion of chitosan, but not of PLL, into CaAlg beads. We similarly

found that exposure of the Ca(A/A70) beads to PLL(0.5%) in 1.1% CaCl₂, 0.45% NaCl instead of the standard 0.9% saline, did not lead to significantly increased in-diffusion of PLL (images not shown).

The capsule shell plays important roles in permeation and biocompatibility and, thus, it may be advantageous to be able to carry out shell formation independent of the core-crosslinking process. In order to test the scope for separately controlling core-crosslinking and shell formation, CaAlg beads were sequentially coated with two PLL solutions of different MWs, a variation of the approach described by Prokop et al²⁴ of coating simultaneously with a blend of low and high MW polycations. The expectation was that sequential coating would ensure that the higher MW PLL could coat the outside of the bead, without competition from the more mobile low MW PLL. Subsequently, the lower MW PLL would be able to diffuse through the outer PEC shell to crosslink inner regions not accessible to the high MW PLL. Hence, Ca(A/A70f) beads were first exposed to 0.05% PLL (15-30k) for 1 min, followed without washing by another exposure to 0.5% PLL (4-15k) for 6 min, and after a wash step, by the usual final coat with 0.03% Alg for 4 min. The resulting capsules, after manual cutting and exposure to citrate and 2 M NaCl, show both the presence of an outer shell formed by reaction of the higher MW PLL with A70f near the surface, and core-crosslinking between the lower MW PLL and A70f in the core (Figure 6.7, a-c). In contrast, the capsules prepared using only 0.5% PLL (4-15k) did not show a distinct outer shell (Figure 6.5c). This demonstrates the ability of the two-stage approach to give some independent control over shell and core crosslinking, and may enable tuning of the MW cut-off as required for specific cell immuno-isolations.

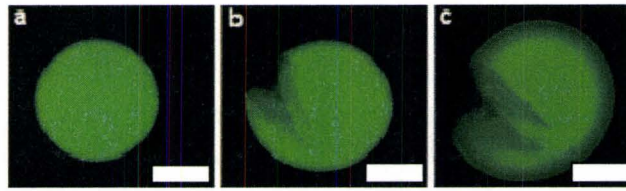


Figure 6.7: Fluorescence microscopy images of (A/A70f)PA capsule prepared by exposure to both high and medium MW PLL. Ca(A/A70f) composite beads were coated with 0.05% PLL (15-30k) (1 min), and then with 0.5% PLL (4-15k) (6 min), followed by 0.03% Alg (4 min). a. As formed, b. After challenge with citrate and manual cutting. c. After exposure to excess 2 M NaCl. The scale bar is 300 μm .

6.3.3 *In-vitro cell viability:*

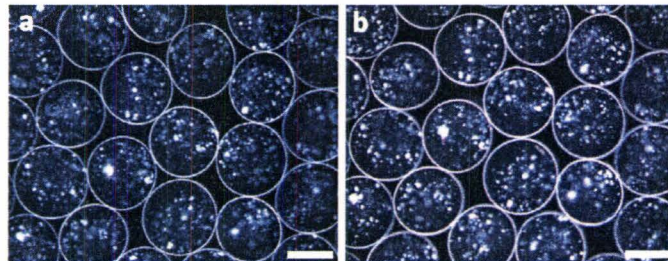


Figure 6.8: Phase contrast microscope image of C_2C_{12} mouse cells 7 days after being encapsulated in a) APA and b) (A/A70)PA microcapsules. Coating conditions: PLL (15-30 kDa, 0.05%)/6 min; Na-Alg (0.03%)/4 min. Scale bar: 400 μm .

C_2C_{12} mouse cells were encapsulated in APA capsules, the shell-crosslinked (A/A70)P(15-30k, 0.05%)A capsules and the core-crosslinked (A/A70)P(4-15k, 0.5%)A capsules. Cell-containing APA and shell-crosslinked (A/A70)P(15-30k, 0.05%)A

capsules are shown in Figure 6.8. The capsules were cultured *in vitro* for one week and the numbers of living cells per capsule were determined with the Alamar Blue assay. Note that the cell viability tests on the two new types of capsules were performed at different times each with an APA control, to take into account variables affecting cell growth that are unrelated to the presence of the new materials. Figure 6.9a shows that the average live cell numbers in these shell-crosslinked capsules are similar to those in APA capsules over the week long incubation, indicating that the A70 in the core of the (A/A70)PA capsules is not detrimental to cell viability.

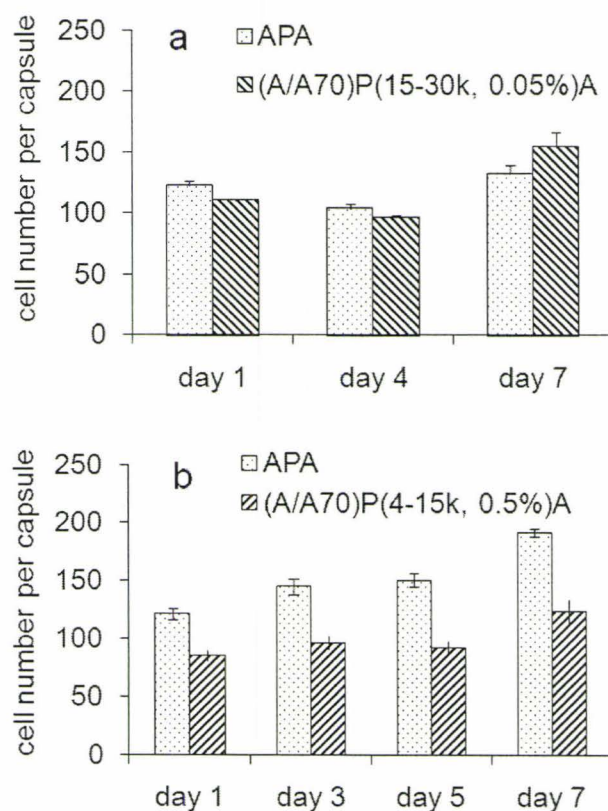


Figure 6.9: *In vitro* cell viability of C_2C_{12} cells encapsulated in APA and (A/A70)PA capsules over time. a) APA and shell-crosslinked (A/A70)P(15-30k, 0.05%)A capsules

and b) APA and core-crosslinked (A/A70)P(4-15k, 0.5%)A capsules. Error bars show the standard deviation. Coating conditions: APA - PLL(15-30k, 0.05 % w/v, 6 min), Alg(0.03% w/v, 4 min); shell-crosslinked (A/A70)PA: PLL(15-30k, 0.05 % w/v, 6 min) Alg(0.03% w/v, 4 min); core-crosslinked (A/A70)PA: PLL(4-15k, 0.5 % w/v, 6 min) Alg(0.03% w/v, 4 min).

The cell viability results for the core-crosslinked (A/A70)PA capsules are shown in Figure 6.10b. The APA capsules show higher cell numbers throughout the incubation although similar relative increases in cell numbers (50-60%) are seen for the two types of capsule. Comparison with the higher cell numbers observed in the case of analogous shell-crosslinked capsules prepared using only 0.05% PLL(15-30 kDa) (Figure 6.10a) suggests that the lower initial cell viability in the present capsules is due to the larger amount of lower MW PLL used.

It was initially surprising that the diffusion of PLL into the capsule core does not have a more negative effect on cell viability. The preferred location of PLL_r (4-15 kDa) in the shell, compared to the homogeneous distribution of A70_f (Figure 6.5) obviously reflects the fact that PLL is applied from the outside, while A70 is found throughout the core. PLL in the bead core may exhibit reduced toxicity towards the encapsulated cells, as verified by the data in Figure 6.9b, because most of the PLL diffusing in from the outside should rapidly react with the A70 present throughout the core. Any residual unreacted PLL would likely be complexed by alginate, and thus rendered much less cytotoxic, as reported previously for the complexes formed between polystyrenesulfonate and polycations.⁴⁹

On the other hand, the presence of excess PLL near the surface may require more than the standard final coating with 0.03% alginate to prevent undesirable interactions with the host. One option will be to apply a coat of A70 to covalently bind this surficial PLL.

6.3.4 MW cut-off of APA and shell-crosslinked microcapsules:

It is important that capsules containing cells allow the diffusion of nutrients and metabolites, while preventing the ingress of components of the host immune system. The good cell viabilities observed for both shell- and core-crosslinked capsules demonstrate reasonable permeability of nutrients into the capsules. The ideal MW cut-off of the microcapsule membrane is one that provides immunoprotection of transplanted cells while allowing release of therapeutic protein. This will depend on the transplant type, with values of about 100 - 200 kDa commonly considered to be suitable for allografts.^{50,51}

The MW cut-off of these new shell- and core-crosslinked capsules was estimated using a series of commercial dextran-FITC samples with nominal MWs of 10, 70, 150, 250 and 500 kDa.^{39,52} GPC analysis showed that the samples had broad MW distributions, with polydispersity indices of 4.7 for the 150 kDa sample and approximately 2 for the other samples, and thus in-diffusion of the low MW fraction may occur with each of the samples. In addition, dextran may behave differently than globular proteins in solution, and as such the use of dextran-FITC provides only a rough indication of the MW cut-off.

Shell-crosslinked (A/A70)P(15-30k, 0.05%)A capsules exposed to 0.0015% dextran-FITC solutions for 24 h and then examined by CLSM showed increasing in-

diffusion with decreasing MW (data not shown). Similarly, core-crosslinked (A/A70)P(4-15k, 0.5%)A capsules containing C₂C₁₂ mouse myoblast cells exposed to dextran-FITC (0.05%) for 24 h (Figure 6.10) showed that dextrans of 500 and 250 kDa are almost completely excluded, while dextrans having MW's of 10 and 70 kDa can diffuse in freely. At least some fraction of the polydisperse 150 kDa dextran also diffuses into the capsules (Figure 6.10c). Both the shell- and core-crosslinked capsules have MW cut-offs that are roughly 100 to 200 kDa, similar to APA capsules (data not shown), and in line with data reported for other capsules.^{31,53,54,55,56} Work is in progress to find additional means of determining the MW cut-off and to explore decreasing this MW cut-off by varying the A70/PLL ratio, and adding additional layers of reactive polymers.

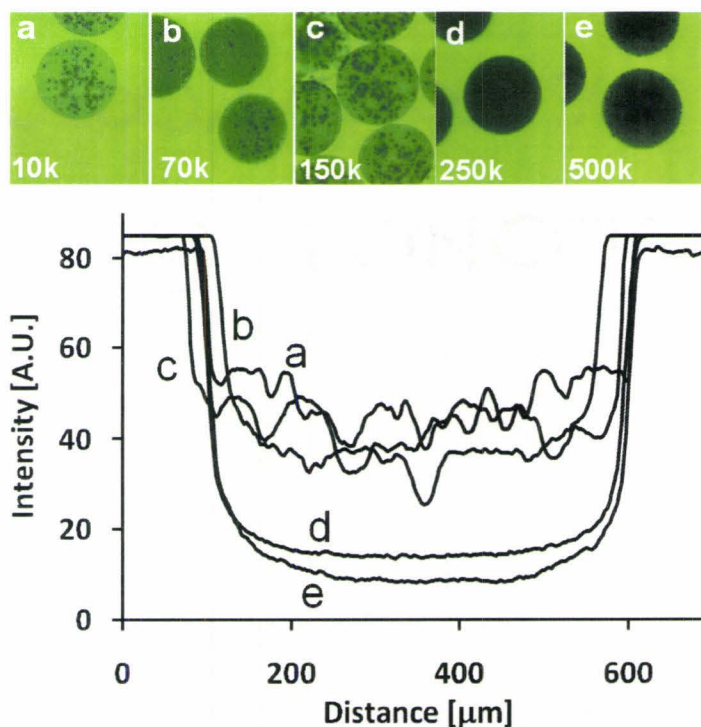


Figure 6.10: *Top*: CLSM middle sections of cell containing (A/A70)P(4-15k, 0.5%)A(0.03%) capsules exposed for 24h at room temperature to 0.05% dextran-FITC

with nominal MWs of a) 10k, b) 70k, c) 150k, d) 250k, and e) 500k. Coating conditions - PLL (0.5 % w/v, 6 min); Alg (0.03% w/v, 4 min). *Bottom:* Line profile from images as above.

The permeability of APA and shell-crosslinked (A/A70)P(15-30k)A microcapsules containing cells was also assessed by looking for the uptake of BSA-FITC (MW 66 kDa) (Figure 6.11). Both types of microcapsules were permeable to BSA-FITC, indicating a MW cut-off greater than 70 kDa, consistent with the dextran-FITC results.

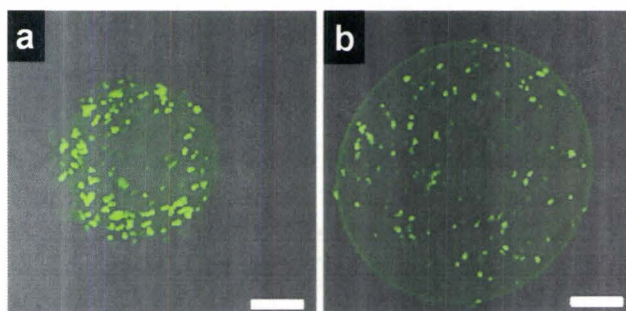


Figure 6.11: CLSM equatorial optical sections of a) APA and b) (A/A70)P(15-30k, 0.05%)A microcapsules exposed to BSA-FITC. The scale bar is 200 μm .

Close inspection of Figure 6.11 reveals that some cells protrude from the surfaces of both APA and shell-crosslinked composite capsules, making them liable to recognition and attack by the host's immune system. This concern has been recognized, and can be addressed by using a double coaxial encapsulation approach that deposits a second, cell-free shell of CaAlg over the cell-containing capsules. In the case of core-crosslinked beads, the inner matrix could provide continued immuno-isolation in capsules whose outer shell has been breached by such surficial cells.

Research is in progress to optimize the amounts of A70 and PLL in such capsules, and to explore their strength and host compatibility.

6.4 Conclusion

We have shown that internally and externally cross-linked networks can be formed in CaAlg beads by inclusion of A70 in conventional APA microcapsule cores. The distribution of the polyelectrolytes in the microcapsules was studied using fluorescently labeled analogs. While a portion of the A70 was lost during gelling, the remainder was distributed evenly throughout bead. The depth of PLL penetration was controlled by varying the PLL MW, which allowed the formation of capsules in which just the shell or both the shell and core were covalently cross-linked. The resistance of these capsules to citrate and high ionic strength demonstrated the cross linked nature of the core as well as the shell. The use of two MWs of PLL can give independent cross linking of core and shell, which should give access to core-cross linked capsules with shells exhibiting MW cut-offs suitable for cell encapsulation. Murine C₂C₁₂ cells were viable within CaAlg composite capsules.

This study describes a promising approach to cell encapsulation and may ultimately be useful for immuno-isolation in cell-based therapies. Research is in progress to optimize the amounts of A70 and PLL in these capsules, and to explore their strength and host compatibility. Studies of the *in vivo* use of these and related capsules are being conducted and will be reported shortly.

6.5 References

- ¹ Chang, T. M. S. *Science*, **1964**, *146*, 524-525.
- ² Bañó, M. C.; Cohen, S.; Visscher, K. B.; Allcock, H. R.; Langer, R. *Biotechnology*, **1991**, *9*, 468-471.
- ³ Uludag, H.; Sefton, M. V. *Biotechnol. Bioeng.*, **1992**, *39*, 672-678.
- ⁴ Thu, B.; Bruheim, P.; Espevik, T.; Smidsrød, O.; Soon-Shiong, P.; Skjåk-Bræk, G. *Biomaterials*, **1996**, *17*, 1031-1040.
- ⁵ Lim, F.; Sun, A. M. *Science*, **1980**, *210*, 908-910.
- ⁶ Peirone, M. A.; Delaney, K.; Kwiecin, J.; Fletch, A.; Chang, P. L. *Hum. Gene Ther.*, **1998**, *9*, 195-206.
- ⁷ Lanza R. P.; Kuhlreiber, W. M.; Ecker, D.; Staruk, J. K.; Chick, W. L. *Transplantation*, **1995**, *59(10)*, 1377-1384.
- ⁸ Soon-Shiong, P.; Heintz, R. A.; Skjåk-Bræk, G. Microencapsulation of cells. US Patent 5762959, 1998.
- ⁹ Zekorn, T.; Siebers, U.; Horcher, A.; Schnettler, R.; Klock, G.; Bretzel, R. G.; Zimmerman, U.; Federlin, K. *Transplant. Proc.*, **1992**, *24*, 937-939.
- ¹⁰ Mørch, Y. A.; Donati, I.; Strand, B. L.; Skjåk-Bræk, G. *Biomacromolecules*, **2006**, *7*, 1471-1480.
- ¹¹ Darrabie, M. D.; Kendall Jr, W. F.; Opara, E. C. *Biomaterials*, **2005**, *26*, 6846-6852.
- ¹² Chandy, T.; Mooradian, D. L.; Rao, G. H. R. *J. Appl. Polym. Sci.*, **1998**, *70*, 2143-2153.
- ¹³ Bünger, C. M.; Gerlach, C.; Freier, T. Schmitz, K. P.; Pilz, M.; Werner, C.; Jonas, L.; Schareck, W.; Hopt, U. T.; De Vos, P. *J. Biomed. Mater. Res.*, **2003**, *67A*, 1219-1227.

-
- ¹⁴ Haque, T.; Chen, H.; Ouyang, W.; Martini, C.; Lawuyi, B.; Urbanska, A. M.; Prakash, S. *Mol. Pharmaceutics*, **2005**, *2*, 29-36.
- ¹⁵ Hubbell, J. A.; Pathak, C. P.; Sawhney, A. S.; Desai, N. P.; Hossainy, S. F. A. Gels for encapsulation of biological materials. U.S Patent 5529914, 1996.
- ¹⁶ Chandy, T.; Mooradian, D. L.; Rao, G. H. R. *Artificial Organs*, **1999**, *23*, 894-903.
- ¹⁷ Dusseault, J.; Leblond, F. A.; Robitaille, R.; Jourdan, G.; Tessier, J.; Menard, M.; Henly, N.; Halle, J. -P. *Biomaterials*, **2005**, *26*, 1515-1522.
- ¹⁸ Leblond, F. A.; Halle, J. -P. Semipermeable microcapsule with covalently linked layers and method for producing the same. U.S. Patent 7128931, 2006.
- ¹⁹ Chen, H.; Ouyang, W.; Lawuyi, B.; Prakash, S. *Biomacromolecules*, **2006**, *7*, 2091-2098.
- ²⁰ Soon-Shiong, P.; Desai, N. P.; Sanford, P. A.; Heintz, R. A.; Sojomihardjo, S. Cross linkable polysaccharides, polycations and lipids useful for encapsulation and drug release. U.S. Patent 5837747, 1998.
- ²¹ Smeds, K. A.; Grinstaff, M. W. *J. Biomed. Mater. Res.*, **2001**, *54*, 115-121.
- ²² Rokstad, A. M.; Donati, I.; Borgogna, M.; Oberholzer, J.; Strand, B. L.; Espevik, T.; Skjåk-Bræk, G. *Biomaterials*, **2006**, *27*, 4726-4737.
- ²³ Crooks, C. C.; Douglas, J. A.; Broughton, R. L.; Sefton, M. V. *J. Biomater. Res.*, **1990**, *24(9)*, 1241-1262.
- ²⁴ Prokop, A.; Hunkeler, D.; Powers, A. C.; Whitesell, R.; Wang, T. G. *Adv. Polym. Sci.*, **1998**, *136*, 53-73.
- ²⁵ Sakai, S.; Hashimoto, I.; Kawakami, K. *Biochem. Eng. J.*, **2006**, *30*, 76-81.
- ²⁶ Prakash, S.; Martoni, C. *Appl. Biochem. Biotechnol.*, **2006**, *128*, 1-21.

-
- ²⁷ Hertzberg, S.; Moen, E.; Vogelsang, C.; Østgaard, K.; *Appl. Microbiol. Biotechnol.*, **1995**, *43*, 10-17.
- ²⁸ Prokop, A.; Hunkeler, D.; Dimari, S.; Haralson, M. A.; Wang, T. G. *Adv. Polym. Sci.*, **1998**, *136*, 1-51.
- ²⁹ Wang, T.; Lacik, T.; Brissova, M.; Anilkumar, A. V.; Prokop, A.; Hunkeler, D.; Green, R.; Shahrokhi, K.; Powers, A. C. *Nat. Biotechnol.*, **1997**, *15*, 358-362.
- ³⁰ Donati, I.; Haug, I. J.; Scarpa, T.; Borgogna, M.; Draget, K.I.; Skjåk-Bræk, G.; Paoletti, S. *Biomacromolecules*, **2007**, *8*, 957-962.
- ³¹ Gåserød, O.; Sannes, A.; Skjåk-Bræk, G. *Biomaterials*, **1999**, *20*, 773-783.
- ³² Wang, M.; Childs, R. F.; Chang, P. L. *J. Biomater. Sci. Polym. Edn.*, **2005**, *16*, 91-113.
- ³³ Mazumder, M. A. J.; Shen, F.; Burke, N. A. D.; Potter, M. A.; Stöver, H. D. H. *Biomacromolecules*, **2008**, *9*, 2292-2300.
- ³⁴ Holme, H. K.; Davidsen, L.; Kristiansen, A.; Smidrød, O.; *Carbohydr. Polym.*, **2008**, *73*, 656-664.
- ³⁵ Eastman Chemical Publication N319c
- ³⁶ Brandrup and Immergut, *Polymer Handbook*, 3rd Ed.
- ³⁷ Ross, C. J. D.; Bastedo, L.; Maier, S. A.; Sands, M. S.; Chang, P.L. *Hum. Gene Ther.*, **2002**, *11*, 2117- 2127.
- ³⁸ Li, A. A, McDonald, N. C, Chang, P. L, *J. Biomater. Sci. Polym. Ed.*, **2003**, *14*, 533-549.
- ³⁹ Vandenbossche, G. M. R, Van Oostveldt, P.; Remon, J. P. *J Pharm. Pharmacol.*, **1991**, *43*, 275-277 .
- ⁴⁰ Shen, F.; Mazumder, M. A. J.; Burke, N. A. D.; Stöver, H. D. H.; Potter, M. A. J.

-
- Biomed. Mater. Res. B: Appl. Biomater.*, **2009**, *90B(1)*, 350-361.
- ⁴¹ Burke, N. A. D.; Mazumder, M. A. J.; Hanna, M.; Stöver, H. D. H. *J. Polym. Sci. A: Polym. Chem.*, **2007**, *45*, 4129-4143.
- ⁴² Strand, B. L.; Morch, Y. A.; Espevik, T.; Skjak-Braek, G. *Biotech. Bioeng.*, **2003**, *82* (4) 386-394.
- ⁴³ Thu, B.; Gåserød, O.; Paus, D.; Mikkelson, A.; Skjåk-Bræk, G.; Toffanin, R.; Vittur, F.; Rizzo, R. *Biopolymers*, **2000**, *53*, 60-71.
- ⁴⁴ Velings, N. M.; Mestdagh, M. M. *Polym. Gels Networks*, **1995**, *3*, 311-330.
- ⁴⁵ Goosen, M. F. A.; O'Shea, M.; Gharapetian, H. M.; Chou, S.; Sun, A. M. *Biotechnol. Bioeng.*, **1985**, *27*, 146-150.
- ⁴⁶ King, G. A.; Daugulis, A. J.; Faulkner, P.; Goosen, M. F. A. *Biotechnol. Prog.*, **1987**, *3*, 231-240.
- ⁴⁷ Gåserød, O.; Smidsrød, G.; Skjåk-Bræk, G. *Biomaterials*, **1998**, *19*, 1815-1825.
- ⁴⁸ Bysell, H.; Malmsten, M. *Langmuir*, **2006**, *22*, 5476-5484.
- ⁴⁹ Vogel, M. K.; Cross, R. A.; Bixler, H. J.; Guzman, R. J. *J. Macromol. Sci. Chem. A*, **1970**, *4*, 675-692.
- ⁵⁰ Morris, P. J. *Trends Biotechnol.*, **1996**, *14*, 163-167.
- ⁵¹ Grigorescu, G.; Rehor, A.; Hunkeler, D. *J. Microencaps.*, **2002**, *19*, 245-259.
- ⁵² Vandenbossche, G. M. R.; Oostveldt, P. V.; Demeester, J.; Remon, J- P. *Biotechnol. Bioeng.* **1993**, *42*, 381-386.
- ⁵³ Awery, D.E.; Tse, M.; Chang, P. L. *Biotechnol. Bioeng.* **1996**, *52*, 472-484
- ⁵⁴ Qi, W.; Ma, J.; Liu, Y.; Liu, X.; Xiong, Y.; Xie, Y.; Ma, X. *J. Membr. Sci.* **2006**, *269*, 126-132

-
- ⁵⁵ Coromili, V.; Chang, T. M. S. *Biomat. Art. Cells Immob. Biotech.* **1993**, *21(3)*, 427-444
- ⁵⁶ Xing, Z. C.; Huh, M. W.; Kang, I. K. *Key Eng. Mater.* **2007**, *342-343*, 417-420

Chapter 7 Summary and Future Work for Cell Encapsulation

7.1 Summary

Cell encapsulation is a technique suitable for the delivery of therapeutic proteins to a patient from transplanted cells. One approach to cell sourcing involves either *ex vivo* or *in vivo* modification of a patient's own cells with viral or plasmid vectors such that the patient's cell will be able to secrete a specific therapeutic protein upon re-implantation. Our collaborators¹ are developing a potentially safer approach that involves immunisolating standard cell lines that have been engineered to secrete a therapeutic protein within alginate-based microcapsules. These microcapsules protect the cells from the patient's immune system, and the success of this approach depends on the long-term structural stability of the microcapsules, as well as their ability to maintain an environment suitable for the long-term survival of the encapsulated cells. In order to increase the structural stability of the microcapsules, this thesis developed a number of synthetic polyelectrolytes capable of forming covalent cross-links, and to form a self-cross-linkable skin either around, or throughout, Ca alginate microcapsules containing viable cells. The encapsulation processes and microcapsule properties were described, including collaborative work on cell viability and host-immune response. The resulting contributions are summarized as follows:

1. Copolymers of [2-(methacryloyloxy) ethyl] trimethylammonium chloride (MOETAC) with 0 to 100% 2- aminoethylmethacrylate hydrochloride (AEM.HCl), the homopolymer of N-(3-aminopropyl) methacrylamide hydrochloride (APM), and

copolymers of methacrylic acid (MAA) with 0 to 70% 2-(methacryloyloxy) ethyl acetoacetate (MOEAA), were prepared by free radical polymerization. NMR, Potentiometric titration, GPC, UV-Vis and Viscometric techniques were used to characterize the polyelectrolytes. Polyelectrolyte complexes of these polyanions and polycations were studied in some detail. They form gel, liquid coacervate or soluble complexes depending on variable such as charge ratio, total polymer loading, polymer molecular weight, and ionic strength. Liquid coacervates were favoured by higher ionic strength, whether from added NaCl or from higher polymer loading, and by using polyelectrolytes of lower molecular weight. The encapsulation of oils with a two-polyelectrolyte system forming a complex coacervate was demonstrated, as was the feasibility of cross-linking the resulting capsule walls. The polyelectrolyte complexes and the encapsulation process were studied in some detail by optical microscopy.

2. We have investigated the feasibility of using the synthetic copolymers of methacryloyl oxyethyl trimethyl ammonium hydrochloride with amino ethyl methacrylate, 70:30 (C70) as a polycation, and copolymers of methacrylic acid sodium salts with methacryloyl oxyethyl acetoacetate, 70:30 (A70) as polyanion to replace the conventional poly-L-lysine and outer alginate, respectively, for the preparation of mechanically stronger microcapsules for therapeutic cell encapsulation. Sequential deposition of these polyelectrolytes on calcium alginate films or beads led to a shell consisting of covalently cross-linked polyelectrolyte complex that resisted osmotic pressure changes as well as challenges with citrate and high ionic strength. Optical, phase contrast and confocal laser scanning microscopy characterized the resultant microcapsules. Confocal laser scanning microscopy revealed that both polyelectrolytes

were concentrated in the outer surface of the calcium alginate beads. The thickness of this cross-linked shell increased with exposure time. GPC studies of solutions permeating through flat analogous model membranes showed molecular weight cut offs between 150 and 200 kDa for poly(ethylene glycol) samples, suitable for cell encapsulation. The encapsulated cells were shown to be viable within calcium alginate capsules coated with the new polyelectrolytes, even though some of the capsules showed fibroid overcoats when implanted in mice, due to an immune response. In addition, preliminary studies have shown that C70 undergoes intra/intermolecular amidation in aqueous solution leading to the formation of cross-linked gels over time, and that C70 coated capsules are more prone to aggregation during the coating process than PLL-coated capsules.

The feasibility of using methacrylate (AEM) or methacrylamide (APM) based homopolymers containing primary amines (C0, PAPM) to replace C70 (and/or PLL) in Ca alginate based capsules was examined in some detail. These results indicate that PAPM is comparable to PLL in terms of shell strength, cell viability and protein binding, in shell cross-linked Ca-Alg capsules formed with the reactive polyanion A70. They also show better capsule strengths compared to C0 and C70. It also showed that PAPM as well as PLL are protected from the undesirable hydrolysis and intra/intermolecular amidation reactions during storage as seen for C70 and for C0.

3. The *in vivo* study of self cross-linked microcapsules in mouse model showed that there is a reaction of the host to the microcapsules or microencapsulated cells after implantation. As C70 and A70 are on the capsule surface, we suspected that C70 and/or A70 might bind to the cell protein or to the component of the culture media. To address this issue, we modified the cross-linked C70-A70 microcapsules by hiding these synthetic

polyelectrolytes (C70, A70) from the capsule surface to improve the *in vivo* performance of the Ca alg-C70-A70 capsules. Four layer-coated capsules were prepared using layer-by-layer method, where calcium alginate beads were sequentially coated with C70, A70, PLL and Alginate. Confocal laser scanning microscopy confirms the location and stability of C70, A70, and PLL polyelectrolyte network within the microcapsules. Interaction between the FITC labelled BSA (analogous to media protein) and the multilayer capsules was studied by CLSM. C70 showed significant protein binding to the microcapsules surface, while A70 had a lesser effect. Reducing the concentration of C70 and A70 lessened this effect. Using serum-free media to culture the microcapsules post fabrication instead of regular medium eliminated this host reaction. Ionic stress test indicates that the 4 layer capsules are covalently cross-linked and are stronger than classical Alginate-poly-L-lysine-Alg (APA) microcapsules. The permeability of multilayer capsules was determined by CLSM and GPC using FITC labelled BSA and narrow dispersed PEG standards, respectively. The pore size of the multilayer capsules was shown to be similar to that of the control APA microcapsules, and is suitable for cell encapsulation. The *in vitro* and *in vivo* biocompatibility of modified capsules was similar to that of APA microcapsules. The multilayer capsules show improved mechanical strength, while maintaining good biocompatibility and permeability

4. The feasibility of using A70, added to the sodium alginate prior to droplet formation, to reinforce the calcium alginate core by forming an interpenetrating network through covalent cross-linking with polyamines was studied in detail. As in conventional APA capsules, the composite cores containing A70 were exposed to PLL to form a covalently cross-linked network with A70 within the Ca alginate composite bead.

Depending on PLL molecular weight, this cross-linked network could be restricted to the capsule surface, or be formed throughout the core. In this context, the interaction between calcium ions and synthetic polyanions was examined. In case of A100, A90 and A80 immediate phase separation occurs to form a liquid coacervate. However, A70 (irrespective of MW) does not phase separate in presence of calcium chloride but forms a soluble complex. The distribution of A70 and PLL in the composite capsules were studied by CLSM using FITC labelled A70 (A70f) and rhodamine labelled PLL (PLLr). A70 and PLL form covalent cross-linked network, which is demonstrated by their resistance to citrate, sodium chloride and sodium hydroxide. The molecular weight cut-off of composite microcapsules was examined by CLSM using FITC labelled protein (BSAf) and different molecular weight of FITC labelled saccharides (FITC-Dextran). The permeability of composite capsules was shown to be similar to those of control APA capsules. Cytocompatibility of composite microcapsules was similar to the control APA microcapsules.

7.2 Future work:

7.2.1 Study New Series of Polyelectrolytes:

The present series of polyelectrolytes form liquid coacervate at 325-450 mM added NaCl, and in screening of the polyelectrolytes, C70 showed significant undesirable protein binding to the microcapsules surface. In addition, C70 undergoes hydrolysis and intra/intermolecular amidation in aqueous solution leading to the formation of cross-linked gels over time and likely for C0. One of the thesis goals was to develop

polyelectrolytes that can form liquid coacervates at physiological salt concentrations (150 mM NaCl), and to use them in cell encapsulation.

In order to address this issue, copolymers with (10, 20, 30%) HEMA or PEO will be prepared which may reduce the electrostatic interactions between chains of a series of polyelectrolyte such as PAPM and A70, and give liquid coacervate at 150 mM added NaCl. These polymers will allow continued exploration of the efficiency of polyelectrolyte complexation, the nature of polyelectrolyte complexes (liquid, gel, solid) and the factors that control them.

Our coacervation research to date involved polyethyleneimine as cross linker to achieve cross-linked coacervate microcapsules. However, polyethyleneimines (PEIs), in linear or branched form showed significant cellular toxicity.² We will continue to explore the possibility to prepare cross-linked coacervate microcapsules using the reduced charge density polyelectrolytes by varying the molecular weight and polymer composition (random, gradient, block), and explore them for cell encapsulation.

7.2.2 Optimization of Composite Capsules:

Our research has shown that synthetic polyelectrolytes (A70) can coexist with alginate in the Ca alginate core, and by varying the molecular weight of PLL, we able to localize the cross-linking reaction at the capsule surface or in the interior for the formation of an interpenetrating network within the classical APA microcapsules. However, PLL, the most widely used polycation is expensive. It has been shown to induce inflammation,³ and also has a pKa (10.5)⁴ well above physiological pH, which is not suitable for covalent cross-linking interactions at physiological conditions. In order to

address this, 3-aminopropyl methacrylamide (APM) copolymers with non-ionic co monomers such as HEMA will be prepared by controlled polymerization such as atom transfer radical polymerization (ATRP) and reversible addition-fragmentation chain transfer (RAFT) polymerization.^{5,6}

Previous study⁷ showed that acrylic acid based polymer adequately binds with PLL, provide a smoother surface and reduce the tissue response when compared with the alginate-coated capsules. To prepare a smoother surface containing capsules, we will use A70 for outer coating, and then optimize the strength of core cross-linked microcapsules by varying the MW and concentration of A70 that will aid to develop smooth surface and doubly cross-linked network (A70-PLL-A70) around or throughout the microcapsule. After optimization of strength of the core cross-linked microcapsules, the permeability and biocompatibility of the doubly cross-linked composite microcapsules will be studied.

7.3 References

- ¹ Dr. Murray A. Potter Lab, Department of Pathology & Molecular Medicine, McMaster University, Hamilton, Canada
- ² Kim, H J.; Kwon, M. S.; Choi, J. S.; Kim, B. H.; Yoon, J. K.; Kim, K.; Park, J. -S. *Bull. Korean Chem. Soc.* **2007**, *28*, 63
- ³ Strand, B. L.; Ryan, L.; Veld, P. I.; Kulseng, B.; Rokstad, A. M.; Skjak-Braek, G.; Espevik, T. *Cell Transplant.* **2001**, *10(3)*, 263-275
- ⁴ Bysell, H.; Malmsten, M. *Langmuir* **2006**, *22*, 5476-5484
- ⁵ Li, Y.; Lokitz, B. S.; McCormick, C. L. *Angew. Chem. Int. Ed.* **2006**, *45*, 5792-5795
- ⁶ Deng, Z.; Boucekif, H.; Babooram, K.; Housni, A.; Choytun, C.; Narain, R. *J. Polym. Sci. Part A: Polym. Chem.* **2008**, *46*, 4984-4996
- ⁷ Bunger, C. M.; Gerlach, C.; Freier, T.; Schmitz, K. P.; Pilz, M.; Werner, C.; Jonas, L.; Schareck, W.; Hopt, U. T.; de Vos, P. *J. Biomed. Mater. Res.* **2003**, *67A*, 1219-1227